Forschungszentrum Jülich



Institut für Chemie und Dynamik der Geosphäre 4:
Erdöl und Organische Geochemie

Gas Generation from Overmature Upper Jurassic Source Rocks, Northern Viking Graben

Michael Erdmann

Jül-3700

Gas Generation from Overmature Upper Jurassic Source Rocks, Northern Viking Graben

Michael Erdmann

Berichte des Forschungszentrums Jülich ; 3700
ISSN 0944-2952
Institut für Chemie und Dynamik der Geosphäre 4:
Erdöl und Organische Geochemie Jül-3700
D 82 (Diss. RWTH Aachen, 1999)

Zu beziehen durch: Forschungszentrum Jülich GmbH · Zentralbibliothek
D-52425 Jülich · Bundesrepublik Deutschland
☎ 02461/61-6102 · Telefax: 02461/61-6103 · e-mail: zb-publikation@fz-juelich.de

Zusammenfassung

Hintergrund und Ziel der Arbeit

Ziel dieser Arbeit war die eingehende Untersuchung der Kohlenwasserstoffgasbildung in der sogenannten überreifen Zone, die dem Ölfenster in höheren Temperaturbereichen folgt. Insbesondere primäre Crackprozesse und das sekundäre Cracken im Muttergestein wurden studiert. Neben den besser untersuchten sekundären Crackprozessen in Reservoirs, die gemeinhin als Öl zu Gas Cracken bezeichnet werden, wird das primäre Cracken immer noch kontrovers diskutiert und ist wenig verstanden. Der weltweit steigende Verbrauch an Kohlenwasserstoffen, als Energieträger oder als Rohstoff zur Herstellung von Plastik, und die daraus resultierenden Anstrengungen der Erdöl/ Erdgas Industrie, diese Bedürfnisse zu befriedigen, indem Exploration in immer größere Teufenbereiche vordringt, sind als Hintergrund dieser Arbeit zu verstehen.

Die vorliegende Studie wurde in der nördlichen norwegischen Nordsee an Gesteinen der oberjurassischen Heather und Draupne Formationen durchgeführt. Aufgrund der geologischen Zeiträume, die die Kohlenwasserstoffbildung in Anspruch nimmt, wurden neben Gasdateninterpretationen aus zahlreichen Bohrungen auch spezifische Laborexperimente unternommen. Die Grundlage für die Relevanz von Ergebnissen aus Kurzzeit-Hochtemperatur-Experimenten für Langzeit-Niedrigtemperatur-Prozesse, welche in natürlichen Petroleumsystemen stattfinden, resultiert aus den chemischen Gesetzen der Kinetik.

Die Ergebnisse dieser Arbeit zeigen unter anderem die Integration von kinetischen Parametern in komplexe Temperaturgeschichten während einer Sedimentbecken-Entwicklung und die Vorhersage von Temperatur-Zeit-Intervallen, in denen Kohlenwasserstoffgasbildung auftrat. Als Konsequenz wurden auch Aussagen über Beiträge der verschiedenen Muttergesteinstypen zu existierenden Lagerstätten im Arbeitsgebiet möglich. Es ist erstrebenswert, solche Ergebnisse an natürlichen Gasdaten zu kalibrieren. Erschwerend sind dabei die auftretenden Heterogenitäten in natürlichen Systemen und das Ablaufen von vergleichsweise schnellen Prozessen, wie z.B. Migration, Biodegradation und anderen.

Neben Temperatur-Zeit-Vorhersagen ist auch die Prognose von Gaszusammensetzungen von großem Interesse, da dies die Korrelation von Muttergestein bzw. Entstehungsgebiet mit der jeweiligen Lagerstätte ermöglichen kann.

Prozesse der Kohlenwasserstoffentstehung

Das mittlerweile unumstrittene, grundlegende Prinzip der Kohlenwasserstoffbildung (Philippi 1975, Tissot & Welte 1984) ist die thermische Spaltung von chemischen Bindungen in fossilem organischem Material, dem Kerogen. Eine Sonderstellung nimmt das Methan ein, das in signifikanten Mengen auch durch bakterielle Abbauprozesse gebildet wird. Die Bereiche der thermischen Kohlenwasserstoffbildung werden mit steigenden Temperaturbereichen, etwas irreführend, als Diagenese, Metagenese und Katagenese bezeichnet. Für die hier diskutierten Fragestellungen sind die Bereiche der späten Metagenese und der Katagenese von Interesse. Allgemein werden Temperaturen von 150-220° C für die Bildung von Methan, Ethan, Propan und Butan angenommen (Quigley & Mackenzie 1988). Neben der Relevanz von Zeit und Temperatur sind auch Druck und Katalysatoren als mögliche Steuerfaktoren denkbar. Der Einfluss von Druck führt nach heutigen Erkenntnissen eher zu einer Verzögerung von thermischen Crackprozessen (Domine 1991), während die Notwendigkeit einer Anwesenheit von Katalysatoren (z.B. Mango 1992) sehr umstritten ist.

Ansatz

Das Gebiet der nördlichen Nordsee, insbesondere der nördliche Viking Graben, bietet für die hier angestrebten Untersuchungen gute Voraussetzungen. Zum einen sind hier zwei grundlegend verschiedene Muttergesteinstypen anzutreffen und zum anderen sind diese bis zu groβen Teufen von mehr als 7000m im Norden des Viking Grabens anzutreffen. Unterschiedliche Expulsionseigenschaften der beiden Muttergesteine resultieren möglicherweise in zwei verschiedenen Wegen der Gasentstehung. Für die Heather Formation nimmt man an, das niedrige TOC-Gehalte (Total Organic Carbon) zusammen mit hohen Anteilen an terrestrischem organischen Material zu einer schlechten Expulsionseffizienz führen. Somit verbleibt ein groβer Teil des gebildeten Öls oder Bitumens im Muttergestein und wird mit fortschreitender Absenkung des Muttergesteins in höhere Temperaturbereiche gebracht (Littke & Leythaeuser 1993). Dies führt schlieβlich zu einer Bildung von Gas durch Cracken des residualen Öls oder Bitumens. Im Gegensatz dazu nimmt man für die Muttergesteine der Draupne Formation eine gute Expulsionseffizienz an und somit eine vorwiegende Entstehung von Gas aus residualem Kerogen.

Der erste Teil dieser Arbeit diente im wesentlichen der Etablierung eines Referenzsystems, dass die unterschiedlichen Kerogentypen und deren Veränderungen mit steigender Reife erfasste und die Einordnung späterer experimenteller Ergebnisse ermöglichen sollte. Daneben wurden *in situ* Gaszusammensetzungen an Muttergesteinsproben unterschiedlicher Reife-Bereiche durch thermische Extraktion ermittelt, sowie Gaszusammensetzungen von „Canned-cuttings" Proben gesammelt.

Der wesentliche experimentelle Teil der Arbeit bestand aus MSSV-Pyrolysen (MicroScale Sealed Vessel), einem geschlossenen System, kombiniert mit offenen Mehrphasen Pyrolysen. Die MSSV Pyrolysen wurden bei unterschiedlichen nicht-isothermen Laborheizraten durchgeführt und bildeten die Basis für die Bestimmung von kinetischen Parametern, während die Ergebnisse der offenen Mehrphasen Pyrolysen eine Unterscheidung zwischen primärem und sekundärem Gas ermöglichten.

Im interpretativen Teil der Arbeit wurden die kinetischen Parameter für Vorhersagen von Gasbildung bei einfachen linearen oder komplexen Heizraten im Rahmen einer Beckensimulation verwendet.

Im letzten Teil der Arbeit wurde auf die zugrundeliegenden chemischen Prozesse eingegangen, soweit es die zur Verfügung stehenden Datensätze erlauben. Unter Zuhilfenahme von großen Datensätzen, die von Norsk Hydro und Saga Petroleum freundlicherweise bereit gestellt wurden, konnten einige empirische Beobachtungen über Gaszusammensetzungen gemacht werden.

Ergebnisse zum Referenzsystem

Mikroskopische organisch-petrologische Untersuchungen, TOC Bestimmungen und Rock-Eval-Analysen lieferten Daten, die eine Klassifizierung des organischen Materials des zur Verfügung stehenden Probensatzes ermöglichten. Vitrinitreflexionsmessungen und der T*max* Parameter der Rock-Eval-Analysen gaben Aufschluss über die Reife der untersuchten Proben.

Die Ergebnisse zeigten, dass die Draupne Formation im wesentlichen Typ II Kerogen enthält, während Heather Formations Proben je nach Anteil terrigener oder mariner Macerale eher als Typ III oder als Mischtyp II / III einzustufen sind. Diese Beobachtungen stimmen mit Ergebnissen von Lafargue & Béhar (1989) überein. Inertinite waren im untersuchten Probenmaterial der Heather Formation häufig. In beiden Formationen traten als fluoreszierende liptinitische Mazerale hauptsächlich Alginite auf. Am häufigsten vertreten waren jedoch Liptinit-Bruchstücke, die wenig Schlüsse auf ihre Herkunft zuließen. Sporinite

ließen sich in beiden Formationen nachweisen. Als eine weiterführende Methode der Klassifizierung wurde offene Pyrolyse-Gaschromatography durchgeführt. Alkanverteilungen, und unterschiedliche Anteile von Aromaten, Thiophenen, und Phenolen ließen die Unterscheidung von marinen, marin-terrigen beeinflussten Muttergesteinen und von Mischtypen zu. Die meisten Proben wurden als unreif bis frühreif eingestuft, der Probensatz deckte jedoch Reifen bis zu 1.6% R_o ab.

Neben der Klassifizierung des organischen Materials und der Reife ließen sich weitere Beobachtungen machen. Die meisten der untersuchten Proben enthielten Vitrinite, wenn auch z.T. in nur geringen Mengen (Draupne Formation). In beiden Muttergesteinen wurde häufig ein Maceral angetroffen, das von Espitalié et al. (1991) als Bituminit beschrieben wurde, eine leicht bräunlich fluoreszierende strukturlose Komponente mit runden Begrenzungen, die leicht mit Vitrinit zu verwechseln ist, jedoch bei gleicher Reife niedrigere Reflexionswerte zeigt. In Proben höherer Reife (R_o=1.0-1.6%) wurde eine Komponente gefunden, die als Migra- oder Pyrobitumen bestimmt wurde, welches als ein nicht expuldiertes Restbitumen verstanden werden kann und somit als Quelle für Gasbildung bei höheren Reifen zur Verfügung steht. Da die stratigraphische Stellung dieser Proben nicht eindeutig geklärt ist, konnte nur aufgrund anderer Muttergesteinseigenschaften impliziert werden, dass es sich um Heather Formation handelt. Die ursprüngliche Hypothese einer bevorzugten sekundären Gasenstehung für Heather Formations Muttergesteine konnte durch diese Beobachtung untermauert werden.

Pyrolyse-Experimente

Im Vorfeld detaillierter Untersuchungen auf der Basis von Pyrolyse-Gaschromatographie, wurden Pyrolysen mit direkter Detektion aller Produkte, sogenannte „Rock-Eval-Typ" Pyrolysen, durchgeführt. Die Anwendung dieser Methode ermöglichte zweierlei. Zum einen konnte gezeigt werden, dass der Einsatz von Kerogen-Konzentraten das Auftreten von katalytischen Hochtemperatur-Mineralmatrix-Effekten vermeidet. Zum anderen lieferten Rock-Eval-Typ-Pyrolysen, die mit Proben unterschiedlicher natürlicher Reife durchgeführt wurden Hinweise, dass die auf Pyrolyse-Experimenten basierenden Kinetiken auf natürliche Systeme anwendbar sind (Schenk & Horsfield 1996).

Zwei Proben, je eine von der Heather Formation und von der Draupne Formation, wurden für Pyrolyse-Gaschromatographie-Experimente selektiert.

MSSV Pyrolysen wurden bei 3 Heizraten von 0,1, 0,7 und 5,0 K/min durchgeführt. Quantifiziert wurden neben dem "gaschromatographisch nichtauflösbaren Bereich", kurz

"hump" genannt, der auflösbare Bereich, sowie eine groβe Anzahl von Einzelkomponenten. Für die Aufgabenstellung erwies es sich als sinnvoll, C_1 -C_5, C_{6+} und C_{1+} zusammenzufassen, wobei C_1 -C_5 im chemischen (wenn auch nicht im physikalischen) Sinn als Gas und C_{6+} als Öl bezeichnet werden kann, auch wenn die Zusammensetzungen dieser künstlichen Produkte nicht wirklich denen von natürlich gebildeten entsprechen. Die kumulativen Produktbildungskurven für diese zwei Gruppen, sowie für die Gesamtprodukte, sind mit steigenden Heizraten zu höheren Temperaturen verschoben. Die Kurvenverläufe für Draupne Formations -Ölbildung zeigen klare Maxima, die die Bereiche für primäres Cracken von Kerogen zu Öl und für sekundäres Cracken von Öl zu Gas trennen. Die Gasbildungskurven zeigen nach Erreichen eines Plateaubereichs ebenfalls eine leichte Abnahme, was ein Resultat des Auftretens von Pyrobitumenbildung im Rahmen des Gas zu Gas Crackens ist. Im Gegensatz dazu, sind für die Heather Formations Ölbildungskurven sehr breite und flache Maxima charakteristisch, während sich die Gasbildungskurven durch stetige Zunahme bis zu den Maximaltemperaturen der verwendeten Messtechnik auszeichnen. Diese liegen je nach Heizrate zwischen ca. 560 und 650 °C. Da Gas bei der Heather Formation einen deutlich gröβeren Teil der Produkte darstellt, steigt auch die Gesamtproduktkurve über den kompletten Temperaturbereich an.

Um die Gesamtgasbildung in eine primäre und eine sekundäre zu unterteilen, wurde ein einfacher mathematischer Ansatz verwendet, so dass später für beide Prozesse kinetische Parameter bestimmt werden konnten. Der Ansatz geht vereinfachend davon aus, dass sekundäres Cracken von Öl zu Gas mit dem Erreichen des kumulativen Maximums der Ölbildung einsetzt. Unter dieser Annahme ergibt sich die Sekundärgasbildung direkt aus der Abnahme des Öls mit steigender Temperatur, multipliziert mit einem Konversionsfaktor, der die Bildung von Teer/Pyrobitumen berücksichtigt. Die Gesamtgasbildung minus berechnetem Sekundärgas ergibt die entsprechende primäre Gasbildung als Funktion der Temperatur.

Etwas genauere Betrachtungen wurden möglich, nachdem zusätzlich offene Mehrphasen-Pyrolyse-Gaschromatographie bei einer Heizrate von 5,0 K/min durchgeführt wurde. Dadurch konnte die primäre Gasbildung direkt gemessen und mit der berechneten verglichen werden. Es zeigte sich für die Draupne Formation, dass beide Kurven gut übereinstimmen, mit Ausnahme von Abweichungen bei hohen Temperaturen (primäres Cracken in offenen und geschlossenen Systemen muss nicht zwangsläufig identisch verlaufen). Für den Fall der Heather Formations -Probe ergab sich hingegen eine beträchtliche Abweichung der primären Ölbildung von der im geschlossenen System beobachteten, so dass eine Berechnung der Sekundärgasbildung mit dem vereinfachten Ansatz zweifelhaft erschien. Die so berechnete Menge an sekundärem Gas erwies sich als sehr klein, wohingegen die resultierende primäre Gasmenge sehr groβ war und einen Hochtemperatur-Gasbildungspuls anzeigte, der im

offenen System nicht erkennbar war. Diese widersprüchlichen Beobachtungen ließen sich durch die Bildung eines intermediären Bitumens oder Residuums erklären, das sich durch Rekombination von primären Produkten mit der Kerogenstruktur bildet. Ein Teil des im offenen System gebildeten Öls wird im geschlossenen System wieder an die Kerogenstruktur gekoppelt und bei höheren Temperaturen als sekundäres Gas freigesetzt. Es wurde im Folgenden versucht, anhand präparativer Experimente Beweise für dieses Model zu finden, was jedoch nicht eindeutig gelang, da Massenbilanzierungen aufgrund experimenteller Einschränkungen schwierig sind. Nichtsdestotrotz vermag das hier entwickelte Model die Ergebnisse der MSSV Pyrolysen zu erklären und steht im Einklang mit Ergebnissen, die von Béhar et al. (1995) und Schenk & Horsfield (1996) über die Verlagerung von Aktivierungsenergiepotentialen bei Typ III Kerogenen und Kohlen berichtet wurden.

Am Ende dieser Untersuchungen und Betrachtungen standen schließlich eine Reihe von Eingangsdatensätzen für die Bestimmung kinetischer Parameter der Gasbildung, als da sind:

- primäre Gasbildung für Heather und Draupne Formation,
- sekundäre Gasbildung via Cracken von Öl, wobei für die Draupne Formation zusätzlich zwischen Gas resultierend aus der Degradation von "Hump-" und "gaschromatographisch nicht auflösbaren Einzelkomponenten" unterschieden wurde,
- sowie für die Heather Formations -Probe ein zweiter Prozess der sekundären Gasbildung aus rekombiniertem Residuum.

Kinetische Parameter

Die bereits erwähnte Beobachtung, dass sich Produktgenesekurven mit steigender Heizrate zu höheren Temperaturbereichen verschieben, läßt vermuten, das diese Prozesse den Gesetzmäßigkeiten der Kinetik folgen. Kann man also die mathematische Funktion und deren Parameter bestimmen, mit denen sich die im Labor beobachtete Verschiebung erklären läßt, so kann man diese verwenden, um Gas- und Ölgenese unter geologischen Heizraten (die um 10 bis 12 Größenordnungen kleiner sind) vorherzusagen. Ob dies möglich ist, wird in der Literatur immer noch kontrovers diskutiert. Da es aber Anzeichen dafür gibt, dass die auf Kinetik basierenden Ergebnisse sinnvoll sind, scheint es zunächst gerechtfertigt, diese Methode anzuwenden. Im Rahmen dieser Arbeit wurde versucht, die ermittelten kinetischen Parameter mit Hilfe von Beckenmodellierung auf ihre Relevanz zu testen.

Es wurde angestrebt kinetische Parameter sowohl für die Gesamtgasbildung als auch solche für primäre und sekundäre Gasbildungen zu bestimmen. Weiterhin wurden die in der MSSV-Pyrolyse beobachteten Ölbildungskurven für Kinetikbestimmungen herangezogen und diese

mit Ergebnissen von Rock-Eval-Pyrolysen für Gesamtkinetiken verglichen, da kinetische Parameter prinzipiell von der verwendeten Analysemethode unabhängig sein sollten. Die Bestimmung von Parametern für die Bildung von Gas-Einzelkomponenten erwies sich als problematisch, da man hier nicht zwischen primär und sekundär gebildeten unterscheiden kann. Solche Bestimmungen wurden nur für Methan und Ethan durchgeführt, um die Ergebnisse für die Modellierung des kinetischen Isotopen-Effekts zu verwenden.

Die Berechnung kinetischer Parameter erfolgte unter den Annahmen, dass die semi-empirische Arrhenius-Gleichung Gültigkeit besitzt und die Reaktionen erster Ordnung sind. Weiterhin wurde die Annahme zugrundegelegt, dass den Reaktionen individuelle Frequenzfaktoren zuzuordenen sind, die durch die "Shift in T*max* Methode" bestimmt wurden. Als Ergebnis erhält man somit Potential *versus* Energieverteilungen mit zugehörigem Frequenzfaktor. Diese Parameter wurden zur Vorhersage von Gasbildungsraten bei einer linearen geologischen Aufheizrate von 5,3 K/MJ verwendet.

Die Ergebnisse für **primäre Gasbildung** zeigten breite Energieverteilungen, wobei die Heather Formation höhere Hauptenergie/ Frequenzfaktor Paare aufwies. Dennoch ergaben sich für die geologischen Vorhersagen für Heather und Draupne Formation ähnliche Temperaturintervalle von ca. 120-225 °C. Die Vorhersagen für die maximal Temperaturen sind höher für die Heather Formation (T_{max} = 190 °C, R_o ~1,7%) als für die Draupne Formation (T_{max} = 175 °C, R_o~1,3%).

Die **sekundäre Gasbildung** führt zu wesentlich komplexeren Ergebnissen. Bestimmungen für das gesamte sekundär gebildete Gas führten für den Fall der Draupne Formation nicht zu sinnvollen Parametern, so das in das Cracken von "hump" und das Cracken von gaschromatographisch auflösbaren Produkten differenziert wurde. Beide Degradations-prozesse zeigten nur wenige Energien, jedoch mit hohen Werten, was auf ein im Vergleich zum Kerogen stabileres und homogeneres Material schließen läßt. Für die Heather Formation wurden Parameter für das Cracken des gesamten C_{6+} Materials bestimmt. Die resultierende Energieverteilung war in diesem Fall etwas breiter. Wiederum ergaben sich ähnliche Temperatur Intervalle für die geologische Prognosen beider Formationen, die mit ca. 170-260 °C deutlich höher waren als vergleichsweise für primäres Gas.

Im Fall der Heather Formation nimmt die sekundäre Gasbildung eine Sonderstellung ein, die aus dem Abbau des rekombinierten Bitumens/ Residuums resultiert. Die wenigen Datenpunkte ließen zwar keine Bestimmung der kinetischen Parameter zu, eine vergleichende Betrachtung aller anderen Reaktionen zeigte jedoch, dass die relative Reihenfolge von Prozessen auch bei geologischen Aufheizraten scheinbar erhalten bleibt.

Somit würde diese Gasbildung bei Temperaturen von mehr als 250 °C bei einer Heizrate von 5,3 K/MJ ablaufen.

Anwendung der kinetischen Parameter in der Beckenmodellierung

Ziel der Anwendung war zum Einen, die Ergebnisse unter nicht-linearen Heizraten zu testen und zum Anderen, ihre Relevanz anhand von Daten eines natürlichen Petroleumsystems zu prüfen. Desweiteren war die Frage interessant, wieviel Gas proportional von beiden Muttergesteinen im Gebiet der Tampen Spur zu existierenden Lagerstätten zugeführt wurde.
Da bei der Modellierung auch Expulsion und Migration berechnet wurden, ließen sich Aussagen über den Anteil des sekundär gebildeten Gases machen. Aufgrund unzureichender Daten über die petrophysikalischen Eigenschaften der geologischen Einheiten in dem betreffenden Gebiet ließen die Ergebnisse allerdings nur erste Hinweise auf die tatsächlichen Vorgänge zu.
Neben der Kinetik und der Versenkungsgeschichte, die sich aus Datierungen und seismischer Interpretation direkt ergibt, ist die Wärmeflussgeschichte der wichtigste Parameter mit Einfluss auf die Kohlenwasserstoffbildung.
Für die hier durchgeführte Simulation wurden 80 mW/m^2 während der oberjurassischen Riftphase und 55-60 mW/m^2 für die Postriftphase angenommen, was zu einer guten Kalibrierung von modellierten Temperaturen und Vitrinitreflexionen im Vergleich mit Daten einer Bohrung führte.
Die Ergebnisse der Simulation zeigten, dass im Zeitraum von ca. 110 - 60 MJ (Millionen Jahre) die Hauptbildung von Kohlenwasserstoffen stattfand, während die Bildung von Gas noch bis 35 MJ fortschritt. Die Bildung von sekundärem Gas aus rekombiniertem Residuum wurde nicht beobachtet, da die maximale Teufe von über 7000m für die Heather Formation in der modellierten Sektion nicht ausreichend war. Daraus folgt, dass Heather Formations Muttergesteine in diesen Teufen noch ein residuales Potential besitzen müßten. Dies ist nicht anhand natürlicher Daten zu belegen, da Teufen von mehr als 4000m i.d.R. nicht erbohrt sind. Sekundäres Cracken von Öl zu Gas wurde für die Heather Formation im Zeitintervall von 50-0 MJ errechnet, während es für die Draupne Formation scheinbar von untergeordneter Bedeutung war. Eine Massenbilanzierung für die gesamten Sektion zeigte, dass die Heather Formation im Vergleich zur Draupne Formation möglicherweise mehr Gas zu Lagerstätten der Region beiträgt. Dieses Ergebnis beruht allerdings auf der Tatsache, dass Verluste von der Sektion für Draupne Formations-Produkte größer sind und die Formation als solche für Produkte der Heather Formation einen effektiven "Caprock" darstellt.

Kompositionelle Betrachtungen

Kompositionelle Betrachtungen an Gasen und an leichten Kohlenwasserstoffen im C_5 - C_7 Bereich wurden durchgeführt, um ein chemisches Verständnis für die Reaktionen, die der Kohlenwasserstoffgenese zugrundeliegen, zu entwickeln, auf denen letztlich die Kinetik basiert.

Die chemischen Mechanismen der primären und sekundären Crackprozesse wurden anhand der Versuchsergebnisse interpretiert.

Hierbei waren besonders Modelle des Crackens in Abhängigkeit von der Bindungsstärke (Sanderson 1976) und alternativ dazu sogenannte Random-Cracking-Modelle (Kissin 1987) interessant. Beobachtungen von Kissin (1987), das molare Mengen *versus* alkyl-Kettenlänge exponentiellen Funktionen folgen, konnten bestätigt werden, während sich keine Anhaltspunkte dafür ergaben, dass langkettige Produkte verhältnismäβig einfacher vom Kerogen abzuspalten wären. Lediglich Methan, Ethan und Propan schienen schwerer vom Kerogen abzuspalten, was jedoch auch durch das Vorhandensein von relativ kurzkettigen "crosslinking" -Strukturen im Ausgangsmaterial erklärbar wäre.

Die bei weitem energieaufwendigste Reaktion, die Spaltung von Methylgruppen von aromatischen Kernen, lieβ sich durch Bilanzierung von Toluol und Benzol belegen. Die Dealkylierung aller Aromaten im System lieferte jedoch nur einen Anteil von 15% des gesamten sekundären Gases. Als interessant erwies sich in diesem Zusammenhang, dass ein Nebenprodukt der Reaktion von Toluol zu Benzol das nicht-alkylierte Biphenyl ist, vorrausgesetzt, dass Wasserstoff in nicht ausreichenden Mengen vorhanden ist. Da Biphenyl ein Produkt in natürlichen Systemen ist, in Pyrolysen jedoch nicht, oder nur in geringen Mengen nachweisbar war, läßt sich die Schlussfolgerung treffen, dass für die hier verwendeten Pyrolyse-Systeme kein Wasserstoffmangel vorliegt und somit keine zusätzliche Anwesenheit von Wasser notwendig ist. Eine weitere Schlussfolgerung war, das Biphenyl in natürlichen Systemen ein Indikator für sekundäres Cracken unter Mangel von Wasserstoff sein könnte.

Empirische Betrachtungen an leichten Kohlenwasserstoffen

Die kompositionelle Zusammensetzung der leichten Kohlenwasserstoffe, d.h. bis zu einer Kohlenstoffzahl von sieben C-Atomen, wurde im Hinblick auf Veränderungen mit Reife und Ausgangskerogen untersucht. Vergleichende Betrachtungen von Labor- und Felddaten zeigten sowohl Parallelitäten als auch Unterschiede.

Es wurde zwischen Gas (C_1-C_4) und sogenannten "light-ends" (C_5-C_7) unterschieden. Letztere sind aufgrund ihrer geringeren Flüchtigkeit, im Vergleich zu Gas, bevorzugt in der Literatur für Untersuchungen herangezogen worden. Man geht davon aus, dass molekulare Verhältniswerte von C7-Isomeren weniger durch sekundäre Prozesse im Zusammenhang mit Migration verändert werden und Verluste durch Probennahme und Lagerung nicht signifikant zum Tragen kommen.

Korrelationen von Reife und organischer Fazies mit molekularen Verhältniswerten von C7-Isomeren wurden unter anderem von Philippi (1975), Thompson (1979, 1983), Schäfer *et al.* (1984) und von Mango (1987, 1990) publiziert. Im Rahmen dieser Arbeit wurden Verhältnissewerte von Molekülen verschiedener Stoffgruppen untersucht: Iso-alkane *versus* Iso-alkane, Cyclo-alkane *versus* Cyclo-alkane, Iso-alkane *versus* Cyclo-alkane und schließlich n-alkane *versus* Cycloalkane. Für Betrachtungen an Molekülverhältniswerten erwies es sich als hilfreich, einfache mathematische Modelle, bestehend aus zwei differentiellen oder integralen Gauss'schen Molekülbildungskurven, als Analoge zu verwenden. Es zeigte sich, dass Veränderungen in Standardabweichung und Amplitude keinen Einfluss auf das Vorzeichen der Steigung der resultierenden Verhältniskurve haben. Der Verhältniswert ändert sich nur über die relativen Lagen der Hauptbildungs-geschwindigkeiten. Neben der Bildungsgeschwindigkeit hat die Degradationsgeschwindigkeit eines Moleküls oder einer Molekülgruppe den gleichen Einfluss auf einen Verhältniswert (was allerdings nur im Experiment zu zeigen ist, da in der Natur in der Regel kein Maß für das "Verschwinden" einer Komponente vorhanden ist). Bildungsgeschwindigkeit und Degradationsgeschwindigkeit zusammen ergeben sehr komplexe Verhältniskurven mit zunehmender Reife, und gehen über die publizierten einfachen Zusammenhänge hinaus. Für das Verhältnis von Heptan zu Methylcyclo-Hexan (paraffinicity 2 nach Thompson 1979) konnte gezeigt werden, dass sowohl im Experiment als auch bei natürlichen Proben ansteigende Werte während der Hauptbildungsphase des Öls zu erwarten sind. Im Gegensatz dazu lassen sich sinkende Werte für das sogenannte Gasfenster beobachten.

Für die eigentlichen Gaskomponenten zeigte sich das iso/n-Butan Verhältnis und der C_1-C_4 "fingerprint" als besonders informativ. Beide Charakteristika ergeben sowohl signifikante Unterschiede für die Draupne und Heather Formation, als auch klare Reifetrends. Große Ähnlichkeiten zwischen Laborwerten und Daten aus dem Gebiet der nördlichen Nordsee ließen eine Interpretation der Datensätze einzelner Bohrungen unter Zuhilfenahme der Clusteranalyse zu. Sowohl Heather Formations -Gas von hoher Reife als auch sekundäres Gas konnten identifiziert werden.

Schlussfolgerung

Die kinetischen Parameter primärer Gasgenese zeichneten sich durch breite Aktivierungsenergieverteilungen aus während sekundäre Gasbildungen einzelne Energien aufwiesen, was mit der heterogeneren Zusammensetzung des Kerogens im Vergleich zum primären Bildungsprodukt (Öl) im Einklang steht. Die Anwendung der kinetischen Parameter im Rahmen einer Beckenmodellierung zeigte neben den kritischen Zeitintervallen, dass die sekundäre Gasbildung möglicherweise eine größere Rolle für die Muttergesteine der Heather Formation spielt. Dieser Schluss wird von kompositionellen Beobachtungen (molekulare Verhältniswerte und Gas-Isotopen) untermauert. Als Schlussfolgerung aller Beobachtung und experimentellen Ergebnisse scheint es wahrscheinlich, dass Heather Formations-Muttergesteine im Vergleich zur Draupne Formation eine wichtigere Rolle für die Enstehung von Gas in der überreifen Zone des untersuchten Gebietes haben. Dies gilt insbesondere für den hier postulierten Rekombinationsmechanismus, der zu einer sekundären Gasbildung bei besonders hohen Temperaturen im geologischen System führen würde. Weiterhin zeigt sich, dass geschlossene Pyrolysen eine realistischer Einschätzung von Gaspotentialen zulassen, die von offenen Pyrolyse-Systemen unterschätzt werden würde.

ABSTRACT

The overall goal of this study was to build a model of gas generation from overmature Heather and Draupne Formation source rocks utilising observations from the Northern North Sea Viking Graben hydrocarbon system, hydrocarbon gas generation predictions obtained from artificial maturation experiments and results from numerical modelling using Petromod©. Heating experiments were conducted to determine the kinetic parameters of gas generation, which were subsequently applied to a complex burial history. This approach was thought to provide an understanding of gas generation in terms of basin development, heating history and the type of the organic matter.

Laboratory experiments were performed on solvent extracted immature kerogen concentrates of 2 Upper Jurassic Heather and Draupne Formation samples. Information used to help choosing these samples from a larger sample set included observations on organic petrology, Rock Eval analysis, kerogen typing by pyrolysis-gas chromatography and determination of bulk generation kinetic parameters. The Draupne Formation sample is characterised by a marine type II kerogen with a strong aliphatic hydrocarbon signature and contents of organic sulphur. The Heather Formation has a high proportion of aromatic hydrocarbons and phenols due to higher contributions of terrigenous type III organic matter. Both samples revealed similar alkyl-chain length distributions pointing to similarities in the marine proportions of the kerogens. It was decided that detailed work on gas generation should consider these typical end-member kerogen compositions.

The kinetics of primary and secondary gas (C_{1-5}) generation was recognised and kinetic parameters assigned to them. The results of extrapolations to a linear geological heating rate of 5.3K/ma can be summarised in short as follows

- Primary gas generation
  Peak generation temperatures are higher for Heather Formation (T_{max} = 190°C, R_o appr. 1.7%) compared to Draupne Formation (T_{max} = 175°C, equivalent to R_o 1.3%) at 5.3K/ma.
- Secondary gas generation
  Peak generation temperatures at 5.3K/ma are 220°C for Heather Formation and 205 to 215°C for Draupne Formation secondary gas generation from the cracking of oil. These temperatures correspond to R_o values of 2.4% and 2.0% respectively. The high temperature secondary gas formation from neo-formed bitumen as detected for the Heather Formation is outstanding and is suggested to occur at very high temperatures (max appr. 250°C) for geological heating rates.

The observation of such a bitumen formation with subsequent secondary cracking has profound implications for petroleum exploration, in that a significant charge of dry gas from the Heather Formation can be expected at very high maturity levels. Moreover it shows that closed system pyrolysis is the appropriate technique for assessing hydrocarbon gas generation potentials. Open system pyrolysis will underestimate late stage high temperature gas generation. From these findings and in combination with the application of parameters using basin modelling and correlations by gas range molecular parameters and isotope compositions an overall scenario for gas generation in the Viking Graben was obtained. Gas from overmature settings was recognised and assigned preferentially to the Heather Formation.

Acknowledgements

First of all I would like to thank Brian Horsfield who initiated the project and supervised this study and who helped direct the research towards success. His informative reviews and numerous discussions improved the manuscript. Prof. Ralf Littke and Prof. Dietrich Welte are acknowledged for reviewing the dissertation. Thanks especially to H.J.Schenk who provided invaluable help during completion.

Norsk Hydro and Saga Petroleum are acknowledged for funding and support of this research study. I thank especially Nigel Mills, Nils Telnæs and Arnd Wihelms who provided always a lot of help. Special thanks to Rolando di Primio for helping to set up the basin modelling at Saga Petroleum and for the wonderful fishing tours in Norway's fjords.

I wish to express sincere appreciation to Keith Hall and Chris Boreham for rapid performance of the isotope analyses under the pressure of time and to Malvin Bjorøy for performing the headspace gas analyses.

Thanks are extended to all my colleagues at the Institute, in particular to Gary Muscio who helped me much during the first time and to Volker Dieckmann and Matthias Schulze who were always willing to discuss not only on scientific issues. Bernhard Cramer and Roland Gaschnitz were always ready to discuss matters of kinetic isotope effects which helped improving the corresponding chapter.

I am pleased to acknowledge also the considerable laboratory assistance given by Franz Leistner and all scientists and technicians of the ICG 4.

Last but not least the help and encouragement of my parents is gratefully acknowledged here.

Abbreviations

A	frequency factor
API gravity	density = 141500/(kg/m^3)-131.5
appr.	approximately
ARO	aromatic hydrocarbon fraction
CO_2	carbon dioxide
Ea	activation energy (1kcal = 4.1868 kJ)
ESR	electron spin resonance
FID	flame ionisation detector
gc	gas chromatography
gc ms	gas chromatography mass spectrometry
GOR	gas oil ratio
HC	hydrocarbons
H/C	hydrogen / carbon ratio
HCl	hydrochloric acid
HI	Hydrogen Index
IR spec.	infrared spectroscopy
IR MS	isotope ratio mass spectrometry
KCF	Kimmerdige Clay Formation
MK EC	kerogen concentrate/ extracted
MSSV	MicroScale Sealed Vessel
m/z	mass/ charge
NMR	nuclear magnetic resonance
NNE	North Northeast
NSO	nitrogen-sulfur-oxygen components
O/C	oxygen/ carbon ratio
OI	Oxygen Index
pers. comm.	personnel communication
pic.	picture
PVT	pressure volume temperature
py	pyrolysis
r	heating rate
R_o	vitrinite reflectance, oil immersion
S/C	sulfur/ carbon ratio
S_{org}/C	organic sulfur/ carbon ratio
SSW	South Southwest
TIC	total ion current
t_{max}	temperature of maximum product yield
TOC	total orgainc carbon
tvap	thermovaporisation

ABSTRACT

CONTENTS

Acknowledgements
Abbreviations

1 INTRODUCTION 1

1.1 Problems and Objectives 1

Precursors
Driving Forces
Northern North Sea Hydrocarbon System

1.2 Approach 6

2 METHODOLOGY 7

2.1 Sampling and Data 7

2.2 Analytical Program 9

2.2.1 Geochemical Evaluations 9

2.2.2 Heating Experiments 12

2.2.3 Kinetic Modelling 14

3 RESULTS AND DISCUSSION 16

3.1 Reference Systems 16

3.1.1 Kerogen Types 16

Organic Petrology 16

Bulk Kerogen Classification 18

Detailed Kerogen Composition 20

3.1.2 Maturity 25

Vitrinite Reflectance 25

T_{max} and Hydrogen Index (HI) 27

3.2 Choice of Samples for Heating Experiments 29

3.2.1 Kerogen Concentration versus Whole Rocks 29

3.2.2 Bulk Hydrocarbon Generation 30
3.2.3 Applicability of Kinetics 30
3.3 Heating Experiments simulating Gas Formation 33
3.3.1 Evolution of Boiling Ranges during MSSV Pyrolysis 35
3.3.2 Evolution of Boiling Ranges during Multistep Open System Pyrolysis 36
3.3.3 Product Amounts 37
3.3.4 Compositional Details from MSSV and Open System Pyrolysis 38
3.3.5 Calculation of Primary and Secondary Gas Formation 40
Conservative Evaluation 40
Refined Evaluation Draupne Formation 42
Refined Evaluation Heather Formation 47
3.3.6 Recombination and Cracking of Neoformed Residues 50
3.4 Kinetics of Gas Formation 56
3.4.1 Determination of Kinetic Parameters and Extrapolation to Linear Geological Heating Conditions 58
Primary Gas Generation 59
Secondary Gas Generation 61
Gas Formation versus Oil and Bulk Products 64
3.4.2 Application of Kinetic Parameters using Basin Modelling 67
Principles of Basin Modelling 68
Input 68
Calibration 71
Results of the Simulation 74
Burial and Temperature History 74
Gas Generation 75
Whole System Mass Balance 77
Timing of Hydrocarbon Gas Generation 78
Migration and Gas Losses 79

3.5 Compositional Considerations 82
3.5.1 Petroleum Forming Reactions 82
Primary Cracking 82
Secondary Cracking 84
3.5.2 Gas and Lightend Hydrocarbons 90
Gas Oil Ratio (GOR) 91
Compositional Features of Light-ends 94
Compositional Features of Gas 102
3.5.3 Stable Carbon Isotopes 111

4 CONCLUSIONS 115

5 REFERENCES 118

6 APPENDIX

1 INTRODUCTION

Human interest in energy resources and the chemical industry's need for raw-materials is still strongly focussed on organic fossil fuels, including the hydrocarbon gases methane, ethane, propane and butane. Hence, petroleum exploration proceeds to successively deeper areas of sedimentary basins and seeks to understand processes happening therein. Questions that arise deal with the process of hydrocarbon formation under conditions encountered in deep basins, such as the breakdown of oil either in reservoirs or in source rocks and the question of whether a "gas-floor" exists or not.

1.1 Problems and Objectives

The thermal energy driven evolution of hydrocarbon gases from deeply buried petroleum source rocks of the Norwegian Northern North Sea in the so-called "overmature zone" is the topic of this work.
The main objectives are the evaluation of the timing and the extent of gas generation from different types of source rocks or different types of precursors and the discrimination among their related gases. Different types of precursors are, for instance, residual unexpelled bitumen and kerogen in source rocks. Special emphasis is placed not only on the prediction of gas generation under geological conditions but also on an understanding of different gas-forming mechanisms. In this regard, *product prediction* by means of heating experiments, for instance in terms of gas-oil ratios or individual component distributions, was considered. Results from these investigations are thought to provide a reliable basis for exploration work such as the prediction of reservoir filling scenarios where gas flushing from deep kitchen areas may occur. Furthermore the contributions of gas from different Upper Jurassic source rocks to Northern North Sea reservoirs are discussed.

Precursors

A number of different origins for hydrocarbon gases are known. In general these are subdivided into b*iogenic* gas that results from microbial action, *inorganic* gas which is thought to be formed in the deeper crust or upper mantle and *organic thermal* gas. The latter evolves during the degradation of fossil organic matter in the subsurface (Philippi 1975, Tissot & Welte 1984) during diagenesis, catagenesis and metagenesis in the so-called early-mature, mature and overmature zones (Tissot & Welte 1984, p.72). Late catagenesis and early metagenesis are particularly significant for gas generation.
Hydrocarbons are the proportion of thermal gases that are of economic interest. They are generated from two major precursors namely kerogen and petroleum/ bitumen. Kerogen, commonly described as the insoluble proportion of organic matter in sedimentary rocks (Robinson *et al.* 1953) can be investigated by optical microscopic methods (Teichmüller 1986), pyrolysis (Horsfield 1984), or chemical degradation methods (Rullkötter & Michaelis 1989) and by non-destructive spectroscopic methods (Schenk *et al.* 1986, Durand 1980, Marchand & Conard 1980). Kerogens are commonly classified according to Tissot *et al.* (1974) as types I, II and III which are defined by their atomic ratios H/C and O/C according to earlier work of Van Krevelen (1951). Based on these observations it was found that different types of kerogen can be discriminated which have different potentials for gas generation as well as differences in the resulting gas compositions (Leythaeuser *et al.* 1979). Concerning gas and condensate compositions the question is not yet settled, as to whether gas precursors as a part of the kerogen-structure are predominantly formed during diagenesis (Erdman

1961), or if they can be considered to be original moieties inherited from the biological matter (Thompson 1979, 1983) or even if they form through intermediates during primary cracking reactions (Mango 1987).

A bulk-concept for the origin of petroleum (i.e. both oil and gas) which accounts for educts and products without considering single chemical reactions was introduced by Cooles *et al.* (1986). The model assumes kerogen to comprise an inert and a reactive proportion with the latter further subdivided into labile and refractory proportions. Empirical observations in many petroleum basins world-wide led to the discrimination of zones with either low or high contributions of gas which consist predominantly of methane (dry gas) or high C_{2-4} gas concentrations (wet gas). The reactive-inert kerogen degradation model was founded on these observations. The labile fraction is thought to produce mainly oil and minor amounts of wet-gas whereas the refractory proportion is thought to be thermally more stable, producing mainly dry gas at higher maturities.

The secondary cracking of reservoired oil and unexpelled oil or bitumen in source rocks is the second major gas-forming process (e.g. Tissot & Welte 1984, p.200). Some authors believe secondary cracking to be the major source of gas formation *per se* (Monin *et al.* 1989, Pepper *et al.* 1995). Other authors objected the relative thermal instability of oil, for instance for the decomposition of the cycloalkane ring Mango (1991) calculated a period of time that exceeded the lifespan of the earth. To date there is no evidence for the relative importance of these processes for naturally occurring gas accumulations. The possibility for secondary cracking of petroleum in reservoirs has long been recognised (Barton 1937, Landes 1967, Connan *et al.* 1975, Béhar *et al.* 1992, Kuo & Michael 1994). In the overmature zone on which interest is focussed here higher molecular weight petroleum species are considered unstable (Hunt 1984, 1996). Data published by Price (1982) and Whelan *et al.* (1990) are contradictory because appreciable amounts of C_{15+} bitumen were observed at temperatures as high as 300°C and maturities exceeding 4% vitrinite reflectance. Detailed investigations by Horsfield *et al.* (1992) support the degradation of reservoired oils during experiments that allowed the extrapolation of results to geological heating conditions. They found that gas generation starts at relatively high temperatures compared to kerogen degradation and is of a simpler chemical nature as compared to primary cracking. These findings were based on the observation that secondary cracking occurred in a much more narrow temperature interval as did the cracking of oil and gas from the kerogen. In contrast little is reported about in-source secondary degradation (Pepper & Dodd 1995). The breakdown of petroleum in source rocks, i.e. the unexpelled fraction of first-formed products can be assumed to work differently from in-reservoir cracking. The composition of unexpelled petroleum differs from reservoired oil in that aromatic-, NSO- and asphaltene fraction contents are higher than in related oils (Connan & Cassou 1980). Eglinton *et al.* (1990) reported that the presence of sulphur linkages reduces the bulk thermal stability of kerogen. Moreover the residual kerogen that stays in contact with the unexpelled products is known to have an increasing content of free radicals with maturity, the increase of which depends on the kerogen type (Pilawa *et al.* 1996). Thus it is likely that the in-source degradation of residual petroleum by secondary cracking to form gas proceeds faster and at lower temperatures than observed for reservoirs.

Driving Forces

Temperature is the critical driving force for petroleum formation with the most prolific generation of gas thought to take place at high temperatures (Philippi 1975). These temperatures are expected to be

in the range of 150-220°C (Quigley & Mackenzie 1988). Aside from increased temperatures, elevated pressures also occur in deep basin parts. Tissot & Welte (1984, p.196) concluded the influence of pressure to be negligible. Other investigators stated the importance of elevated pressure (Louis & Tissot 1967, Bostick 1973, Behar & Vandenbroucke 1996) and also the presence or absence of catalysts and/ or water (Hoering & Abelson 1963, Hoering 1984). The role of these parameters is still controversially discussed but the generally accepted view is that their contribution to petroleum and especially gas formation is small compared to temperature, and in the case of pressure rather retard petroleum formation (Dominé 1991, Price & Wenger 1992, Michels *et al.* 1995, Jackson *et al.* 1995). Still these answers are uncertain and not quantifiable.

Not only temperature but also time is thought to control the formation of gas (Philippi 1965, Quigley & Mackenzie 1988). The time-temperature dependence was recognised early by coal investigators (Karweil 1955, Juentgen & van Heek 1968) leading to the widely accepted point of view that chemical kinetics govern hydrocarbon gas formation. Attempts to establish kinetics from naturally observed data have been performed (Pepper *et al.* 1995) but, especially for the overmature zone, these data are hard to obtain because wells are usually situated in structurally high positions. Moreover the mobility of gas creates uncertainties in observations. Alternatively gas formation can be investigated in heating experiments (pyrolysis) using either source rock samples or model substances. Using generation kinetic parameters that can be obtained from those experiments allows the extrapolation of short-time high-temperature observations to long-time low-temperature conditions.

As chemical kinetics usually deal with well defined reactions, which to date cannot be determined for cases of kerogen breakdown or bitumen degradation, bulk chemical concepts have been designed instead. These concepts, which were thoroughly reviewed by Ungerer (1990) and recently by Schenk *et al.* (1997), all assume that bulk reactions can be expressed as an unimolecular decay according to the equation A > B+ C + ...

The question of whether equilibrium processes, which are thermodynamically instead of kinetically controlled, are of importance for the generation of gas is not settled yet. Most authors consider these processes to be of minor importance because petroleum formation is considered to be quasi-irreversible. Individual reaction steps like for instance the addition or combination of radicals are however reversible. Still, equilibrium was reported to control the occurrence of methane in deep basins (Takach *et al.* 1987) by interaction of rock, water, CO_2 and methane. Similarly, Seewald (1994) found metastable equilibria for the system ethane, ethene, water and an inorganic redox-buffer based on reversible thermodynamically controlled reactions. However, the author did not object the absence of stable equilibrium in natural systems. It is known from the chemical industry that even solid - gas phase equilibria exist. An example is the so-called Boudouard-equilibrium where the concentrations of CO_2 and CO in the presence of graphite adjust to a temperature-dependent equilibrium. Investigations of similar processes during petroleum generation have not been reported in literature.

Northern North Sea Hydrocarbon System

Gas encountered in the Viking Graben, a major structural element of the northern North Sea, was reported to be mainly of thermogenic origin (Tissot & Welte 1984, p.212). The importance of gas in this area was emphasised by Chung *et al.* (1995), whereby 40-90 mole % of the total petroleum hydrocarbons in the Viking Graben were reported to consist of gas, so that the physical properties and secondary migration behaviour of petroleum will be strongly controlled by the amounts of gas.

The Viking Graben hydrocarbon system is substantially restricted to the Jurassic. Tertiary units are of importance in some areas. Here migration through Cretaceous strata comprising predominantly shale and siltstone lithologies with some carbonates has to be considered. In the eastern part of the northern North Sea upper Jurassic sandstone intercalations of the Sognefjord and Fensfjord Formations are important reservoir rocks and migration pathways whereas in western areas the lower Jurassic Statfjord Formation and sandstones of the middle Jurassic Brent group gain importance.

The major source rock units are the Upper Jurassic Draupne and Heather Formations of Bathonian to Kimmeridgian age. Additionally middle Jurassic coals of the Brent group and shales of the lower Jurassic Dunlin group have to be considered (Skervoy & Sylta 1993). Whereas their contributions to oil accumulations are evidently negligible, the respective contributions of the latter source rocks to reservoired gas are still uncertain (Goff 1983, Cooper & Barnard 1984, Chung *et al.* 1992). In the case of gas the task of source correlations is clearly of great difficulty. This becomes obvious when reviewing opinions about the relevance of gas derived from Heather Formation and Brent coals. Rønning *et al.* (1986) outlined that the Hild gas/condensate field would be of Brent origin because they detected terrigeneous biomarkers. A detailed investigation by Skålnes *et al.* (1993) of the same field using biomarkers and n-alkane isotope compositional data led to the conclusion that several source rock units must be involved, one of them with a clearly terrigeneous signature, leaving the choice between Heather Formation and Brent coal. Chung *et al.* (1995) stated straightforward: "the Lower Jurassic Brent group is responsible for the bulk of gas and condensates in many accumulations in the Viking Graben" based on terrigeneous isotope signatures. These conflicting statements reveal the lack of a reliable basis for the interpretation of the origin of gas.

The regional distribution of source rock sedimentary facies also plays an important role as demonstrated by a strong dependence between sedimentary facies and the distribution and quality of organic matter as recognised by Hunt (1963). A lot of research on the geology of the north Viking Graben area was undertaken (for example Goff 1983, Thomas *et al.* 1985, Rawson & Riley 1982 a.m.m.), in particular on the Draupne Formation. Both the Draupne and Heather Formations were deposited under marine conditions, while the Jurassic rift-regime provided a strong tectonic activity resulting in numerous sub-basins which led to a regional definition of the Draupne and Heather Formations applying to the Norwegian Northern North Sea (Vollset & Doré 1984). The Draupne Formation depositional environment can be described as shallow to deep-marine with subbasins and intramarine highs, which were responsible for abundant debris flows or turbidite currents charging into the deeper basin areas. On high positions occurred thin condensed or eroded units with organic matter of poor quality. In the basin centers homogenous claystones are intercalated vertically and laterally with coarse grained lithologies, closely related to fluctuations in the total organic carbon (TOC) content. In spite of this unsteady morphology and tectonic setting overall dys- or anaerobic conditions caused by a stratified water column are assumed for the Draupne Formation (for example Lallier-Vergès & Bertrand 1993). In contrast the underlying Heather Formation is believed to have been deposited under shallow and more aerobic conditions with less tectonic activity but with an increased input of clastic detritus from the eastern deltaic systems. This resulted in poor preservation conditions for organic matter whereas in basin centers the quality can resemble that of the Draupne Formation.

Field (1985) mapped the maturity of the upper Jurassic using vitrinite reflectance (Fig. 1) in the northern North Sea between 58°N and 62°N. The distribution of maturity boundaries within the upper

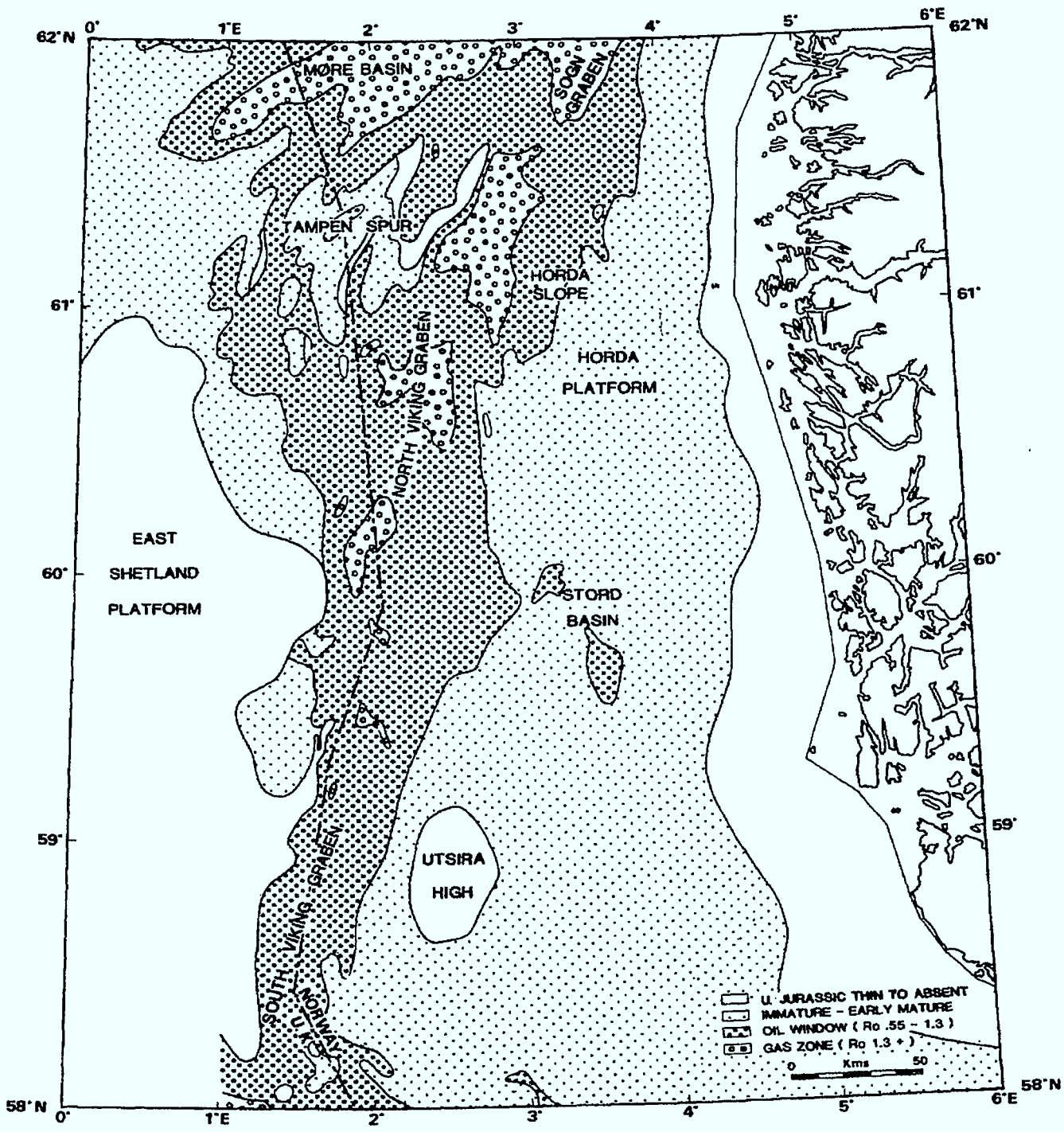


Fig. 1: Northern North Sea. Maturity expressed as vitrinite reflectance encountered in the Upper Jurassic.From Field (1985).

Jurassic corresponds well with structural trends of the Viking Graben. The highest maturities occur along the Graben axis striking from SSW to NNE. In the northernmost part, in the Sogn Graben and the Møre Basin the base of Cretaceous exceeds depth of 9000 m, ensuring the presence of overmature settings.

Reeder & Scotsman (1985) concluded that the present day condensate window in the northern North Sea is at depths of 4500-5400 m based on simple observations of API gravity-distributions and Kimmeridge Clay burial depth. However, this was a rough estimate without any quantitative measure of gas formation during burial of the source rocks through time. Predictions resulting from the

combination of kinetic modelling and basin modelling are more appropriate and became possible during the last years.

1.2 Approach

For the purpose of this study Draupne and Heather Formation source rocks from the northern Viking Graben were chosen for investigation as they represent two types to which different gas generation characteristics might be assigned. Two pathways for gas generation in the overmature zone were considered. The Draupne Formation is organic-rich and contains marine oil-prone kerogen, resulting in a high expulsion efficiency (Larter 1985, Cooles *et al.* 1986) which in turn is thought to result in low amounts of residual bitumen available for subsequent secondary cracking. In contrast the Heather Formation with low average TOC contents and a more terrigeneous influenced kerogen is likely to be a less efficient expeller resulting in high proportions of residual bitumen. Under these assumptions an investigation of in-source secondary cracking of unexpelled bitumen alternatively to gas formation from kerogen was planned.

The successively deeper burial of source rocks towards the Graben centers, especially towards the north, provides ideal conditions for the investigation of gas generation in overmature settings. Additionally the intense research in the area during decades of exploration provides a good regional knowledge and data.

Working-plan

- Establishment of a framework for the examination of gas generation. Kerogen quality and distribution and maturity were investigated for the selected samples.
- *In-situ* hydrocarbon gas compositions were determined by thermal extraction (thermovaporisation) and headspace and occluded gas analyses. The initial plan to include gas compositions obtained from oil samples was rejected because compositional alterations by separators at wellsites were considered to be too strong.
- A major part of the work was to investigate the gas formation under laboratory conditions. This is useful because the number of contributing parameters is small in comparison with natural systems and additionally the products are not altered by post generation processes like expulsion, migration etc. Pyrolysis experiments were performed on low maturity samples by employing closed and complementary open system devices thus considering primary as well as secondary processes. Closed system MSSV pyrolysis experiments were run at three different heating rates.
- Use of different heating rates allowed the calculation of kinetic parameters for gas generation, with the help of which experimental rate curves were extrapolated to reasonable linear geological heating rates.
- Extrapolations to complex heating histories in a Graben flank scale with the help of basin modelling software were the next step to be done.
- Gas generation predictions as well as compositional changes encountered during pyrolysis experiments and their respective isotopic compositions were used in a final step for comparisons with naturally occurring features obtained from thermovaporisation and headspace gas analyses. Additionally at this point a database of Viking Graben geochemical information was employed for interpretations.

2 METHODOLOGY

2.1 Sampling and Data

During the time of the project the sample set was extended repeatedly and data were collected from the funding companies. The former was done because high-maturity samples were difficult to obtain and because in the first year of the study low maturity samples often turned out to be impregnated by migrated hydrocarbons, especially Heather Formation samples from quadrant 35. The final sample set is listed in Table 1. The map in Fig. 2 gives an overview of the research area showing main structural features, blocks where samples stem from and some of the major hydrocarbon accumulations (for instance Oseberg (30) and Snorre (34)). Samples from the wells M, N and O were received during the final stage of the study and analysis were restricted to thermovaporisation-gc-ms in order to investigate the gas range composition of these high maturity samples.

Table 1: Sample set for the project.

	R_o (%)	conventional cores		cuttings		sidewall cores		canned cuttings	
Well	range	Draupne	Heather	Draupne	Heather	Draupne	Heather	Draupne	Heather
A	0.35-0.4	2	1	-	-	-	-	-	-
B	0.36	2	-	-	-	-	-	-	-
C	0.4-0.5	-	2	-	-	-	-	-	-
D	0.45	1	-	-	-	-	-	-	-
E	0.4-0.5	-	-	-	-	2	-	-	-
F	0.4-0.5	-	7	-	-	-	-	-	5
G	0.5	-	9	-	-	-	-	2	10
H	0.5	-	4	-	-	-	-	-	-
I	0.6	3	2	-	-	-	-	5	3
J	0.7-1.0	-	2	9	17	-	-	-	-
K	0.8-1.0	-	-	3	17	-	-	-	1
L	1.0	1	-	-	-	1	-	-	-
M	0.8	-	2	-	-	-	-	-	-
N	>0.8	2	-	-	-	-	-	-	-
O	>0.8	2	-	-	-	-	-	-	-
P	1.0-1.6	8 (Viking group)		-	-	-	-	8 (Viking group)	

Data bases

The following data were provided by the funding companies (Table 2, Appendix):

- Depth of stratigraphic boundaries for wells in quadrants 30, 31 and 35.
- Completion logs and geochemical reports for wells from which samples were selected.
- Vitrinite reflectance measurements for quadrants 30, 31, 34 and 35.
- Extractable organic matter (EOM) - Iatroscan group-type separation data for Norwegian North Sea quadrants 30, 31, 34 and 35.

- Headspace and occluded gas data for quadrants 30, 31, 34 and 35 and headspace gas isotope data for the same quadrants and wells from Mid-Norway.
- Bulk-kinetic analyses data including activation energy potentials and frequency factors. These data were provided to help choose samples for detailed analyses.
- An interpreted seismic section from quadrant 33 was provided for basin modelling (Fig. 2).

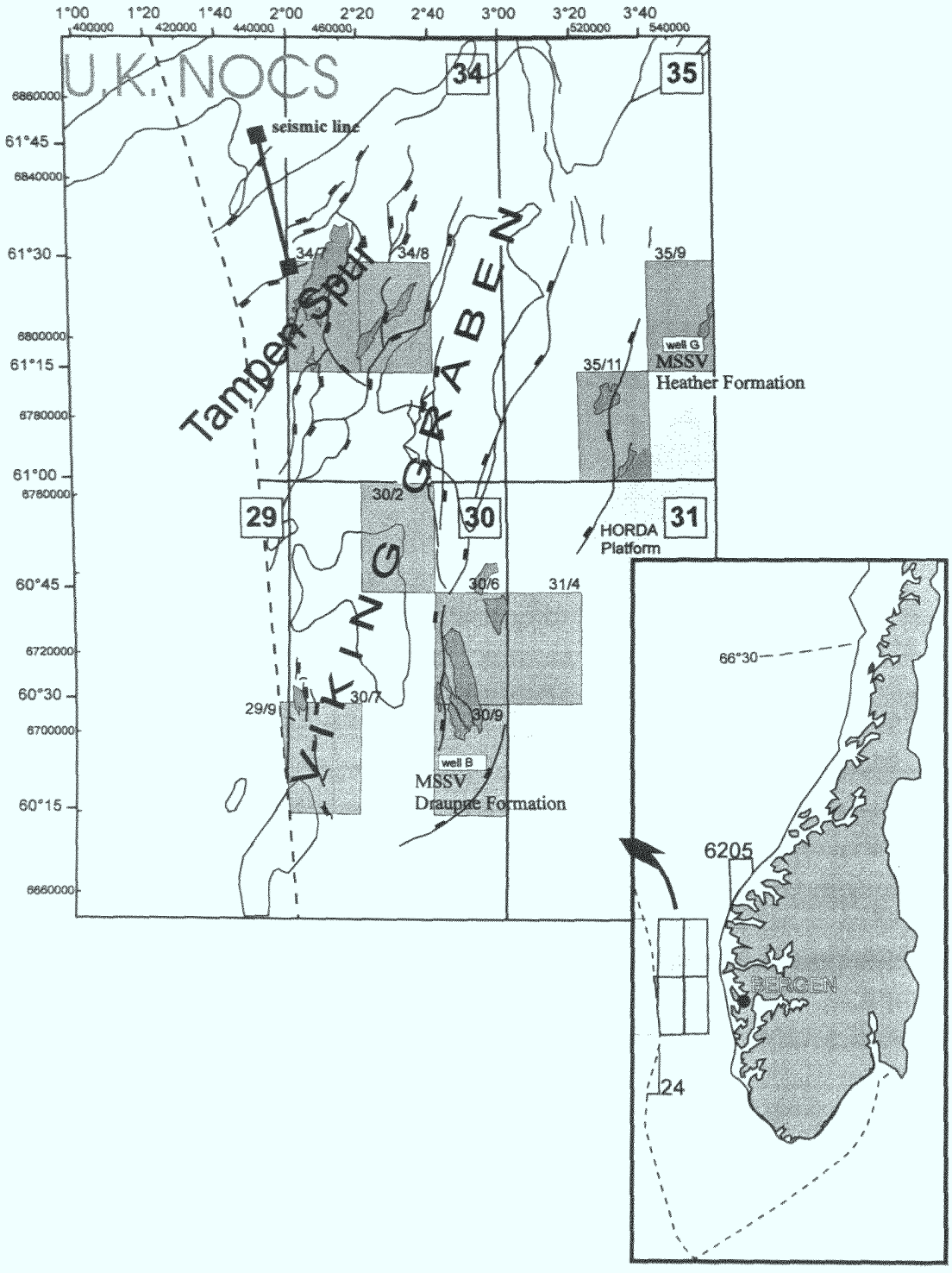


Fig. 2: Norwegian Northern North Sea quadrants. Highlighted are blocks where wells are located, major structural elements and petroleum accumulations. Locations inscribed MSSV will be referred to later. Gas kitchens (see Fig. 1) along the Graben axis are included as light grey areas. The stippled line indicates the border between the U.K. and Norwegian continental shelf.

2.2 Analytical Program

The flow chart in Fig. 3 gives an overview of the different methods which were employed and are described below. Almost only core samples were analysed except for the wells J and K where cuttings were used as well. The flow chart discriminates between three main stages, the first of which, geochemical evaluation, includes analyses which provided basic informations about kerogen quality, maturity, bulk petroleum formation properties and gas potentials. The second stage comprises heating experiments performed on two selected source rock samples from the Heather and Draupne Formation. Finally a third part shows analyses which were carried out exclusively on the Heather Formation sample and which were designed to solve problems that arose during the course of investigations. This third complex is described in chapter 3.3.

2.2.1 Geochemical Evaluations

Organic petrology

In order to characterise organic matter, polished sections of conventional core samples and kerogen concentrates were investigated (Taylor *et al.* 1998) using fluorescence microscopy. A Zeiss Universal Microscope at magnifications of 10X, 20X, 50X and 100X was employed with violet/blue light excitation.

Vitrinite reflectance

was measured in oil immersion using polarised monochromatic light (wavelength of 546nm) over a measuring area of 0.16µm in diameter. More than 50 readings for each sample were recorded, with the exception of samples which contained only low amounts of vitrinite. The indigenous populations from histograms were interpreted according to microscopic observations. Other constituents like inertinites and bituminites and migra- or pyrobitumen were measured for completeness.

Total organic carbon (TOC) determinations

were made via LECO carbon-analyser IR112 and the successor CS-225. The samples were treated with HCl prior to analyses in order to remove inorganic carbon. Analyses was performed in duplicate at 1100°C in an oxygen atmosphere. The detection of the oxides of carbon by infrared detector allowed the calculation of TOC as weight-percent of the rock sample.

Rock Eval pyrolyses

was carried out using a Rock Eval II apparatus from DELSI according to the method described by Espitalié *et al.* (1977, 1985). Sample weights were adjusted by TOC content so as to avoid detector saturation. IFP standard 55000 was used for calibration. Heating was done under He flow with the help of which products were immediately removed and detected by FID. In theory this combined thermal extraction and open system pyrolysis system produces two well-defined peaks, S1 and S2, and an additional peak S3 for CO_2. S1 represents the extractable products at $T < 300°C$ which were formed during natural maturation. S2 evolving at $T > 300$ up to 550°C at a heating rate of 25 $Kmin^{-1}$ represents the remaining hydrocarbon potential.

"Closed system" Thermovaporisation gas chromatography (tvap-gc)

Tvap-gc (Jonathan *et al.* 1975) was employed using a system consisting of a sample holder with a programmable furnace, a cryogenic trap, and a gas chromatograph (HP 5890) in order to measure the concentrations of volatile organic species. The analyses was performed on the 45 whole rock samples listed in Table 4. Each of the samples was coarsely crushed and inserted immediately in an MSSV glass capillary tube (Horsfield *et al.* 1989) of approximately 40µl volume which was sealed with a hot

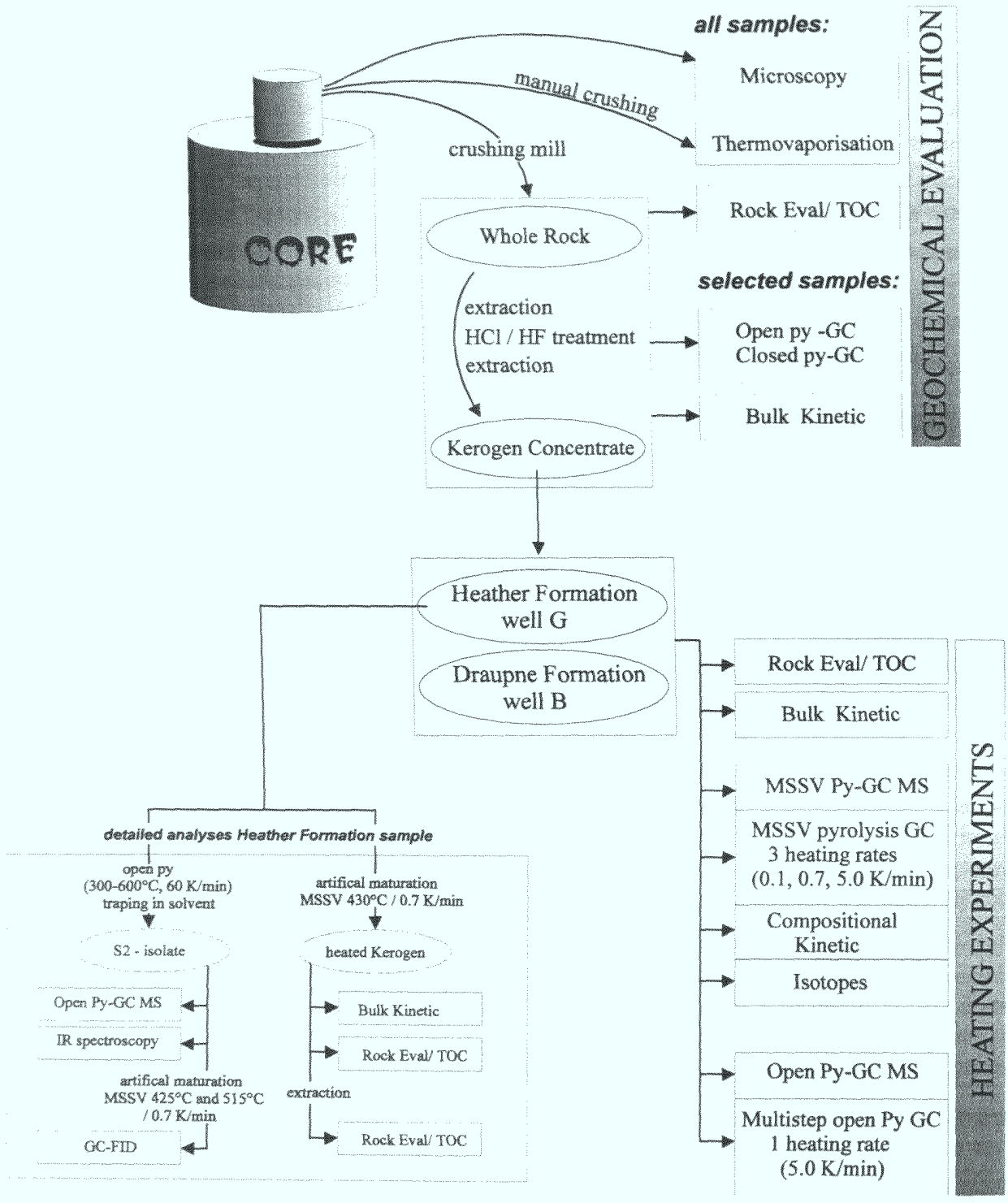


Fig. 3: Flowchart showing the analytical program performed during the study.

hydrogen flame. This method ensures that no further losses of gas species can occur after crushing. Coarse crushing is important as experience did show lower yields when crushing the samples too thoroughly. The sealed glass tube was inserted into the sample holder with programmable furnace which provided a constant temperature of 300°C. After flushing for 3min with helium the glass tube was broken manually using the piston device. The thermally releasable organic matter was focused in a liquid nitrogen-cooled trap. The liquid nitrogen supply was stopped 10 min after crushing the glass tube and a temperature program started (from 40°C to 300°C at 5.0 $Kmin^{-1}$, and 25min at 300°C

isothermal). The products were transmitted directly onto a 25m X 0.32mm column with 0.5µm film thickness (HP1). Products were detected by flame ionisation detection (FID) and quantified using an external n-butane standard. The computerised examination of obtained data was done with the VG Multichrom system.

Thermovaporisation gas chromatography-mass spectrometry (tvap-gc-ms)

For identification of single compounds tvap-gc-ms analyses were carried out using a Fisons Quadrupole MD 800 mass spectrometer. The sample treatment and the gas-chromatographic configuration and conditions were identical to those described for thermovaporisation, except that a 50 m column was used to compensate the vacuum of the ionisation chamber of the mass spectrometer and allow optimised flow. Analyses were performed in full scan mode. Full scan mass spectra were recorded over the mass range *m/z* 10 to *m/z* 450.

Headspace and occluded gas analyses

Headspace and occluded gas analyses on 33 canned wet cuttings of Heather and Draupne Formation and Viking group of well P were carried out by Geolab Nor including TOC determination for each sample. As samples stem from source rock intervals it was inferred to detect most likely in-situ generated gases. The analyses were performed according to the „Norwegian Industry Guide to Organic Geochemical Analyses".

Cluster analyses

The chemical and isotope compositions of gases were investigated by cluster analyses. This statistical method allows similarities or dissimilarities to be expressed in distances. Results are depicted in tree-diagrams in which branches represent clusters or families of similar parameter sets. The distances i.e. dissimilarities were calculated as Euclidean distances which is the standard method. Euclidean distances can be described as the diagonal distances in an n-dimensional system where n is the number of parameters employed. Finally the linkage method determines whether two samples, a sample and a cluster or two clusters will be merged in a calculation step. The complete distance method was used for linkage which employs the distance of the two most distant pairs.

Open and closed pyrolysis-gc-FID

experiments were conducted to provide a quick measure of minimum and maximum gas potentials for Heather and Draupne Formation samples of different maturities. Minimum because an open system produces primary fragments which in a closed system will be further cracked resulting in maximum gas amounts. For the closed pyrolysis-gc-FID (maximum gas potentials) extracted kerogen concentrates of nine samples, from the immature and mature Heather and Draupne Formation and Viking Group, were inserted into MSSV glass tubes (1.3 cm length, inner diameter approximately 1mm, volume of 40 µl). Pyrolysis was performed with the same external oven used for closed-system programmed-temperature MSSV pyrolysis (see below). A single heating rate of 0.7 $Kmin^{-1}$ was applied to reach a single end temperature of 520°C. The gas-chromatographic analyses was identical to those described for tvap-gc. Results are given in Table 9.

Open pyrolysis gc FID (minimum gas potentials) was carried out on 30 samples, both whole rocks and kerogen concentrates, in order to investigate compositional details of S2 which provided also

information about kerogen types on a molecular level. Glass capillary tubes with both ends open were used. Approximately 5 to 10 mg sample were inserted and fixed in the tubes with glass-wool. The temperature program started with a 300°C isotherm (5 min) to remove volatile hydrocarbons corresponding to the Rock Eval S1 peak. During pyrolysis the temperature was increased up to 600°C with a heating rate of 60 $Kmin^{-1}$ and a final holding time of 2 min. The results are given in Tables 6-8.

2.2.2 Heating Experiments

Samples used for the investigation of the thermal kerogen decomposition were treated by extraction and kerogen concentration, followed by repeated extraction in order to remove in-situ soluble organic components and mineral matrix.

Soxhlet-extraction was conducted with an azeotropic mixture of 23.4 % methanol, 29.9% acetone and 47.6% chloroform for several (3-5) days and temperatures of approximately 60°C. After extraction samples were dried for several days followed by a thermal extraction at 280°C for 5 min in order to remove the remaining solvent completely. Control measurements indicated that especially acetone seems to have a high affinity to be adsorbed by kerogen.

The kerogen concentration procedure comprised two steps and corresponds to the method described by Durand & Nicaise (1980). In a first step carbonates were removed by treatment with hot (70°C) hydrochloric acid for 2h. After washing the sample with distilled water the remaining mineral matrix was removed by treatment with hydrochloric and hydrofluoric acid (1:1) for 12h at 70°C. The obtained kerogens were concentrated by factors ranging from 4 to 18, averaging 9. Varying, but overall high amounts of pyrite remained within the concentrates, as confirmed by microscopic observations.

Pyrolysis-gas chromatography-mass spectrometry using open and closed pyrolysis was performed on Heather Formation E 41716 well G and Draupne Formation E 43254 well B samples in order to ensure correct peak identifications and also to enable detailed comparisons between hydrocarbon compositions obtained from these two principle systems. For all pyrolysis methods the analysis of pyrolysis products was performed with the same gas-chromatographic set-up and procedure as described for thermovaporisation gc-FID or gc-ms respectively.

"Bulk kinetics" open-system pyrolysis

The method is a modified regular Rock Eval analyses and was performed on 12 finely ground Heather and Draupne Formation samples, whole rock samples as well as kerogen concentrates, extracted but also unextracted aliquots. The main reason for employing the method was to screen samples to see if more detailed laboratory derived kinetic determinations were warranted.

The apparatus described by Schaefer *et al.* (1990) was made up of a two-zone furnace (Carbolite), with a Eurotherm-controller. Pyrolysis products were removed from the heating zone by a constant argon flow of 45ml/min, and detection was by FID. Temperatures from 150-700°C were applied using linear heating rates of 0.1, 0.7 and 5.0 $Kmin^{-1}$.

Closed-system programmed-temperature MSSV pyrolysis

Detailed kinetic determinations were made using this system. More than 150 aliquots, each weighing 5-8 mg, of immature extracted kerogen concentrates of the Heather Formation (well G; 2138.75m)

and Draupne Formation (well B; 2764.7m) were inserted into MSSV capillary glass tubes. Using such small sample amounts has got the advantage that the temperature of the aliquot is likely to match precisely the temperature detected by the thermocouple. For very high temperatures quartz tubes had to be used instead of glass tubes. The remaining volume in the tubes was reduced with glass beads so that the system had a high confinement. The tubes were sealed by using a hydrogen-oxygen flame. Pyrolysis were performed off-line, using an external oven consisting of a metal core surrounded by several heating coils, at heating rates of 0.1, 0.7 and 5.0 $Kmin^{-1}$. The metal core served as a sample holder and provided a very homogeneous temperature field. Temperature control was guaranteed by a thermocouple, which was introduced directly into one sample holder. The temperature program started at 200°C and ranged up to different temperatures depending on the chosen heating rate. Every 5, 10 or 20 degrees a sample was removed from the oven and analysed by gas chromatography-FID. The analytical system is described by (Horsfield *et al.* 1989). Total product (integration to column blank) and resolved product (skim baseline) amounts and more than 77 different compounds were identified and quantified, listed in Tables 14-19. For the case of the Draupne Formation sample a series of 22 control measurements were performed at all three heating rates. This was done because at higher temperature scattering of the total amounts C_{1+} occurred and preliminary results for the calculation of kinetic parameters resulted in unexpectedly high values. However, the validity of measurements was verified and high temperature scattering must be assigned to real processes happening in the reaction vessels.

Isotopic composition of MSSV pyrolysates

Stable carbon isotope compositions of C_{1-4} gases from MSSV pyrolysates of the Heather and Draupne Formation samples were investigated.

Twelve MSSV pyrolysis samples (6 for each source rock) were pyrolysed to different temperatures at a heating rate of 0.7 $Kmin^{-1}$. Products were analysed by continuous flow mass spectrometry at the Australian Geological Survey Organisation, Canberra. The analyses were performed with the following procedure. After cracking the MSSV tube in the injector at 60°C, the C_{1+} volatile pyrolysate was focussed at the front of a 25m QPLOT megabore fused silica capillary column by immersing a 10 cm length of column in liquid nitrogen. After 10 minutes, the trap was removed and the C_1-C_5 pyrolysis products separated under gc temperature programming conditions from 30°C to 220°C at 10 $Kmin^{-1}$. Carbon monoxide, methane and C_2-C_5 hydrocarbons were quantitatively converted to CO_2 after passing through the Finnigan combustion interface I at 1000°C (the initial generated CO_2 remained intact). The CO_2 was introduced via an open split into a Finnigan 252 mass spectrometer and isotopically analysed using the *m/z* 44 response and *m/z* 45/44 ratio trace. Up to three repeated measurements were performed. Since the dynamic range of the gc-IR MS technique is limited, ^{13}C could not be determined for all peaks in a single run. A full dataset was therefore obtained by changing the split flow or in extreme cases decreasing the electron emission. For the latter case corrections were calculated. Finally data for n-butane turned out to be disturbed slightly by an unidentified shoulder limiting the accuracy of measurements for butane and C_4 total.

Multistep open pyrolysis gc

During closed-system pyrolysis primary and secondary gas generation are difficult to discriminate. In order to gain a better understanding about the evolution of primary gas an multistep open pyrolysis gc

approach was employed.

20 aliquots of the Heather and Draupne Formation samples employed for MSSV pyrolysis were pyrolysed at a single heating rate of 5.0 $Kmin^{-1}$. The temperature program started from 300°C and ended with temperatures between 350 and 570°C. The oven used here is different to the oven used for MSSV pyrolysis in that it is directly on-line with the gas chromatographic system. Therefore the comparability of the results depends on the comparability of the temperature fields of both ovens. From experiments with the Posidonia Shale and from determinations of the temperature field within the oven it was implied that for a heating rate of 5.0 $Kmin^{-1}$ the differences in the temperature fields would be too small to produce any significant errors in the hydrocarbon formation curves. Each run consisted of two parts. The first part was necessary for the detection of methane which could not be focused in the cryogenic trap. Thus FID signals had to be recorded for the whole pyrolysis program (up to 54 min). Reaching the end temperature for each step a temperature-holding time of 2 min followed in order to remove all methane from the system. The second part was a regular gc-analysis of compounds focussed in the cryogenic trap, while the pyrolysis-oven temperature was lowered to 250°C to make sure that no additional generation of products could take place. For results see Tables 20,21.

2.2.3 Kinetic Modelling

Product yields from MSSV closed-system pyrolysis but also reaction rates from Rock Eval type pyrolysis provided the input for the calculation of kinetic parameters, termed "bulk kinetic parameters" for the open system and "compositional kinetic parameters" for the MSSV closed system. The mathematical routine published by Schaefer *et al.* (1990) was used for these determinations. This approach is based on non-isothermal kinetics (Juentgen 1964, Hanbaba 1967 and Juentgen & Van Heek 1970). An advantage of MSSV pyrolysis data in this context is the possibility to obtain specific frequency factors and activation energies for individual compounds, compound groups or hydrocarbon boiling ranges. Specific frequency factors can be considered as mathematical optimisation parameters (Schaefer *et al.* 1990).

The procedure which was used especially for handling of the MSSV raw data sets can be described as follows. Spline curves were approximated to the measured hydrocarbon formation curves for the three linear heating rates. Yields measured with the MSSV closed pyrolysis are cumulative yields. In a second step these spline functions were numerically differentiated in order to produce formation rate versus temperature curves from which kinetic parameters were calculated according to Schenk & Horsfield (1993). The heating rates of 0.1, 0.7 and 5.0 $Kmin^{-1}$ were reported to be sufficiently different so that accuracy for the determination of a start-frequency factor is ensured (Van Heek & Juentgen 1968). Using the start frequency value, formation rate curves based on activation energy distributions allowing up to 40 parallel reactions (spacings of 1 kcal are commonly used) with corresponding partial hydrocarbon potentials were calculated for 200 temperatures per heating rate. Linear and non-linear least square iteration procedures allowed to find an optimised parameter set of activation energy distributions and frequency factor which results in a best-fit for calculated curves and measured curves. This method is very sensitive due to the number of calculation steps. For this reason most calculations were performed several times by carefully checking the cumulative plateaus, different spline approximations and the resulting first derivations.

Basin modelling

The 2 dimensional basin simulation program *Petromod*®, versions *3.1* and *3.5* from IES (Integrated Exploration Systems) was used for testing kinetic parameter sets under non-linear heating conditions. The software allows the calculation of the temperature development within a given source rock layer as a function of time. Apart from the temperature history, the generation kinetics is governing the timing of gas formation.

In a basin modelling program all processes which are relevant for the reconstruction of the history of a given sedimentary basin are integrated to give a dynamic mathematical model. These processes include the burial of layers, the development of the temperature field as well as pressure, maturation in terms of changes in vitrinite reflectance or transformation of the kerogen into oil and gas and finally migration of hydrocarbons within the model. The reconstruction of the burial history is based on the geometry of the geological model, the assigned ages of layers and their lithologies. Physical compaction of sediments during burial is part of this calculation. An interpreted 2D seimic section was used to construct the geological model. Compaction as well as the temperature development are controlled by the petrophysical properties which describe different lithologies. For the temperature development the heatflow is even more important. It is calculated as a lower boundary condition at the base of the model. Vitrinite reflectance data and temperature data from wells allow the calibration of this parameter.

For basin simulations usually no probabilities of results can be derived because of the complexity of dynamic models, instead sensitivity analyses are performed like done here for the case of reaction kinetics (Yükler 1979, Wygrala 1989, Poelchau *et al.* 1997).

3 RESULTS AND DISCUSSION

3.1 Reference Systems

A geochemical framework must be constructed which is able to account for the differences in hydrocarbon gas generation properties. For this purpose the *geological source rock unit* and the *generalised type of organic matter* are most frequently used as reference systems. Actually the chemical structure of the initial kerogen dictates the range of possible gas occurrence and makes a determination of kerogen structural types on a molecular level necessary. *Maturity* can be considered as an expression of the changes of the initial kerogen structure with temperature and time and has an additional impact on the gas generation.

The investigations performed to establish such a reference system include microscopic methods, Rock-Eval analyses combined with total organic carbon (TOC) determinations and pyrolysis-gaschromatography. Organic petrology, the Rock Eval parameter Hydrogen Index (HI) and compositional information derived from pyrolysis gas chromatography provide information about the quality of organic matter. Optical reflectance measurements of organic detritus and the Rock-Eval parameter T_{max} ensure maturity evaluation.

3.1.1 Kerogen Types

Organic Petrology

The advantage of organic petrological analysis is that all variations of the organic matter can be observed, maturity induced as well as initial properties. Unfortunately it is hard to quantify the observations. For the characterisation, immature to early mature samples were investigated. Some observations on overmature samples from well P were included because they revealed important features described below.

It has to be noted that the particulate organic matter that can be identified unambiguously contributes only minor amounts to the bulk of organic matter. Cooper *et al.* (1995) reported the range of 10-90 % of the TOC for North Sea source rocks to be represented by amorphous organic matter. This is confirmed by investigations of Knudsen *et al.* (1988) who reported similar proportions for two wells of the Oseberg area. From kerogen concentrate microscopy sections (Draupne Formation (E 41691), Heather Formation (E 41711) and Viking Group (E 41699)) it became evident that a major part of the organic matter consists of finely disseminated fluorescing and non-fluorescing amorphous contributions.

Observations on particulate macerals

In spite of its low contribution the particulate organic matter can give valuable information on source areas and kerogen types. An abundant characteristic maceral that occurs in almost all investigated samples of both source rock units, was classified as bituminite, a brown fluorescing amorphous liptinite component often associated with pyrite (Plate 1 and 2). Bituminite was described by Teichmüller (1974) and Gutjahr (1983). Espitalié *et al.* (1991) observed important amounts of bituminite in Heather Formation source rocks. Teichmüller (1985) stated that this maceral often surrounds particles of yellow fluorescing liptodetrinite (Plate 1, pic. 1) and occurs as lenses and

irregular streaks, thereby matching the features of components described here. The morphological characteristics and the fluorescence colour excluded the possibility that this particle could be vitrinite 2 (Buiskool Toxopeus 1983). Alternatively the constituent was considered to be a sort of solid bitumen (Pickel,W. pers. comm.). This could theoretically be possible for well I which is in the beginning of the oil window ($R_o \cong 0.6\%$) where expulsion may not have started yet. Clarification was attempted by performing the following experiment. After microscopic observation, two polished samples were extracted with a of organic solvent mixture (chloroform, methanol, acetone) for three days at temperatures of 60-75°C in a Soxhlet apparatus. A second microscopic investigation of the sections revealed that none of the compounds had vanished, only the maceral surfaces appeared to be dissolved to different degrees. It may be concluded that the consituents do not fulfill the requirements to be termed bitumen and will be classified as bituminite.

Contents of Draupne type

Yellow fluorescing liptinites probably parts of algal bodies are among the most abundant macerals. Sometimes unalterated Tasmanites algae (Plate 2, pic. 2 and 3) with a strong yellow fluorescence can be found. The bituminite, mentioned above is common. Finely disseminated fluorescing organic matter including liptodetrinite (Plate 2, pic. 3) is predominantly present in clay-rich layers. Khorasani & Michelsen (1992) suggested that this maceral type, which they observed as a consituent of Draupne Formation, is likely to be degraded alginite matter. Evidence was provided by SEM observations. The authors proposed the incorporation of oxygen into the kerogen structure by primary oxidation as degradation mechanism and stated that the oxygen would be unreactive within aromatic systems rather than occurring as carbonyl or carboxyl functional groups. Vitrinite contributes overall minor amounts and is absent in some cases as for instance in the well A. Instead of vitrinite different types of bituminite were found. A sample of well D reveals a prominent bituminite content (plate 1, pic.3).

Contents of Heather type

Well H samples contain similar constituents as described for Draupne Formation though the amount of finely disseminated fluorescing organic matter seems decreased relative to the amount of vitrinite and inertinite. The wells F and G contain high amounts of vitrinite and inertinite and sometimes bituminite. Here the liptinites are different to those of Draupne. Thin laminar structures which surround grain boundaries or fragments of these are common (Plate 3, pic. 1). Though they are not subparallel to sedimentary bedding planes they show similarity to lamalginite as described by McKirdy & Kantsler (1980). Other liptinitic components, which can be found quite often, are fragments of a cellular structure (Plate 3, pic. 2 and 3). Sporinite was detected (Plate 4, pic. 1) but its abundance is difficult to assess because fragments resemble other liptinite macerals. The same is true for cutinites (Plate 4, pic. 2) which were identified in rare cases by their typical "toothed" structures.

Contents of overmature samples

In samples of well P no fluorescing particles could be detected. Vitrinite and inertinite are present in fair amounts but the dominant contributor was classified as pyro- or migra- bitumen (Jacob 1989). It occurs as a three-dimensional web or as finely disseminated fillings (Plate 4, pic. 3) and must be considered as a quantitatively significant material from which gas might be generated at higher levels of maturity.

Concluding remarks, organic petrology

Both source rock formations contain finely disseminated amorphous fluorescent and non-fluorescent organic matter, the proportions of which are difficult to determine. In any instance they seem to be of major importance. The detrital fluorescent matter of Heather and Draupne revealed similar compound spectra in block 34/8 but crucial differences in block 35/9. The overall content of vitrinite and inertinite is higher for Heather Formation samples. Nevertheless, Heather Formation samples, which are relatively rich in TOC (i.e. exceeding average of appr. 3%), can show a remarkable similarity to Draupne Formation with an abundance of liptinitic phytoclasts. This was observed for Heather Formation samples of the western Graben flank (wells H and I) where the influence of near landmasses during Jurassic seems to be smaller as observed for samples from the eastern flank (wells F and G).

Bulk Kerogen Classification

The classification of kerogens by means of bulk properties as for instance the atomic ratios H/C and O/C (van Krevelen *et al.* 1951) or their Rock Eval counterparts Hydrogen Index (HI) and Oxygen Index (OI) (Espitalié *et al.* 1977, 1985) is a method which provides information about kerogen type, maturity and hydrocarbon generation potential. The HI is defined as the hydrocarbon generation potential S2 normalised to TOC. Screening data are given in Table 3.

A diagram depicting HI versus OI (Fig. 4) using additional literature data from Thomas *et al.* (1985) implies a hydrogen-rich type I-II kerogen for the Draupne Formation. At least two kerogen types have to be expected for the Heather Formation. One data envelope overlaps with the Draupne Formation field

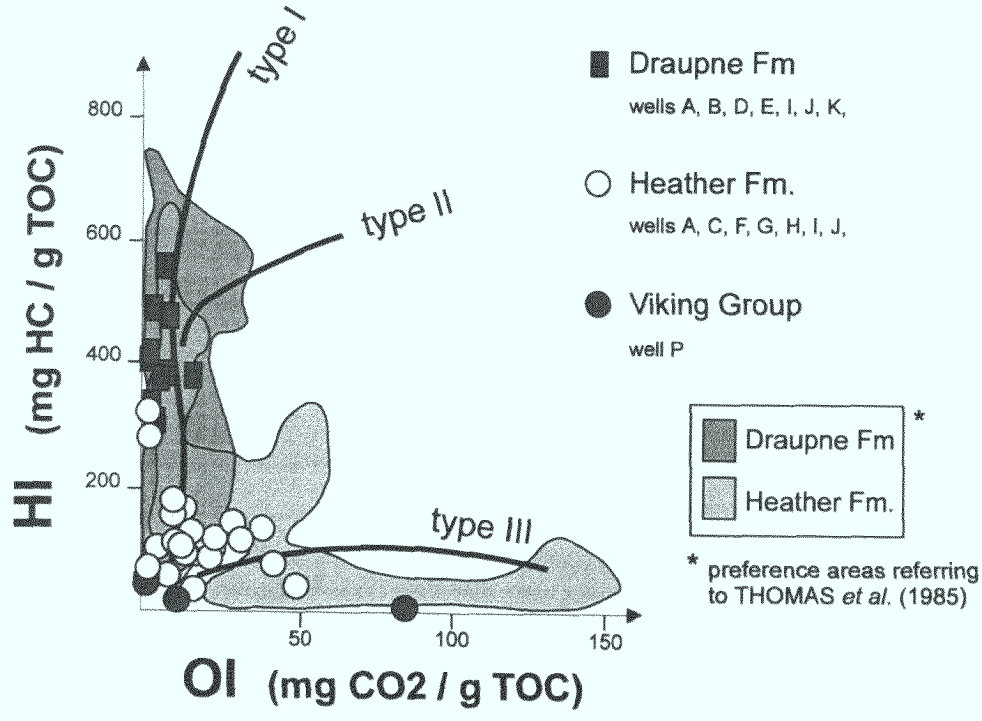


Fig. 4: Kerogen type discrimination on the basis of the Rock Eval parameters Hydrogen Index (HI) and Oxygen Index (OI).

Table 3: Sample-numbers, wells and depth. Rock Eval screening data, TOC and vitrinite reflectance.

sample key					*screening data*						
E.nr.	Well	depth (m)	fm	sample	TOC (%)	Ro (%)	S1 (mg HC/g samp)	S2	Tmax (°C)	OI	HI
41725	K	4027	dr	cutting	2.93		0.22	0.46	420	62	16
41739		4345	hea	cutting	2.58	1.22 ?	0.45	1.16	441	50	45
43256	C	3265.1	hea	core	4.45	0.43	3.50	8.26	430	9	186
43257		3266.6	hea	core	3.51		2.05	4.95	429	9	141
41746	J	3818	dr	cutting	4.07		2.03	5.16	434	61	127
41748		3823	dr	cutting	2.96		1.30	1.78	428	52	60
43252		3890.3	hea	core	6.74	0.94	4.35	6.30	447	6	93
43253		3896.2	hea	core	5.47	0.86	5.14	5.98	447	8	109
43254	B	2764.7	dr	core	11.9	0.37	2.77	59.76	428	4	502
43254 MK EC		2764.7	dr		44.8	0.37	3.15	248.50	423	7	555
43255		2767.7	dr	core	8.39	0.36	2.36	30.86	422	6	368
43249	A	2110.9	dr	core	8.28	no vit.	0.99	31.79	418	8	384
43250		2118.9	dr	core	7.03	no vit.	1.17	29.81	421	10	421
43251		2141.8	hea	core	3.07		0.15	1.19	424	16	39
42180	D	TVD 2644.15	dr	core	7.25	0.45	2.07	34.27	418	8	473
42382	E	2905	dr	swc	5.1	0.44	1.90	15.80	427	4	310
42383		2911	dr	swc	6.5	0.5	0.20	24.80	427	16	381
41690	I	3573.75	dr	core	8.12	0.61	6.36	33.49	436	2	412
41691		3575.8	dr	core	9	0.53	6.37	36.49	434	1	406
41691 Mk		3575.8	dr	kerogen	37.5	0.53					
41692		3578.6	dr	core	9.8	0.64	7.40	32.52	433	3	329
41692MK		3578.6	dr	kerogen	41.6	0.64	19.91	87.93	429	5	211
41693		3582.55	hea	core	4.9	0.59	5.60	13.62	432	1	276
41694		3583.55	hea	core	7.3	0.56	5.86	23.28	431	1	320
42384	L	4478	dr	swc	1	0.98	0.10	0.50	468	0	54
41695	H	2902.8	hea/dr	core	4.5	0.49	0.82	13.46	425	4	300
41695 MK		2902.8	hea/dr	kerogen	38.3	0.49	16.15	141.17	431	9	369
41696		2903.45	hea	core	3.7	0.51	0.61	2.10	426	5	57
41697		2904.8	hea	core	2.1	0.5	0.21	2.15	425	8	103
41698		2907.3	hea	core	2.3	0.53	0.30	3.64	430	10	159
41707	F	2041.6	fens	core	1.6	0.42	0.59	1.6	423	17	102
41708		2043.65	U.hea	core	1.8	0.4	0.62	2.1	426	32	117
41709		2045.45	U.hea	core	2.3	0.43	0.77	2.65	427	32	118
41710		2058.95	U.hea	core	1.8	0.39	0.61	2.06	424	15	113
41711		2064.8	U.hea	core	3	0.45	0.82	3.43	424	12	115
41711 MK		2064.8	U.hea	kerogen	23.9	0.45	5.49	32.71	430	15	137
41712		2094.3	U.hea	core	1.1	0.42	0.36	0.83	423	42	78
41713		2094.9	U.hea	core	1.4	0.45	0.54	1.27	426	21	94
42502		2140.65	L.hea	core	0.97		0.46	1.28	430	568	132
42503		2142.8	L.hea	core	1.52		0.63	2.05	427	13	135
42504		2143	L.hea	core	0.75		0.24	0.89	422	13	119
42505		2146	L.hea	core	1.2	0.42	0.80	1.65	431	38	138
42506		2150.4	L.hea	core	1.83		0.89	2.44	428	25	133
41714	G	2130.95	U.hea	core	2.6	0.48	0.97	1.66	420	2	64
41715		2134.95	U.hea	core	5.5	0.43	3.56	8.25	422	28	151
41715 MK		2134.95	U.hea	kerogen	52.2	0.43	18.50	58.63	427	13	112
41716		2138.75	U.hea	core	5.9	0.45	2.90	9.59	420	10	164
41716 MK		2138.75	U.hea	kerogen	47.6	0.45	17.29	64.03	428	10	135
41717 MK EC		2138.75	U.hea	kerogen	33.1	0.45	1.50	48.28	421	7	146
41718		2140.97	U.hea	core	3.1	0.47	1.28	3.08	426	12	99
41719		2522.9	L.hea	core	2.2	0.47	0.28	2.52	426	24	116
41720		2535.7	L.hea	core	1.9	0.52	0.24	1.76	429	12	91
41721		2546.9	L.hea	core	2.7	0.5	0.30	2.47	429	9	93
41721 MK		2546.9	L.hea	kerogen	30.8	0.5	5.99	32.13	430	11	104
41722		2549.9	L.hea	core	1.2	0.5	0.16	1.54	430	15	123
41723		2553.95	L.hea	core	1.9	0.5	0.19	2.76	429	13	142
41699	P	4449.13	vik	core	6.38	1.01	0.96	2.43	465	0	38
41699 MK		4449.13	vik	kerogen	37.5	1.01					
41700		4449.33	vik	core	5.4	1.09	0.79	1.96	469	1	36
41701		4451.4	vik	core	4.5	1.11	0.79	1.41	468	1	31
41701 MK		4451.4	vik	kerogen	45.2	1.11	5.23	6.32	446	4	14
41702		4971.45	vik	core	0.78	1.38	0.03	0.12	510	12	15
41703		4973.45	vik	core	3.2	1.33	0.06	0.35	473	0	11
41703 MK		4973.45	vik	kerogen	32.1	1.33	1.17	1.56	443	4	5
41704		5021.5	vik	core	0.13	Sst	0.00	0.00		77	0
41705		5253.85	vik	core	5.4	1.5	0.03	0.60	483	0	11
41706		5262.6	vik	core	1.9	1.45	0.05	0.13	487	0	7
41706 MK		5262.6	vik	kerogen	36.8	1.45	1.93	1.03	420	5	3

fm= Formation, hea= Heather Formation U= upper L= lower, dr= Draupne Formation, vik= Viking Group, fens= Fensfjord Formation, core= conventional core, swc= sidewall core, MK= kerogen concentrate, EC= extracted, TWD= total vertical depth.

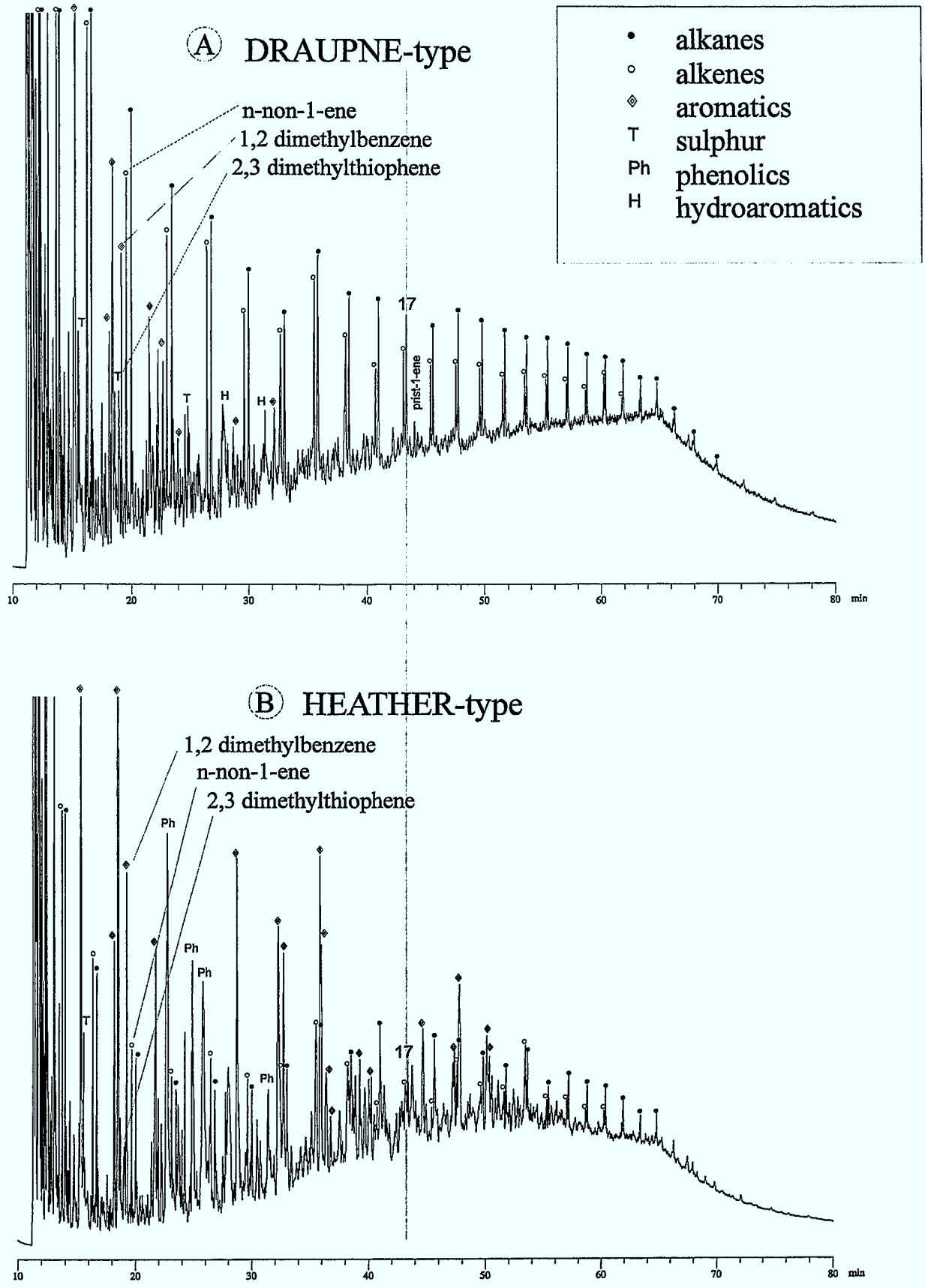
and should therefore represent a kerogen type II. Preferentially block 34/8 data follow this trend. A second branch of the data envelope can be interpreted as a mixture of kerogen type II and III thus confirming observations from organic petrology. The conclusions of a mixed marine-terrigeneous type of kerogen typical for the Heather Formation was also reported by Lafargue & Behar (1989). A third branch reported by Thomas *et al.* (1985), probably kerogen type III/IV, is of minor importance for the sample set used in this study.

However there are a number of restrictions to the method. For example, in spite of the low maturity that most samples exhibit (Table 3), it has to be noticed that their representing points in the HI / OI diagram are already quite far proceeded on the so called maturity paths for kerogens I, II and III (Tissot & Welte 1984, p.511). Moreover Langford & Blanc-Valleron (1990) stated that HI as ratio of S2/TOC may involve scattering of data in the HI / OI diagram for kerogens of the same type and maturity. This is valid for the here investigated Heather Formation samples which revealed a poor correlation between S2 and TOC (first progress report) and will become again of importance when gas potentials are considered later in this study. Also the classification takes no account of the real variety of different kerogen types. A classification scheme incorporating petrologic observations proposed by Cooper *et al.* (1995) goes some way towards a more refined approach. Their results indicated that Draupne organic matter consists of contributions from kerogens Ib (microbial), IIa (alginite) and IIb (microbial) with minor contributions of different subtypes of the general types III and IV, the abundances of these depending on the depositional environment. However, molecular characterisation is required to provide a quantitative basis for elucidating petroleum generation potential (Horsfield 1984, 1989, Larter & Senftle 1985).

Detailed Kerogen Composition

In a review article Horsfield (1997) indicated that the pyrolysis-gc technique provides information about the kerogen structure itself in that the overall composition of the pyrolysate mirrors that of the kerogen. Comparison of pyrolysate aromaticities with results from ^{13}C NMR spectroscopy backed up these findings and were also reported to be valid by other authors. Lafargue & Behar (1989) for instance described a Draupne Formation sample to contain normal marine type II kerogen and a Heather Formation sample to contain a mixture of marine type II and terrigeneous type III organic matter based on the interpretation of pyrolysis gas chromatograms. Tegelaar & Noble (1993) outlined that a classification using pyrolysis-gc also correlates well to hydrocarbon onset, peak and end of generation.

Three pyrograms, one for Draupne and two for Heather Formation (Fig. 5) typify the different organic matter qualities. Draupne Formation is characterised by the abundance of saturated and mono-unsaturated aliphatic hydrocarbons. The most prominent components occur in the C_{1-7} range and are methane, ethane, propane and butane. A large variety of mono- and di-aromatic components and their respective sulphur-containing counterparts are present. In contrast the Heather Formation pyrogram is mainly made up of a complex mixture of aromatic components with major contributions from phenolic components. Aliphatics are of subordinate importance. The pyrogram of a Lower Heather Formation sample (Fig. 5, p.22) seems to represent a mixture of both types in that phenolic and aromatic components are present, which is a typical Heather Formation feature, but hydroaromatic components such as indane and methylindane are present as well. The aliphatic fraction is


A DRAUPNE-type
n-non-1-ene
1,2 dimethylbenzene
2,3 dimethylthiophene
• alkanes
○ alkenes
◈ aromatics
T sulphur
Ph phenolics
H hydroaromatics
17
pris-1-ene
10
20
30
40
50
60
70
80
min
B HEATHER-type
1,2 dimethylbenzene
n-non-1-ene
2,3 dimethylthiophene
Ph
T
17
10
20
30
40
50
60
70
80
min

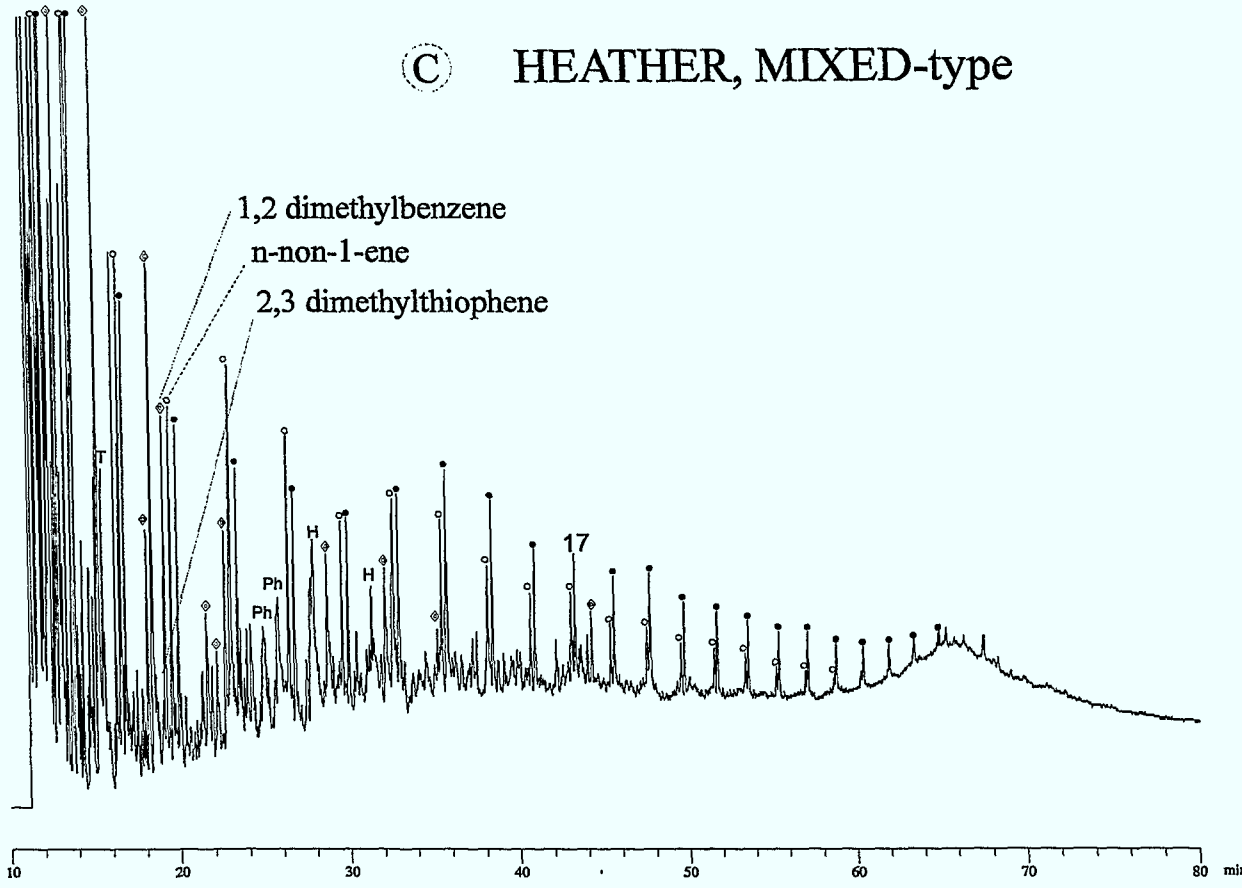


Fig. 5: Open pyrolysis gas-chromatography FID (300-600°C, at 60 $Kmin^{-1}$). A: Draupne Formation well B (2764.7m), B: Upper Heather Formation well G (2134.95m) and C: Lower Heather Formation well G (2546.9m). The three highlighted peaks are used for kerogen characterisation (page 24) in a ternary diagram according to Eglinton *et al.* (1990).

predominant and alkylated naphthalenes and phenanthrenes are of minor importance, these being typical features for the Draupne Formation. For identified components and quantitative data see Table 7. Hydroaromatics were not quantified because they were encountered later by gc-ms.

An approach for kerogen classification given by Horsfield (1989) which employs the aliphatic fraction of pyrolysates was applied (Fig. 6). The distribution of the data points in the diagram infers a somewhat similar type of kerogen for Draupne and Heather Formations, though with strongly varying aliphatic proportions, probably related to varying marine contributions, in the case of the Heather Formation. The center of gravity for data points of this source rock is only slightly shifted to the gas/condensate corner indicating a higher relative gas-proneness compared to Draupne Formation. The distribution of data points in the diagram is consistent with oil compositions reported from the Viking Graben. Leith *et al.* (1993) characterised the Snorre field oil as paraffinic-naphthenic with an n-alkane profile biased towards low molecular weight compounds. Draupne Formation pyrolysate data points instead are shifted slightly into the field of paraffinic oils if compared to petroleum compositions. The observable differences are however small. Horsfield (1989) pointed out that the effect of maturity on samples with very similar compositional patterns in alkyl-chainlength can be markedly different. Some kerogens preserve their pattern up to high degrees of maturity whereas others release their alkyl-moieties rather fast. These differences are consistent with kerogen degradation models comprising a labile and a refractory kerogen proportion. The here employed

samples from Heather and Draupne Formations do not show significant changes in compositions for the range of 0.4-0.9% (R_o) and 0.37-1.0% (R_o) respectively. Yet, the cluster of Viking group samples of well P occurring in the gas field is likely to represent a maturity trend as these samples have corresponding vitrinite reflectance values of 1.0 to 1.5%, although a different type of kerogen cannot be ruled out.

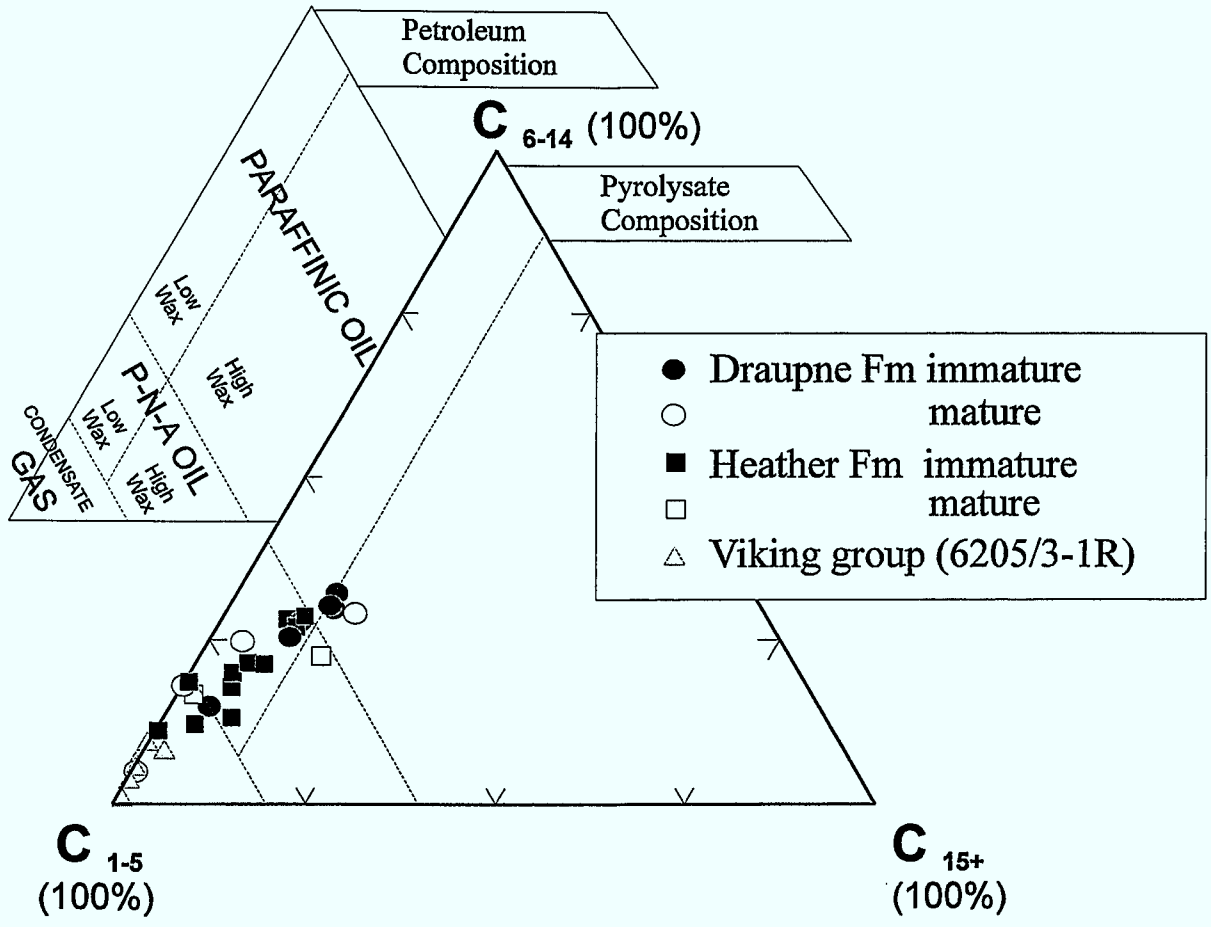


Fig. 6: Kerogen typing on the basis of alkyl-moiety distributions derived from open system pyrolysis gc (300-600°C, at 60 $Kmin^{-1}$) modified from Horsfield (1989). For data see Table 8 in the Appendix.

Concerning kerogen types it may be concluded from the diagram that mainly the marine proportion of both kerogens is considered and seems to have similar characteristics for both source rock units with Heather Formation organic matter being more gas-prone. It was reported by Boucher *et al.* (1990) that the abundant occurrence of alkylgroups with less than 20 carbon atoms is a typical feature for algal derived matter. Furthermore the authors found for a Kimmeridge Clay *Dorset type* sample that alkyl-moieties in the range of C_1-C_{10} with a maximum at C_6 predominantly contribute to crosslinking structures in the investigated kerogen. These alkyls occurred as dicarboxylic-acids upon RuO_4 treatment of the kerogen, where the carboxyl groups mark connecting points. Even if no evidence can be drawn from the results of open pyrolysis concerning the role of cross-linking alkyls, it might be possible that this structural type applies to the here investigated kerogens as well. It will be later discussed that such a structural type is likely to have an impact on gas generation.

The presence of sulphur-containing or phenolic groups has a strong impact on hydrocarbon generation profile characteristics (Tegelaar & Noble 1993). Sulphur, if part of the kerogen structure is thought to decrease the thermal stability of the macromolecular matter (Orr 1986). Consequently petroleum generation would take place at lower maturities. It is not reported what the impact for gas generation might be. The degree of primary gas generation might be enhanced as well, but this is rather unlikely as sulphur-rich oils were reported to have low yields in the gasoline range (Baskin & Peters 1992).

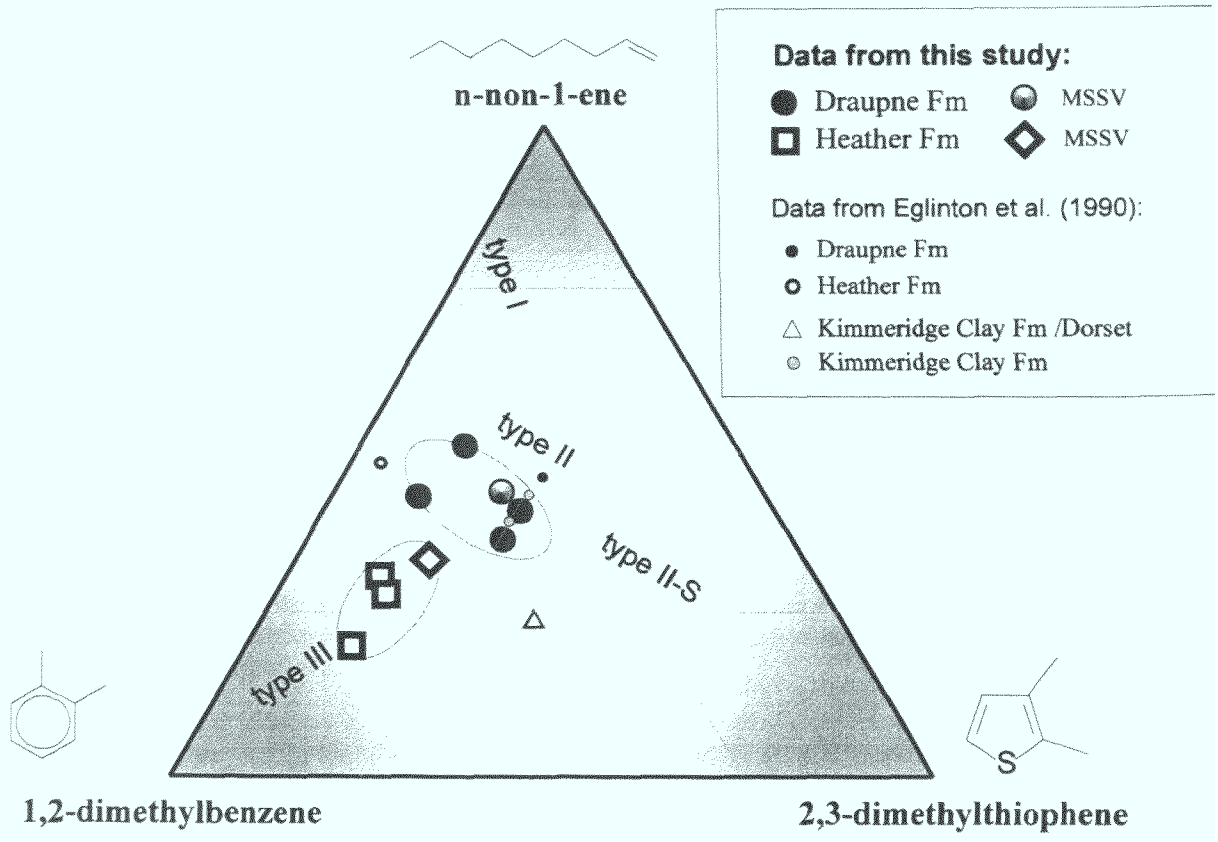


Fig. 7: Ternary diagram modified from Eglinton *et al.* (1990), scales are from 0 - 100 percent. Kerogen typing using aromatic, sulphur-containing and alkyl- compound groups. Two samples, termed MSSV are also highlighted, but are discussed later in the course of this study (in "Heating Experiments").

Eglinton *et al.* (1990) outlined the difficulties in determining the organic sulphur content and offered an easy applicable method using py-gc data. The diagram (Fig. 7) employs the open system pyrolysate components n-non-1-ene, 1,2-dimethylbenzene and 2,3-dimethylthiophene. The authors report the ratio of these components to correlate well with atomic S/C ratios. Two distinctive groupings can be observed which clearly distinguish between Heather Formation, which is shifted in the type III terrestrial-derived kerogen corner, and Draupne Formation which is near the position of marine type II kerogen, as proposed by Eglinton *et al.* (1990). For both formations the sulphur content varies, but certainly stronger for the Draupne Formation. The 2,3-dimethylthiophene contribution ranges from 10-25 % which translates to S_{org}/ C atomic ratios ranging from 0.005 to 0.02 according to the correlation proposed by Eglinton *et al.* (1990). For comparison, the Dorset type sample in Fig. 7 has a value of 0.047 and Monterey type II-S kerogens were reported to have values ranging from 0.054 to

0.102. With regard to the products of natural maturation, namely oils from the Draupne Formation, the sulphur contents are reported to be small. For instance Leith *et al.* (1993) reported 0.5 % sulphur for a Snorre oil. This is paradoxical in view of the high organic sulphur contents of the organic matter in the source rocks.



Concluding remarks, kerogen composition

Draupne Formation contains predominantelly marine kerogen with relatively increased sulphur contents whereas Heather Formation can contain higher amounts of oxygen functional groups. Both formations reveal similar alkyl-chainlength distributions thus corroborating similar kerogen types for the marine proportions of the kerogens. Especially towards the west where the terrigeneous influence for Heather Formation decreases the overall kerogen compositions become similar for Heather and Draupne. For these reasons it was decided that detailed work on gas generation should consider typical end-member compositions for Heather and Draupne Formations (cf. Fig. 5). Hence, the chosen Draupne Formation was a marine kerogen with a strong aliphatic hydrocarbon signature whereas the chosen Heather Formation had a high proportion of aromatic hydrocarbons and phenols due to increased terrigenous organic matter content and had a higher relative gas-proneness as compared to Draupne.

3.1.2 Maturity

Vitrinite Reflectance

The chemical structure and the related physical properties of kerogen undergo changes during maturation and hydrocarbon formation (van Krevelen 1961, Durand 1980) providing the means for the assessment of source rock maturity. The reflectance of light on polished maceral surfaces especially vitrinites is the most frequently used method because vitrinites are thought to be ubiquitous in sedimentary rocks. The use of other macerals than vitrinite, here for the case of pyro- or migra-bitumen, can give additional information. The vitrinite reflectance values determined for this study are reported in Table 3. All measurements were ensured to be in good agreement with measurements provided in a Norsk Hydro database (Fig. 8 right). Care was taken to check for other macerals that might be mistaken for vitrinite or for alteration of reflectance due to oxidation by pore waters and other processes (Tissot *et al.* 1987, Price & Barker 1985, Pollack & Cercone 1994, Radke *et al.* 1997, among others). In this context suppression due to bitumen staining was excluded by Radke *et al.* (1997).

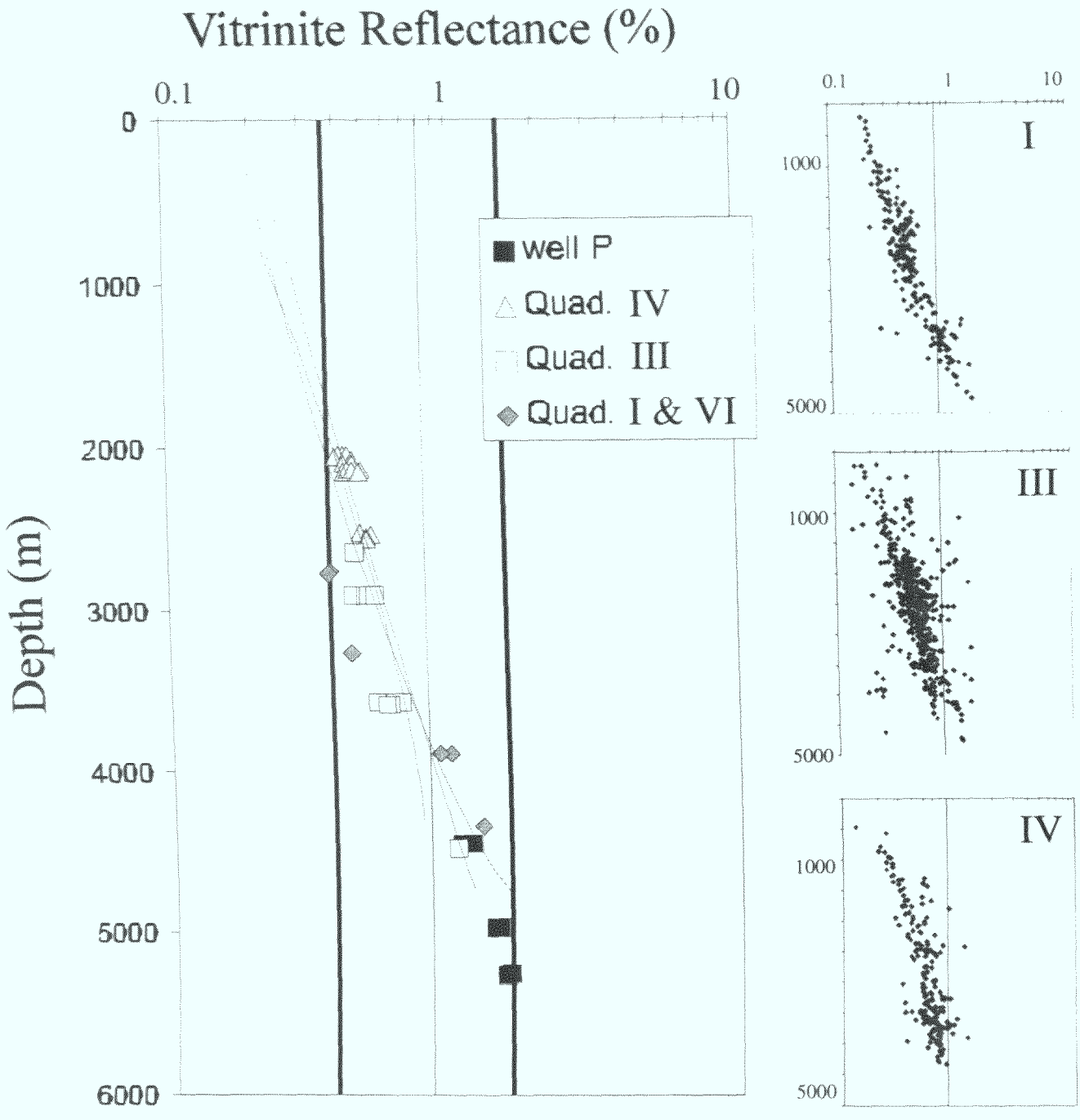


Fig. 8: Vitrinite reflectance (R_o %) versus depth for the here investigated sample set (left) listed in Table 3. Mean trend-lines from diagrams on the right are included. Right: distributions of R_o (%) versus depth in the Norwegian Quadrants I, III and IV (Norsk Hydro data).

Although the samples as reported in Table 3 cover a maturity range of 0.36 % to 1.5 % immature samples in the range 0.4 to 0.5 % predominate the sample set. The covered maturity range is depicted in Fig. 8 and corresponds with a larger database for the quadrants I, III and IV. Even if the trends are relatively broad especially for quadrant III the mean trends fall close together indicating an overall similar heating history. From Fig. 8 it becomes clear that the limit for observations on the natural system is at appr. 1.5 % R_o source rock maturity. Observed gas compositions however may originate from higher levels of maturation.

The samples of well P contain significant amounts of pyro-/ migra-bitumen besides vitrinite. For each sample vitrinite reflectance and pyrobitumen reflectance were measured and plotted in an X/Y-diagram (Fig. 9). A linear relationship with a high correlation index is evident. The pyrobitumen reflectance increases slightly faster than the vitrinite reflectance. Compared with results given by Jacob (1989) it can be stated that the data in the R_o range 1.0-1.6 % are in agreement only Jacob's regression envelope is clearly steeper. This relationship can be used to evaluate maturity in cases where vitrinite is absent but pyro-/ migra-bitumina can be recognised.

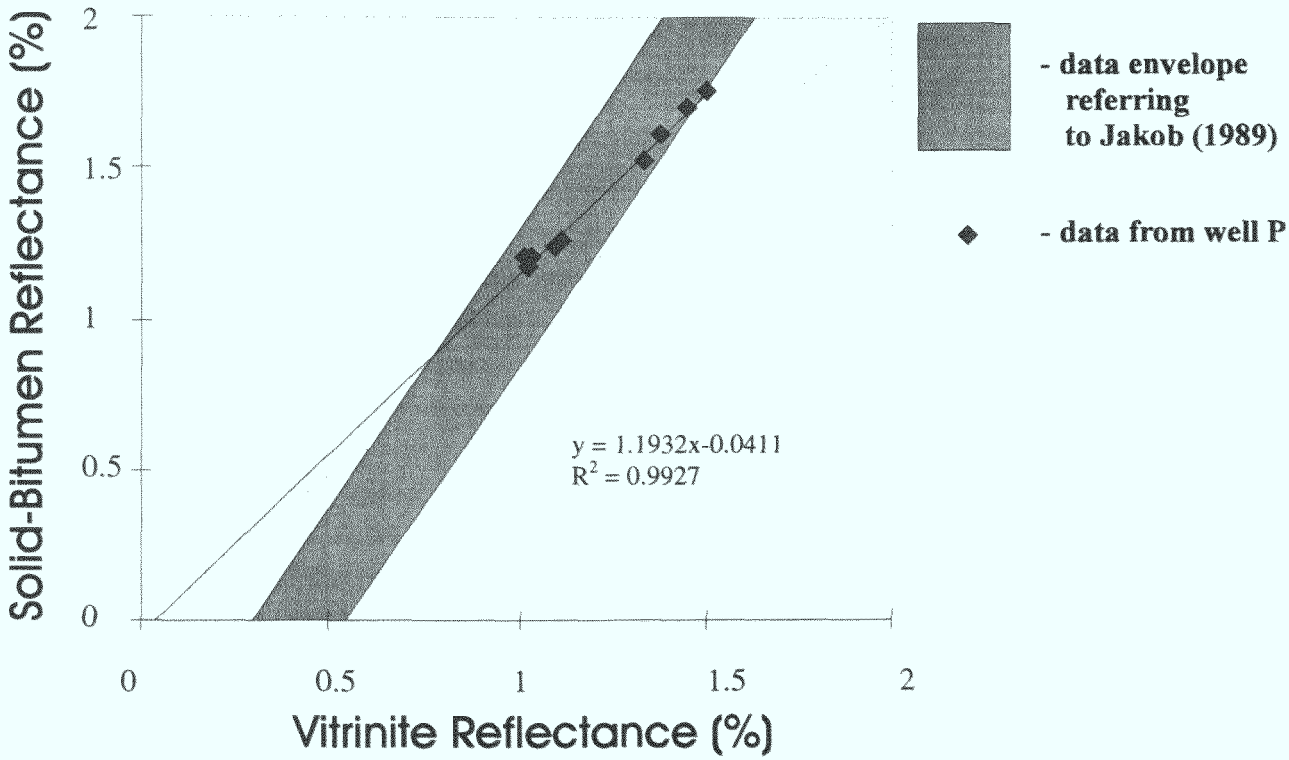


Fig. 9: Correlation between changes in vitrinite reflectance and pyro- or solid-bitumen reflectance.

T_{max} and Hydrogen Index (HI)

In contrast to vitrinite reflectance, T_{max} is dependent on the "bulk kerogen" maturity because it is not based on the measurement of a single organic matter constituent. The principle of changes in T_{max} with maturity is not founded on physical-chemical relationships but on chemical changes in the hydrocarbon potential. The maximum of the product generation curve in Rock Eval experiments displays the stability of bonds between potential products and the kerogen. The more labile products were removed during natural maturation, the higher the observed T_{max} will be, provided that significant differences in bond types and strength are present.

The diagram of the remaining hydrocarbon generation potential (HI) versus T_{max} shows that Draupne and Heather Formation samples fall within two principle groupings which were proposed by Skervoy & Sylta (1993). Viking Group data of well P fall within the high maturity part of the envelopes which are reported to be essentially the same for Heather and Draupne. In the immature zone the Draupne Formation envelope is defined by overall higher values but both source rock envelopes show a

considerable overlap due to Heather Formation which probably contains appreciable proportions of marine type II kerogen. The center of gravity for the here investigated sample set shows however low HI values of 100-150 (mg/g TOC). The most important information from Fig. 10 is that both principle

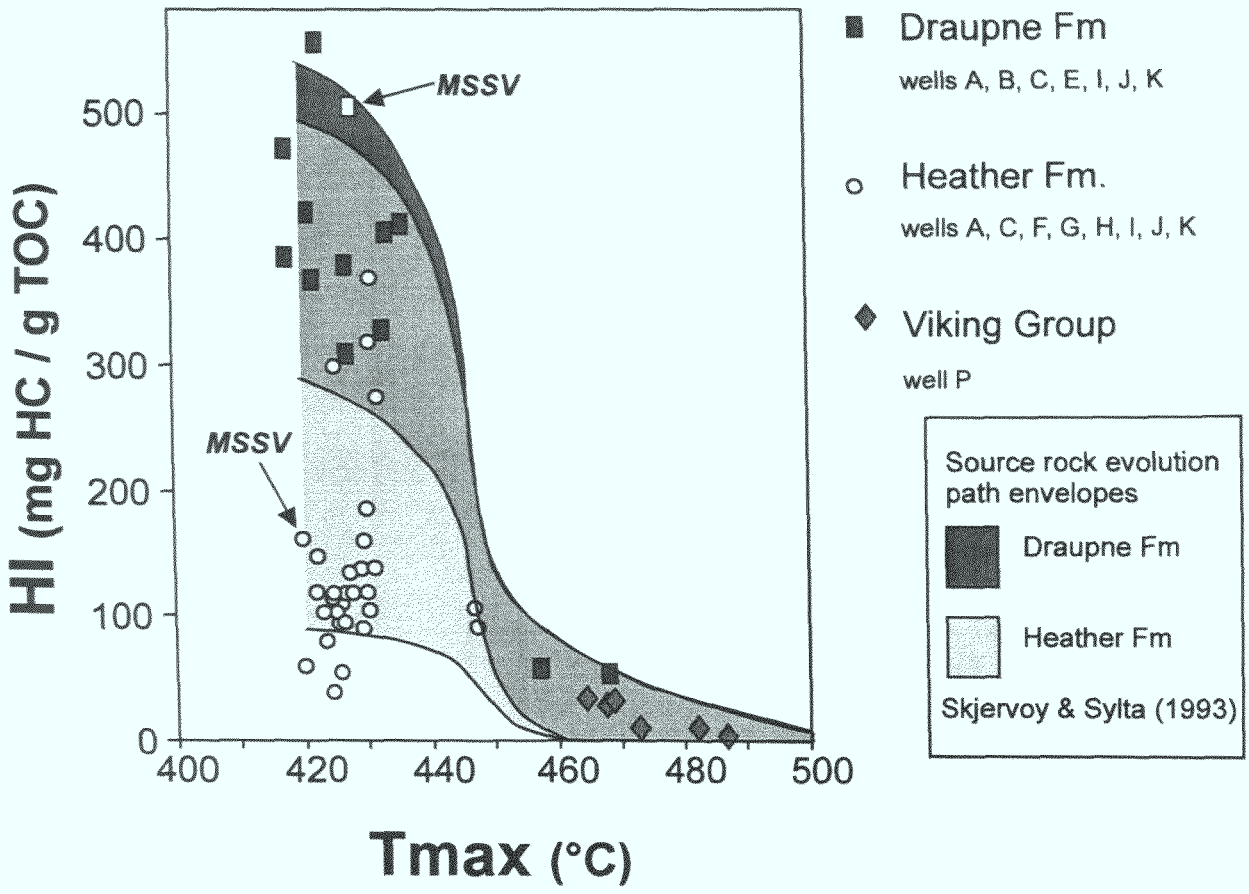


Fig. 10: Draupne and Heather Formation source rock envelopes and samples in a Rock Eval parameter plot , HI versus T_{max}. Data points highlighted by MSSV correspond to samples used for detailed investigations in the chapter "Heating Experiments".

kerogen types seem to cover similar T_{max} intervals, inferring that similar bond-strength distributions are present. Secondly the main decrease of hydrocarbon potentials seems to fall in the same narrow T_{max} range of approximatelly 440 to 455 °C. It must be stated however that no information about the "true" maturation pathway can be obtained from the diagram. Especially the Heather Formation envelope is large, allowing numerous alternatives.

Concluding remarks, maturity

The maturity parameters vitrinite reflectance, and for high levels of source rock maturity in addition the reflectance of pyro- or soild-bitumen and also the Rock Eval parameter T_{max} were shown to be applicable for the task of this study. Data obtained from the sample set were checked for validity using information reported in literature and from databases.

3.2 Choice of Samples for Heating Experiments

Aside from a reference systems for kerogen types and maturity established above, bulk kinetic parameter determinations for hydrocarbon generation were used to help select samples suitable for MSSV pyrolysis studies. This additional criterion was employed because even for kerogens, which reveal similar properties by bulk and molecular characterisations, differences in hydrocarbon generation might occur. Furthermore Schenk & Horsfield (1996) detected from investigations of different source rock sample sets covering maturity ranges that not all types of kerogens are suitable for laboratory investigations. This point is discussed in the following, as well as the general problem of using kerogen concentrates or whole rocks.

3.2.1 Kerogen Concentration versus Whole Rocks

The main objection for using whole rock samples is the possibility that high temperature catalytical effects occur which are not likely in lower temperature natural systems. It is well known that quartz, clay minerals, carbonates and pyrite can have a strong impact on laboratory pyrolysis reactions because of such high temperature catalytic effects (Horsfield & Douglas 1980, Monthioux & Landais 1988, Lillack 1992, Dembicki 1992, a.o.). A possibility to ensure that these effects do not occur is the isolation of the kerogen from the surrounding mineral matrix. On the other hand it is uncertain if the kerogen isolation or rather concentration procedure alters the kerogen structure itself (Reynolds & Burnham 1995). The latter authors stated that their results were in good agreement for shales and kerogens for a series of samples from different locations and source rock types while a Kimmeridge Clay sample exhibited the largest differences. Monthioux & Landais (1988) investigated coal pyrolysis residues by IR spectroscopy and found that sample treatment with HCl had no influence on the structure of solid residues.

Results from Rock Eval screening analysis (Table 3) infer that the concentration procedure results in T_{max} values being reduced by 20-67°C for samples of high maturities. For low maturity samples differences were less striking. It was decided to use kerogen concentrates for closed system pyrolysis experiments for three reasons:

- Low maturity samples revealed only small differences in T_{max} for whole rocks and kerogens.
- Secondly the amounts of product per g sample are higher so that the detection of compounds is more reliable, and
- finally open pyrolysis experiments (Table 6, Appendix) indicated a higher relative proportion of gas for most of the whole rock samples pointing to retention or high temperature catalytic effects of the mineral matrix.

In contrast to T_{max}, the Hydrogen Index values show strong deviations between whole rock and kerogen concentrates up to ± 50%. This cannot be explained exclusively by mineral matrix catalysis because HI sometimes increases due to concentration. This phenomenon was also reported by Espitalié *et al.* (1980) who explained it by the retention of heavier hydrocarbons by the rock matrix, especially the clay mineral fraction. On the other hand the reduction of HI indicates an alteration of the kerogen structure and removal of labile organic matter.

3.2.2 Bulk Hydrocarbon Generation

As outlined above a number of samples were investigated by Rock Eval type open system pyrolysis at three heating rates with subsequent determination of bulk kinetic parameters (Schaefer *et al.* 1990) in order to provide information supplementary to those of the reference system. 12 samples from both source rock units, immature as well as mature, were investigated. The activation energy distributions and frequency factors for all investigated samples are listed in the Appendix (Table 10). The range of the results is for the immature Heather Formation:

$Ea = 57\text{-}62$ kcal/mol

$A = 1.2*10^{15} - 3.2*10^{16}$ sec^{-1}

(Sample E 41694 from well I was not considered for this range because it contains marine type II organic matter resembling Draupne Formation kerogen.)

and for the immature Draupne Formation:

$Ea = 55\text{-}56$ kcal/mol

$A = 3.0*10^{14} - 1.1*10^{15}$ sec^{-1}.

An overview of results from selected recent literature (Table 11) shows that for both source rocks under investigation the determined kinetic values are in a similar range of magnitude. Heather Formation values are found to be higher than those reported. Especially the mean activation energy and the frequency factor values for the whole rock sample of well G; 2138.75m (E41716) are relatively high reflecting probably the high terrigenous contributions to the organic matter.

Table 11: Reaction kinetic parameters reported in literature.

Ritter *et al.* (1995)	Ea = 53.2 kcal/mol A = $5.0*10^{13}$ sec^{-1}	KCF/ MSSV isothermal on whole rocks
Espitalié *et al.* (1988)	Ea = 56 kcal/mol A = $0.52*10^{15}$ sec^{-1}	KCF/ Rock Eval type kerogen concentrates
Wei *et al.* (1994)	Ea = 52-54 kcal/mol A = $5.0\text{-}9.0*10^{13}$ sec^{-1} Ea = 52-54 kcal/mol A = $7.0*10^{13} - 1.6*10^{14}$ sec^{-1}	Draupne/ Rock Eval type kerogen concentrates Heather/ Rock Eval type
Reynolds & Burnham (1995)	Ea = 54-57 kcal/mol A = $2.9*10^{14}$ sec^{-1}	Rock Eval type on whole rocks & kerogen concentrates

(KCF = Kimmeridge Clay Formation)

The samples of higher maturities (E 42384 - Draupne Fm well L and E41700 & E 41705 - Viking group of well P) have lower product yields but higher residual or new evolved activation energy distributions and frequency factors (Table 10, Appendix). Comparing the predicted hydrocarbon generation temperature windows (Fig. 12) generation starts at 10-30°C higher temperatures for Heather Formation source rocks and Draupne Formation total petroleum formation rates are at least 2-3 times faster.

3.2.3 Applicability of Kinetics

Schenk & Horsfield (1996) outlined that extrapolation of petroleum formation to geological heating conditions using laboratory-derived kinetic parameters is not valid for all types of kerogen. Formation rate curves of naturally matured marine type II kerogen samples (Posidonia Shale) were shown to

remain always within the original envelope defined by the least mature sample (Fig. 11). This indicates that both natural and artificial maturation proceed through the release of hydrocarbons, so that preferentially low activation energies are stripped away. Further observations indicated that the same mechanism applies in the case of artificial maturation. In contrast, formation rate curves of Carboniferous coals of higher maturities do not fit within the envelope defined by the least mature sample. Here the natural mechanism must be different, because new potentials are formed at high activation energies. This could be explained by aromatisation and condensation processes. As a matter of fact these cannot be reproduced by artificial maturation in the open system.

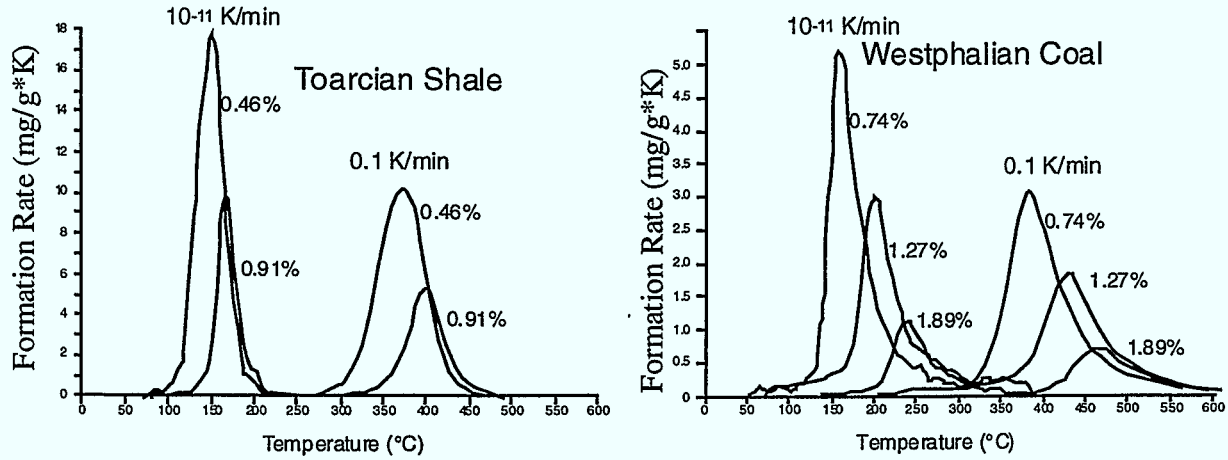


Fig. 11: Total product formation rate curves for samples of increasing natural maturation (given in % vitrinite reflectance), Toarcian Shale and Westphalian Coal. From Schenk & Horsfield (1996).

Thus it became necessary to investigate prior to more detailed studies whether natural maturation of Heather and Draupne Formation source rocks behave like the first or the second scenario described above. Especially the Heather Formation was thought likely to show hydrocarbon formation features similar to Westphalian coals because of the presence of a very heterogeneous type of organic matter.

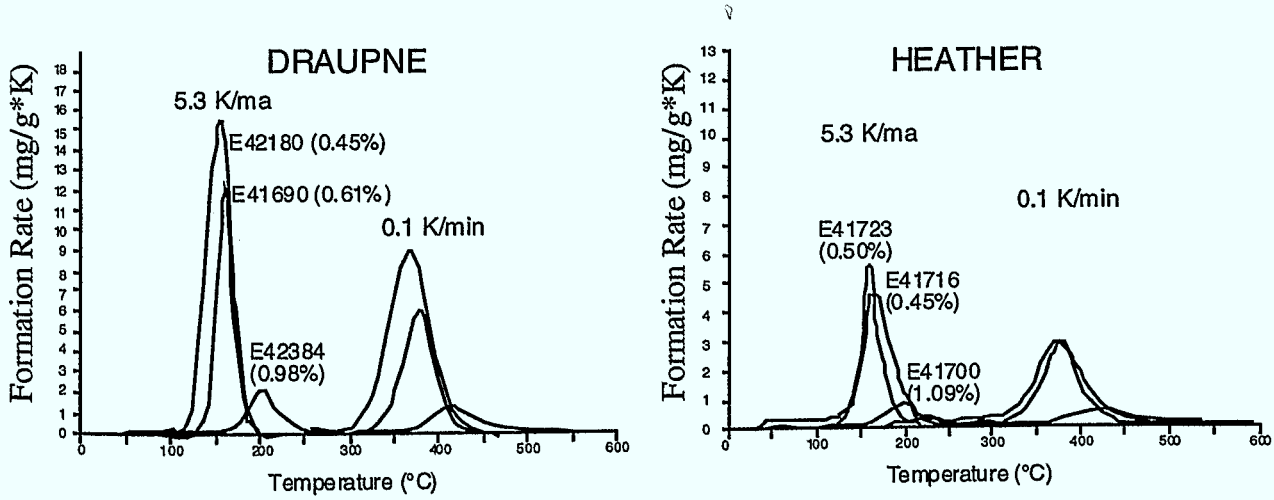


Fig. 12: Bulk hydrocarbon formation rate curves for samples of different degrees of natural maturation (vitrinite reflectance), Heather and Draupne Formation.

Fig. 12 displays the results for the Draupne Formation. Results similar to those observed for the Posidonia Shale (Schenk & Horsfield 1996) were expected because of similar types of organic matter.

Actually the formation rate curve of the most mature sample is not within the immature envelope suggesting aromatization / condensation. Unfortunately only one sample of higher maturity (well L) was available at that time, which was a sidewall core of poor sample quality, so that the reliability of the data is uncertain. Another point to state is that in spite of screening analysis indicating a homogeneous type of organic matter for Draupne Formation, hydrocarbon generation kinetic parameters for a much larger sample set are known to be variable (Telnæs, pers. comm.) indicating appreciable kerogen type differences on a molecular level. Hence, the samples analysed for the determination of bulk kinetic parameters might not be directly comparable.

The Heather Formation also gives ambiguous results. The high maturity sample (R_o=1.09%) curves (Fig. 12), both measured and predicted, remain under the envelope of the immature sample E41716 but not of the immature sample E41723 (both immature samples stem from well G). This confirms the heterogeneity of organic matter and means that extrapolation of hydrocarbon generation using the kinetic parameters determined here is not categorically right or wrong. Anyhow, the number of measurements performed is too small to provide evidence on a statistical basis. New aspects concerning this topic are put forward later in this study when results from MSSV programmed temperature pyrolysis for an immature Heather Formation sample are considered.

Concluding remarks, choice of samples for heating experiments

Based on the above described considerations two samples, one of Heather Formation and one of Draupne Formation were chosen for detailed analysis.

For the case of the Heather Formation an immature sample was chosen that might represent an end-member of the kerogen types present in the Upper Jurassic of the northern Viking Graben. Especially for immature Heather Formation source rocks Rock Eval HI values strongly vary from 100-500 (mg/g TOC) (Fig. 10). The sample (E 41716 MK EC) from well G (2138.75 m) contains a high proportion of land derived organic matter, (vitrinite and inertinite) and a minor contribution of liptinitic organic matter and has a hydrogen index (HI) of 146 (mg/g TOC). In contrast the Draupne Formation sample (E 43254 MK EC) from well B (2764.7 m) has the opposite end-member character with low contributions of vitrinite and inertinite and high hydrogen index (HI) of 555 (mg/g TOC) reflecting mainly marine type II organic matter.

3.3 Heating Experiments simulating Gas Formation

Thermogenic gas can form via the primary cracking of kerogen (Robinson 1966; Speers & Whitehead 1969) and by secondary cracking of already formed oil or bitumen. The secondary cracking of oil in reservoirs was considered early (Barton 1937, Landes 1967, Connan & Cassou 1980) and investigated in detail using heating experiments (Horsfield *et al.* 1992, Kuo & Michael 1994). Insights into chemical mechanisms for both primary and secondary processes were mainly gained by performing heating experiments of various types. Model compounds as for instance behenic acid, n-alkanes (Fabuss *et al.* 1965, Weres *et al.* 1988, Jackson *et al.* 1995, Behar & Vandenbroucke 1996) and branched alkanes, alkylated aromatics, ethers and other components (Kissin 1987, Savage & Klein 1988, Malhotra *et al.* 1989, Enguehard *et al.* 1990, Dominé 1991) were employed. Especially asphaltenes are suitable model compounds (Savage & Klein 1988, Behar & Pelet 1988) because new formed residues can be investigated separately, which is virtually impossible for the case of kerogens. Tissot & Welte (1984, p.150) and Pelet *et al.* (1986) pointed out that kerogens and related asphaltenes reveal significant compositional similarities, based on observations from IR spectroscopy, elemental analyses and pyrolysis gas-chromatography.

Arising from heating experiments with model compounds two conceptual mechanisms were proposed which are discussed in Greensfelder *et al.* (1949). The first concept is the thermal cracking via free radicals, the so-called Rice - Herzfeld or Rice - Kossiakoff mechanism (Kossiakoff & Rice 1943) and the second alternative mechanism is the acidic catalysed cracking with carbonium ion intermediates. The validity of the former mechanism, or alternatively the acid catalysed cracking for the case of natural petroleum generation, continues to be debated (Kissin 1987, Ungerer 1990, Poutsma 1990).

The Rice-Herzfeld mechanism is a chain reaction consisting of initiation, chain propagation and termination reaction steps. *Initiation* of the chain mechanism involves the formation of a radical. Subsequent β-scission and hydrogen-transfer reactions are *propagation* reactions. The transfer of hydrogen was impressively demonstrated by Hoering (1984) who pyrolysed shale in the presence of heavy water and could show that deuterium was incorporated into the products. *Termination* of chain reactions works by radical recombination / addition and by disproportionation.

The acid catalysed mechanism comprises similar reactions based on ions but produces preferably branched products because hydrogen shift or methyl shift are more common than for radical supported mechanisms. The occurrence of branched hydrocarbons in nature and experiments can either be related to the contribution of the ionic mechanism (Kissin 1987) or to structural units of kerogen (Ungerer 1990). Because of the occurrence of olefins during pyrolysis it is often assumed that thermal cracking via free radicals is the more important process in nature (Jurg & Eisma 1964). Conversely the occurrence of core aromatic structures was used as an argument for the ionic mechanism by Hansford (1953) who found that dealkylation in the ipso-position is preferred by acid catalysis whereas the radical mechanism results in primarily substituted aromatics. Finally the detection of free radicals in kerogens using the ESR technique (Ishiwatari *et al.* 1976, Marchand & Conard 1980) supported the significance of chain reactions over free radicals in natural systems.

Apart from pure thermal or acid catalysed cracking a third concept exists, the catalysed thermal cracking. In contrast to the acid catalysed cracking this type of process is accelerated by transition metals. Mango (1992) has inferred that transition metal complexes like nickel and etioporphyrin III have catalytic properties, which might take part in natural gas generation reactions. The process,

which he deduced, from molecular compound ratios uses cyclopropane intermediates for structural rearrangements (Fig. 13).

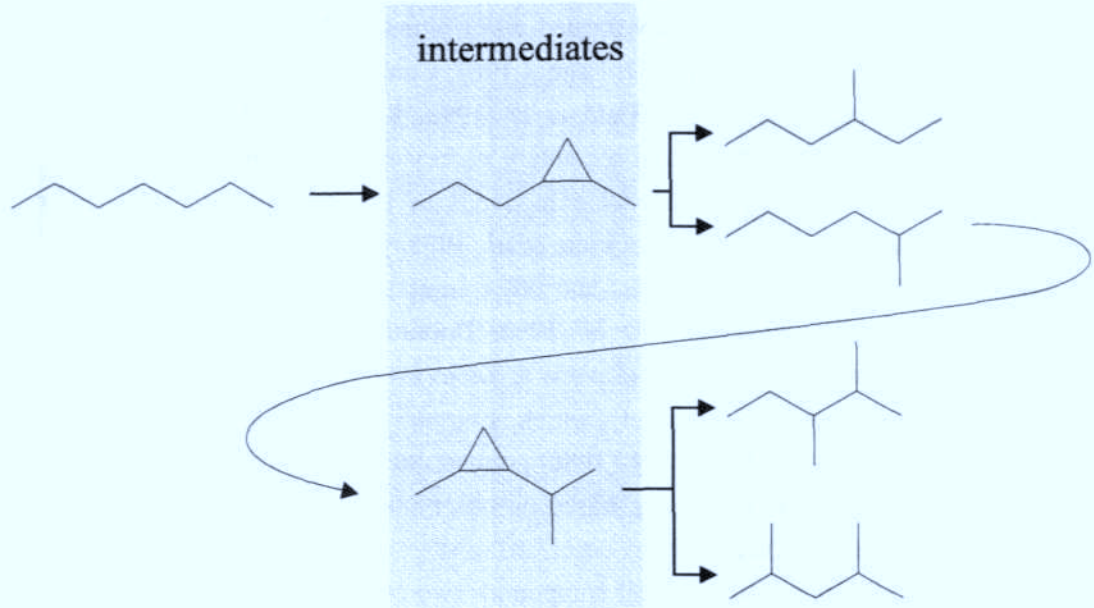


Fig. 13: Reaction scheme after Mango (1987) for the formation of isoheptanes by a steady state catalytic process over short-lived unstable cyclopropane intermediates.

So far Mango's model is the only model that takes account of the observation of regularities in light end hydrocarbon compositional patterns which can hardly be explained by simple cracking of irregular precursor structures. Still the importance of the process might be restricted to rearrangement of components subsequent to thermal cracking reactions.

The above described knowledge about reaction mechanisms for hydrocarbon forming processes is strongly concerned with molecular processes while the focus of this work is to investigate gas generation in a more geologically related framework. Nevertheless the knowledge of reaction mechanisms can help improve the interpretation of heating experimental results.

The question of the validity of laboratory investigations (either on model compounds or on kerogens) for processes occurring in geological systems was discussed controversially in the literature as well. The approach presented above to determine whether the formation of new precursor structures at higher activation energies takes place or not (Section 3.2.3) is certainly only one aspect. Other aspects like compositional differences between pyrolysates and natural occurring petroleum will be the subject of further discussion during the course of this study. The conceptual kerogen decomposition model of Larter & Horsfield (1993) tries to explain differences in that natural petroleum formation is considered to go through NSO-rich bitumen intermediates whereby their release is enhanced in artificial maturation due to the differences in heating conditions.

One thing is for certain, conclusions drawn exclusively on the basis of observations of natural systems or on the other hand exclusively of laboratory experiments may lead to large errors. For the observations from nature it is almost impossible to register the multiple parameters which have had an impact on the observed data. In contrast parameters in a laboratory system are relatively restricted and allow a more complete registration. Therefore, first of all the experimental results are discussed below with regard to different gas forming modes. Respective mechanisms will be discussed and reaction kinetic parameters will be determined.

3.3.1 Evolution of Boiling Ranges during MSSV Pyrolysis

The results from programmed-temperature closed system MSSV pyrolysis provide a platform for considerations about different gas forming modes, mechanisms and related reaction kinetics. It must be noted that for MSSV pyrolysis, as well as the subsequently discussed open system pyrolysis, the measured datapoints represent the sum of all products up to the temperature of each datapoint, thus curves in the following section are cumulative yield curves if not stated otherwise. The MSSV pyrolysis method (Horsfield *et al.* 1989) provides a tool for the investigation of the compositional development of artificial maturation products gas as well as heavier components. Boiling range C_{1-5}, C_{6-14}, C_{15+} (Fig. 14) or individual component concentrations can be determined for temperature intervals depending on the preselected heating rate. With increasing heating rate the onset, increase and end of product generation are shifted to higher temperatures.

Draupne Formation (well B, 2764.7 m)

Fig. 14 (left) shows the evolution of total gc-detectable products and two boiling range fractions at heating rates of 0.1, 0.7 and 5.0 $Kmin^{-1}$. The overall C_{1+} products reach a preliminary maximum followed by a second maximum and a subsequent decrease of total products probably due to the formation of coke. This is most readily seen for the 0.7 and 5.0 $Kmin^{-1}$ experiments. The gas fractions

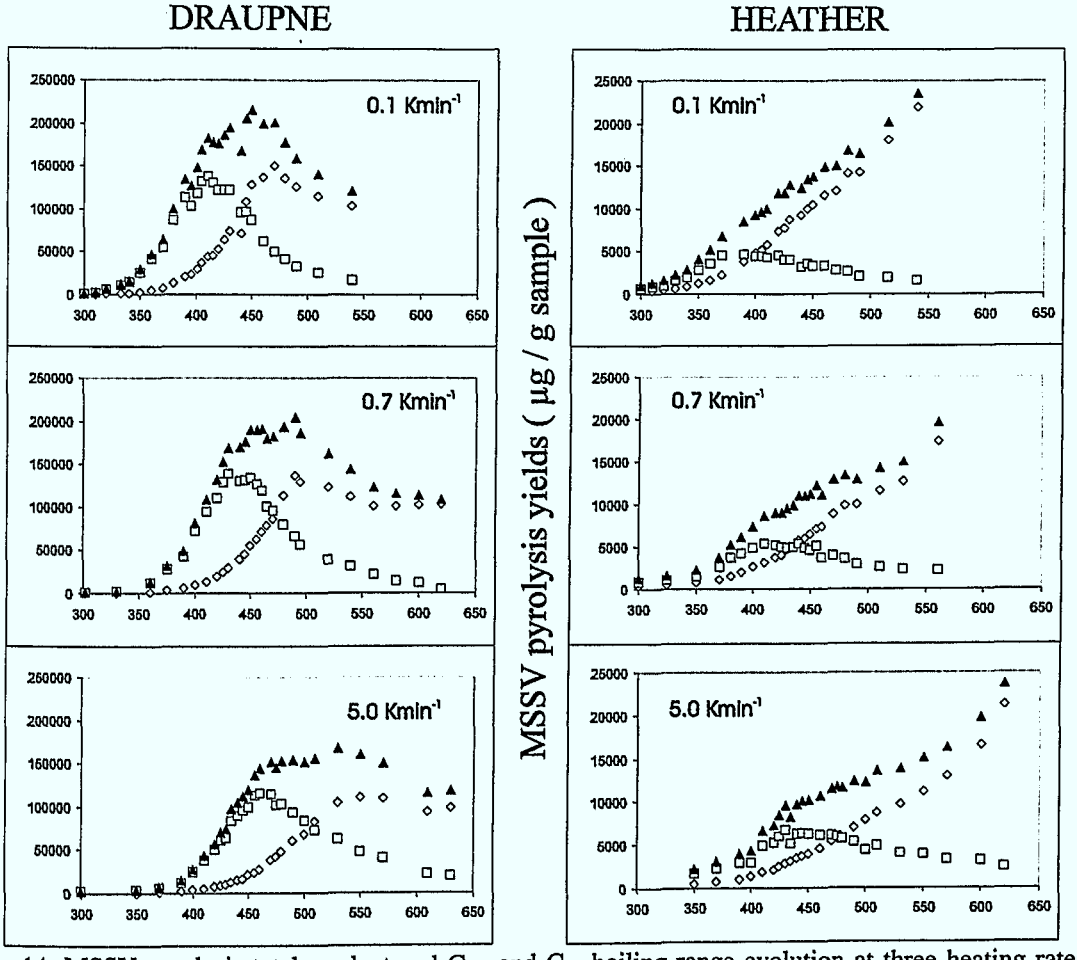


Fig. 14: MSSV pyrolysis total product and C_{1-5} and C_{6+} boiling range evolution at three heating rates, Heather and Draupne Formation (full triangles = C_{1+}, squares = C_{6+} and rhombuses = gas C_{1-5}).

reach their maxima at slightly higher temperatures as observed for the final C_{1+} maximum. The C_{6+} fractions, which are important for considering secondary cracking, show increasing yields until they reach their maximum near the "first" C_{1+} plateau. The slopes of their decreasing parts are subdivided into a first steeper part and a second shallower part. The difference between C_{1-5} and C_{6+} maxima is at least 50°C for all heating rates. The contribution of unresolved hump (not depicted, see Table 17) is relatively high at low temperature and decreases from 45-66 % to low values of 1-2 % at high temperatures indicating that hump components undergo secondary cracking or aromatisation.

Heather Formation (well G, 2138.75 m)

For the Heather Formation (Fig. 14, right) the scenario is significantly different compared to Draupne Formation. Considering the total product evolution the curves appear somewhat irregular, meaning they do not show the usually well-defined shape but instead continue to increase with increasing temperatures. Gas formation becomes more prominent over the measured temperature intervals with a pronounced increase at highest temperatures, which is obviously the reason for the unusual C_{1+} curve shape. The C_{6+} fractions show increasing yields until they reach their maximum. Up to this point they make up the highest proportion of products. The decrease is especially slow and can be termed plateau for the first interval so that it becomes difficult to define an exact peak temperature or an exact onset of decrease. The contribution of unresolved components in form of a hump is lower than for Draupne and ranges from 30-42 % to 1 %.

3.3.2 Evolution of Boiling Ranges during Multistep Open System Pyrolysis

Both samples were analysed also by multistep open system pyrolysis at a heating rate of 5.0 $Kmin^{-1}$. Here in contrast to MSSV pyrolysis the development of primary products is considered exclusively. The results for C_{6+} and C_{1-5} gas formation are summarised in Fig. 15. The scale is adapted to the maximum product amounts (C_{1+} totals) of each source rock to enable a better comparison, also with regard to published values for characteristic source rock gas proneness.

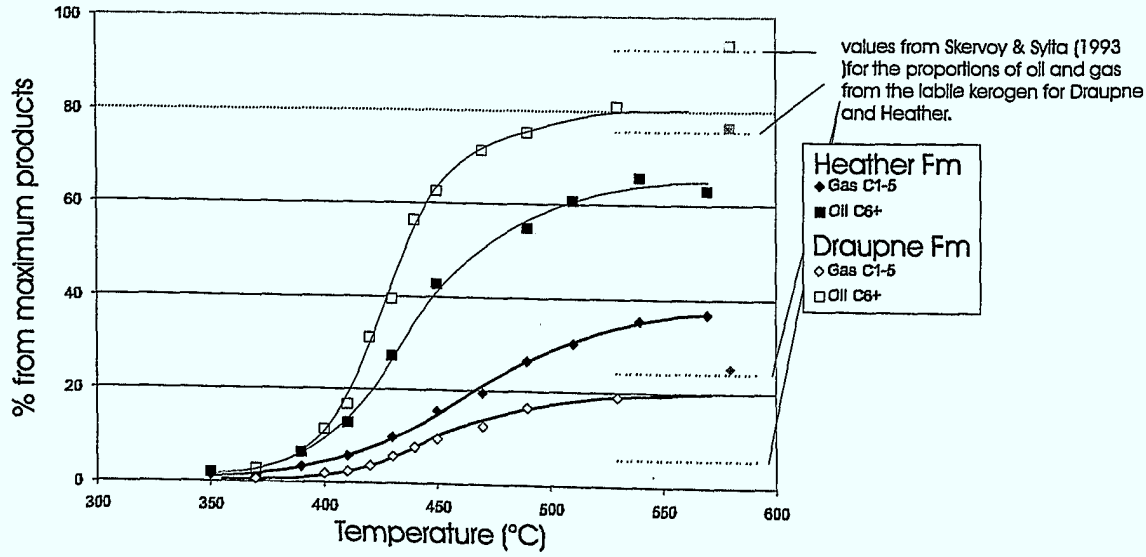


Fig. 15: Multistep open system pyrolysis at 5.0 $Kmin^{-1}$ for Heather and Draupne Formation and in comparison with published potentials. Values are normalised to maximum product yields.

The relative proportion of gas from open system products reaches 20 % for Draupne and 38 % for Heather Formation, confirming that Heather Formation kerogens have a higher relative potential for gas. Gas formation covers a similar or even broader temperature interval than does the C_{6+} generation with the latter reaching the highest formation rates at lower temperatures.
It must be stated at this point that a second aliquot of the Heather Formation kerogen concentrate was employed for multistep open system pyrolysis because the original supply was exhausted by MSSV experiments. Compositional differences of this second aliquot, such as an increased relative abundance of alkanes and a higher proportion of gas means that only a qualitative comparison between open pyrolysis and MSSV pyrolysis are allowed.

3.3.3 Product Amounts

Table 12 gives an overview on product amounts expressed as fraction of TOC for Heather and Draupne Formation, different sample types, analytical systems and heating rates. First of all it stands out that the Draupne Rock Eval HI is increased by approximately 10 % due to kerogen concentration whereas it is reduced for Heather by the same proportion. A reduction of the HI during kerogen concentration can be explained by the removal of macromolecular precursors by solvent and acid treatment whereas the increase in HI was reported (Espitalié *et al.* 1980) to be a retention effect of heavier hydrocarbons by clay minerals.

Table 12: Hydrogen Index from Rock Eval and MSSV and open system pyrolysis equivalents.

sample type	**Draupne well B**	**Heather well G**
system	**2764,7m**	**2138,75m**
whole rock HI	502	164
concentrate HI	555	146
concentrate TOC	44.8%	33.10%
MSSV py HI		
0.1 K/min	502	~75 (generation still in progress)
0.7 K/min	473	~75 (generation still in progress)
5.0 K/min	368	~75 (generation still in progress)
open multistep HI		
5.0 K/min	362	103

(HI values in mg/ g TOC)

Product yields show heating rate dependence. During MSSV pyrolysis the Draupne HI increases with decreasing heating rate, coincidentally the value for the slowest heating rate matches that from Rock Eval pyrolysis of the whole rock sample. The lowest values of 362 and 368 (mg HC/g TOC) were measured for both MSSV pyrolysis as well as multistep open system pyrolysis at 5.0 $Kmin^{-1}$. Hence it can be suggested that the proportion of not-gc-amenable compounds increases with heating rate and is essentially independent of the pyrolysis system employed. In contrast for Heather Formation the product evolution is not ceased during MSSV pyrolysis. The realised HI at highest experimental

temperatures is only about 75 mg HC /g TOC in contrast to 146 and 164 mg HC /g TOC measured by Rock Eval and 103 mg HC /g TOC for the open multistep pyrolysis. The generation of MSSV products obviously did not reach an end (also indicated by the high temperature increase in Fig. 14) but final amounts can be assumed to equal those of open multistep pyrolysis, like it is the case for Draupne Formation at 5.0 $Kmin^{-1}$. The expected amount of gas that remains to be produced would be 28 mg/ g TOC or 8.4 mg/ g sample.

3.3.4 Compositional Details from MSSV and Open System Pyrolysis

Compositional details as revealed by the here employed open and closed heating experiments were investigated by coupled analyses with mass spectrometry. Fig. 16 shows TIC chromatograms for the

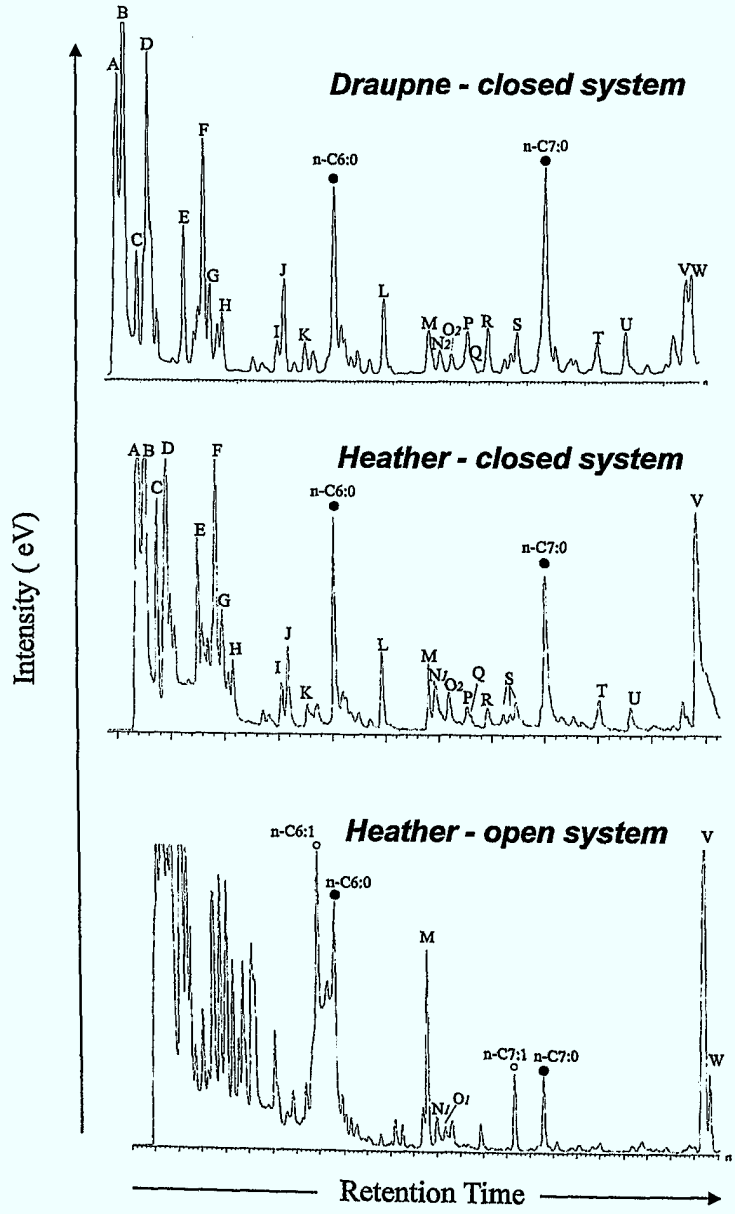


Fig. 16: Compositions in the light hydrocarbon range (Total ion-chromatogram TIC, ethane - toluene) for samples chosen for detailed investigations. Draupne Formation well B 2764.7m (E 43254 MK EC) and Heather Formation well G, 2138.75m (E41716 MK EC). For peak-key see Table 13 Pyrolysis conditions: MSSV closed system - 460°C at 5.0 $Kmin^{-1}$ (Draupne) and 430°C at 0.7 $Kmin^{-1}$ (Heather) and open system - 300-600°C at 60 $Kmin^{-1}$.

light hydrocarbon range up to toluene. MSSV pyrolysis is characterised by a component spectrum similar to naturally occurring petroleums. All components listed in Table 13, except for olefins, were also detected by thermovaporisation (Table 4, Appendix). Draupne and Heather Formation MSSV runs reveal almost the same component spectrum. Differences are specified by the relative abundances of n- and i-alkanes, cycloalkanes, aromatics and thiophenes. Thiophenes are for instance more dominant for Draupne whereas aromatics show higher contributions to Heather Formation, which is in accordance with results from py-gc kerogen typing. In contrast the open system is characterised by high abundances of olefins and inorganic gases in the C_2-C_5 range (CO_2, H_2S, a.o.), where unambiguous peak identifications became impossible. Moreover benzene and toluene predominate whereas, cyclic- and

Table 13: Peak identification, light HC. Open and closed py-gc-ms. see Fig. 16

	compound name	base	mol	further
A	ethane +	28	30	
A	CO2	44	44	
B	propane	29	44	
C	i-butane	43	58	
D	n-butane	43	58	
E	i-pentane	43	72	
F	n-pentane	43	72	
G	2-pentene	55	70	
H	2-pentene ?	55	70	
I	cyclopentane	42	70	55
J	2 methyl-pentane	43	86	71
K	3 methyl-pentane	56	86	57,41
L	methyl-cyclopentane	56	84	41,69
M	benzene	78	78	50,51
N1	methyl-cyclopentene	67	82	
N2	thiophene	84	84	45,58
O1	cyclohexene	67	82	39,41,54
O2	cyclohexane	56	84	
P	2 methyl-hexane	43	100	57,85
Q	2,3 dimethyl-pentane	56	100	71
R	3 methyl-hexane	43	100	71,70
S	1,cis-3,dimethyl-cyclopentane	41	98	55,70
S	1,trans-2,dimethyl-cyclopentane	41	98	56,70
S	1,trans-3,dimethylcyclopentane	41	98	56,70
T	methyl-cyclohexane	83	98	41,55,69
U	ethyl-cyclopentane	69	98	41
V	toluene	91	92	
W	3 methyl-thiophene	97	98	

branched alkanes are almost absent. This supports the idea of the importance of rearrangement reactions subsequent to primary cracking resulting in branched and cyclic alkanes, as implied in the beginning from mechanisms proposed by Mango (1987, 1990). In other words, the large amount of olefinic structures obtained from the open system is likely to correspond to i-alkanes and cycloalkanes in the closed system.

The MSSV pyrolysis gc-ms runs depicted in Fig. 16 were performed to temperatures of 430°C at 0.7 $Kmin^{-1}$ and 460°C at 5.0 $Kmin^{-1}$ which are in both cases intermediate heating conditions where secondary cracking is not severe. In contrast Fig. 17 shows the full extent of secondary cracking with methane and simple aromatic hydrocarbons like benzene and naphthalene being the visible final end

products of the destructive processes. A hydrogen poor residue is a further but not gc-detectable product (Connan *et al.* 1975, Horsfield *et al.* 1992) produced by aromatisation. The formation of such a residue is obvious for Draupne Formation at the highest MSSV pyrolysis temperatures, indicated by a decrease of total product amounts (Fig. 14).

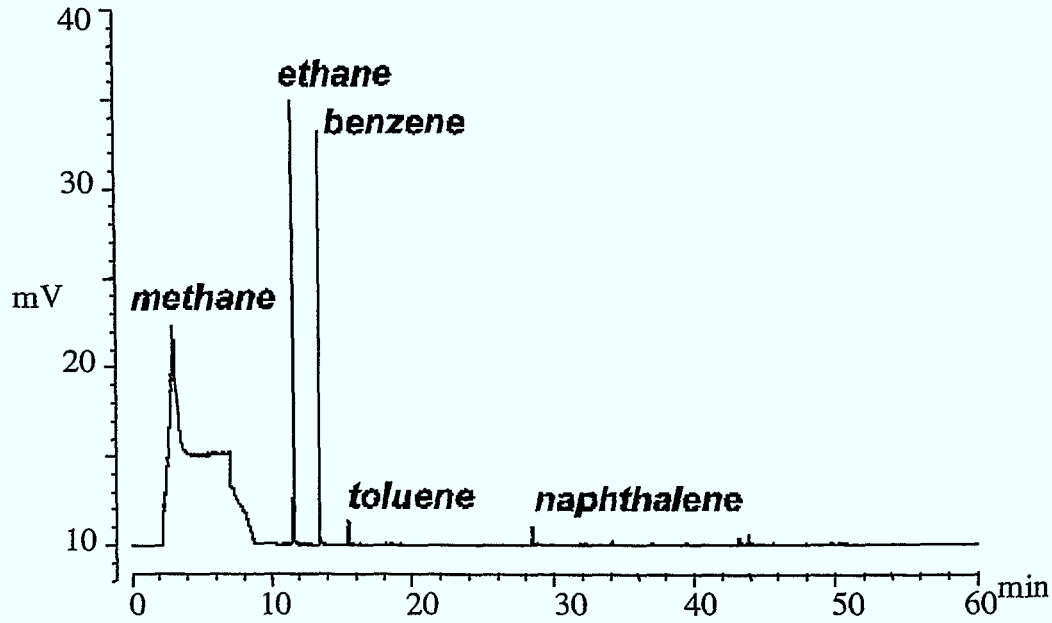


Fig. 17: Terminal MSSV pyrolysis products. Exemplified by the Draupne Formation sample (well B, E43254) at 620°C, heating rate 0.7 $Kmin^{-1}$. The presence of ethane and toluene indicates that secondary cracking is still in progress.

Secondary cracking like shown in Fig. 17 must be considered as an extreme case in that all first formed products are successively degraded. The complete conversion of primary products is unlikely to happen this way in natural systems where varying proportions of petroleum will be released from the source rock during expulsion. The proportions which remain in the source rock and also expelled trapped petroleum which underwent further burial will be degraded.

3.3.5 Calculation of Primary and Secondary Gas Formation

Primary and secondary gas generation both occur in the closed system. In order to enable the determination of reaction kinetic parameters for each of both processes their individual formation curves were evaluated by unravelling the cumulative gas generation curves, using also information derived from multistep open system pyrolysis. The evaluations of the respective proportions of primary and secondary gas are based on an approach described by Dieckmann *et al.* (1997) which is termed here *conservative evaluation.* For the cases of the two source rocks central to the theme of the current study this conservative evaluation was extended resulting in *refined evaluations.* The choice of the different methods discussed below has a strong impact on the results of predictions for gas generation under geological heating conditions.

Conservative Evaluation

It was initially assumed that the formation of gas by secondary cracking starts at the temperature of the cumulative maximum of the C_{6+} fraction (Sweeney *et al.* 1987; Schaefer *et al.* 1990; Horsfield *et*

al. 1992) usually assumed to correspond to "oil". The decrease of the boiling range fraction C_{6+} depicted schematically in Fig. 18 is an indicator of the ongoing secondary cracking which produces gas. As a consequence a proportion of the measured gas C_{1-5} (Fig. 14, p.35) in a closed system must be derived from the degradation of primary products. This proportion can be evaluated using simple stoichometric assumptions demanded by the hydrogen balance (equation 1). The degradation of a stoichometric average "oil" is assumed to form secondary gas (C_{1-5}) and coke in the simplest case (Sweeney *et al.* 1987, Braun & Burnham 1992).

$$\mathbf{CH_{2.2} \rightarrow x\,CH_{3.2} + (1\text{-}x)\,CH_{0.2} \quad x \sim 0.67} \qquad (1)$$

$\mathbf{CH_{2.2}}$ = assumed average composition of C_{6+} (average of hexane and tricontane)
$\mathbf{CH_{3.2}}$ = assumed average composition of secondary gas C_{1-5} (average of methane and pentane)
$\mathbf{CH_{0.2}}$ = assumed average composition of coke (reported by Behar *et al.* 1991)

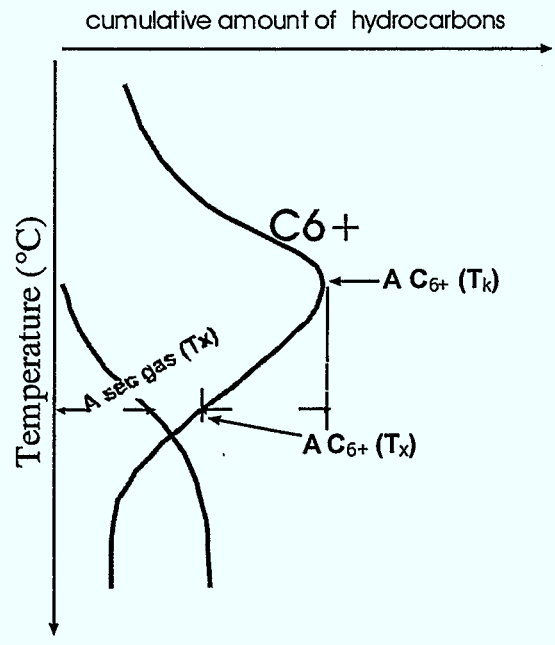


Fig. 18: Model for the calculation of secondary gas formation from the decrease of C_{6+} components.

The assumed average compositions are hypothetical and can be adapted to different scenarios where x= 0.7 might be too optimistic. Skervøy & Sylta (1993) for example used a conversion factor of x= 0.5 in their study.

Based on these prerequisites, the formation of secondary gas can be calculated by equation (2), (provided that all generated C_{6+} products are detected). The amount of secondary gas $\mathbf{A}_{\text{sec G}}$ for a temperature $(\mathbf{T_x})$ equals the difference between the amount of C_{6+} hydrocarbons at the cumulative maximum $\mathbf{A}\,(\mathbf{T_o})$ and the amount of C_{6+} hydrocarbons for an increased temperature $\mathbf{A}\,(\mathbf{T_x})$ (2). The primary gas results from equation (3) and is simply that "*remaining*" when subtracting the calculated secondary gas from the total amount of gas.

$$\mathbf{A}_{\text{sec G}}(T_x) = [\mathbf{A}\,(T_o) - \mathbf{A}\,(T_x)] * 0.67 \qquad (2)$$

$$\mathbf{A}_{\text{primary G}}(T_x) = \mathbf{A}_{\text{total G}}(T_x) - \mathbf{A}_{\text{sec G}}(T_x) \qquad (3)$$

This approach was successfully applied to the secondary gas generation of the kerogen type II containing Toarcian Shale (Dieckmann *et al.* 1997) where the remaining gas was confirmed to be of primary origin. A comparison of closed and open system gas generation, reported below, was employed to see if this applied to the source rocks under study.

Refined Evaluation Draupne Formation

The prerequisite for the conservative evaluation, that secondary cracking of oil to gas starts when primary generation of C_{6+} products ended turns out to hold roughly for the case of the Draupne Formation. This can be inferred from a comparison of C_{6+} generation curves obtained at a heating rate of 5.0 $Kmin^{-1}$ from open and closed system systems (Fig. 19). Both curves display the gc-detectable fraction of oil-like C_{6+} pyrolysate produced from comparable but slightly different heating devices (see analytical section). The curves show excellent agreement up to temperatures of 460°C. Starting from this point the closed system product curve decreases indicating that secondary cracking overcompensates primary generation, whereas the open system curve still increases. The amount of educts converted into secondary gas is highlighted for the conservative evaluation which is clearly much smaller than the observed area inscribed "refined".

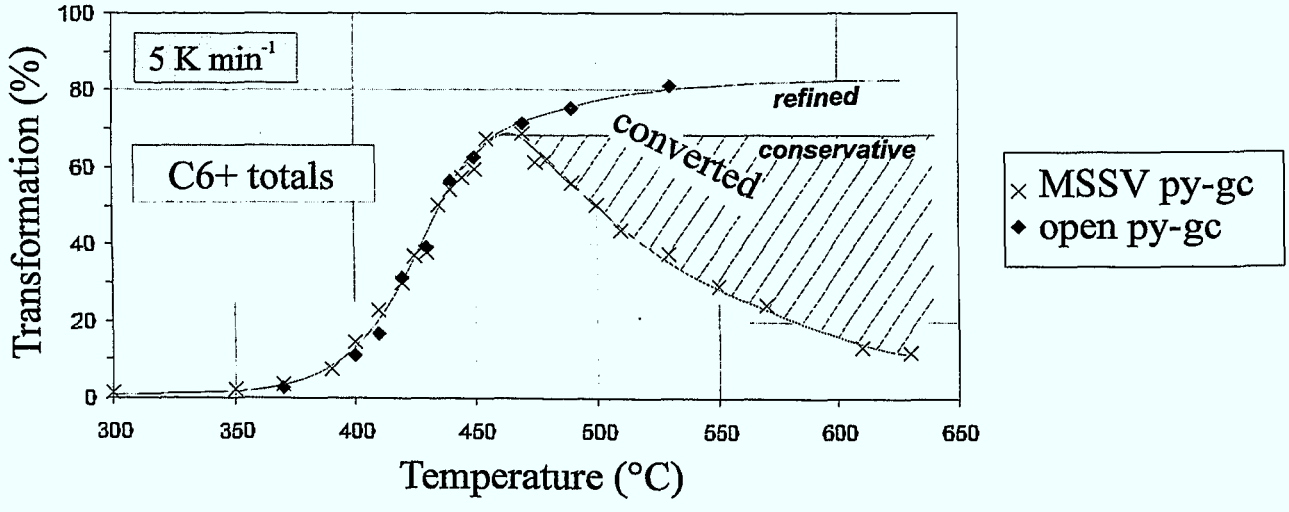


Fig. 19: Comparison of open and closed system C_{6+} temperature versus transformation curves. Transformation is calibrated using the C_{1+} total product yields maximum. The onset of secondary cracking occurs before primary generation ends. Two different scenarios for the amount of educts for secondary gas generation are displayed.

The refined evaluation method is used for further calculations. A problem arising from this choice is that the open system analytical device cannot be adapted to heating rates of 0.1 and 0.7 $Kmin^{-1}$. Thus no measurements for the calculation of refined amounts of secondary educts are available for those heating rates. Nevertheless the following can be stated. The closed system C_{6+} curves (Fig. 20) all reveal maxima in the same range of 65 to 70% of transformation of the total product potential for each heating rate. That is within the error introduced by analytical reproducibility and heterogeneity variabilities. The curves also show excellent agreement with regard to the shape of the open system

5.0 $Kmin^{-1}$ evolution profile. These arguments provide some evidence that the same difference between conservative and refined educt amounts exists for all three heating rates.

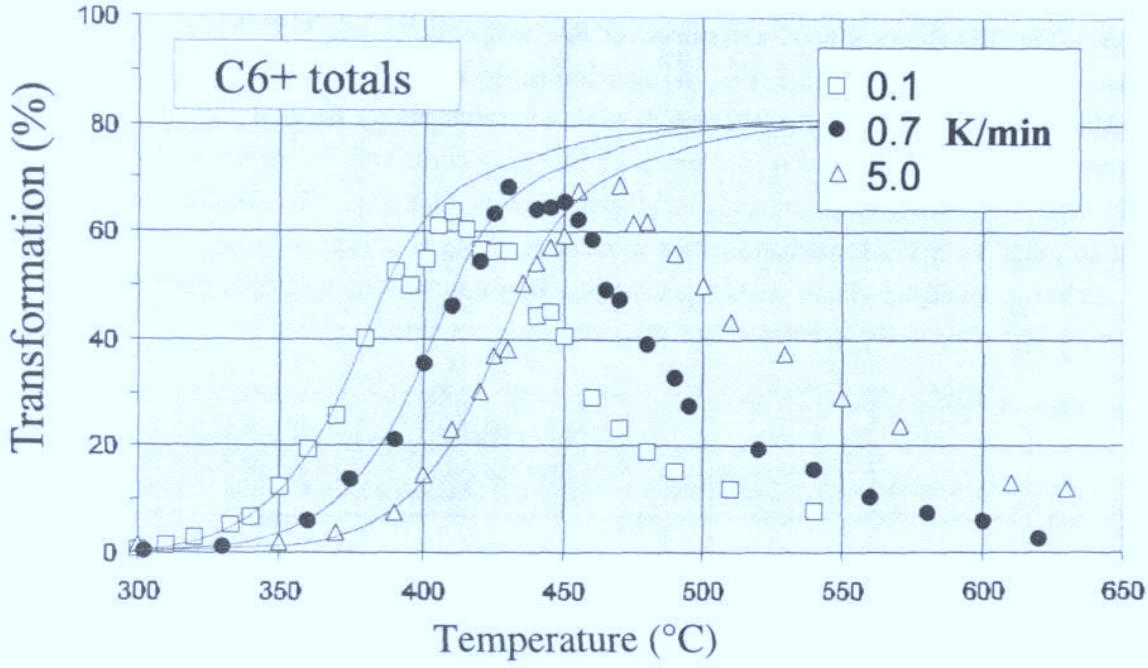


Fig. 20: MSSV pyrolysis C_{6+} cumulative formation curves normalised to C_{1+} total products. The curves are compared to the open system derived C_{6+} curve determined at 5.0 $Kmin^{-1}$.

Under these prerequisites the amount of 81% of C_{6+} fraction was used for the calculation of secondary gas for all three heating rates. The calculated secondary and primary gas formation curves using the equations (2) and (3) are shown in Fig. 21 for the 5.0 $Kmin^{-1}$ heating rate. Both curves add up to the

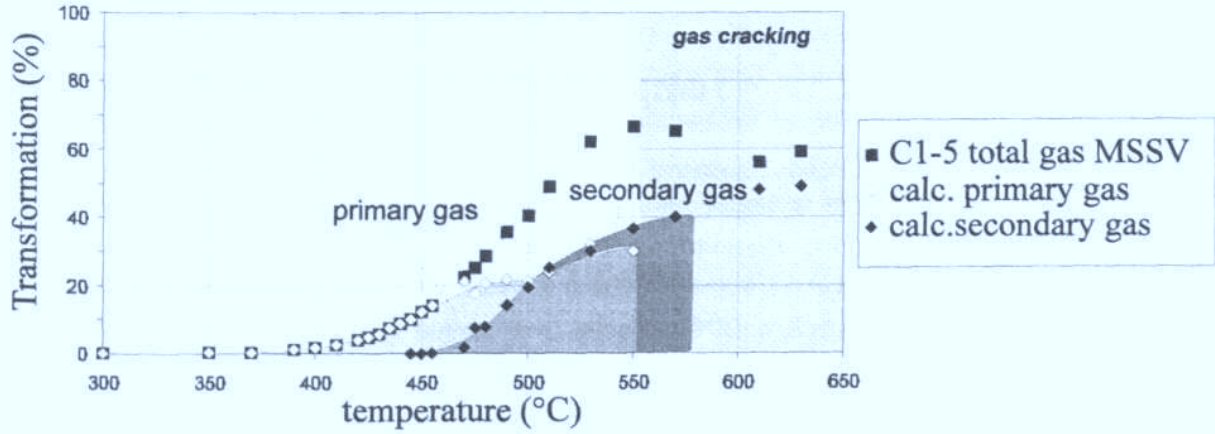


Fig. 21: Example for the results of primary and secondary gas generation evaluation using the refined mode. The sum of both curves equals the measured C_{1-5} total gas curve as derived from MSSV pyrolysis at 5.0 $Kmin^{-1}$ heating rate.

total gas curve which was initially measured. Primary gas generation starts at lower temperatures than does secondary gas generation and the amount of the latter exceeds the primary gas contribution. It can be observed that at temperature higher than 550 °C the total gas curve shows a slight decrease.

This feature must be related to the secondary cracking of gas components yielding methane and pyrobitumen or coke.

A comparison of the calculated primary gas curve with the gas generation obtained from open system pyrolysis (Fig. 22) shows a good agreement for low temperatures and a divergence for increasing temperatures. This might indicate that the stoichiometric assumptions in equation (1) are not in accordance with reality. Actually it is not possible to match reality because the compositions and therefore the H/C ratios of educts and products change successively as shown by Horsfield *et al.* (1992) and confirmed by the compositional development (see Fig. 51). Another reason for the deviation might be that the mechanisms for primary cracking reactions in closed and open systems work different. Catalytic effects of kerogen or petroleum as well as hydrogen partial pressure are among possible reasons for an enhanced primary cracking in a closed system.

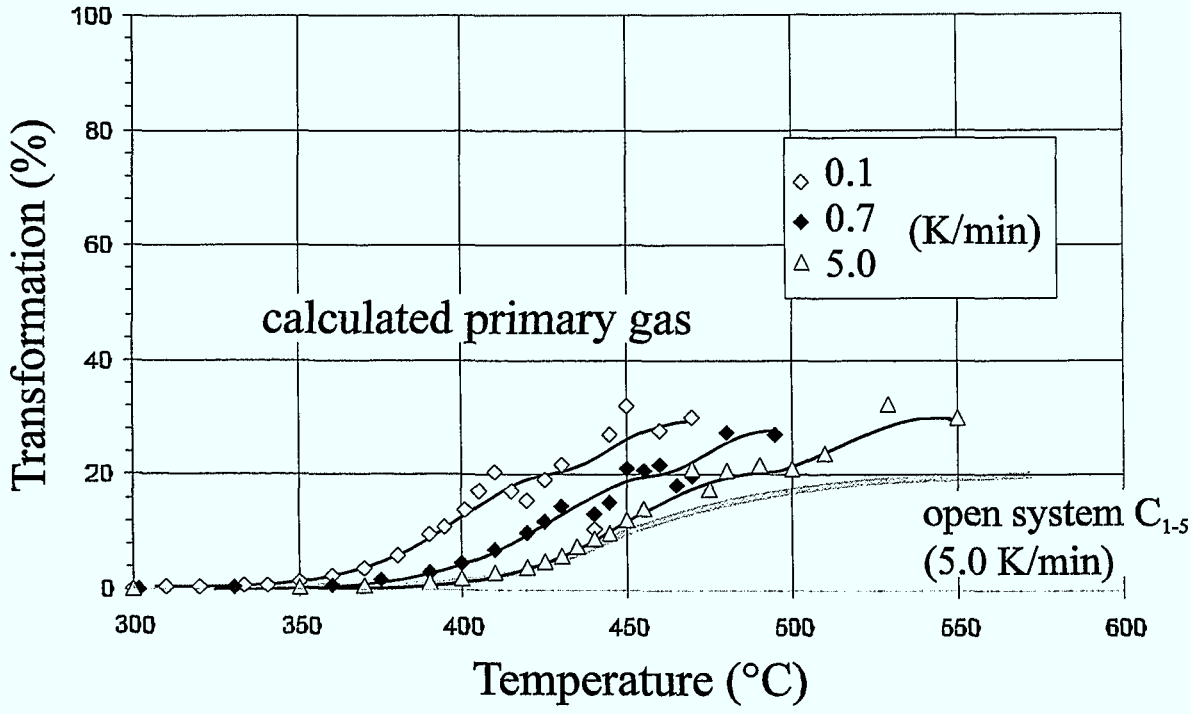


Fig. 22: Primary gas C_{1-5} generation cumulative curves. Calculated curves for MSSV pyrolysis at three heating rates and measured open system gas generation at 5.0 $Kmin^{-1}$.

The calculated gas formation curves reveal similar features for all three heating rates in that they show a flattening when they reach 20% whereas the overall maxima are attained at higher temperatures with approximately 30% of total product yields.

The respective formation curves resulting for secondary gas are depicted in Fig. 23 as amounts per sample weight. They are relatively smooth with a tendency to flatten in shape at higher heating rates while they exhibit sudden onsets due to the calculation procedure. Temperature spacings between the curves are relatively large and the total yields are lower for the 5.0 $Kmin^{-1}$ heating rate compared to 0.1 and 0.7 $Kmin^{-1}$. This observed heating rate dependence of pyrolysis yields for secondary gas is a

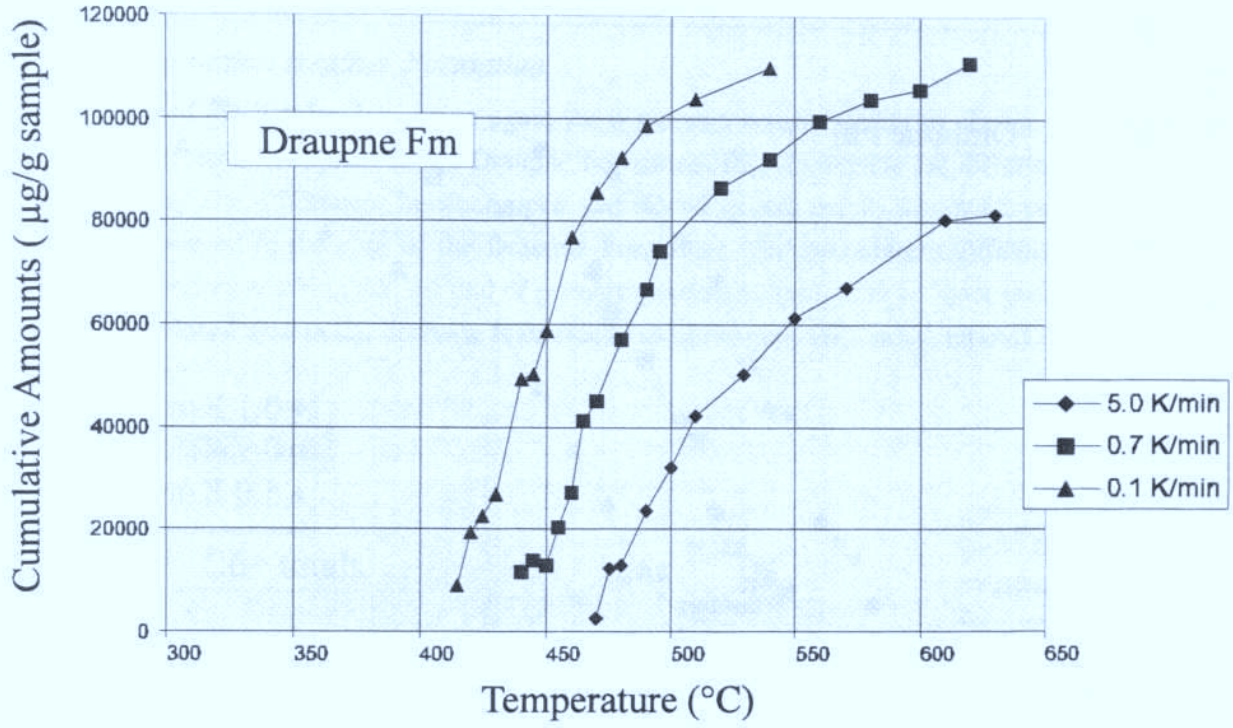


Fig. 23: Draupne Formation secondary gas formation curves. Calculated with the refined evaluation from MSSV pyrolysis at three heating rates.

consequence of lower C_{6+} and total product yields (cf. Fig.14, p. 35). The diagrams in Fig. 24 provide more information about the quality of the determined secondary gas generation curves. Fig. 24 (top) shows that the discrepancies in total amounts for the curves of different heating rates vanish if the curves are normalised to the total C_{1+} maximum pyrolysate yield.

The diagram in Fig. 24 (bottom) explains some of the irregularities in curve-shapes observed in Fig. 23. Secondary gas formation is calculated using the same equations but C_{6+} is split into two parts, the unresolved hump fraction and the resolved C_{6+} fraction (skim baseline). It is evident that the C_{6+} hump fraction undergoes secondary cracking much faster and with an onset at lower temperatures. The temperature intervals covered by the reaction are narrow by about 50°C and followed by well defined cumulative plateaus. Contrary to these observations the degradation curves calculated for the C_{6+} resolved fraction reveals by 25°C higher onset temperatures and changing curve shapes with increasing heating rates. In must be noted that the discrimination between secondary gas from hump and from resolved products as done here is theoretically possible but not necessarily valid because the cracking of C_{6+} hump probably results in C_{6+} resolved compounds as well as gas. However, the amount of secondary gas is in the same range compared to calculations using total C_{6+} (Fig. 23). It can be concluded that cracking of hump C_{6+} seems to be governed by significantly different processes compared to the cracking of C_{6+} resolved fraction. Therefore both were used for determination of kinetic parameters, instead of "bulk" secondary gas. The narrow temperature interval observed for the cracking of C_{6+} hump, indicates that few types of bonds seem to be present.

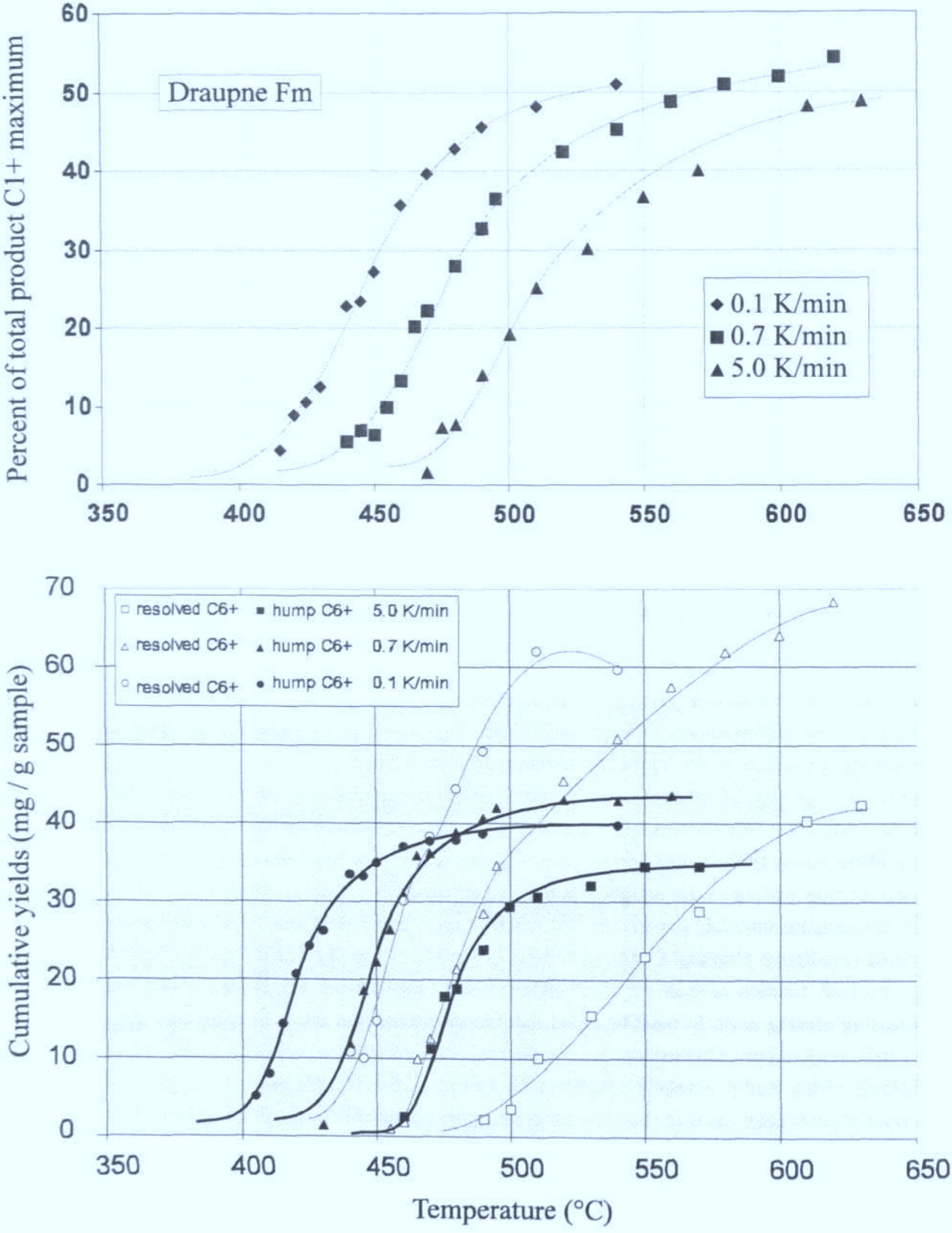


Fig. 24: The diagram at the top displays essentially the same curves as depicted in Fig. 23 but values are normalised to C_{1+} cumulative maximum yields. The bottom diagram shows secondary gas discriminated into a C_{6+} resolved fraction and C_{6+} hump.

Refined Evaluation Heather Formation

For the case of the Heather Formation again the discussion arises whether to use the conservative or the refined evaluation applied to the Draupne Formation. Fig. 25 depicts the different potentials for both methods. The differences between open and closed system curves are much more pronounced than was observed in the case of the Draupne Formation. The temperature difference between the onset of secondary cracking and the end of primary generation appears to be more than 100°C and the slope of the closed system C_{6+} decrease is markedly shallow, especially in the interval of 430-460 °C.

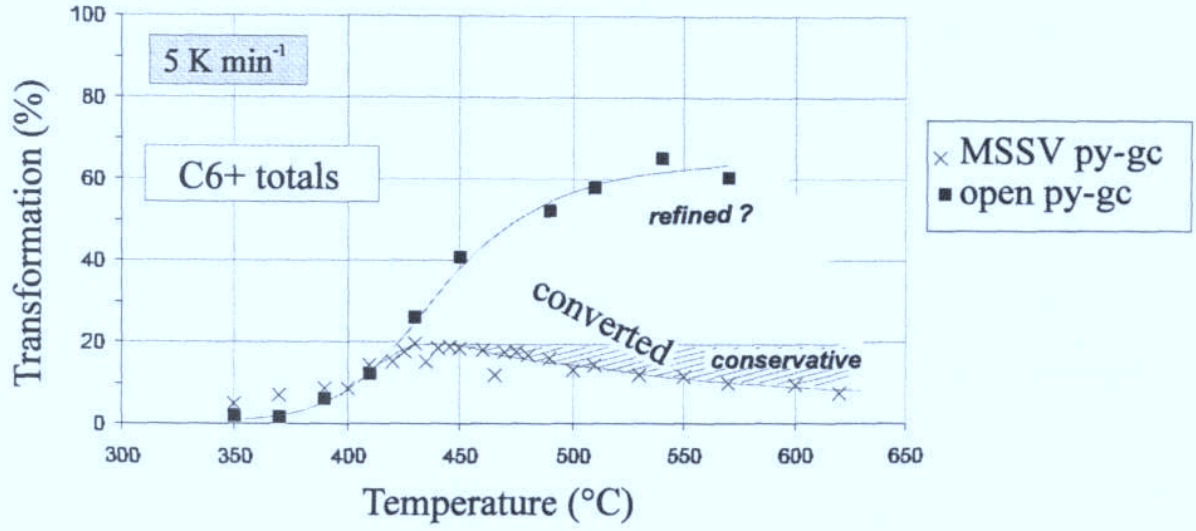


Fig. 25: Conservative and refined areas for conversion into secondary gas. The closed system transformation was calculated by using the open system as reference because the generation of products in MSSV pyrolysis was not completed.

Using the *refined evaluation* that considers the open system C_{6+} fraction would result in a tremendous amount of secondary gas (Fig. 26, left). This is not realistic because the calculated secondary gas even exceeds the amount of total gas that was measured. As a consequence the *remaining* or primary gas becomes negative according to equation (3). This is also not in accordance with the relatively high amounts of gas obtained from the open system (Fig. 26). Hence, it already becomes clear that in spite of the significant differences with regard to onset of secondary cracking and end of primary generation the evaluation like it was performed for the Draupne Formation is not applicable here. In contrast only minor amounts of secondary gas result from the *conservative evaluation* because only small amounts of oil (C_{6+}) are present. Consequently the "*remaining*" or primary gas makes up the major proportion of gas products (Fig. 26, right). The remaining gas curve is in accordance with the observed open system gas up to temperatures of 550°C. From this point the curves start to diverge in that the calculated remaining gas yield starts to increase strongly whereas the primary gas generation in the open system already reached an end. The increase of calculated gas can therefore be excluded to be of primary origin. The end of any primary processes at least at temperatures higher than 550°C (5.0 $Kmin^{-1}$) is additionally confirmed by Rock Eval type open system pyrolysis.

It is inevitable that the formation of gas at temperatures higher than 550°C in the closed system is a secondary cracking process whereby the source of the gas must be another as the volatile gc-

detectable C_{6+} fraction which was already consumed for calculation. Even the choice of a conversion factor higher

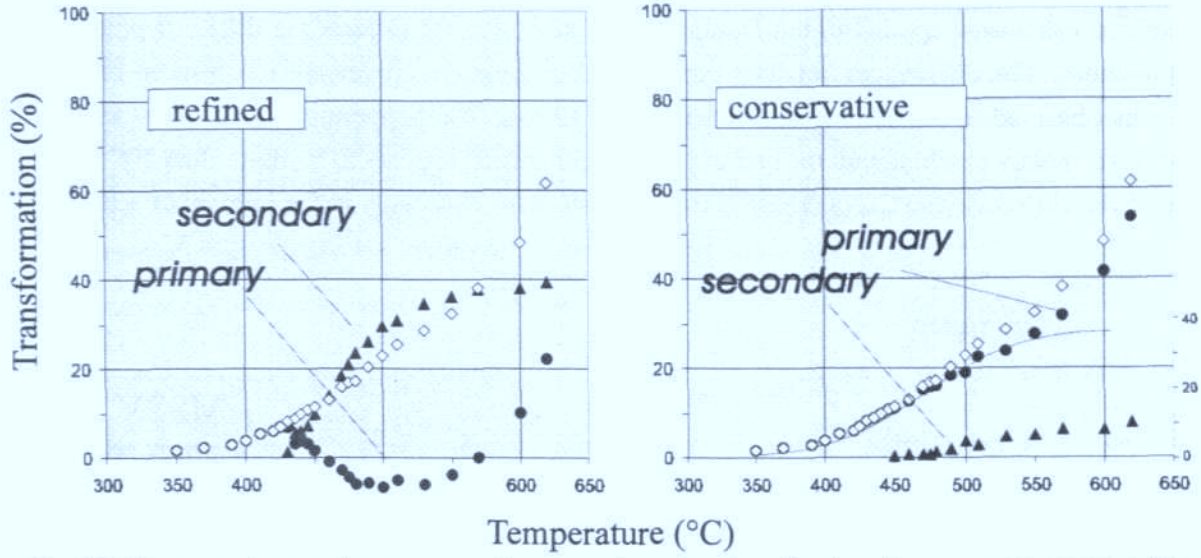


Fig. 26: Primary and secondary gas generation scenarios using the refined or the conservative evaluation method, the former was applied successfully to Draupne Formation (white rhombus total measured gas). In the right diagram the open system gas C_{1-5} generation curve shape is superimposed (thin line, different scale see Fig. 15).

than 0.7 (equation 2) would not result in amounts of gas which would be sufficiently high and finally it was stated in the beginning (page 36) that the gas generation can be assumed to continue until a value of approximately 103 mg/g TOC or 31 mg / g sample is reached.

Fig. 27 exhibits some features encouraging a new idea for the origin of the gas. The C_{1+} and C_{6+} curves are measured curves. The MSSV pyrolysis remaining area comprises calculated primary and

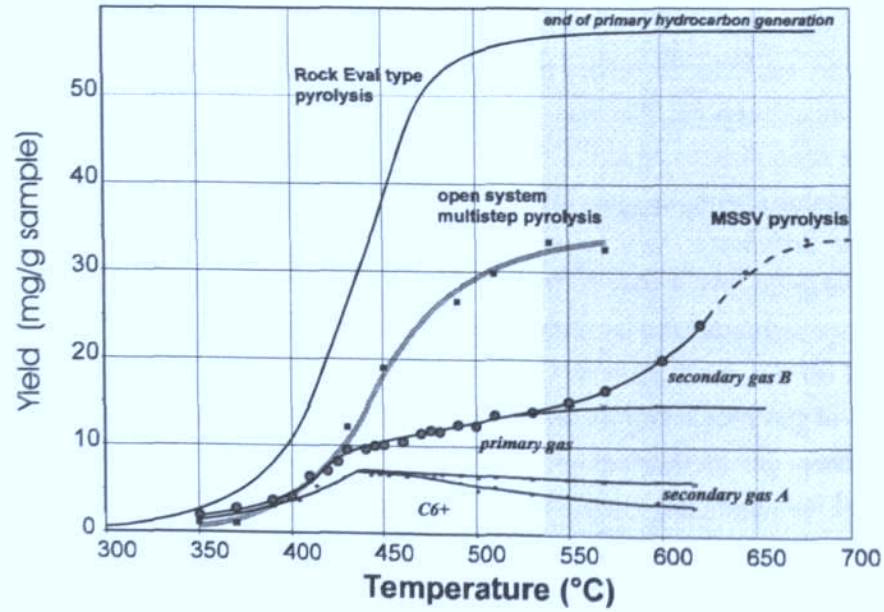


Fig. 27: Comparison of the results of Rock Eval type integrated total product generation, multistep open pyrolysis cumulative total product generation and closed system MSSV pyrolysis total product generation extended by questionmark to higher temperatures. The interpretation of the composition of MSSV pyrolysis products is discussed in the text. All data for a heating rate of 5.0 $Kmin^{-1}$.

secondary gas. C_{1+} is extended to the open pyrolysis plateau by questionmark. The delayed high temperature increase of the MSSV products compared to the open system C_{1+} is striking. The delay could be explained to result from the immobilisation of C_{6+} compounds in the closed system what would also explain the discrepancies for C_{6+} in Fig. 25. This immobilised C_{6+} proportion undergoes secondary cracking at temperatures higher than 550°C. Moreover the retention must be one which does not allow the products to be disconnected from the kerogen or removed from the MSSV glass tubes by temperatures as high as 300°C (temperature at which MSSV tubes are cracked open to analyse the products). Thus the immobilisation must be due to an extremely high average molecular weight of the C_{6+} fraction or to the formation of new chemical bonds. Two possibilities were considered:

A.) The high temperature gas is of secondary origin:

- The fact that secondary cracking starts before C_{6+} compounds reach their cumulative plateau (implied from the open system Fig. 25 and 27) gives ample evidence that a possible source results from an underestimate of the C_{6+} compound cumulative plateau. Thus one of the basic assumptions for the calculation of secondary gas is not valid for this type of kerogen. However, the application of the refined evaluation used for the calculation of the Draupne Formation gas did not yield reasonable results and the temperature range in which the repeated increase in gas formation occurs points to the presence of another process.
- It was suggested and shown in Fig. 27 that a proportion of the C_{6+} first formed products recombines with the kerogen structure (in the closed system). This would give rise to neo-formation of a thermally stable high molecular weight residue which undergoes secondary cracking at very high temperatures taking account for the delayed increase in gas formation. An investigation of this hypothesis as a gas generation-related process was performed and is described in the next chapter.

B.) The high temperature gas is the result of a mineral matrix retention effect:

- The possibility of simple retention of C_{6+} components on mineral surfaces can be ruled out with a high probability. The clay and pyrite assemblages which remain in the kerogen concentrate after the isolation procedure did not show comparable effects for any other experiment. However, it has been shown by Solomon & Rosser (1965) that clay mineral surfaces are able to catalyse the polymerisation of styrene. This was monitored by the authors for temperatures from 130 to 680 °C. Based on their findings it might be assumed that a recombination or above assumed neo-formation occurs with additional help of clay minerals.

The different types of gas as derived from the above performed investigations are summarised in Fig. 28. Primary gas generation dominates the overall scenario up to temperatures of 460, 490 and 520°C with increasing heating rate. Secondary gas generation from the decrease of C_{6+} compounds produces small amounts of gas and is of minor importance. The high temperature secondary gas formation which is assumed to be produced by the degradation of a neoformed bitumen or residue cannot be observed to its final stage but clearly provides a major source of gas. Because of this reason and in order to verify this process at least for the experiment the neo-formation and subsequent cracking is subject of the next chapter. The primary and different secondary gas formation curves presented in Fig. 28 provide the input data sets for the calculation of kinetic parameters

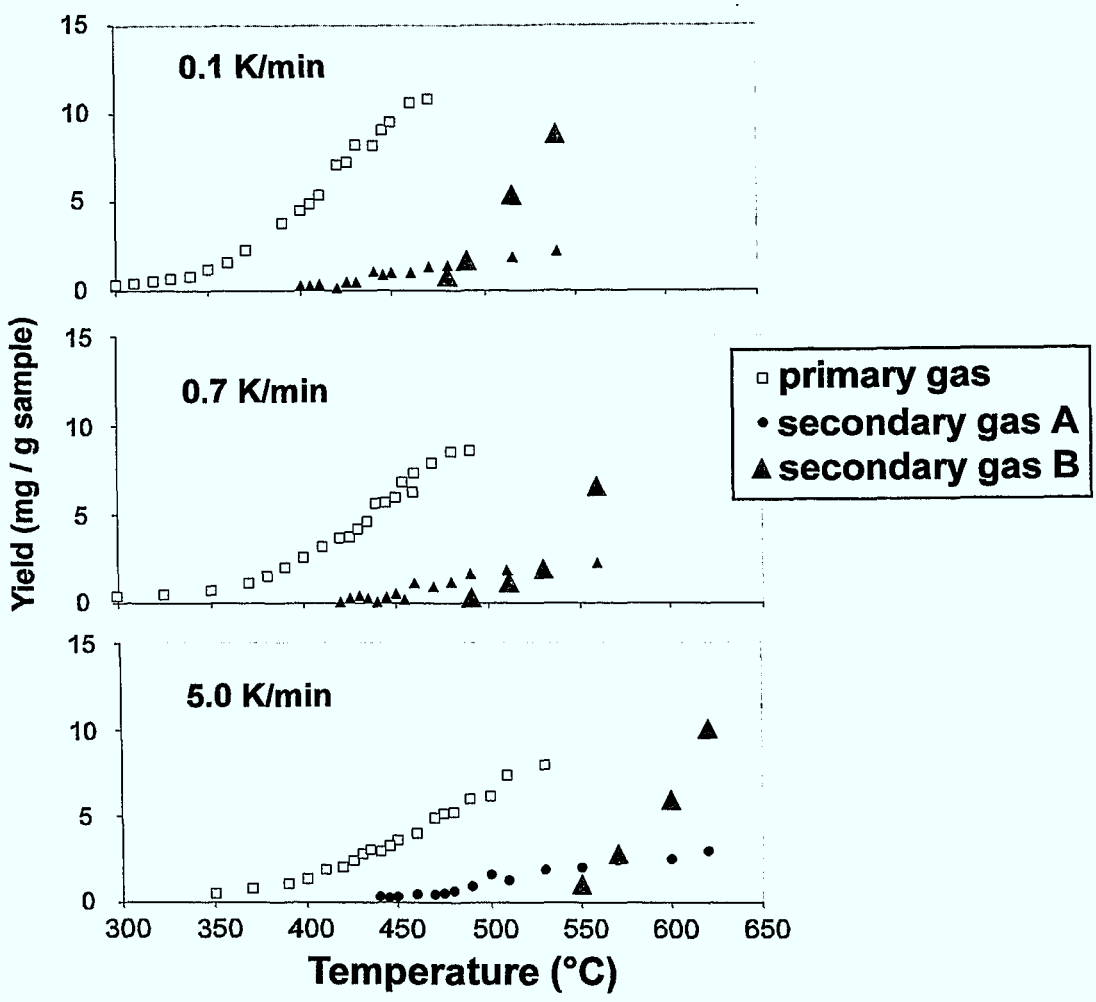


Fig. 28: MSSV pyrolysis. Calculated primary gas formation and two types of secondary gas formation, A = from total detected C_{6+} and B = from neo-formed residuum. Secondary gas A was calculated from the decrease of C_{6+} according to the equations 1-3. Secondary gas B is assumed to equal the gas formation above 550°C because primary production can be excluded.

3.3.6 Recombination and Cracking of Neoformed Residues

It was shown that for the case of Heather Formation MSSV pyrolysis a secondary gas generation was detected for which the cracking of the measured C_{6+} fraction could not account for. Therefore it was assumed that recombination of first formed C_{6+} products would take place to give a kerogen-like residue which underwent secondary cracking at elevated temperatures. This hypothesis was already confirmed to some degree by multistep open pyrolysis product evolution profiles. A review of literature revealed that a similar observation was made by Behar *et al.* (1991) for a type III kerogen. They observed an increased formation of methane at high temperature closed system conditions which they could not explain by degradation of first formed products, because of the overall small amounts of the latter. An origin of methane was thought to be the degradation of residual kerogen, which should be detectable by open systems. By comparison of gas generation from open and closed systems Behar *et al.* (1995) found that this "residual kerogen" (they stayed with this term) must be an intermediate product resulting from recondensation of products creating an asphaltene-like structure. To demonstrate the presence of a recombination residue for the case of the here investigated Heather Formation and in order to gain a better understanding of the respective processes several experiments were designed (Flow chart, p. 10).

The source or at least a part of the source for the high temperature secondary cracking gas was made visible by simple Rock Eval analyses (heating rate 25 $Kmin^{-1}$) of an extracted and an unextracted artificially matured aliquot. An artificial maturation temperature of 430°C at 0.7 $Kmin^{-1}$ was chosen with regard to avoid significant cracking of higher molecular weight compounds and in order to be close to the maximum of C_{6+} compound formation. It was assumed that the maximum of residuum formation could occur at temperatures comparable to the "visible" C_{6+} product maximum.

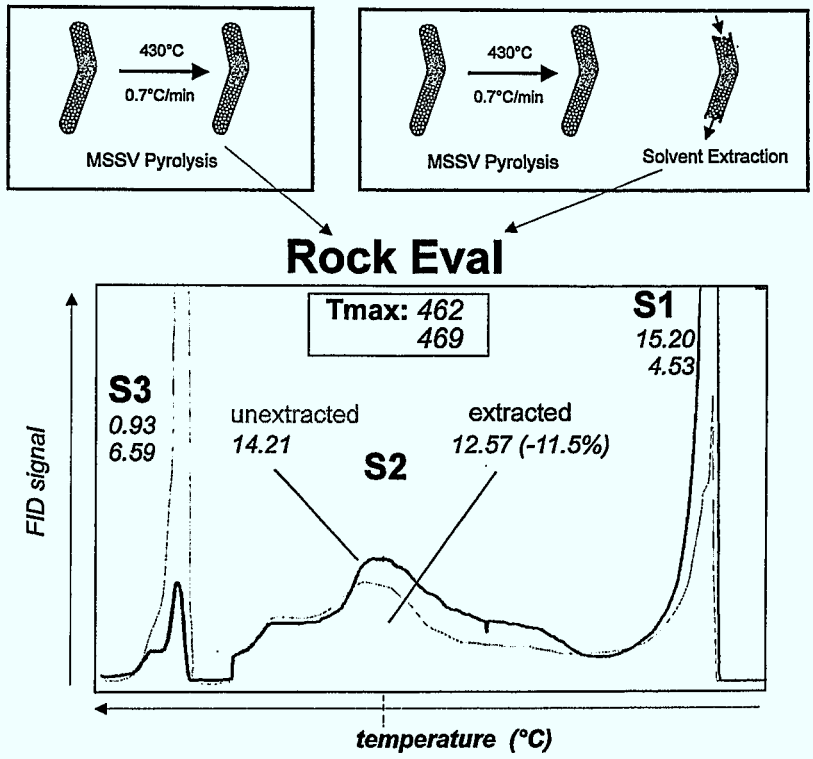


Fig. 29: Rock Eval screening analyses of an extracted and an unextracted aliquot of artificially matured (430°C at 0.7 $Kmin^{-1}$) Heather Formation sample E 41716 MK EC.

The idea was that recombined products might occur as a part of S2 which cannot be released by temperatures as low as 300°C but perhaps can be extracted by organic solvents. As a result the S2 was reduced by 11.5% (Fig. 29). This proportion is too small to explain the amounts of gas (Fig. 28) but the value must be considered as a minimum because extraction was not exhaustive and even S1 is not removed completely. Nevertheless it is also possible that the neo-formed organic matter cannot be removed by organic solvents. This corroborates that the neo-formation of bitumen was accompanied by the formation of chemical bonds, i.e. carbon-carbon or carbon-oxygen to the kerogen. The latter hypothesis would be favoured by the high abundance of phenolic structures in the kerogen, as inferred by open system pyrolysis (Fig. 5, p.21). The importance of oxygen is also confirmed by the strong increase of S3 (Fig. 29) for the extracted sample. It seems that the extraction made a release of CO_2 possible which was impossible before extraction for reasons that are unclear. Concerning the role of oxygen Enguehard *et al.* (1990) found from experimental decomposition of dibutylether serving as an oxgen containing model-component, that addition and recombination take place during closed pyrolysis. Besides of expected cracking products such as butane and propane they detected C_7 and C_8 alkanes and C_8 aldehydes. They stated that the role of pressure would be crucial for this type of reactions. This cannot be ruled out by interpretation of the here presented data.

Rock Eval type open system pyrolysis was performed on the artificially matured aliquot and compared to the results obtained from the immature sample in order to gain more information. It was attempted to see whether the neoformed bitumen can be observed by the occurrence of new potentials at higher activation energies as it was demonstrated by (Schenk & Horsfield 1996) for a naturally matured sample series of Westphalian coals. The authors stressed that for the case of a simple release by thermal cleavage the product formation curves of mature samples should be completely within the formation curve envelope of the most immature sample. This was not the case for the Westphalian coals where formation curves of mature samples indicated the formation of new activation energies. This approach was used in the beginning for the purpose of selecting samples for detailed analyses. From Fig. 30 it can be concluded that for the artificial maturation of Heather Formation exactly that seems to happen what was described for the natural maturation of Westphalian coals.

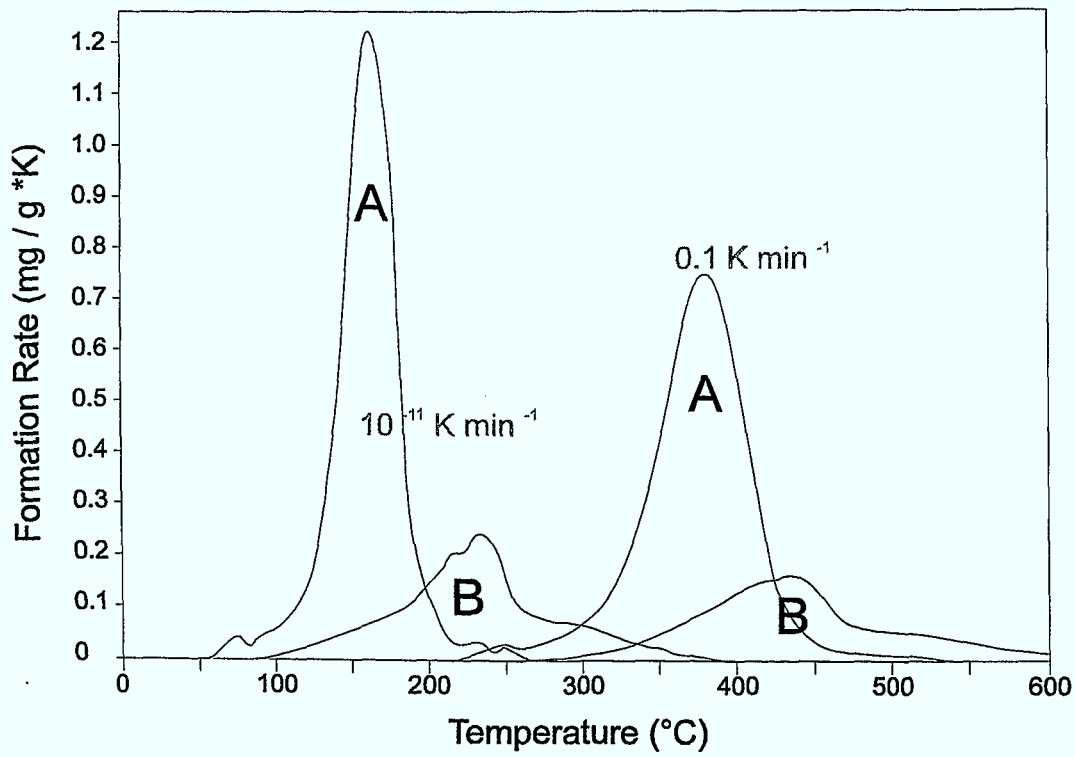


Fig. 30: Rock Eval type pyrolysis. Experimental (0.1 $Kmin^{-1}$) and extrapolated (10^{-11} $Kmin^{-1}$) product formation rates of the **A** immature (Ro=0.45%) and an **B** artificially matured sample (MSSV pyrolysis 430°C at 0.7 $Kmin^{-1}$).

Even if this new experiment confirms the formation of new activation energies and thus the formation of a thermally stable residuum which undergoes secondary cracking at higher temperatures, the obtained formation rate curve (Fig. 30, B) does not show the expected increase at temperatures higher than 460°C for the 0.1 $Kmin^{-1}$ heating rate. This indicates that the artificial maturation, which was performed in much larger glass tubes (150µl volume) compared to those of MSSV experiments, did not match the conditions of the small tubes pointing to the before mentioned role of pressure.

A more detailed investigation of the recombination product was attempted by employing pyrolysis of the isolated reactive proportion of kerogen. Therefore the Rock Eval S2 was isolated from the kerogen in order to be able to produce a neoformed material which is not in contact with the kerogen. This might of course not necessarily work because the kerogen itself probably plays an important role in

the recombination process. It was outlined by Lewan (1994) that free radical sites in the kerogen structure could be terminated by generated hydrocarbons what implies automatically that a part of the products is reconnected to the kerogen. He argued that this was inhibited in hydrous pyrolysis because free radical sites could be terminated by water derived hydrogen. In contrast Lillack (1992) and Monthioux (1988) stressed that sufficient amounts of hydrogen are also present if water lacks, due to hydrogen providing reactions during pyrolysis. Hence the subject is still controversial and the MSSV pyrolysis of isolated S2 might reflect the process under investigation to some degree.

The isolation procedure was simply an open pyrolysis using temperatures of 300-600°C at 40 $Kmin^{-1}$. The pyrolysates were trapped in an organic solvent and the procedure was repeated several times in order to obtain sufficient amounts of S2 for further investigations.

First of all the composition of the S2 isolate is addressed. The gc-ms run in Fig. 32 (top) shows that the isolated S2 proportion is made up of phenolic and aromatic compounds, n-alkanes/-alkenes and unresolvable compounds. The isolated S2 is depleted in light end products (< $n\text{-}C_{12}$) and might have lost some of its high molecular weight polar compounds on the furnace-cold trap interface but it is likely to contain large amounts of the moieties which react to form the neoformed residue in the closed system. Analyses of the isolated S2 by IR spectroscopy (Fig. 31) shows strong disturbing silicate bands for the kerogen concentrate and diffuse adsorptions for the S2 isolate. The latter is due to the difficulty in producing a homogenous mixture of isolated S2 with KBr. Nevertheless the aliphatic bands at 2900, 1443 and 1378 (1/cm) are present in both kerogen concentrate and isolated S2 and indicate that minor structural alterations occur during the isolation.

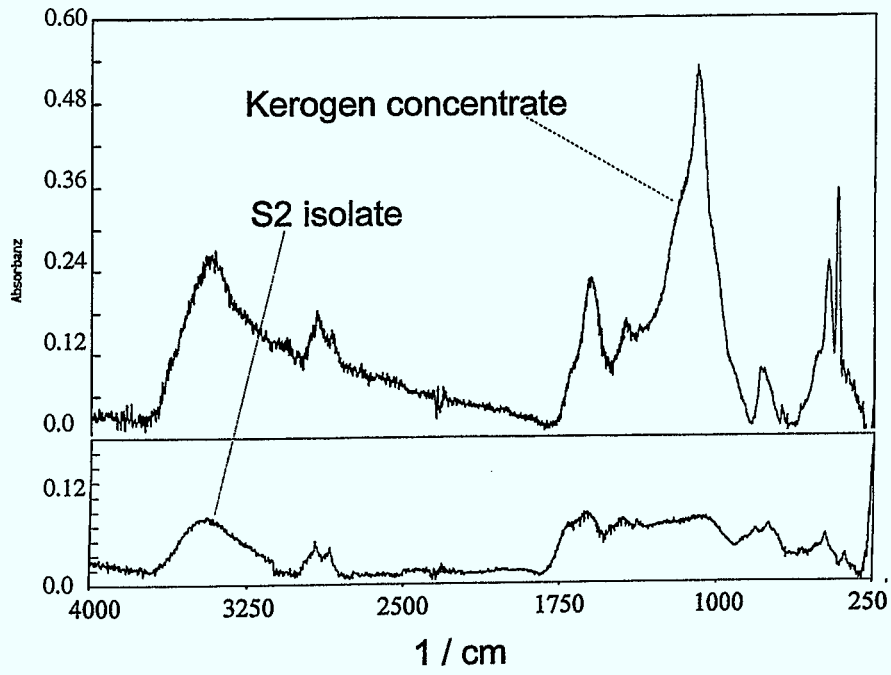


Fig. 31: IR spectroscopy of kerogen concentrate and isolated S2. Comparison of bands at 2900, 1443, 1378 and 780 (1/cm).

Independent MSSV pyrolysis using two temperatures (425°C and 515°C) were undertaken on the isolated S2 (Fig. 32, middle) and compared to the development of S2 in contact with the kerogen (left). The pyrolysis of the isolated S2 in the closed system produced a large proportion of residue

(78%) of golden-yellow colour which could not be removed by temperatures of 300°C from the MSSV glass tube, and a volatile pyrolysate (22%). Whereas the release of S2 in the presence of kerogen under closed system conditions resulted in the formation of simple mono- and di-aromatic hydrocarbons and mono- and dimethylated phenols, the pyrolysis of isolated S2 forms mainly saturated hydrocarbons with a maximum in chainlength at about n-C_{20} and a great variety of polyalkylated aromatic and phenolic components. Thus, apart from the contribution of chromatographically unresolvable compounds also long alkyl-moieties, alkyl- aromatics and -phenols seem to be involved in neo-bitumen formation. Observations of Monthioux (1988) might yield some additional evidence for the involvation of alkyl-groups in that aromatic but also aliphatic C-H bonds were shown to increase with maturity in naturally matured coals before they started to decrease. In the here discussed experiments the main proportion of S2 pyrolysate is however already implemented into the solid residue which makes up approximately 70-80% of total products.

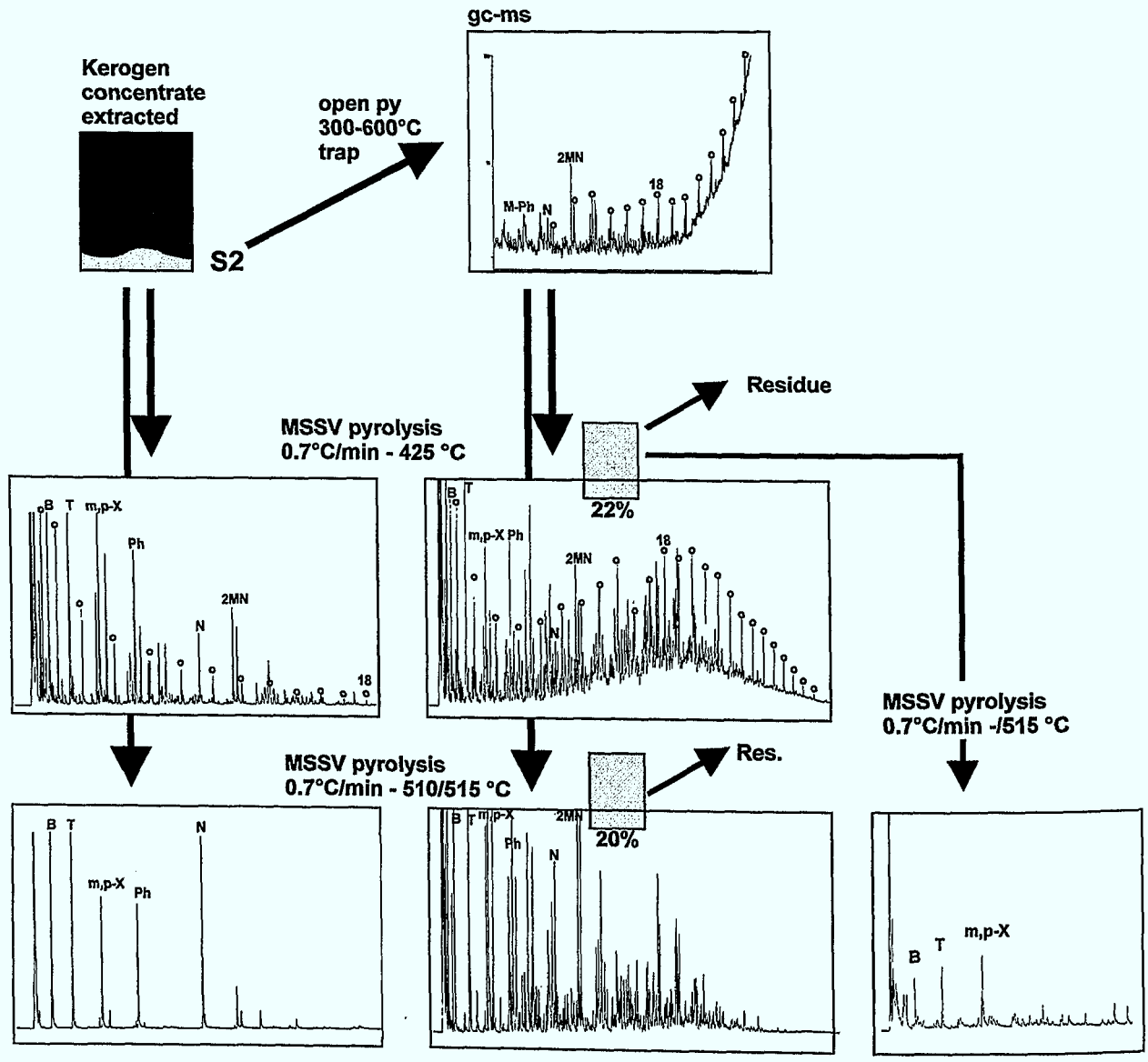


Fig. 32: Heather Formation (E 41716 MK EC), evolution of pyrolysis products from kerogen concentrate versus evolution from isolated Rock Eval S2. Implications for the composition of neoformed bitumen, and gas from cracking of this bitumen (bottom, right).

Pyrolysis of this char or neoformed bitumen was thought to simulate the secondary cracking of the substance when it is not in contact with the kerogen (Fig. 32 right). The pyrolysate consists of gas C_{1-4} and some mono-aromatic components and is actually not as rich in methane as expected. The gas wetness is 40% and the i/n butane value is high with 2.22.

Different arguments for the formation of a thermally stable residue which undergoes secondary cracking at high temperatures were presented. The assumed responsible process, recombination, is part of the generally accepted chain reaction mechanism.

- The formation of MSSV products is partly delayed to higher temperatures compared to open pyrolysis.
- The Rock Eval S2 of an artificially matured sample aliquot decreases upon solvent extraction.
- The bulk petroleum formation rate curve of this artificially matured aliquot is shifted to higher temperatures and does not fall within the envelope of the immature sample, thus indicating the formation of new activation energies.
- Pyrolysis of an isolated S2 proportion yields a golden yellow residue which remains in the glass tubes at T=300°C and yields also a pyrolysate which is rich in aliphatics and complex alkylated aromatic and phenolic components, indicating that these components form part of the neo-formed residue structure during kerogen pyrolysis.
- Pyrolysis of the golden yellow residue yields C_{1-4} gas, confirming the presence of a remaining potential of this residue, which can be assumed to be higher, if the residuum is formed in contact with kerogen.
- The formation of such residues during experiments was also reported by Béhar *et al.* (1991, 1995) and their significance for natural systems might be inferred from the formation of new activation energies in coals upon maturation (Schenk & Horsfield 1996).



Concluding remarks, heating experiments

- Primary and secondary cracking was quantitatively determined from results of MSSV closed pyrolysis in order to obtain input data sets for both processes for kinetic modelling.
- Input data sets established for Draupne Formation comprise primary gas and two types of secondary gas, which are secondary gas from cracking of hump and from cracking of C_{6+} resolved fractions.
- Input data sets established for Heather Formation are primary gas and two types of secondary gas, which are secondary gas from cracking of total detectable C_{6+} and secondary gas from the cracking of a neo-formed residuum, which is actually no visible gc-product.

3.4 Kinetics of Gas Formation

The before discussed chemical reactions, i.e. primary and secondary gas formations, can also be described in terms of reaction velocities or reaction rates, that means the change of educt and product concentrations for a given reaction with temperature and time. The determination of corresponding rate laws is the task of kinetic considerations which are thought to be applicable for gas generation since Tissot (1969) and Lopatin (1971). The knowledge of such rate laws enables predictions for low-temperature long-time conditions on the basis of observations at high-temperature short-time conditions, e.g. various pyrolysis experiments. Well defined reactions cannot be recognised for the case of kerogen degradation or oil breakdown, and therefore "bulk" kinetic concepts are used, as reviewed by Ungerer (1990) and lately by Schenk *et al.* (1997). Most of these models are based on the assumption that the overall reaction for petroleum and gas formation can be expressed as an unimolecular decay,

$$A > B + C + .. \tag{4}$$

where A is the kerogen, oil or bitumen and B, C .. are products. This type of reactions follows a first order kinetic law with respect to the educt and can be expressed as

$$-d(A)/\,dt = k * (A) \tag{5}$$

The temperature dependence of this law can be expressed by the semi-empirical Arrhenius law which describes the "rate constant" k as a function of temperature.

$$k\,(T) = A * \exp^{(-E/RT)} \tag{6}$$

where A is a pre-exponential factor (1/t), E the activation energy (J/mol or kcal/mol), R the gas constant and T the temperature (K). A further development is the determination of the temperature dependence of the frequency factor A in the transition state theory. But for the case of petroleum formation measurements are not accurate enough for such evaluations (Schenk *et al.* 1997).

The overall reaction of gas formation is assumed to consist of multiple parallel and consecutive component reactions. Schenk *et al.* (1997) explained that for the case of consecutive reactions the slowest elementary reaction and for the case of parallel reactions the fastest elementary reaction will govern the overall reaction rate. For chain reaction systems which are composed of the reaction rates of all participating reactions initiation is of first order, propagation reactions can be of order 1 or higher and terminations are of orders higher than 1 (Ungerer 1990). In this regard Rice and Herzfeld (1959) could show that the decomposition of acetaldehyde did not follow first order kinetics. The authors suggested a reaction order of 1.5 due to a chain terminating mechanism. Moreover hydrodealkylation reactions which occur in closed systems are of reaction orders higher than 1 (Malhotra *et al.* 1989, Silsby & Sawyer 1956) because they depend on the availability of hydrogen. Beside the reaction order, chain reaction steps are also known to have different ranges of activation energies/ frequency factors. Ungerer (1990) reported that initiation reactions have the highest, termination reactions have zero and propagations have intermediate kinetic parameters. Some evidence will be shown in the next chapter however, that for initiation not necessarily the bond-strength is the controlling parameter but random cracking, i.e. the formation of radical centers.

Translated to gas formation these considerations mean that the knowledge is important whether reactions can be considered consecutive or parallel and which chain-reaction step wins and looses importance during maturation and experiment.

In this context it becomes automatically important whether kinetic parameters derived from laboratory measurements remain valid under geological heating conditions because reactions might be parallel in the experiment whereas they are consecutive in nature or vice versa. Larter & Horsfield (1993) outlined this possibility using a bulk chemical concept. They concluded that the reactions kerogen > bitumen and bitumen > oil have only slightly different kinetic parameters so that they appear be the same from laboratory observations. Consequently the hardly detectable crossover in an Arrhenius plot based on laboratory measurements would lead to the bitumen > oil reaction as the rate controlling reaction whereas in nature it would be the kerogen > bitumen reaction. This might be an explanation for differences in pyrolysate compositions and naturally occurring petroleum, still being a point which cannot easily be explained. Juentgen & Van Heek (1968) and references therein stated that heating rates might have an impact on the composition of products from thermal degradation reactions which is in line with the idea of competing reactions.

The applicability of laboratory derived kinetic parameters was objected by Snowdon (1979). His views focussed on the uncertainty of the Arrhenius law temperature independence of kinetic parameters so that competing and consecutive reactions might yield different results in low and high temperature regimes. An interesting point also connected to the temperature dependence of kinetic parameters that was raised by Snowdon (1979) derives from quantum chemistry, namely the effect of tunneling. In short, this mechanism can be explained as the probability that low-mass particles like electrons overcome energy barriers, which are higher than the particles own energy without raising the latter. This effect might have an impact on the reaction rates of radical supported chain reactions in low temperature regimes, especially for the formation of radical centers. The tunneling effect was also reported as a possible reason for deviations from the Arrhenius law in the context of ethane cracking (Pilling 1980). However, Braun *et al.* (1991) rejected these objections when they stated: "a change in reaction mechanisms cannot cause a deviation from the Arrhenius law", and Schenk *et al.* (1997) concluded that: "from a physico-chemical point of view and in terms of applicability the Arrhenius theory is considered as the most adequate approach taking account of the temperature dependence of petroleum generation reactions". Finally the applicability of laboratory kinetic parameters was tested by Juentgen & Van Heek (1968). They predicted the formation of gas products for a higher heating rate and verified their predictions by measurements. Barth *et al.* (1996) tested the applicability of open system derived kinetics by comparing the predictions obtained from such a system to the formation of products from hydrous pyrolysis experiments. They could not confirm the overall applicability but obtained some encouraging results. Braun *et al.* (1992) used a similar approach but concentrated on the generation of acetic acid. They stated a favourable agreement between predictions and hydrous pyrolysis results. For the case of predictions for geological heating conditions based on laboratory derived kinetic parameters detailed studies of Ungerer & Pelet (1987) and Quigley & Mackenzie (1988) confirmed that natural basin geochemical data can satisfactorily be matched.

To obtain measurements for kinetic analyses one can choose between isothermal or non-isothermal pyrolysis, the latter occupying different heating rates. The validity of non-isothermal kinetics has been discussed by Schenk (1997) and references therein. Tang & Stauffer (1993) found from their

investigations good agreement between the kinetic parameters derived from both approaches, but non-isothermal kinetics has a crucial advantage, that is the determination of the frequency factor by the shift in T_{max}. Additionally a systematic control during the first phase of experiments is provided. For isothermal experiments a short ramp (non-isothermal step) has to be used as well in order to reach the temperature which was selected for investigation. Even if this time is very short significant errors might be produced. Not the least the non-isothermal heating comprises a better similarity to gradual heating of source rocks in nature. Data which are employed below are produced by non-isothermal MSSV pyrolysis, and the determination of input data sets was described in the previous chapter.

3.4.1 Determination of Kinetic Parameters and Extrapolation to Linear Geological Heating Conditions

Details of the procedure employed to determine kinetic parameters from MSSV pyrolysis data are described in the chapter *Methodology*. It should be noted here again that specific frequency factors for compound groups or hydrocarbon boiling ranges are obtained by this method. The authors outline this to be realistic for complex hydrocarbon forming systems of n-parallel reactions where specific frequency factors can be considered as mathematical optimisation parameters.

Bulk gas formation was investigated as well as the different primary and secondary gas formations which were found to be relevant. Additionally the kinetic parameters for the formation of oil (C_{6+}) were evaluated mainly for reasons of comparison with results from bulk kinetic determinations by open system pyrolysis. This is an important thing to be done because the determination of kinetic parameters should be independent of the analytical device. Schenk & Horsfield (1993) could show that kinetic parameters derived from Rock Eval type open system pyrolysis and MSSV pyrolysis were almost identical for the case of a Toarcian shale sample. The analytical systems used here are essentially the same as in the work presented by Schenk & Horsfield (1993).

Single gas components were found to be extremely affected by secondary cracking of long-chain hydrocarbons. The impact on MSSV pyrolysis cumulative formation curves is significant in shifting the maxima to much higher temperatures leading to a steady increase of methane the end-point of which is beyond the normal operation of MSSV pyrolysis. It was concluded from this observation which is also addressed later (see *Petroleum Forming Reactions*) that the individual gas component curves incorporate the largest number of contributing reactions. In contrast to the approach used for secondary and primary gas calculation, primary and secondary ethane for instance cannot be discriminated. An evaluation of kinetic parameters for a single gas component includes therefore primary as well as different secondary product formations. Despite being formed from a large number of reactions with high activation energies / frequency factors, the model assigns only one broad energy distribution with spuriously low mean Ea and A values to the formation curves (Juentgen & Klein 1975). Ethane and propane are the only components which were used for analyses despite of these objections and the results are further employed for the extrapolation of isotope-fractionation effects to geological heating conditions, later in this study.

The input for the calculation of reaction kinetic parameters is provided by the MSSV pyrolysis gas formation rate curves determined at three heating rates. The output is in form of potential versus activation energy distributions with a corresponding frequency factor. Predicted gas formation rate curves for reasonable linear geological heating rates are calculated from these parameters. In the following chapter these will be extended to non-linear heating rates of a heating history by using a

basin modelling case study. The quality of predictions of this type either linear or not depends on the quality of laboratory measurements. Especially the correct determination of T_{max} peak generation is crucial, because the shift in T_{max} for different heating rates determines the start frequency factor in the kinetic parameter calculation. Schenk *et al.* (1997) explained that for open system measurements an error of +/-1°C arises from the experimental system which translates to a prediction error of 4%. For a geological T_{max} of 400K (127°C) this would be an error of 12°C. For the case of closed system pyrolysis the error is probably higher caused by the introduction of cumulative plateaus, spline approximations and subsequent differentiation of the curves. Results presented below are also listed in Table 22 and 23 in the Appendix.

Primary Gas Generation

Draupne Formation

The differentiation of cumulative primary gas curves resulted in first derivations with a shoulder on the left flank, which originate from the irregularities in slopes as shown in Fig. 22. Because of these irregularities relative simple spline approximations had to be chosen which in turn result in the somewhat rough shape of the differentiated curves. Calculation of best fitting model curves resulted in the kinetic parameter set displayed on the left hand side in Fig. 33. A broad activation energy distribution with a pronounced main energy of 54 kcal/mol and a low frequency factor are significant results which fall in the range of bulk petroleum kinetic parameters often reported for kerogen type II.

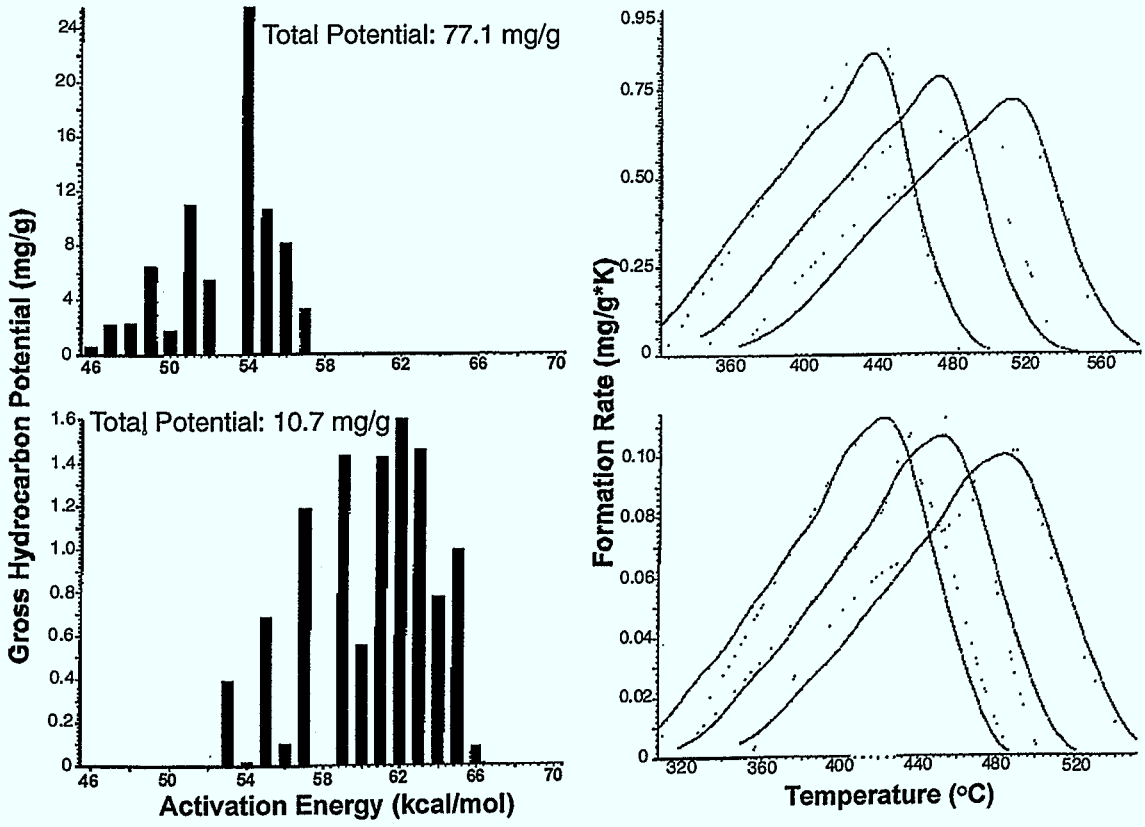


Fig. 33: Measured and calculated formation rate curves for primary gas generation at heating rates of 0.1, 0.7 and 5.0 $Kmin^{-1}$ (right) and kinetic parameters for **Draupne Formation (top)** and **Heather Formation (bottom)**. Potentials are in mg per g sample.

Heather Formation

The primary gas curves were used for analysis of kinetic parameters. Fig. 33, bottom shows that there is a good agreement for the first derivations of curves with the iterative approximated calculated curves as derived from the kinetic parameter set on the left hand side. The spacings between the T_{max} values for different heating rates are relative close (appr. 30-33 K) if compared to those for Draupne Formation (appr. 40 K). This is the reason for the much higher frequency factor. The activation energies range from 53 to 65 kcal/mol which is an even broader distribution as detected for Draupne Formation. The main energy is 62 kcal/mol with a corresponding high frequency factor.

The extrapolation of primary gas generations of both source rock units to a geological heating rate of 10^{-11} $Kmin^{-1}$ 5.3 K/ma is depicted in Fig. 34. Heather Formation primary gas generation is predicted to cover a slightly broader temperature range (~130°C) and to have a higher peak generation temperature (190°C, Ro appr. 1.7%) compared to Draupne (T_{max} 175°C, equivalent to Ro 1.3%, Fig. 40). This is in accordance with the differences described for the kinetic parameter set. The predicted onset of gas generation is in the range of 100 / 120°C for Heather and Draupne, corresponding to Ro =0.53 / 0.66%.

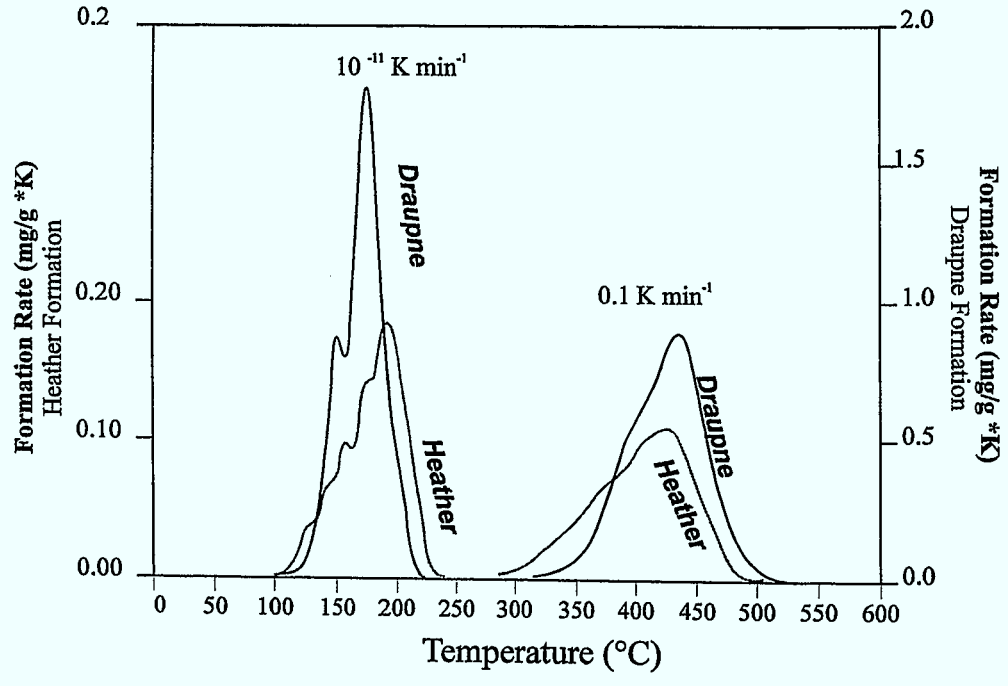


Fig. 34: Primary gas C_{1-5} formation rate curves for Heather and Draupne Formation. Slowest laboratory heating rate and extrapolation to a geologically reasonable heating rate. Note different scales for Heather and Draupne.

From the change in the relative order of generation curves from both samples at fast and slow heating rates it can be further predicted that for heating rates slower than 10^{-11} $Kmin^{-1}$ the Draupne Formation generation window will shift faster to lower temperature as will Heather Formation. The specific shape and kinetic parameters found for primary gas generation from both source rocks corroborates the accepted opinion that gas generation from terrigenous organic matter requires higher temperatures. The shape of Heather Formation gas generation is especially biased to high temperatures probably due to high contributions of methane.

Secondary Gas Generation

Draupne Formation

Attempts to determine kinetic parameters for C_{1-5} secondary gas generation from C_{6+} failed, probably because differences in kinetic parameters from contributing reactions are too large. In the chapter *Heating Experiments simulating Gas Formation* in was outlined that several processes, most likely three of importance, are involved in the secondary cracking of C_{6+} components. The discrimination between cracking of hump and resolved compounds resulted in well defined curves for the hump and heating rate dependent alterating curves for C_{6+} resolved (page 45). In the latter curves also two processes which obey different kinetic parameters are involved. These might be for instance, cracking of n-alkanes and dealkylation of aromatics. For the differentiated secondary gas formation curve (C_{1-5}) these features become pronounced again, in that two maxima appear (Fig. 35, bottom). Consequently this results in the calculation of two main energies at 62 and 66 kcal/mol. The "measured" differentiated curves clearly follow a heatingrate dependence and therefore the accuracy of the best fit calculation is poor. Fig. 35 (top) in contrast shows narrow curves for secondary gas from hump degradation with small temperature differences of about 30°C between T_{max} values. The activation energy distribution which results in a best fit comprises 3 energies of 70-73 kcal/mol .

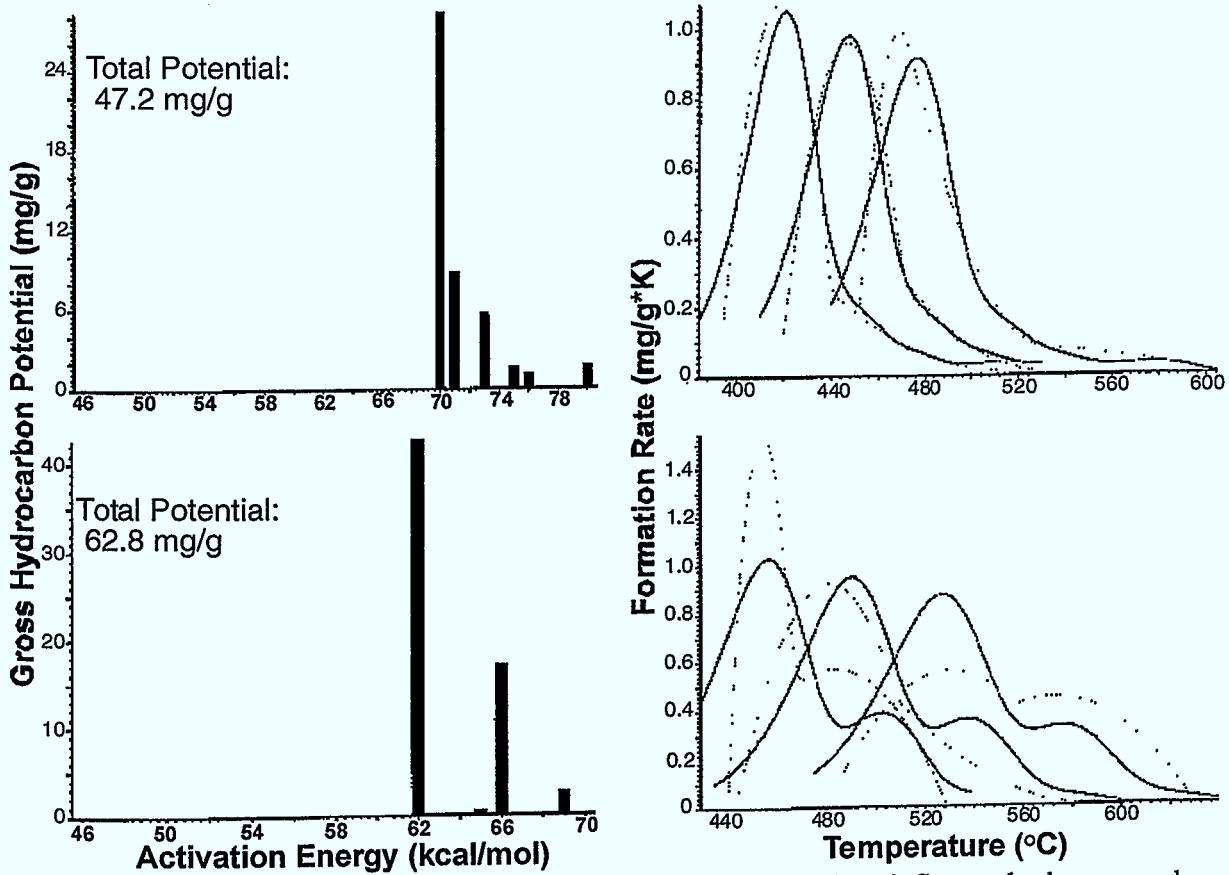


Fig. 35: Secondary gas formation from C_{6+} hump degradation (top) and C_{6+} resolved compound degradation (bottom). „Measured" and calculated formation rates (right) and corresponding kinetic parameters (left). Draupne Formation.

This implies a homogeneous composition for the hump with thermally relative stable constituents. Hence, even if a determination for C_{1-5} secondary gas from the decomposition of total C_{6+} was not possible, a splitted secondary gas generation from the cracking of hump and C_{6+} resolved fractions resulted in reasonable kinetic parameters sets.

Heather Formation

The secondary gas for the Heather Formation was calculated from the decrease of total C_{6+} compounds. In Fig. 36 the "measured" and the calculated best-fit curves are displayed. The quality of the measured curves seems to be poor at first glance but the results from kinetic analysis (Fig. 36, left) with a main energy of 66 kcal/ mol are in a similar range as values determined for Draupne Formation secondary gas from C_{6+} resolved compounds. Moreover it must be kept in mind that because of the small amount of C_{6+} compounds no discrimination between different secondary processes as considered for Draupne was performed. Interestingly the activation energy distribution is not restricted to one or two energies but relative broad by covering 10 energies (kcal) and the potentials do not show any gaussian like distribution but reveal values which are all of the same order of magnitude except for the lowest and the highest values.

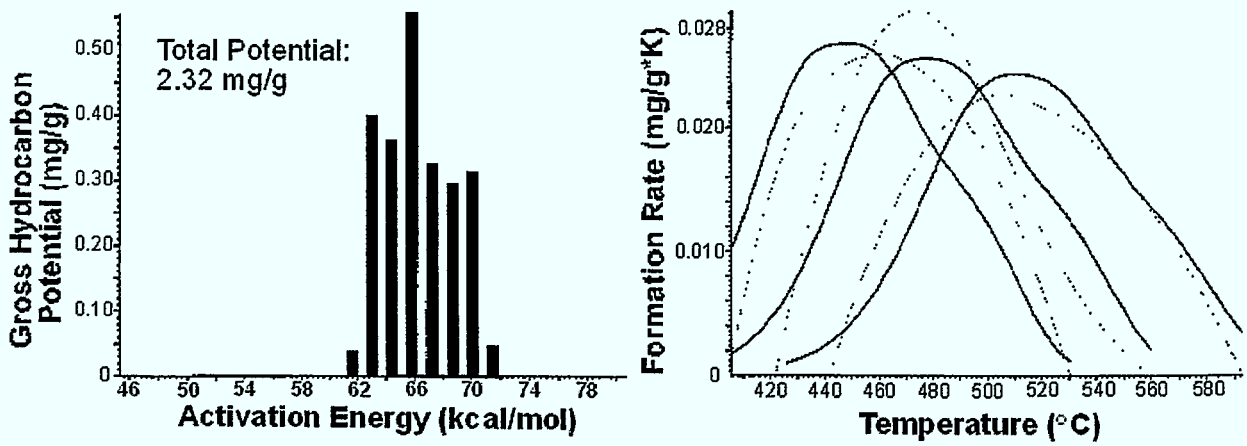


Fig. 36: Heather Formation secondary gas from C6+ degradation. Right: "measured" and calculated formation rate curves for three heating rates. Left: Corresponding kinetic parameter set.

A second type of secondary gas, i.e. the cracking of a neoformed bitumen (page 48) was found to be of importance for Heather Formation. It was not possible to perform a determination of kinetic parameters for this type of gas seeing as only 3-4 data-points in the appropriate high temperature range for each of the three heating rates were available. From considerations using open system total product amounts it was concluded before that the overall amount for this type of gas generation could reach values of more than 13 mg/g. The required experimental temperatures to reach the end of this process which must be assumed to more than 700°C are too high to be performed with the employed analytical set-up. Based on the observation that the relative order of compound group formation curves remains more or less the same for a single sample this mode of methane generation can be predicted to be a high temperature process in the geological system. This is also documented in Fig. 37 where the expression E/(lnA -ln r) as a measure of T_{max} is plotted versus the logarithm of the heating rate (ln r). The relative order of primary gas, secondary gas and oil (C_{6-14}) remains essentially

the same for all laboratory and geological heating rates. For the purpose of demonstrating the importance of this type of gas a conservative

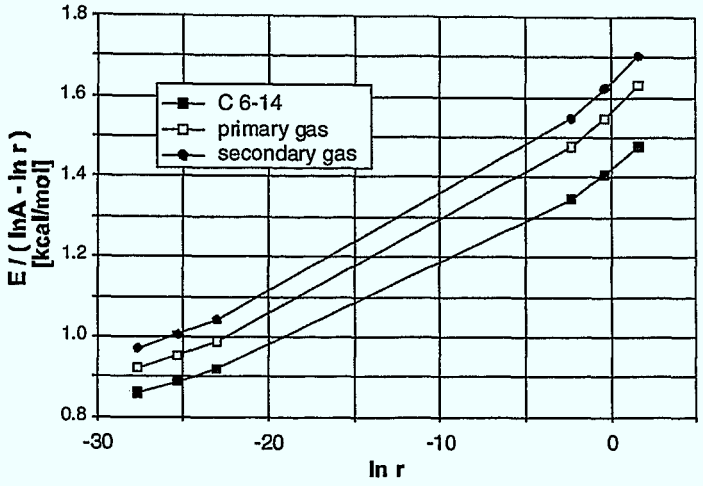


Fig. 37: T_{max} as an expression of kinetic parameters and heating rate. T_{max} measures for C_{6-14}, primary gas and secondary gas (C_{6+} decrease) from Heather Formation.

assessed maximum amount of 13 mg/g sample was used to calculate a differentiated laboratory curve for experimental conditions (Fig. 38). The amount stems from the calculated yields for this type of gas which range from 7-10 mg/g sample plus 8 mg /g sample (page 37) of gas that remains to be produced.

The measured and predicted secondary gas formation rate curves for Heather and Draupne Formation (Fig. 38) both indicate higher temperature ranges as found for primary gas generation in Fig. 34. The T_{max} for Heather secondary gas from C_{6+} cracking at a heating rate of 10^{-11} $Kmin^{-1}$ (5.3 K/ma) is approximately 220°C and for the two types of Draupne gas 205 to 215°C. This is equivalent to

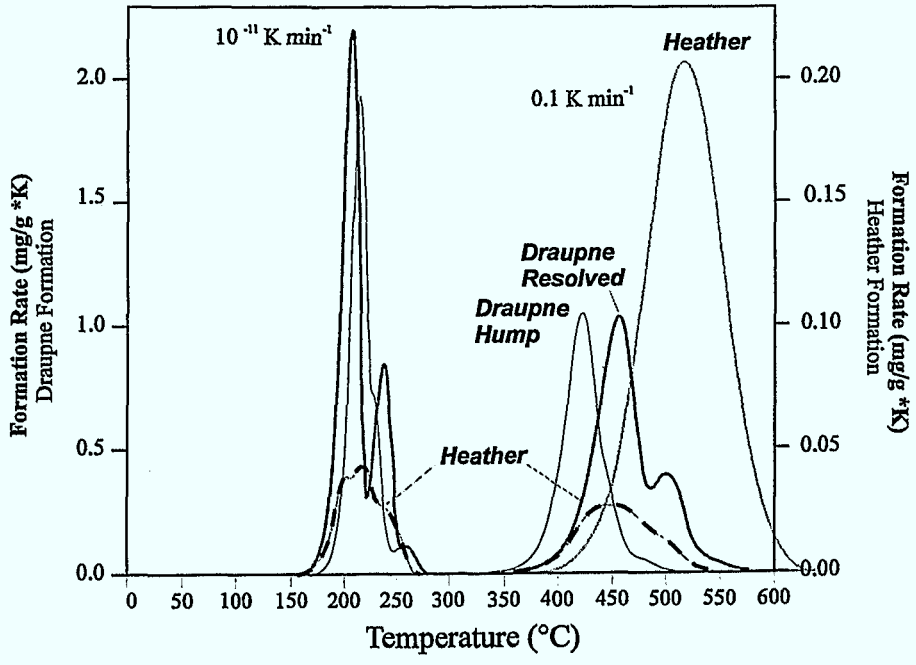


Fig. 38: Secondary gas from cracking of C_{6+} hump and C_{6+} resolved compounds, Draupne Formation and C_{6+} total Heather Formation. For secondary cracking of neoformed bitumen a formation rate curve for laboratory conditions was constructed (see text). Left, predicted rate curves at a geological heating rate and right, measured rate curves at an experimental heating rate.

Ro values of 2.4% and appr. 2.0% respectively (Fig. 40). The outstanding laboratory curve for secondary gas from cracking of neoformed bitumen for the case of Heather Formation has a much higher T_{max} (515°C) than any other observed secondary gas. Heather Formation secondary gas from C_{6+} was not investigated for separate gas forming proportions like performed for Draupne Formation. In spite of this, it turns out from Fig. 38, that the secondary gas covers an identical temperature interval for both measured and predicted hydrocarbon formation rate curves as Draupne Formation gas. In combination with the broad activation energy distribution that was detected it seems likely that the same number of three gas forming mechanisms is present. The occurrence of a maximum with two shoulders, which all together mirror the distribution of the three Draupne Formation secondary gas formation rate maxima, seems to underline this assumption but must be considered as a coincidence.

Gas Formation versus Oil and Bulk Products

Laboratory and predicted geological formation rate curves for primary and secondary gas are compared to oil formation as derived from MSSV pyrolysis and bulk product formation derived from Rock Eval type open system pyrolysis in Fig. 39.

For the case of the Heather Formation the C_{6-14} boiling range was used for "oil" generation instead of C_{6+} because of the overall small amounts of C_{15+} which resulted in a reduced accuracy of measurements or a relative strong scattering of data. For the C_{6-14} boiling range (Table 22, Appendix) the activation energy distribution is narrow with a main energy value of 60 kcal/mol. A main activation energy of 59 kcal/mol is assigned to Draupne Formation oil generation as determined from MSSV pyrolysis. This is in a similar range as detected for Heather Formation oil. In spite of the slightly lower kinetic parameters for Draupne Formation, the peak oil generation is predicted to occur at higher geological temperatures. This is due to the higher experimental peak oil generation temperatures (appr. 375°C) compared to Heather Formation (appr. 355°C).

The bulk kinetic parameters (open system, Table 10 Appendix) for Heather Formation show higher values (58 kcal/mol, $1.68*10^{17}$ min^{-1}) than Draupne Formation (55 kcal/mol, $2.88*10^{16}$ min^{-1}). The fact, that oil and primary gas for both source rocks and for laboratory as well as for predicted conditions fall more or less within the Rock Eval type pyrolysis curves shows the results are essentially independent of the analytical system. In detail, however, this is not precisely true. All Draupne Formation MSSV pyrolysis results are shifted to slightly higher temperatures, a feature that will become even more pronounced at slower geological heating rates, due to the differences in kinetic parameters. Another point to note is that primary gas generation curves for both source rocks fall slightly out of the Rock Eval curve envelope on the high temperature side, an effect which derives from the fact that primary gas yields from the closed system were found to be higher than those from open systems. An expected and reasonable feature is that the secondary gas formation rate curves for both source rocks are lying at the high-temperature edge of the bulk generation curves or fall out of this envelope. This is pronounced for Draupne secondary gas from cracking of the C_{6+} resolved fraction and most outstanding for the Heather Formation high temperature secondary gas. The question-marked curve for geological heating conditions for this type of gas was obtained under the aforementioned assumptions by using an activation energy of 70 kcal/mol.

Finally the Rock Eval pyrolysis indicate much higher product amounts especially for Heather Formation a feature which was explained by Schenk & Horsfield (1993) to be a condensation phenomenon of proportions of the polar fraction to form tarry residues in the analytical MSSV system

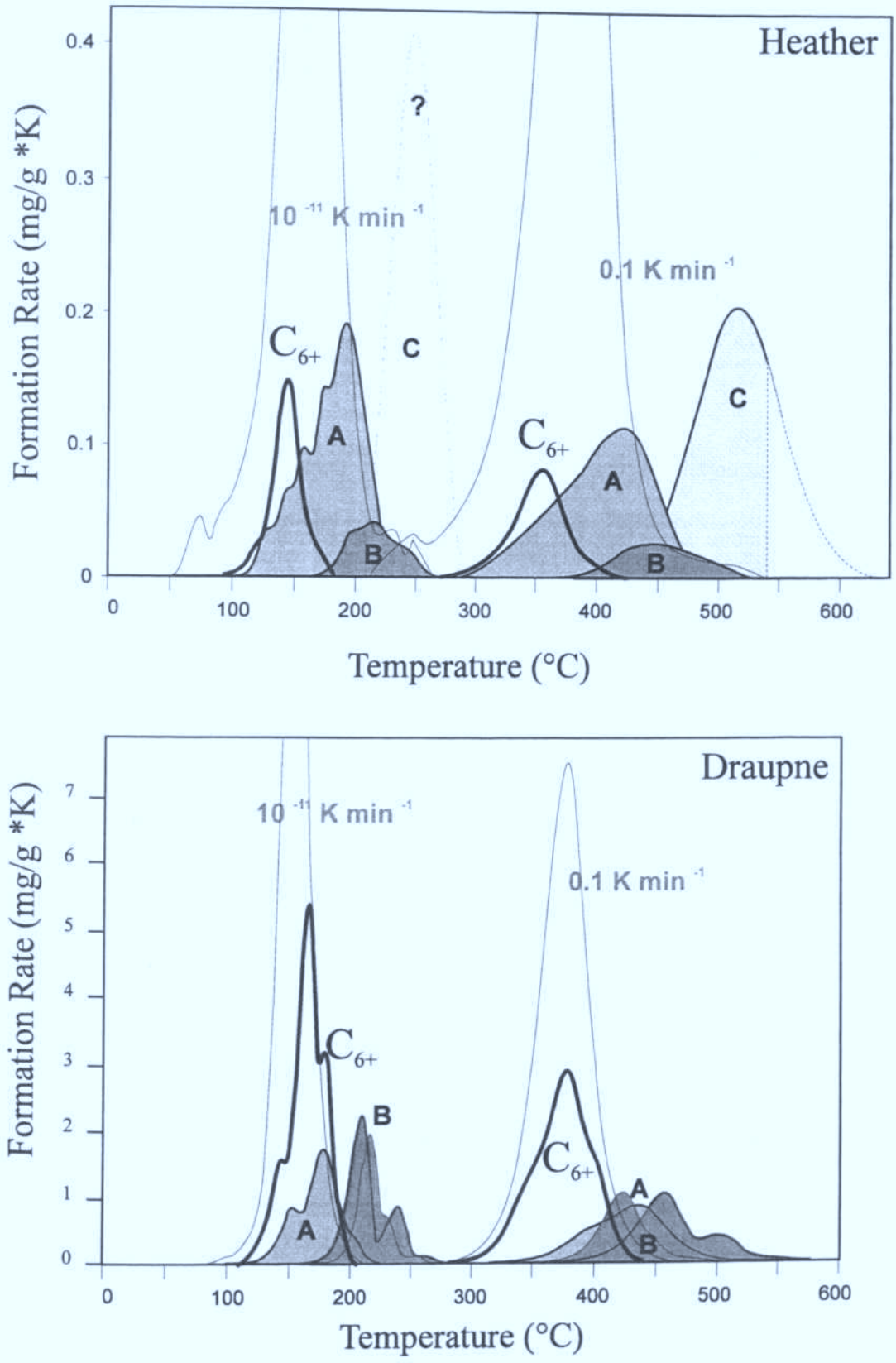


Fig. 39: Comparison of overall results. Experimental curves (right) at 0.1 $Kmin^{-1}$ and extrapolated curves (left) at 10^{-11} $Kmin^{-1}$. Depicted are Rock Eval bulk kinetic curves (thin lines) and for MSSV pyrolysis: C_{6+} (bold lines, it is C_{6-14} for Heather Formation, for explanation see text), primary gas (**A**), secondary gas (**B**) from cracking of C_{6+} and high temperature secondary gas (**C**). Top is Heather Formation, bottom is Draupne Formation. Kinetic parameters for Rock Eval type total products and C_{6+} and C_{6-14} MSSV products are included in the Appendix.

as for instance on the column. As a further contributing mechanism responsible for lower pyrolysate yields the authors mentioned the formation of coke, but both processes were reported to have no effect on the results of kinetic parameter determination.

Concluding remarks, kinetics of gas formation

For a linear geological heating rate of 10^{-11} $Kmin^{-1}$ (5.3 K/ma)

- primary gas generation was found to occur in a broad temperature interval (appr. 110-230°C, max 195°C) for Heather Formation and a slightly less broad range (appr. 120-220°C, max 180°C) for Draupne Formation.
- Secondary gas generation occurs at higher temperatures (appr. 175-260°C, maxima from 205-220°C).
- The high temperature secondary gas formation from neoformed bitumen as detected for the Heather Formation is outstanding and was inferred to occur at very high temperatures (max appr. 250°C) for geological heating rates.
- Overall results are in accordance with oil generation and bulk product generation.

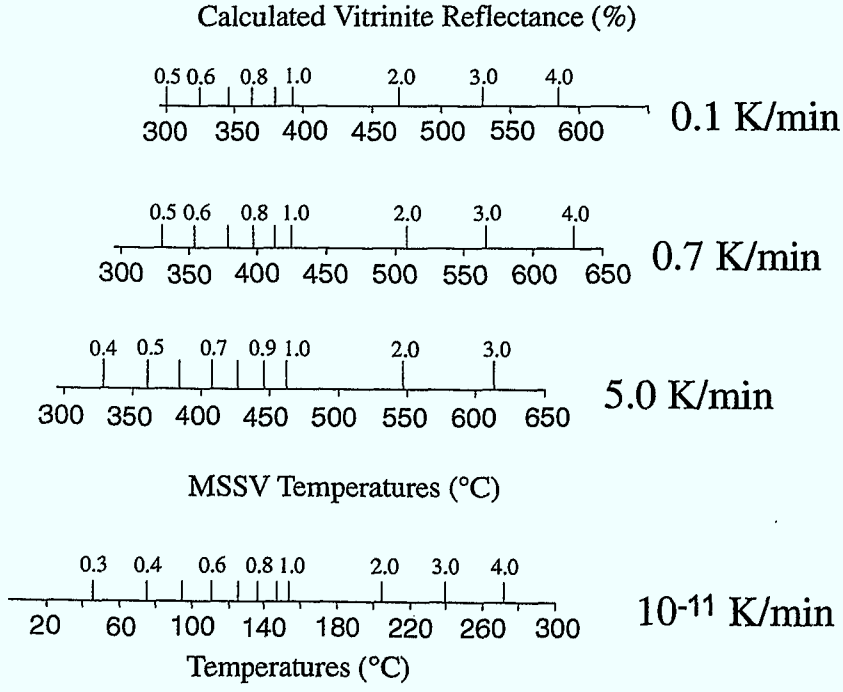


Fig. 40: Calculated vitrinite reflectance (after Sweeney and Burnham 1990, EASY Ro) correlated to pyrolysis and geological temperatures at 4 heating rates. The calculation is based on reaction kinetics for the release of methane CO_2 and water from the vitrinite. In order to provide an additional measure of maturity and because vitrinite reflectance is the most commonly used calibration parameter the correlation is included here.

3.4.2 Application of Kinetic Parameters using Basin Modelling

The major goal of using basin modelling was to apply the compositional kinetic parameters for the prediction of hydrocarbon gas formation under the non-linear heating conditions given by a burial and heating history of the investigated area. It is attempted to show that the choice of the kinetic parameter set has a significant impact on the results for gas occurrence predictions and thus for exploration. For this purpose the results from the determination of kinetic parameters were implemented into the basin modelling software Petromod 2D *Version3.1* and *Version 3.5* as user-defined kinetics (Tab. 25). The experimental values were adapted to the limitations of the *Petromod* input spreadsheet.

A second goal to comply with, was to get an idea about the distributions and contributions of gas from the two different source rock units Draupne and Heather Formations in a natural system. Therefore the modelling included also expulsion and migration of hydrocarbons, both oil and gas. Migration has to be considered a process of similar complexity, as is generation. Migration includes phase changes contemporaneous to pressure / temperature changes and compositional as well as isotopic changes due to migration fractionation or migration contamination. Moreover, the process strongly depends on the petrophysical properties of carrier beds. Because numerous petrophysical parameters must remain unknown in the framework of this test, only a limited approximation could be done to match a „realistic" model. Nevertheless, expulsion and migration have also an impact on the generation of gas, in that they control the availability of unexpelled petroleum for secondary cracking. It was stated in the beginning that different expulsion efficiencies of Heather and Draupne are thought to lead to Heather Formation source rocks producing gas mainly by cracking of unexpelled residual bitumen and Draupne Formation source rocks preferentially from kerogen.

Principles of Basin Modelling

Present day conditions, which as a rule are provided by interpreted seismic lines, are used to create a conceptual model of the investigated area, which functions as an input for basin modelling. Commonly the basin history, that is the subsidence in dependence of time and heating history, has to be unravelled. The first step towards this task is to decompact the sedimentary column by "backstripping" layers or events from the top. Repeated "forward modelling", i.e. sedimentation and compaction of events, beginning with the oldest event, results in an optimisation of the conceptual model. For each deposition, non-deposition or erosion-event calculations of energy-transport, maturation of the organic matter and mass transports are performed taking account of the respective boundary conditions.

The conceptual model has to be calibrated by comparison of calculated results like temperature, pressure or others with measured field data obtained from wells. Data such as thickness, duration and age, depositional sedimentary facies of individual layers and their respective physical properties (e.g., thermal conductivities) can be considered as fixed, meaning they cannot be changed for calibration purposes. Conversely, the timing and extent of erosion, heat flow, sea bottom temperatures and water depth are allowed to be optimised in order to attain a basin history reconstruction fitting present day conditions. Temperature over time, in addition to sediment input, erosion or non-deposition, are the most crucial parameter for the basin simulation because most basin evolution controlling processes, whether physical or chemical, are temperature dependent. At least two different independent calibration tools are necessary for a reliable reconstruction of the burial history (Leischner *et al.* 1993,

Yalcin *et al.* 1997). For this study additional calibration data sets were not available as for instance, apatite fission tracks or fluid inclusion homogenisation temperatures.

Input

A seismic line from the area north of the Tampen Spur was chosen (Fig. 2) to provide the basis for applying compositional kinetics to model hydrocarbon gas generation. The investigated area is part of the northern North Sea Viking Graben system and can be considered as a part of possible migration pathways for the filling of Tampen Spur reservoirs from the Møre basin kitchen. In short, the area can be explained to be an extensional plate tectonic setting and the history is described best by three major events (Ziegler *et al.* 1986, a.o.):

- *the Permo-Triassic initial rift system,*
- *the middle to upper Jurassic early rifting, producing tilted fault blocks,*
- *the full marine subsiding basin from Cretaceous to the present day.*

Each of the tectonic environments was accompanied by related sedimentary environments, i.e. lithologies, water depth, sediment water interface temperatures and by a related heatflow history.

26 events and 60 gridpoints were defined to describe the stratigraphic model resulting in at least 1560 finite elements. For the calculation of migrating petroleum masses the events are further subdivided automatically by the computer program in circumstances where they are too thick, resulting in an increased number of finite elements and thus higher accuracy of simulation. In order to allow also the simulation of deeper basin parts and consequently the prediction of high maturity gas formation the section was extended. The distances between the last two gridpoints (59 and 60) was increased to 6 km and the thickness of each layer raised by 100 m, resulting in a "virtual extension" (Fig. 41).

Lithologies and ages were assigned to each event. The lithologies (Fig. 41) were interpreted using 2D seismic information and knowledge from wells in the vicinity and was undertaken by Saga Petroleum. The interpreted section consists predominantly of clay rich strata. The upper Jurassic source rock units (events 8 and 9) are depicted in dark grey, the underlying middle Jurassic potential reservoir sandstones in light grey. A thin layer of Palaeocene sandstone (event 17) was introduced as an additional potential reservoir. Some of the original shale strata were changed during modelling into more silty layers, as for instance for event 12, in order to investigate the impact of sedimentation rate, pressure build up and migration losses from the section.
The event boundaries are isochrons in the model, this must not necessarily be correct but cannot be verified due to a lack of data. The time values of the event boundaries (Tab. 24) were derived from micro-palaeontologic age determinations provided by the sponsors.

The source rock properties *initial TOC* and *initial HI* were assigned to Draupne and Heather Formation (events 9 and 8). Draupne Formation values were chosen to be: HI = 532 mg HC / g TOC and TOC = 10 % and Heather Formation values to be: HI = 300 mg HC / g TOC and TOC = 5 %, based on Rock Eval data for immature samples and published values (see *Reference Systems*). Dunlin Group and Brent coals were not considered as source rocks for this simulation.

The heatflow history is the main parameter controlling temperature and vitrinite reflectances. As no paleotemperature determinations were available the heatflow history was designed according to literature data for different tectonic settings. Published values from Allen & Allen (1995) for

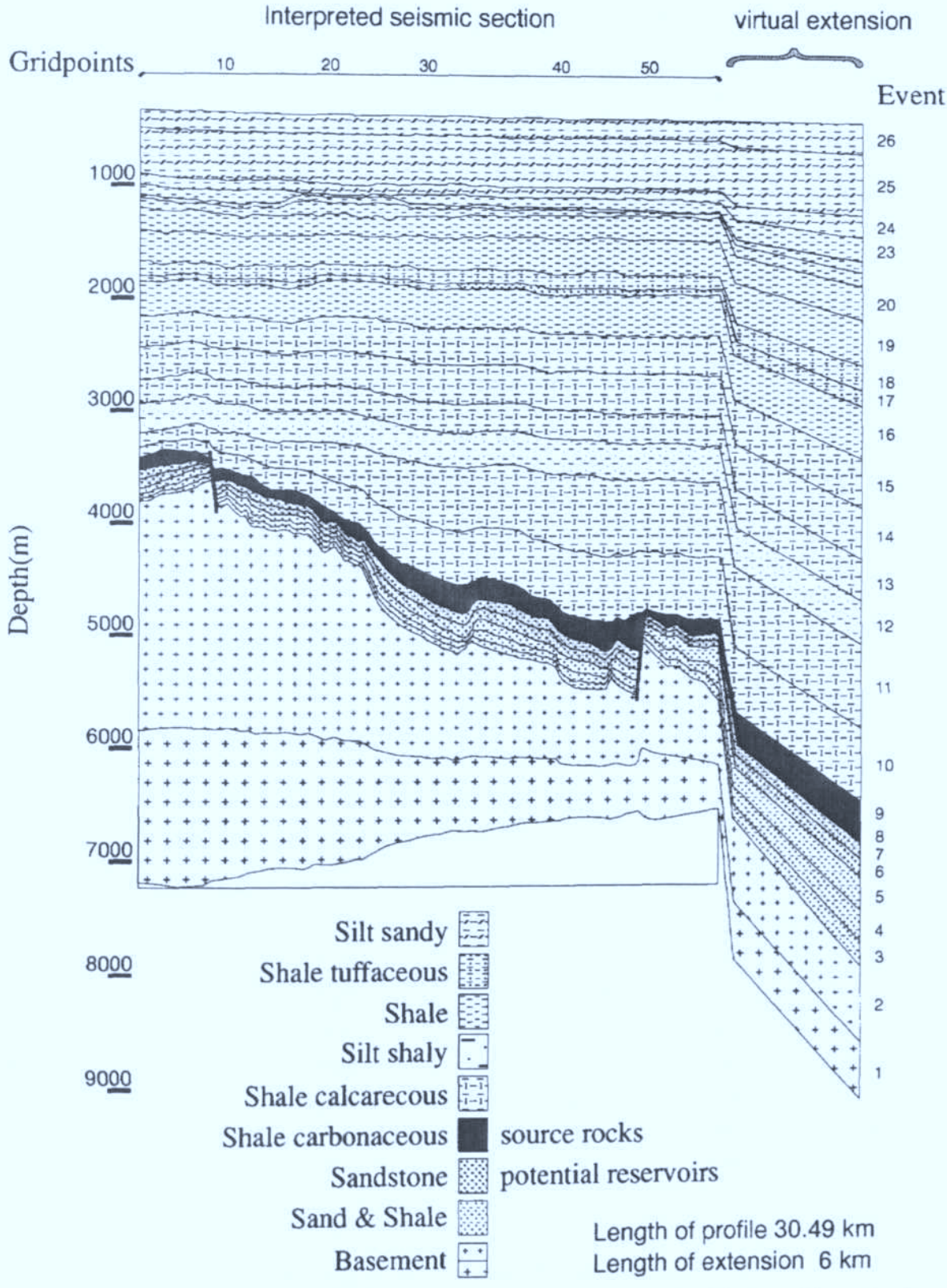


Fig. 41: Petromod-input: Interpreted seismic section including lithologies. 26 events. The section is oriented as left = south, and right = north (see Fig.2 for location).

extensional basins during active syn-rift phase and post-rift phase were selected. The active phase was assumed to have occurred during the upper Jurassic with maximum values of 80 mW/m^2. 55-60 mW/m^2 were assigned to the passive post-rift phase. These values are also confirmed by present day heatflow values and heatflow histories published by Goff (1983) who assumed a stretching factor β=1.5 for 155 mabp and 100 mabp.

Table 24: Stratigraphy for the investigated section.

event	time at base (mabp)	chronostratigraphy
Event 26	2.36	Quarternary
Event 25	8.63	
Event 24	10.00	
Event 23	16.00	
Event 22	21.16	
Event 21	33.00	Tertiary
Event 20	41.80	
Event 19	55.00	
Event 18	62.00	
Event 17	65.00	
Event 16	76.61	Upper Cret.
Event 15	87.72	
Event 14	99.11	
Event 13	107.66	Cretaceous
Event 12	118.00	
Event 11	131.00	
Event 10	142.00	
Event 9	152.00	Draupne
Event 8	164.00	Heather
Event 7	171.00	Brent
Event 6	180.00	Jurassic
Event 5	192.52	
Event 4	202.50	
Event 3	210.00	
Event 2	219.02	Triassic
Event 1	225.00	

Note, that time boundaries do not always coincide with stratigraphic units. This is because the definition of events is based on seismic interpretations where lithologic differences are considered.

The Petromod program offers default values for many parameters, which can be used if no measured data, exist or even are indeterminable as for example for the initial porosity. These default values are usually in geologically and physically reasonable ranges but may lead to errors in the basin simulation if real properties deviate considerably (Poelchau *et al.* 1997). Because no "real property" data were available in the timeframe of this test case, the following lithology defaults were used: density, thermal conductivity and its anisotropy, heat capacity, compressibility, initial porosities and porosity-permeability relationships, permeability anisotropy and migration saturation and capillary pressures. Especially porosity and permeability relationships and anisotropies are crucial for migration modelling. Also as defaults assigned to lithologies are paleo-waterdepth and sediment-water-interface temperatures, which were already implemented in the section by Saga Petroleum, based on palaeo-latitudes. These parameters have an impact on the temperature field development and therefore for hydrocarbon generation.

Hydrocarbon generation reaction kinetic parameters for primary generation of gas and oil and secondary cracking of oil were implemented into the basin modelling software as user-defined kinetic files (Table 25) for both source rock formations. The kinetic parameters from MSSV pyrolysis were

adapted to the Petromod input sheet. The formation of a neoformed bitumen (Heather Formation) cannot be simulated by the program, therefore the gas generation by cracking of the neoformed residue was included in the primary generation of gas from kerogen (K>G). This resulted in a bimodal activation energy distribution with a single frequency factor. The input spreadsheet of the Petromod software allows to define individual kinetic parameter sets for each source rock unit which alternatively can be switched on or off, to enable investigation of generation from single source rocks. However there are two serious limitations:

- Only three main reactions are allowed (K>O, K>G and O>G).
- For oil to gas cracking only one activation energy can be defined when it is attempted to include expulsion/ migration modelling.

For the case of Draupne Formation even two secondary gas formation distributions had to be condensed to one. Especially for the simulation of secondary cracking reactions it is however crucial to include expulsion, which can be considered a limiting factor for the presence of cracking educts in the source rock. Moreover the here employed secondary kinetic parameters are valid for in-source cracking which was assumed before to be favoured by catalytic effects of the kerogen in contrast to in-reservoir or in-carrier cracking. Consequently the latter types of cracking might be overestimated.

Expulsion "is treated as a pressure driven transport process in a separate phase along the pore system and microfractures" (Petromod manual). It was modelled with the default saturation model. For the case of gas no saturation threshold is necessary. The saturation threshold which is necessary for the onset of expulsion for oil is defined as a lithologic property. It is 5% of the porespace for the case of carbonaceous shale. This is actually not the only controlling parameter. Expulsion is additionally defined by the in-situ physical properties that accelerate or inhibit the process. This complex expulsion module takes account of the changes in petroleum composition expressed as GOR and the resulting volume and pressure changes as well as the decreasing volume of the organic matter and the respective impact on pressure. Additionally the resulting pore size distributions and an expression for microfractures are included. Finally the residual saturation which is also very important for the occurrence of secondary cracking is defined as a proportion of the migration saturation. Values of 10-20% of the migration saturation were chosen.

Finally a carrier system and migration properties had to be assigned. All rocks above the basement, above as well as subjacent to the source rocks were allowed to function as migration pathways. 3-phase flow (oil, gas and water) or 3-phase flow and gas diffusion were used to model migration. Especially the middle to lower Jurassic events 3 to 7 can be considered as potential migration pathways because of their lithologies.

Calibration

A well located in the vicinity of the seismic line (Fig. 2) provided the calibration data set for the simulation. The data consisted of pore pressure, vitrinite reflectance and temperature. The well is situated near gridpoint 16. The calibration (Fig. 42) shows a good fit with the observed *vitrinite*

reflectance data. The calculated values are slightly higher than those observed. It is noteworthy that the calculated values strongly depend on the employed calculation model which is the model of Sweeney & Burnham (1990) for the depicted case. The model of Larter (1989) resulted in higher Ro values at shallow depth and is additionally not applicable to very high maturities. Consequently the heatflow history would have to be changed to lower values to match the observed vitrinite reflectance profile with Larter's (1989) vitrinite kinetics. In contrast the temperature versus vitrinite reflectance correlation reported by Bakken (1993) is not based on kinetic calculations but on empirical observations of vitrinite reflectance versus borehole temperatures and indicates for the overmature zone lower temperatures for a given Ro value than it results from the Sweeney & Burnham model (1990). As present day temperatures do not reflect the time-temperature history this correlation must be objected.

The calculated *temperatures* in Fig. 42 are higher by approximately 10-15°C than the observed value at 1600 m depth. Borehole temperature measurements tend to give too low values because temperature field equilibration times are known to be relatively long (Yalcin *et al.* 1997). The here reported temperature was obtained from a temperature log with no information about the test method Therefore the value was not further used for calibration. The temperature profile obtained from the simulation

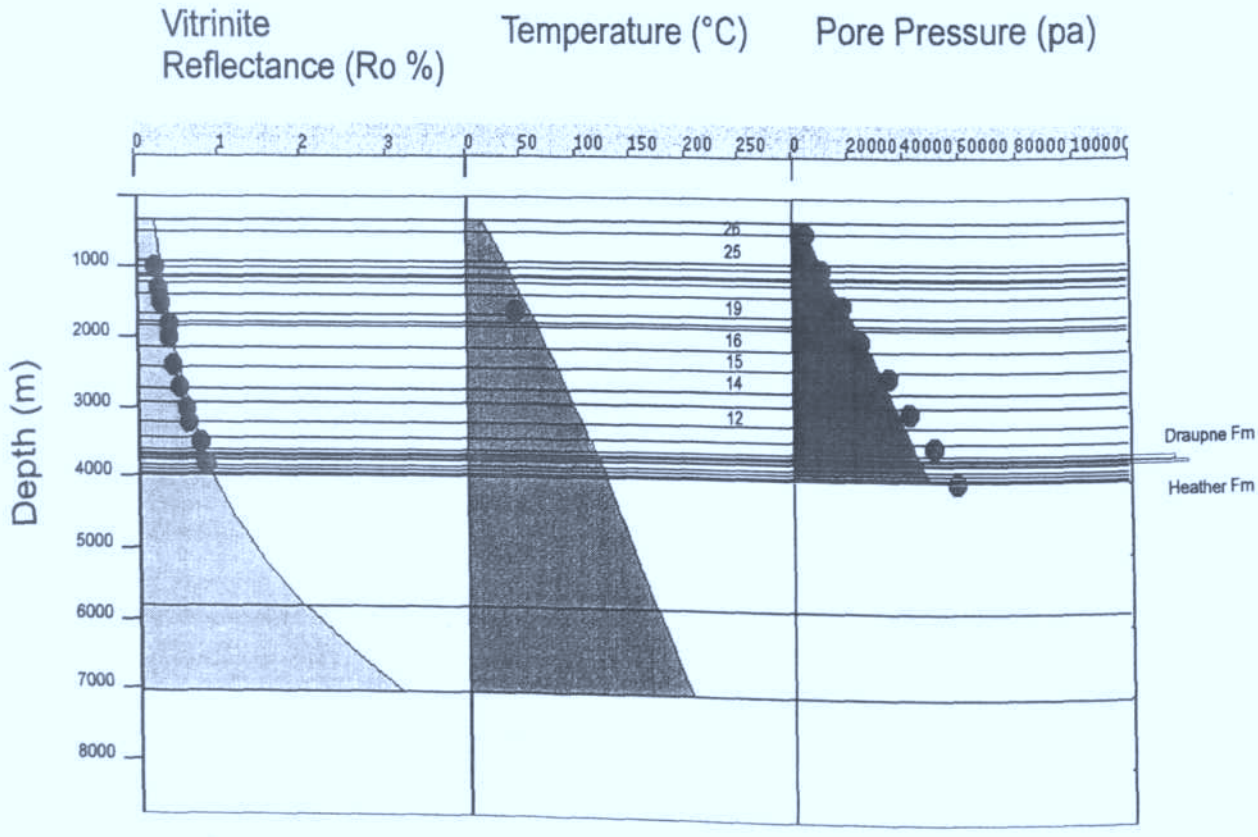


Fig. 42: Calibration of simulation at gridpoint 16, using comparison data of a well in the vicinity.

is however in accordance with published measured corrected bottom hole temperatures (Goff 1983). The calculated *pore pressure* is in good agreement with observed pressures down to a depth of 2000m. The observed pressures are converted from mudweight logs (Saga data report 1994). Below

2000m the calculation shows lower values than observed indicating either deviations in the assigned lithologies to the natural system or unrealistic sedimentation rate calculations. However, while the natural system is not in equilibrium the simulation achieves this state. As a consequence migration for which pressure is a crucial parameter will not be matched realistically.

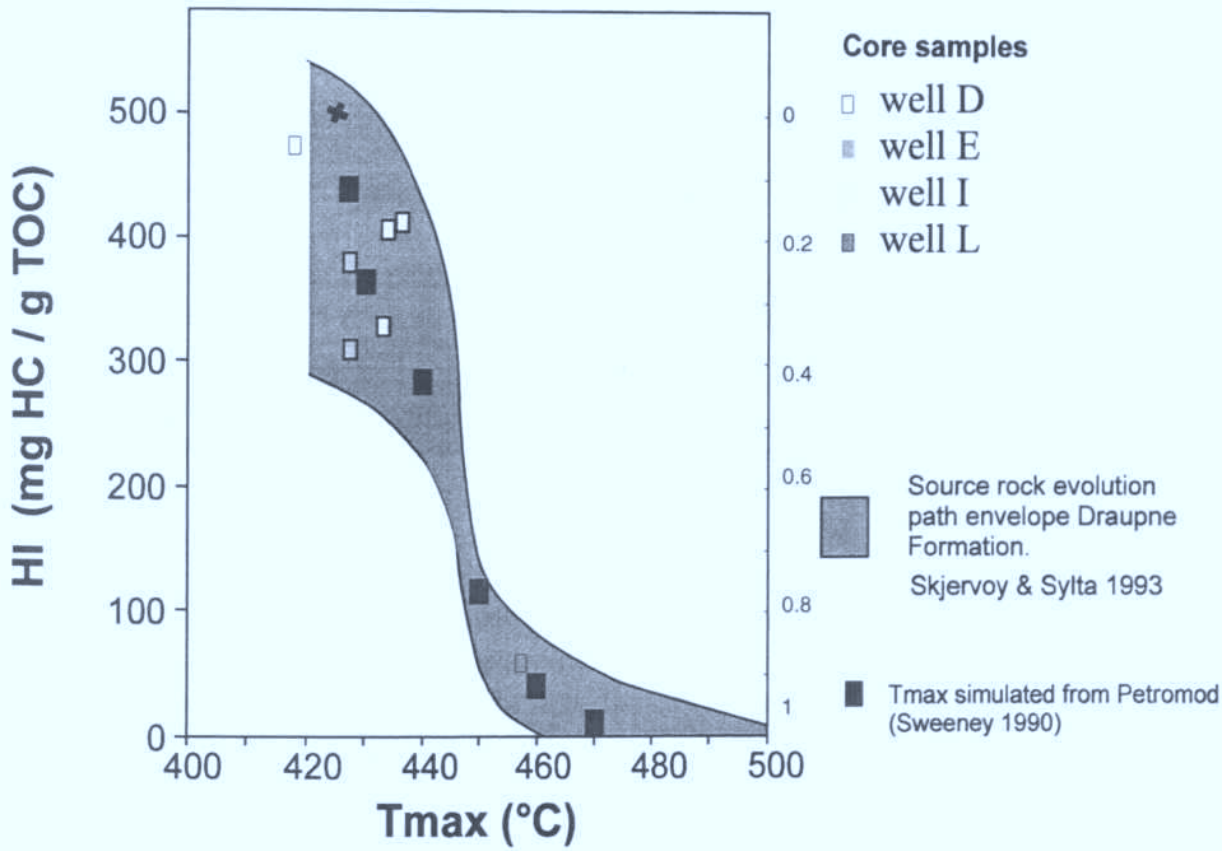


Fig. 43: Comparison of calculated Tmax for Draupne Formation with measured data. The scale on the right gives the calculated transformation ratio for an initial HI of 532 (mg/g TOC), which was used for the Draupne Formation.

An additional calibration tool is provided by the possibility to calculate the Rock Eval Tmax parameter (25 $Kmin^{-1}$ heating rate) using the method of Sweeney (1990). For the case of the Draupne Formation the comparison of calculated HI versus T_{max} maturation pathway results in excellent agreement with the natural source rock evolution presented by Skervoy & Sylta (1993) in Fig. 43. For the case of the Heather Formation the calculated T_{max} values were unrealistically low (<400°C). This is probably connected to the effect of recombination of products. The Heather Formation Transformation Ratio when calculated from total MSSV pyrolysis products shows only a shallow increase in the interval where a major part of the products recombines before the high temperature gas generation starts and the TR increases again. This interval is probably mistaken as no maturation in terms of Transformation Ratio by the Sweeney (1990) model. The consequence is that the calculation of Tmax results in unrealistic low values and therefore must be considered a mathematical problem.

Results of the Simulation

Burial and Temperature History

Fig. 44 shows the burial history near the deepest part of the profile (gridpoint 58) in a depth versus time diagram with the corresponding temperature field evolution. The maximum temperature at grid-

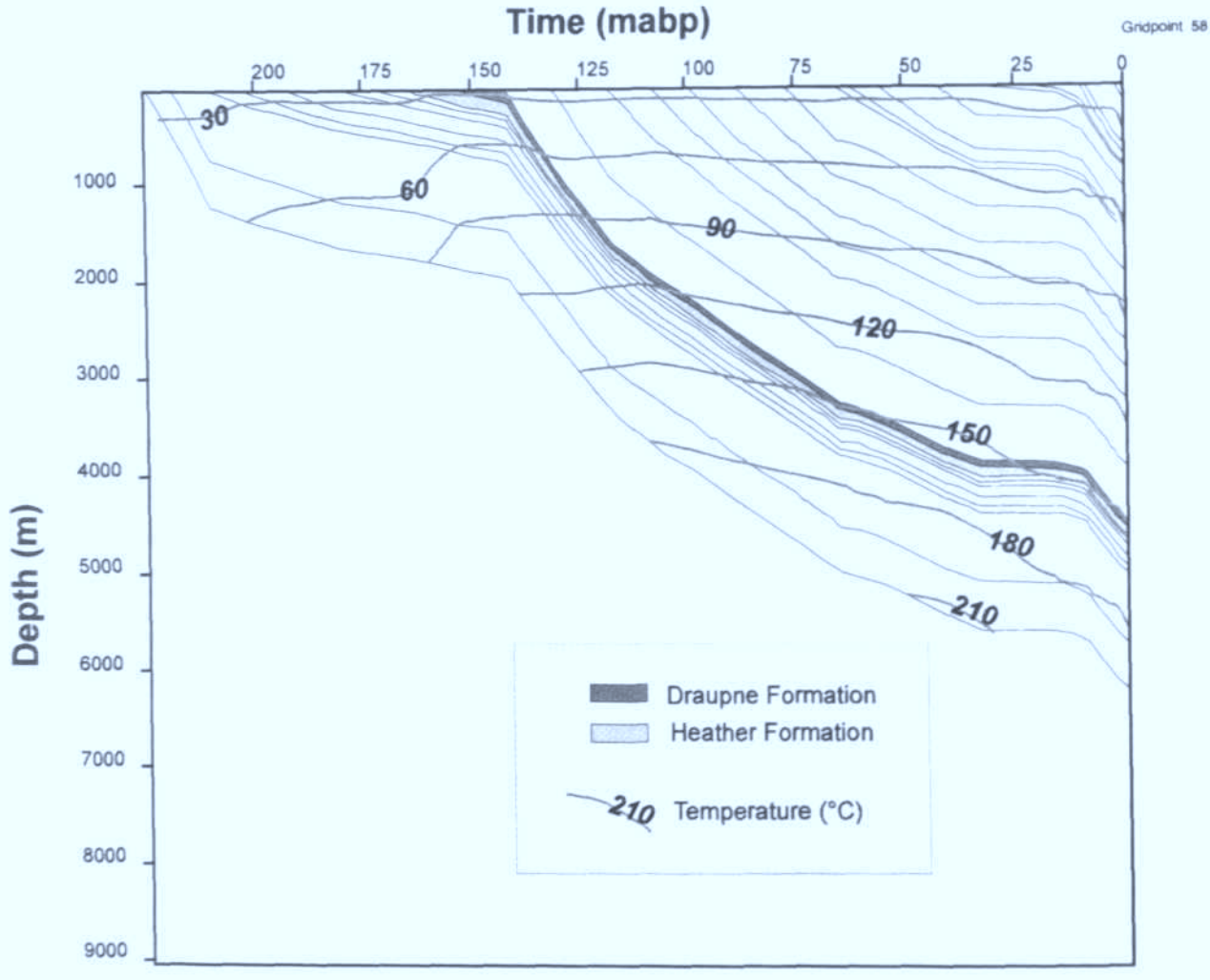


Fig. 44: Reconstructed burial history at gridpoint 58.

point 58 for the highlighted source rocks reaches approximately 160°C at 40 mabp, whereas the maximum temperature within the virtual extension is approximately 200°C. The burial history can be divided into several intervals. The fastest subsidence rates occur from 142 mabp to 118 mabp (u. Jurassic) and during the last 10 ma (Nordland Group to present day). In-between, the subsidence becomes successively slower. Heating rates relevant for the hydrocarbon generation can be determined from the subsidence and the temperature distribution. Three major intervals were found, as there are 142-118 mabp with 3.3 K/ma, 118-62 mabp with 1.16 K/ma and a heating rate of 0.7-1.0 K/ma for the interval of 62-33 mabp.

Gas Generation

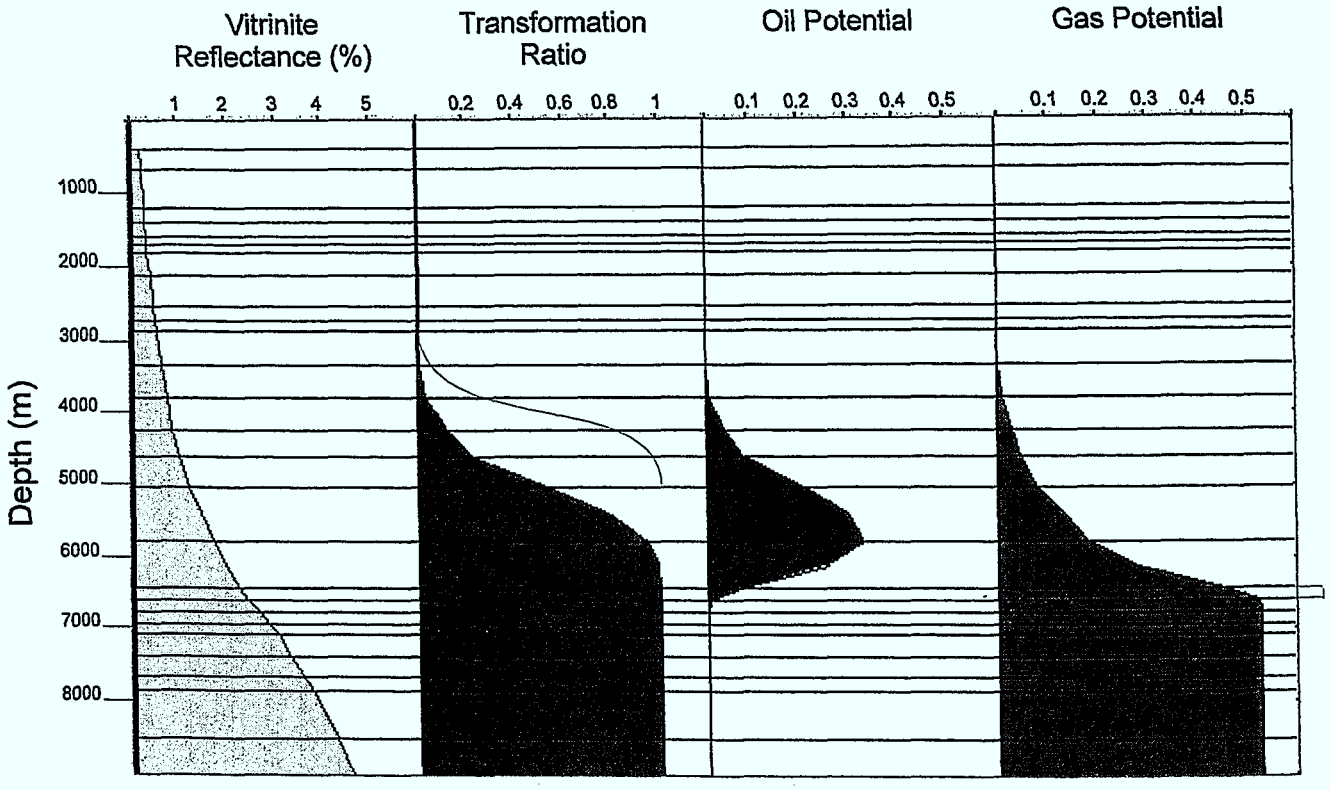
Fig. 45 shows the gas and oil generation potential and the transformation ratios for Heather and Draupne Formations in relation to maturity expressed as R_o (%) and in relation to depth at present day at gridpoint 60.

- Gas formation is indicated to start at 3500 m depth and the transformation of the kerogen is completed at 6500m. However, thresholds based on depth change through time and for a scenario at for instance 90 mabp the generation threshold was situated at approximately 1000m shallower depth. The onset for both oil and gas corresponds roughly to 0.5-0.6 % vitrinite reflectance, which is an accepted boundary condition for the northern Viking Graben area (Dahl & Augustson 1993). The complete transformation is predicted to occur at appr. 2% vitrinite reflectance in contrast to 1.2% obtained from kinetic parameters of Burnham (1989) for kerogen type II (uses same parameter set for both oil and gas generation). The strongly increasing gas potential at R_o>1.6% in Fig. 45 results from the secondary cracking of oil.

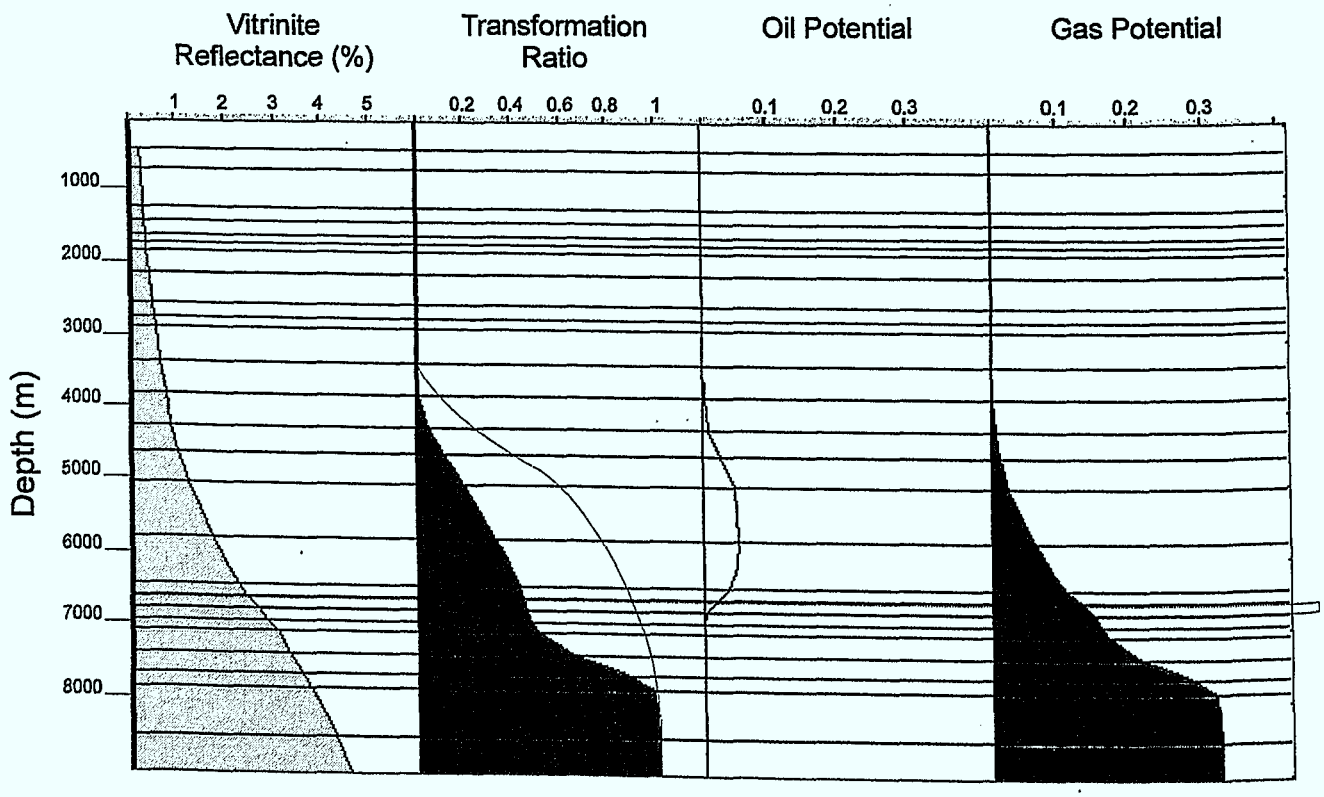
- The Transformation Ratio indicates complete conversion of the kerogen for a depth of more than 7500m with a corresponding vitrinite reflectance of 3.7%. This is in agreement with the prediction based on Burnham (1989) kinetic parameters, but with a significantly different evolution profile. The onset of hydrocarbon gas formation is 500m deeper than determined for Draupne Formation. At gridpoint 60 the major proportion of the Heather Formation oil potential has been realised, but the gas potential is realised for only less than 50 %. Especially the high temperature secondary gas from cracking of assumed recombination residues occurs at high maturities (R_o>3%).

Fig. 45 (next page): Results from simulation. Heather and Draupne Formation Transformation Ratios and Oil and Gas potentials at Gridpoint 60 as a function of depth and in comparison with vitrinite reflectance. Source rock units are highlighted as bars. Thin lines are Transformation Ratios from Burnham (1989) kinetic (type II for Draupne and type III for Heather), for kinetic parameters see text.

Draupne Formation



Heather Formation



Whole System Mass Balance

The conversion of the total potential of the organic matter into oil and gas was calculated as a function of time taking the whole section into account. The present day conditions are depicted in Fig.

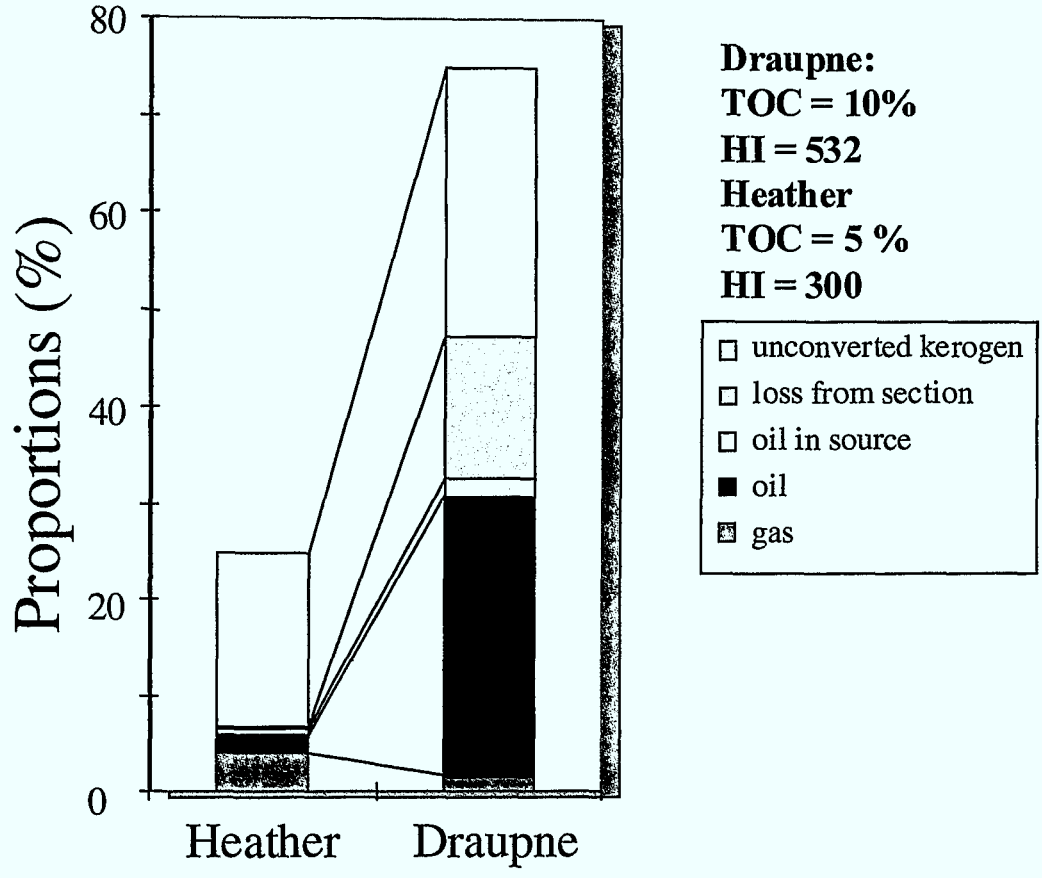


Fig. 46: Mass balance for the present day situation. The depicted distribution results from both generation and migration. Losses from the section are upward losses as basin sides were modelled as closed.

46 and the evolution through time in Fig. 47. Due to the similar thicknesses of Heather and Draupne Formations for the investigated section the proportions of convertible kerogens for the whole system depend predominantly on the source rock properties HI and TOC. Therefore Draupne Formation holds approximately 75% of the convertible mass and Heather formation the remaining 25% on a basin scale. A larger proportion of Draupne Formation (~2/3) compared to Heather Formation kerogen (~1/4) is converted. The depicted product distribution (oil versus gas) has to be considered carefully. Heather Formation contributes more gas to the overall products because Draupne Formation gas is mainly lost from the section (upward loss, into the atmosphere). It is uncertain whether this might be realistic or not. However, this scenario indicates that the larger proportion of gas present in the Viking Graben derived from Heather Formation. Additional arguments are that the unconverted Heather Formation kerogen will yield mainly high maturity gas and Heather Formation thickness in contrast to this section often exceeds Draupne thickness. In any way it is clear that the Heather Formation gas contributions are likely to be very significant even if the losses for Draupne Formation gas are unrealistic.

Timing of Hydrocarbon Gas Formation

A short review of published generation-timing data yields very different results. Dahl *et al.* (1987) for instance investigated the Oseberg area in quadrant 30 and stated that oil generation has been going on since the early Maastrichtian (74 mabp) with an additional heat input during Eocene/Miocene resulting in enhanced hydrocarbon formation. In a combined 1 & 2 D basin modelling approach for quadrant 34 (Norsk Hydro Report 1992) oil and gas generation was predicted to have started during Turonian to Coniacian time (92-80 Ma) in the Viking Graben. Oil generation was stated to level out in early Maastrichtian (74 Ma) in the Graben whereas gas generation increased. Two more phases of oil generation were determined, one in early Miocene and a third phase in Pliocene at 4 ma. The most deviating results were given by Leadholm *et al.* (1985) who predicted the oil generation in block 33 and 34 (i.e. this study area) to occur from early Miocene to middle Pliocene times by using thermal history (K-MOD) and maturation (M-MOD) computer simulations.

From the here presented simulation it results, that oil and gas generation were active for a much longer period of time because immature Draupne and Heather Formation source rocks were buried more or less successively into the generation window throughout the time interval of 110-40 mabp (Fig. 47). The most pronounced formation for both source rock units is centered around 80 mabp.

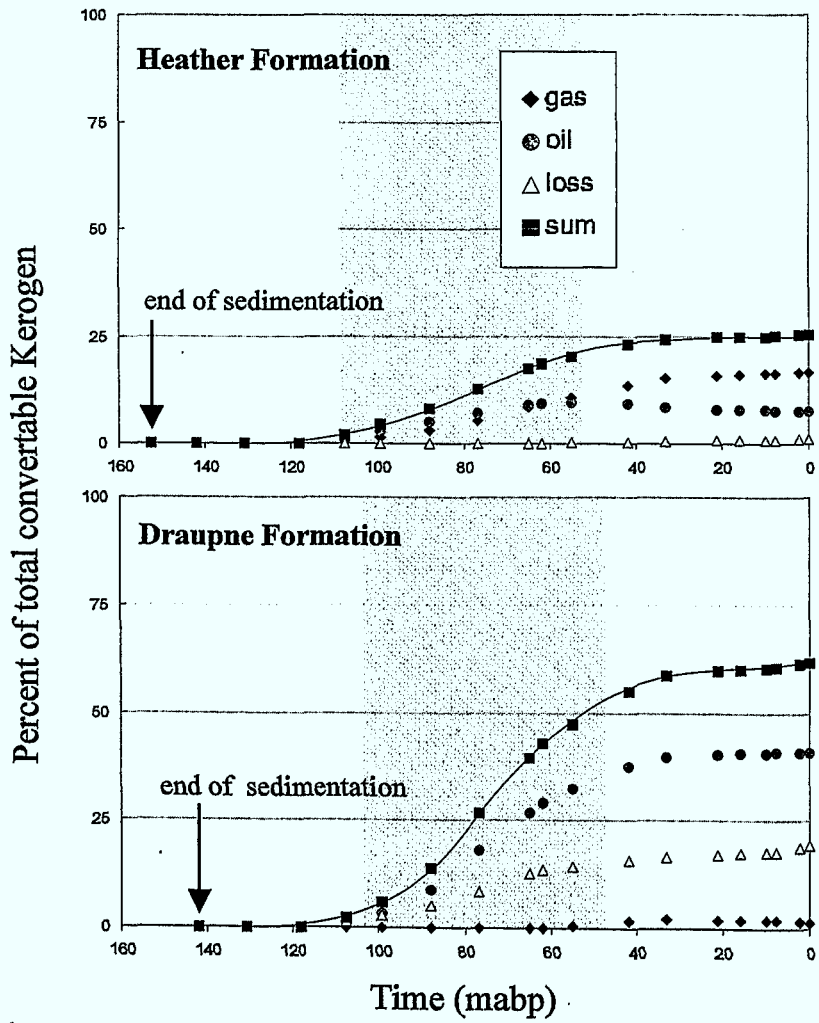
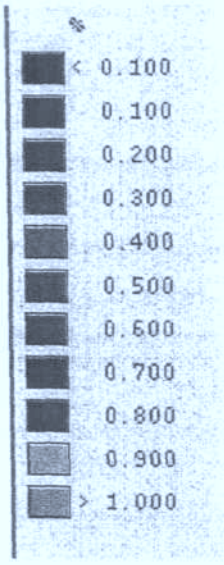


Fig. 47: Petroleum product balancing taking account for the complete section (100%). Kerogen conversion is by far more complete for Draupne Formation. Heather Formation shows oil to gas cracking, but the contribution of high maturity methane seems to be still negligible.

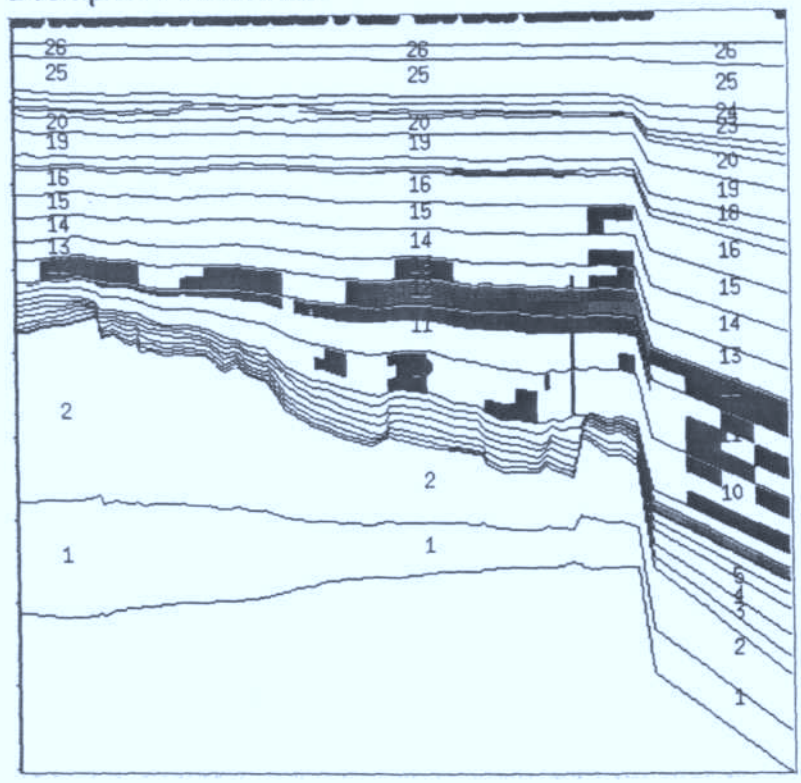
These different findings are in the first instance a result of different determinations of the subsidence history and in the second instance a result of different reaction kinetic parameters. Nevertheless is the timing of generation one of the most crucial parameters in exploration because older migration pathways might vanish and new pathways might evolve during time. The same is true for structures which can trap petroleum or as another possibility the structure of traps might change as for instance recently reported for the Troll structure (Horstad & Larter 1997).
Another feature resulting from Fig. 47 is the increase of gas formation at 50 mabp for Heather Formation with a contemporaneous decrease in the amounts of oil, which indicates the secondary cracking of oil. A similar feature is not present for Draupne Formation confirming the assumption presented in the approach, that secondary cracking of unexpelled bitumen might be more relevant for the Heather Formation because of lower expulsion efficiencies.

Migration and Gas Losses

The results of the included migration modelling are expressed as hydrocarbon saturations (Fig. 48) and have to be considered as only one scenario among many others with an uncertain degree of probability. In considering gas versus oil distributions Schroeder & Sylta (1993) have shown that 2D migration modelling is a very sensitive tool demanding a calibration by existing reservoirs. Because this was not possible for this section, and in view of the restricted information about petrophysical properties, faults properties and others, the results must be considered as a hypothetical model. Nevertheless some useful information can be obtained especially because this seismic line is parallel to a possible migration pathway of petroleum into the Tampen Spur area and because the question remains why the simulation resulted in such high gas losses for Draupne Formation gas.
In Fig. 48 most of the Heather Formation hydrocarbons are expelled downwards caused by a high degree of compaction already reached by Draupne Formation shales during the time that Heather Formation generation started. A further reason and perhaps the more important one is that high pressures probably accompanied the generation of petroleum for the Draupne Formation due to the increase in volume when petroleum is released from the kerogen. Thus upwards hydrocarbon losses for Heather Formation gas are small except for cases where faults provide migration possibilities. In contrast Draupne Formation expels mainly upwards in the model. This seems to be unrealistic because only minor amounts of oil would ever reach the Jurassic reservoir rocks in the Tampen Spur area. Instead of that reservoirs situated directly in top of the source strata can be filled with this scenario, like realised here for the small layer of Palaeocene sandstones (event 17). Moreover another consequence are the observed high losses of gas from the section. In this context Welte *et al.* (1984) reported that substantial gas leakage may be common for most reservoirs. Additionally Karlsson (1986) reported a lack of tight caprocks for the Tampen Spur area and Leith *et al.* (1993) confirmed the presence of migrated petroleum above the Snorre field by gas and n-alkane compositional observations. They concluded from their observations that not only diffusion would be a responsible process but also bulk flow because they found a relationship between oil-column height in the reservoir and gas wetness above the reservoir. Montel *et al.* (1993) quantified the reservoir leakage using a one-dimensional numerical model which resulted in losses of 13-22% of the reservoired gas. The sum of these published observations and opinions might indicate that losses as large as those observed from the simulation might be possible.



Draupne Formation



Heather Formation

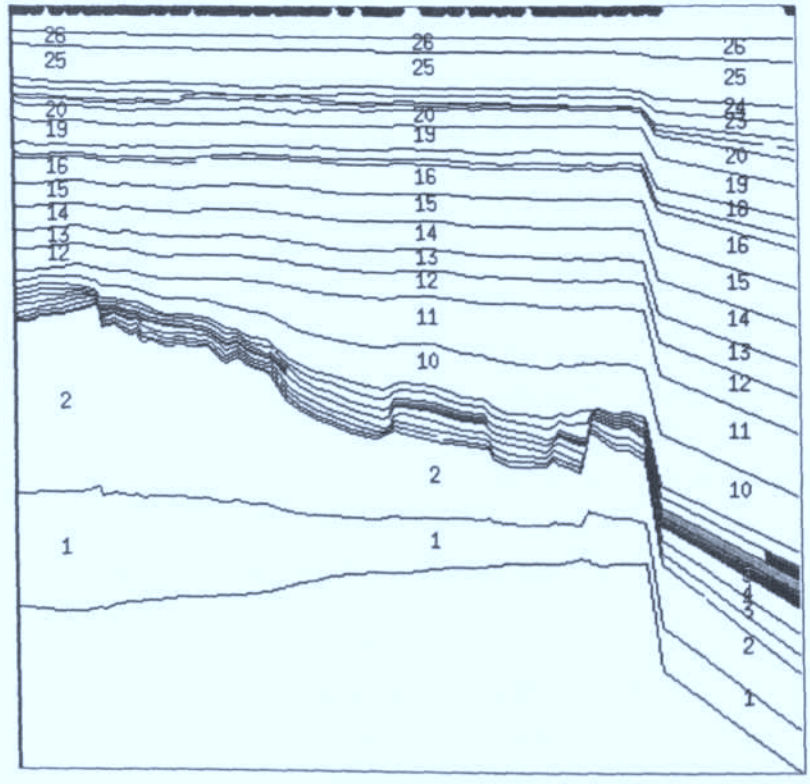


Fig. 48: Petroleum (both oil and gas) saturation expressed as % of porespace. South = left, North = right.

Concluding remarks, application of kinetic parameters using basin modelling

- A heating rate of 1.16 K/ma for the time interval of 118-62 mabp is the most relevant heating rate for oil and gas generation in the investigated system.
- High temperature gas formation by cracking of neoformed bitumen as proposed for the Heather Formation did not occur in the employed section, even though the section was extended and the source rock burial increased. Temperatures were not high enough resulting in significant remaining gas potentials for areas deeper than 7000 m or vitrinite reflectances >3%.
- Secondary cracking of oil to gas was found to be of minor importance for Draupne Formation where oil is efficiently expelled. This corroborates the assumption presented in the approach.
- For Heather Formation a decrease of the overall amounts of oil in the time interval of 50-0 mabp indicates that secondary cracking takes place.
- An overall mass balance implies that Heather Formation gas might contribute higher proportions of gas to Viking Graben reservoirs compared to Draupne Formation.

3.5. Compositional Considerations

The compositional development of pyrolysis products was investigated and subsequently used for comparisons with compositional patterns obtained from the natural hydrocarbon system, i.e. for gas - source correlations. Gas C_{1-4} and light end C_{5-7} compositions are included as well as stable carbon isotope compositions.

3.5.1. Petroleum Forming Reactions

The knowledge about petroleum or gas forming reactions may improve the assessment of the validity of laboratory results but may also clarify the origin of features observed during the calculation of primary and secondary gases from MSSV pyrolysis.

Primary Cracking

Primary gas generation can be understood as the simple cracking of low molecular weight hydrocarbons from the kerogen structure. A commonly accepted mechanism of bond breaking, either from the aliphatic fraction or from alkyl-groups linked to aromatic nuclei, is the scission of the beta bond, i.e. the second bond from a radical center. Kissin (1987) found that the alkane chain lengths (which he discussed for C_{9+}) versus molar amounts seem to follow exponential laws and stated the responsible mechanism to operate randomly. Observations from multistep open system pyrolysis data of Heather Formation depicted in Fig. 49 support this hypothesis. N-alkanes in the C_{1-27} range show overall uniform increasing yields if expressed as a fraction of the maximum potential for each component. This potential was assumed to equal the highest component yield (high py temperatures).

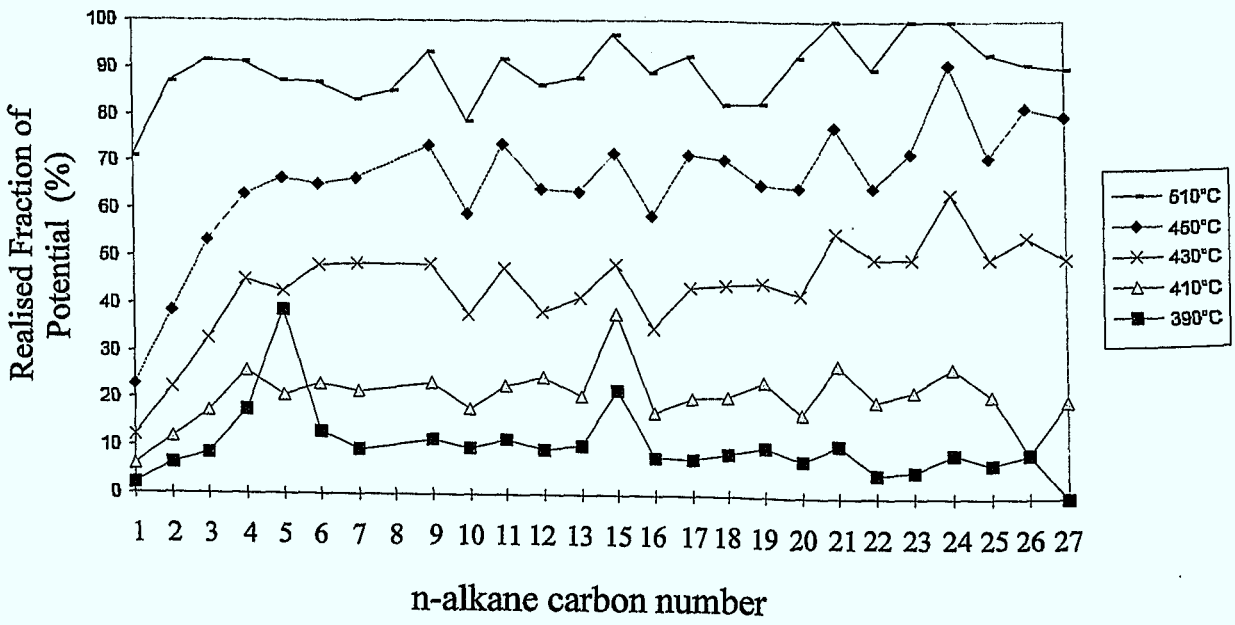


Fig. 49: Evolution of n-alkanes C_{1-27} during multistep open system pyrolysis from Heather Formation.

Exceptions from the uniform increase are obvious for methane, ethane and propane. Their relative increase is lower than for the rest of components. One explanation is provided by considerations about bond energies. Using the model of alkyl-chains attached to an aromatic core it was reported that

the second bond of an alkyl-chain is the weakest (Sanderson 1976). This finding is based on the differences in the bond dissociation energies which are 99 kcal/mol for the first bond (alpha-scission) and 72 kcal/mol for the second bond (beta-scission). These numbers hold for the case that the attached alkyl is an ethyl-group. With increasing alkyl-chain length the bond dissociation energy for the β-bond decreases even further but the effect diminishes for longer alkyl-chains. Consequently, the longer the alkyl-chain, the easier it will be cracked from the kerogen and in terms of generation, long chains are generated first, whereas short chains are generated last. These views about the impact of bond strength are neither in accordance with the assumption of a random process nor with the trends observed in Fig. 49, except for the gases. Alternatively the retardation of gas C_1-C_3 formation could be explained by the occurrence of crosslinking-structures in the kerogen, consisting of short-chain alkyl-groups, because crosslinks would have to be split first and gas components would be released in a second cracking step. In this regard Boucher *et al.* (1990) reported crosslinking-alkyls to have a maximum at C_6 for a Kimmeridge Clay sample.

Additional information can be used from MSSV closed system pyrolysis if considering the low temp-

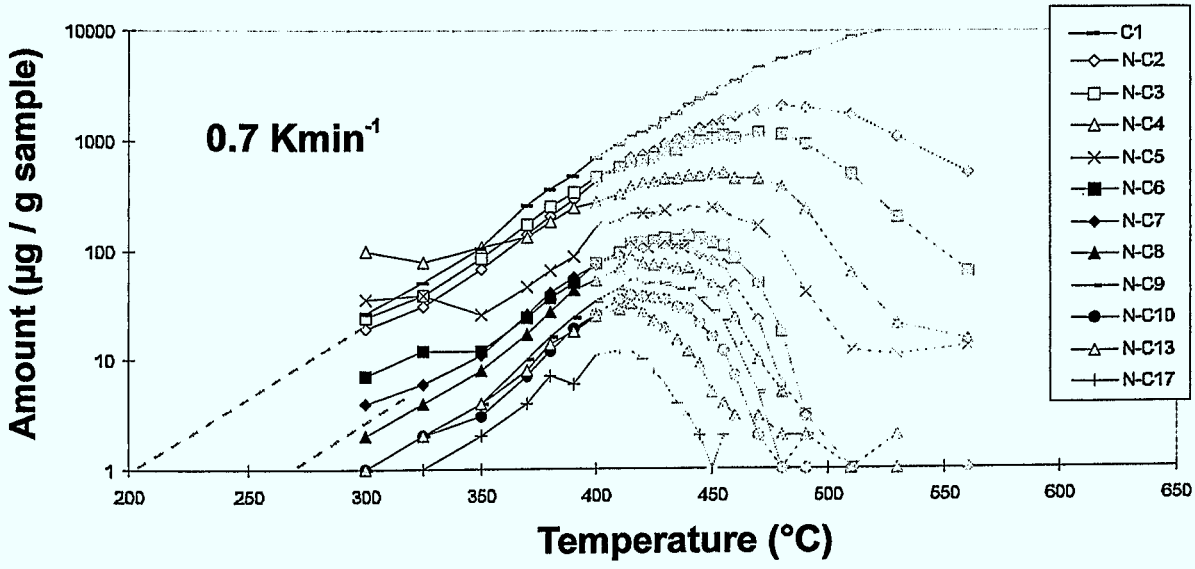


Fig. 50: Formation of n-alkanes during MSSV pyrolysis of the Heather Formation samples. The range which is likely to be exclusively affected by primary cracking reactions is highlighted. The general trends can be observed for Draupne Formation as well (not depicted) and are similar for all heating rates.

erature region where secondary cracking reactions can be excluded. For the case of selected n-alkane formation during the experiment (Fig. 50) no indication can be seen, that longer-chained molecular species evolve at lower temperatures. In contrary if the formation profiles are extrapolated to lower temperatures, it appears that short chain n-alkanes evolve first. These contradictions cannot be explained yet but it is likely that the differences in bond energies are overshadowed by the random cracking, which depends mainly on the position where a radical center forms and which might also explain the prevalence of short moieties. The outstanding dissociation bond energy for the alpha-bond however, should have an impact on the methane formation. It can be summarised:

- A random bond-breaking mechanism for C_{3+} seems to be likely confirmed by observations from both open and closed heating experiments.

- Methane, ethane and propane exhibited a slower relative increase during open system pyrolysis. An elucidation can be that short-chain alkyl crosslinks in the kerogen structure are an important source for the gas. Crosslinkage-alkyls are not visible from pyrolysis-gc but have been detected by oxidative degradation of Kimmeridge Clay kerogen by Boucher *et al.* (1990).
- Cracking-models based on the relative strength of individual bonds cannot explain the generation of components as it was observed, especially the implied onset of generation for short-chain prior to the formation of heavier molecules. However, the very high bond dissociation energy of methyl-groups connected to aromatic cores is likely to have an impact on methane generation.

Secondary Cracking

It was stated before that different secondary cracking processes occur. Cracking of hump resulted in different activation energy / frequency factor parameter sets as determined for cracking of C_{6+} resolved components. The latter seemed to include also two processes indicated by two main energies. In Fig. 51 the evolution of different compound groups due to secondary cracking is highlighted. For Draupne Formation alkanes, alkylated aromatics and alkylated thiophenes are compiled and for Heather Formation alkylated phenols instead of thiophenes. It becomes clear from the diagrams that all of these compound groups undergo decomposition from different temperatures on and with different rates. The decrease of n-alkanes seems to govern the whole process in that the decrease coincides with the decrease of H/C values and the increase of aromaticities of the pyrolysate. This

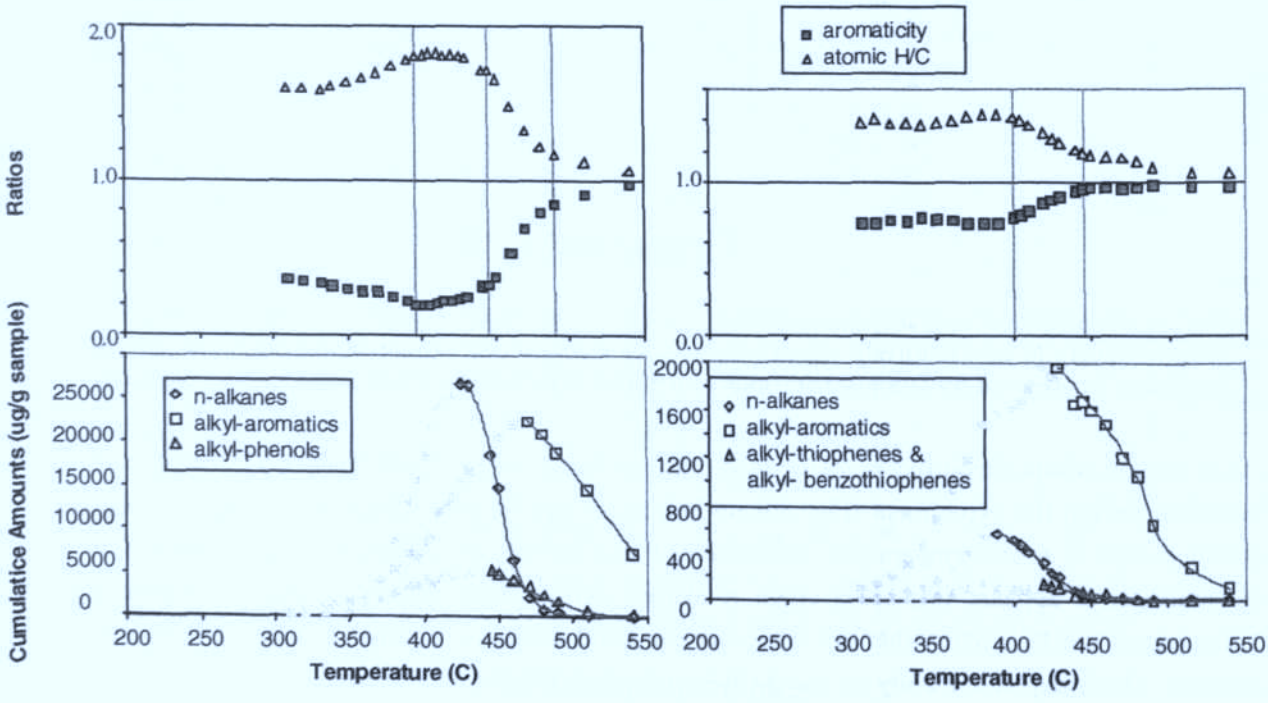


Fig. 51: MSSV pyrolysate (resolved fraction) compositional changes, Draupne Formation (left) and Heather Formation (right). All curves at 0.1 $Kmin^{-1}$. H/C ratios are calculated as the sum of all component H/C ratios weighted by their abundance. Aromaticity was determined as: sum of identified aromatics / sum of resolved C_{6+} pyrolysate.

seems reasonable because the dealkylation of thiophenes, phenols and aromatics yields only relative small amounts of gas components. The longest chainlength of aromatic alkyls considered in the diagrams are pentyl- groups. In addition the cracking of alkyl-chains from aromatics and thiophenes or phenols starts to become pronounced when cracking of n-alkanes has almost reached its end. The relation between the bulk compositional descriptors H/C and aromaticity and the compound group evolution reveals interestingly a delay of the decrease of H/C ratios compared to the onset of secondary cracking of n-alkanes. Probably the decrease of the atomic ratio is compensated for about 10 degrees by the ongoing primary aromatic moiety production.

The cracking of n-alkanes is further investigated by using Draupne and Heather Formation n-alkane cumulative curve inflexion points (as an indicator for the onset of secondary cracking) and data from MSSV pyrolysis of a North Sea oil (Fig. 52). Again the deviating behaviour for short chained alkanes is striking. Whereas long-chain n-alkanes show relative small increases of inflexion point temperatures (see also Fig. 50) compared to the next smaller molecule, gas range hydrocarbons show fast rising inflexion point temperatures. For the North Sea oil additionally iso-alkanes are displayed which are consistent with the n-alkane trend. The oil shows the overall highest temperatures and the steepest trend, i.e. the smallest changes in inflexion-point temperatures, whereas Heather Formation inflexion points occur at the lowest temperatures and with the shallowest trend. The Draupne Formation distribution comes closer to the oil trend.

To explain these kerogen or oil specific features an explanation for the general features must be found. If assuming again random bond breaking, the breakdown of a long chain gives two short chains and thus moves the inflexion points of two short chains to higher temperatures. This could explain the

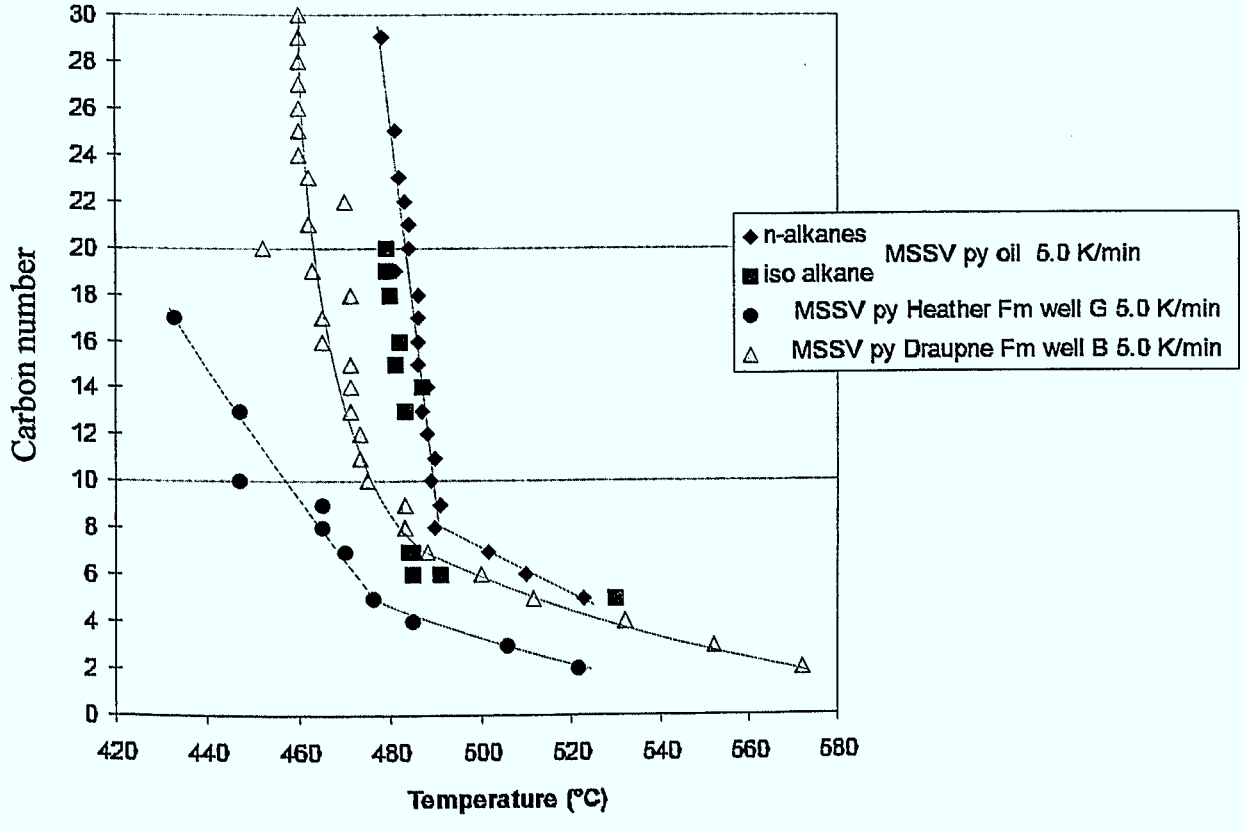


Fig. 52: Alkane inflexion-points in MSSV pyrolysis (maximum amounts, or onset of decrease) as an indicator for secondary cracking?

observed trends, provided that all chains start to undergo cracking from the same temperature on. Thus the longest chains would indicate the real onset of secondary cracking. The influence of ongoing primary cracking cannot be excluded for the source rock MSSV data, but for the oil. This might explain the bigger difference between the inflexion temperatures of tridecane to octane, which is appr. 10°C for the oil and more than 20°C for Draupne Formation. The extreme deviation of Heather Formation inflexion point temperatures in shifting to lower temperatures goes in line with the observation that C_{6+} curves (Fig. 14, p.35) do not show well developed maxima but have flat plateaus before they start to decrease.

The observation of the regular changes in cumulative curve inflexion-points implies a retardation of short-chain inflexion-points due to the adding of cracking products from long chains. A mathematical model designed as a random cracking module was used for an evaluation of the above hypothesis. This random element calculates the cracking of C_1-C_{30} chains with an initial number of ten molecules for each species (Fig. 53, initial composition). Except for methane each molecule undergoes one cracking event resulting in the formation of two smaller molecules the chainlength of which depends on the breaking bond which was randomly chosen. The possibility of no bond-breaking is allowed as well, resulting automatically in a higher stability for smaller molecules, because zero as one possibility out of 0, 1, 2 and 3 (for butane) has a higher probability than for instance out of 18 (for octadecane). Fig. 53 displays the random cracking performed 8 times, each time with the same initial composition of ten molecules. The initial number of 300 molecules multiplied by a factor <2 gives the post cracking composition. Due to the increased stability of short chains the center of gravity of the distribution is shifted to small molecules. Though even if no masses are considered here and instead of the uniform initial composition, this model shows the enhanced formation of low molecular weight components which might cause a pronounced shifting of inflexion points to higher temperatures.

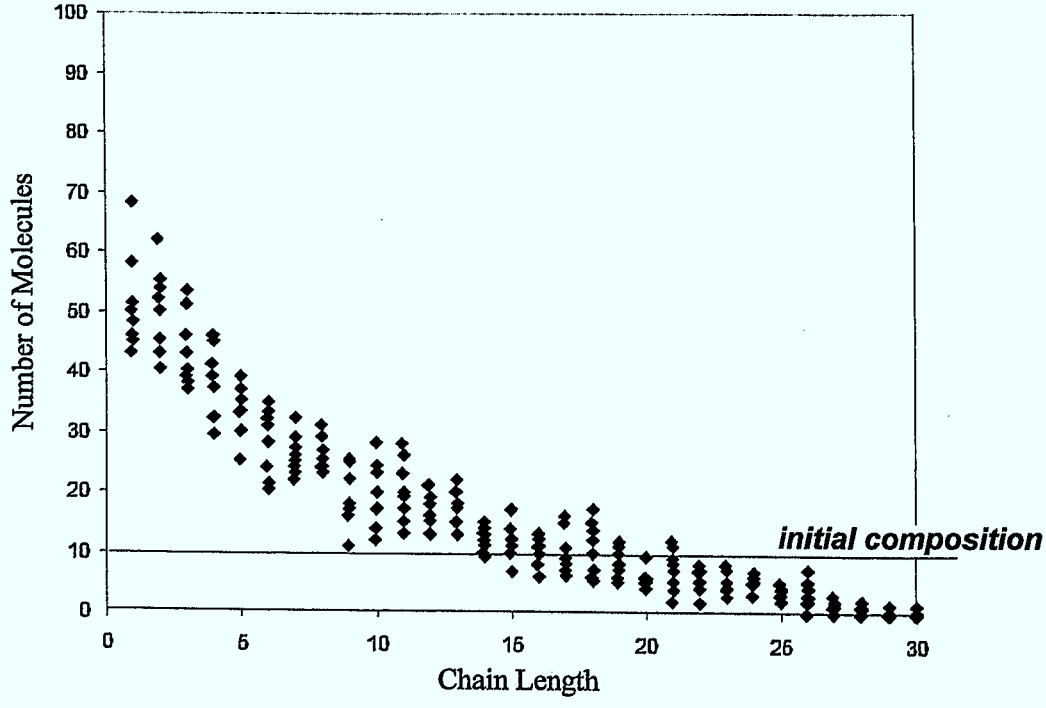


Fig. 53: Result from 1 cracking step of a mathematical random cracking model (performed 8 times. No cracking is optional.

This model takes no account of the role of chain initiation by free radical production, the occurrence of alkanes or alkenes and chain termination or even alkylation. However chain initiation and termination were reported by Weres *et al.* (1988) to be of minor importance because of their low activation energies (in contrast Jackson *et al.* 1995 report Ea for initiation to be high) whereas the cracking step is rate determining.

For the case of the second process of importance, the cracking of alkylgroups from aromatic units, the demethylation of toluene was considered as a model case. Some experience for this process was reported in literature based on the industry interest in converting toluene to benzene (Asinger 1971, p.511 & 589; Silsby & Sawyer 1956). The reaction can be written as

$$C_7H_8 + H_2 \xrightarrow{\Delta T} C_6H_6 + CH_4 \qquad (7).$$

Because hydrogen should be present in excess the reaction is termed hydrodemethylation or hydrodealkylation. Fig. 54 shows that data from MSSV and multistep open pyrolysis confirm the assumed reaction. The toluene decrease (black symbols, MSSV pyrolysis) coincides with the sudden increasing slope of the benzene curve, whereas the benzene formation in the open system reaches a cumulative maximum at approximately 550°C.

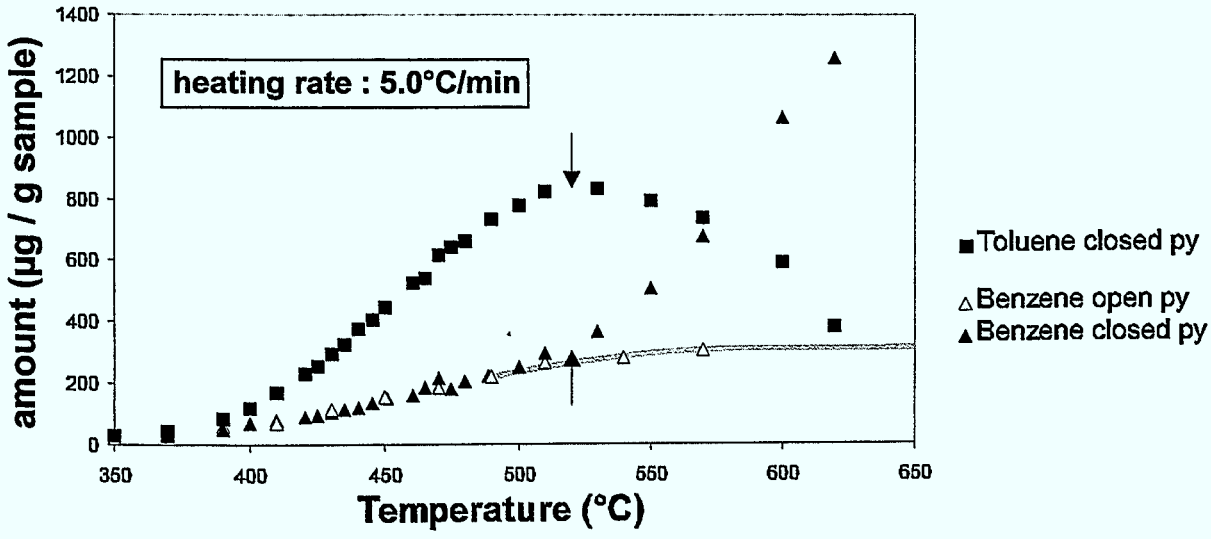


Fig. 54: Comparison of benzene formation in open and closed systems. The deviating formation curve in the closed system seems to be related to the decrease in toluene. Heather Formation.

A model calculation based on Heather Formation MSSV data for a heating rate of 0.1 $Kmin^{-1}$, revealed that 369.9 (µg/g sample) secondary gas could be produced by hydrodealkylation assuming hydrogen to be in excess. Educts used for the calculation were toluene, C_2- and C_3- benzene and C_1-, C_2- and C_3 -naphthalenes. The amount translates to 15 % of the secondary gas calculated from C_{6+} decrease.

Considering the case that for the above-described reaction hydrogen is not present in excess biphenyl occurs as a reaction by-product (Asinger 1971). Observations from thermovaporisation and open

system pyrolysis show that no biphenyl is present at low maturities or under open pyrolysis conditions.

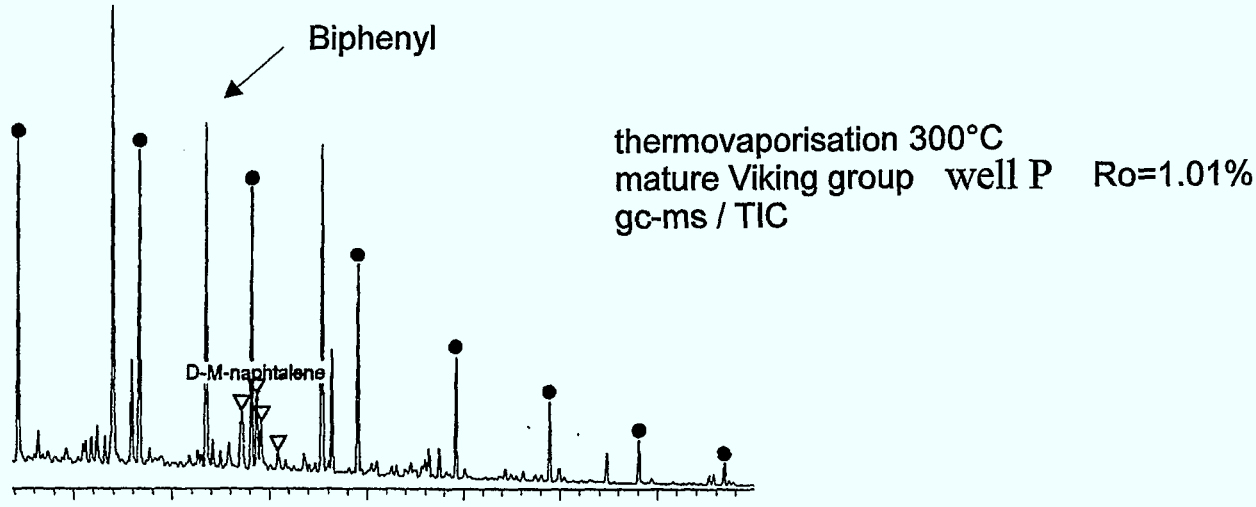


Fig. 55: Occurrence of biphenyl in high maturity settings as observed from thermovaporisation.

In contrast thermal extracts of the high maturity well P (Fig. 55) contain high amounts of biphenyl. Hall *et al.* (1985) confirm increasing biphenyl concentrations with depth for the North Sea area. Based on these observations the occurrence of biphenyl can be interpreted as an indication for in-source rock secondary cracking with an attending hydrogen shortage. The common opinion is in contrast that water derived hydrogen as a reactant is in excess in natural source rocks (for example Lewan 1994). MSSV pyrolysis of two aliquots of sample E 41716 one without and one with added water yielded only 8% more products, the overall composition remained the same. The presence of additional water did not show any significant changes probably because sufficient amounts of hydrogen were already present before. The amounts of biphenyls in both aliquots were small compared to those from well P. In addition to these observations Lin & Wang (1988) presented investigations on crude oils, oil shales and coals and drew the same conclusion from their observations, that is that biphenyls could be high temperature cracking products. The occurrence of this moiety as a simple maturation product a former part of the kerogen especially for terrigeneous kerogens or coals cannot be excluded.

Concluding remarks, petroleum forming reactions

Primary and secondary cracking were discussed on a qualitative basis by considering compositional changes during heating experiments.

- Differences in bond strength could not explain pyrolysate compositions, which instead seem to be controlled by random mechanisms.
- The occurrence of crosslinking structures in kerogens might have a significant impact on C_{1-3} primary gas formation.
- Secondary cracking of the resolved pyrolysate fraction exhibited two stages, the first of which is dominated by n-alkane cracking and a second which starts slightly before n-alkane cracking ceases and is dominated by cracking of alkyl-groups from aromatic units.
- Random cracking was shown to be likely for secondary cracking of alkanes as well. This process could explain the successive increase in temperature for formation-degradation inflexion-points with decreasing carbon chainlength.
- The dealkylation of aromatic hydrocarbons accounts for 15% of secondary gas (cracking of C_{6+}, Heather Formation).
- Biphenyl as a by-product of dealkylation reactions under accompanying hydrogen shortage might indicate secondary cracking in the natural system.

3.5.2 Gas and Light-end Hydrocarbons

Amounts and compositions of gases as observed in hydrocarbon systems can reveal useful hints to clarify the origin of gas with respect to source and maturity. Early attempts to detect gas generation deduced that amounts observed at certain depths would represent generation more or less directly (Landes 1967, Tissot *et al.* 1974, Huc & Hunt 1980, Tissot & Welte 1984, p.182). Cooles *et al.* (1986) however, outlined that the detectable amounts of hydrocarbons and their compositions are a function of generation and migration losses or impregnation, especially for high volatile gas.

Compositional information on gas, associated condensates or even oils were often used for interpretations. Connan & Cassou (1980) observed dry gas with minor contribution of condensate to occur mainly in the immature zone, wet gas associated with paraffinic crude oils at oil window maturity and dry gas associated with mature condensate in the deepest stratigraphic levels. Similar observations were also reported from other places in the world (Leith *et al.* 1993, Evans *et al.* 1971). Hunt (1984) reported for the overmature zone, that even the methane concentration in very deep wells decreases, based on observations from 400 wells in the USA which were deeper than 6.1 km.

The iso-/n-butane molecular ratio for instance has been proposed as a maturity index for gas by Reznikov (1969). C7 hydrocarbons were investigated in detail by Thompson (1979), Mango (1987) and others. Thompson (1979) established a maturity parameter based on changes in the relative concentrations of cyclic and branched alkanes. Using the same components Mango (1990, 1992 & 1994) proposed a parent-daughter scheme involving heptane, isoheptanes and cycloalkanes. Earlier Mango (1987) reported the invariance of isoheptanes which ten Haven(1996) stated to have a high application potential for correlation studies.

For all these investigations the quality of measurements on natural occurring hydrocarbons is a crucial factor. Concerning thermovaporisation measurements it is important to keep in mind that during core storage serious losses of light-end hydrocarbons occur. Headspace gas data also may include large errors due to the sample collection procedure or arising from bit-metamorphism (Faber *et al.* 1988). Sokolov *et al.* (1971) published data according to which the concentration of gas is up to three orders of magnitude lower for conventional sampling procedures compared to a KC-core-lifter technique, which seals the sample at depth *in situ*. Last but not least are "natural" data likely to have undergone crucial changes arising from migration losses, impregnations, water washing effects or biodegradation.

An alternative source for this type of data are artificial heating experiments which allow direct observations on compositional changes upon heating.

Gas Oil Ratio (GOR)

The main bulk gas descriptor is the gas oil ratio (GOR) which is defined as gas (C_{1-5})/ oil (C_{6+}) in kg/kg under surface conditions. It is the GOR which determines the phase-behaviour, density and viscosity of a given petroleum under subsurface conditions (England *et al.* 1987). These properties in turn govern to a large degree the processes of migration and finally accumulation. When petroleum with an inherited GOR is expelled from the source rock, the GOR will be altered by pressure-volume-temperature (PVT) changes (England *et al.* 1987). This is because during decreasing pressure and

temperature liquids lose low molecular weight components to the gas phase or for the case of gases high molecular weight components disproportionate into a liquid phase.

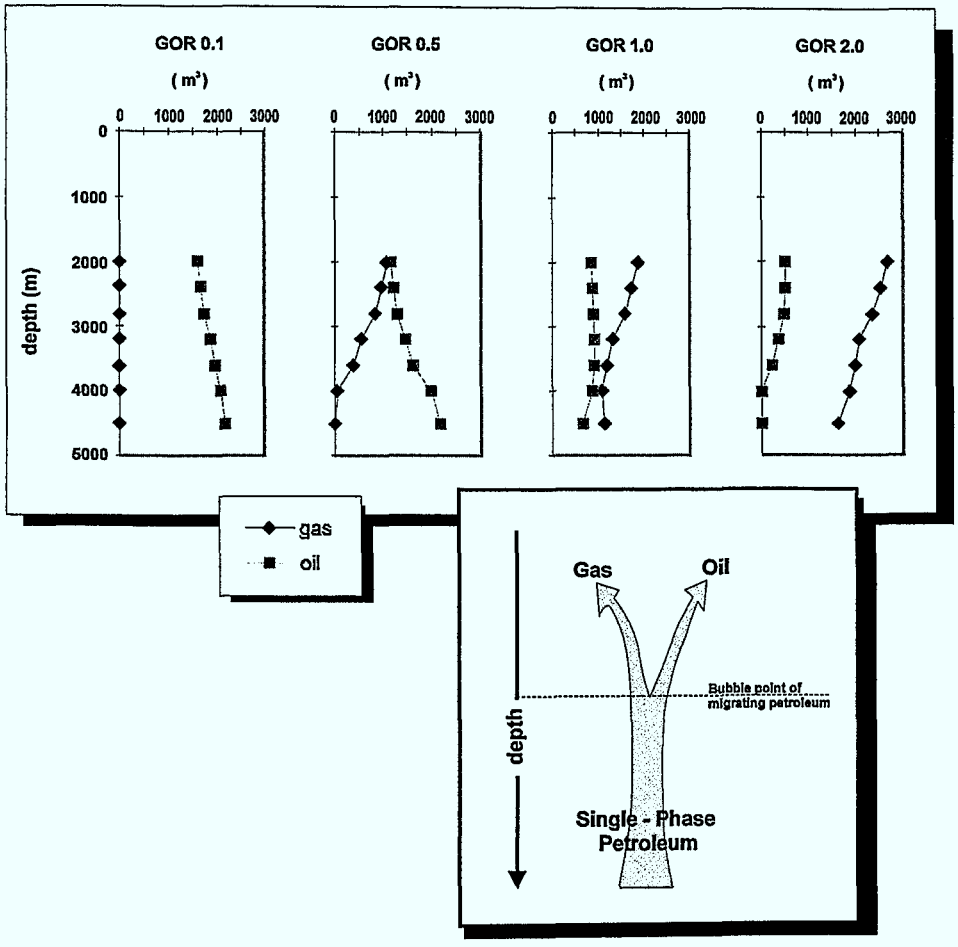


Fig. 56: Volume changes of single gas and oil phases during upward migration after phases have separated above the bubble-point. Four different initial petroleums expressed by their initial GOR's are considered (From Horsfield 1997).

The impact of the initial inherited GOR and the related volume changes of liquid and gas phases was demonstrated by Horsfield (1997) as shown in Fig. 56. An average northern North Sea pressure gradient (13MPa/km) and a temperature-depth relation (Dahl & Augustson 1993) were used to calculate the development of a petroleum with properties published by England *et al.* (1987) during upward migration with the help of *Prospect Analyser* software.

For the case of this study GOR's were determined from the resolved fraction of pyrolysates as proposed by Horsfield & Dueppenbecker (1991). Natural data for purposes of comparison turned out to be difficult to obtain. Thermal extracts were analysed, but are likely to suffer from preferential losses of gas during sampling and core storage as stated above. The overall GOR of the samples investigated here (Table 5) is in the range of 0.1, no matter what type of source rock was investigated. PVT-reconstructed petroleum compositions, i.e. mathematically recombined oil and gas fractions, which were devided by separators at wellsites are the most reliable source of natural system data but were not available for this study.

In Fig. 57 the evolution of GOR's during artificial maturation in closed and open system pyrolysis (top and bottom) is depicted. Results from MSSV pyrolysis indicate first decreasing GOR's with subsequent steadily increasing values for all heating rates and both source rocks. The lowest values for Draupne center around 0.2-0.4 kg/kg. The lowest Heather Formation values are in the range of 0.5-0.7 kg/kg. Data from multistep open pyrolysis on the immature samples indicate only slight increases with temperature, therefore the closed system increase must be assigned to the secondary cracking of oil. GOR's for primary gas generation are 0.3 - 0.8 kg/kg for Draupne and appr. 1.0-2.0

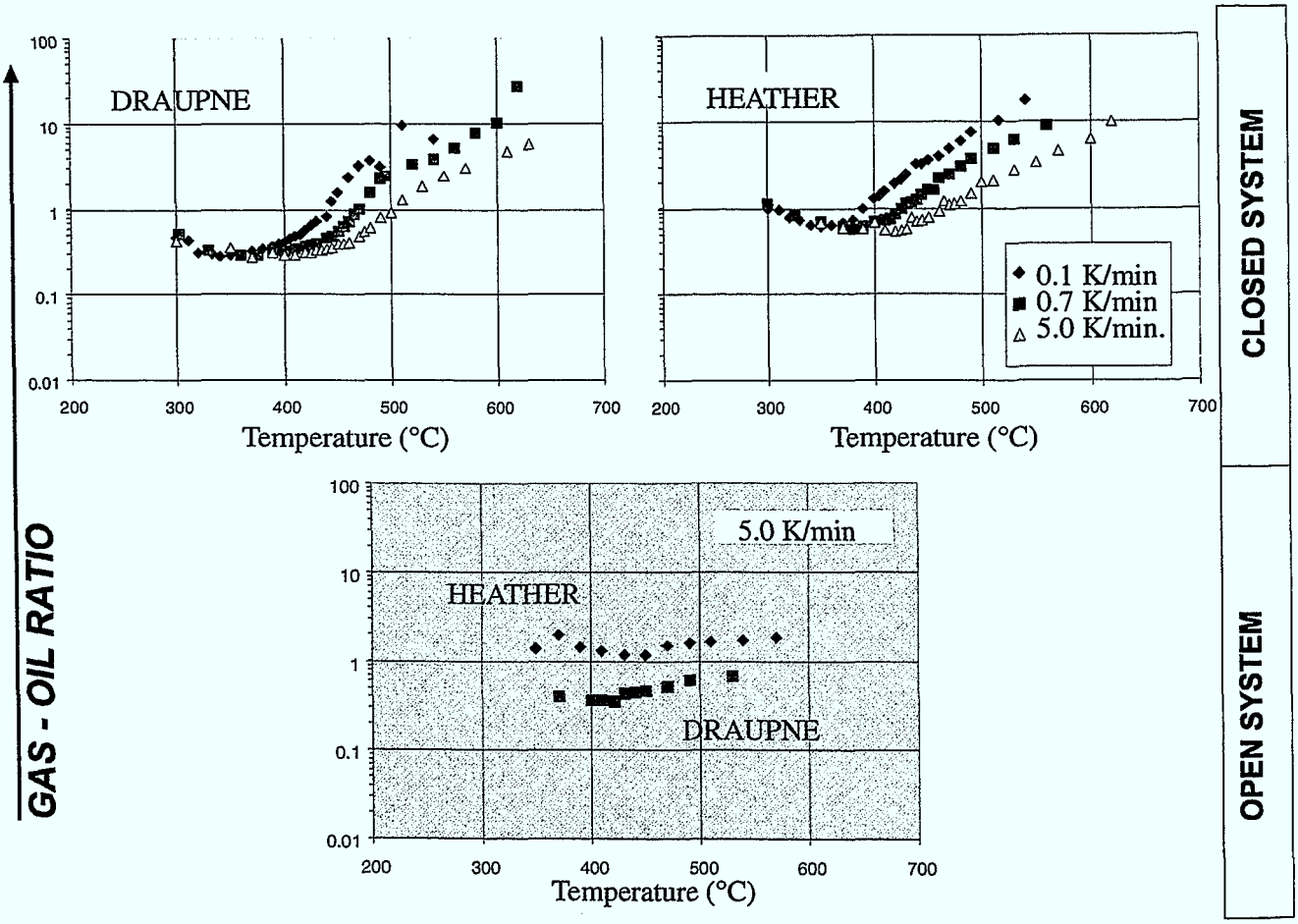


Fig. 57: GOR of products from artificial maturation of immature kerogens during closed (top) and open system pyrolysis (bottom).

kg/kg for Heather Formation. For comparison Skjevrak *et al.* (1994) reported values of 0.46 kg/kg for Heather and 0.24-0.27 kg/kg for Draupne Formation, determined by MSSV pyrolysis and probably based on the total gaschromatographic amenable pyrolysate.

According to the determinations of kinetic parameters for oil and gas (Table 22 & 23) the GOR's for Heather Formation will remain valid under geological heating conditions (cf. Fig. 39, p.65). It was shown that T_{max}-values for primary gas, secondary gas and oil have a preserved relative order for geological heating conditions. In contrast Draupne Formation GOR's should be higher for geological heating conditions than those determined in Fig. 57, this results from the "lower" kinetic parameters for primary gas compared to the formation of oil.

The amounts of gas detected by thermovaporisations were found to be governed by the sorption potential of the organic matter. The higher the TOC-content, the higher is the total amount of gas, this

correlation becomes evident from Fig. 58. Results from Schloemer & Krooss (1996) support this finding by showing the methane diffusion coefficient to be reduced by increasing TOC contents. Both, headspace gas C_1-C_4 and tvap gas C_1-C_5 show amounts which correlate with TOC(%). However the scatter of data is still one order of magnitude. An explanation for the scattering of data especially for headspace gas could be the presence of migrated hydrocarbons instead of indigenous hydrocarbons and variations in sorption potentials due to kerogen types. Methane values from

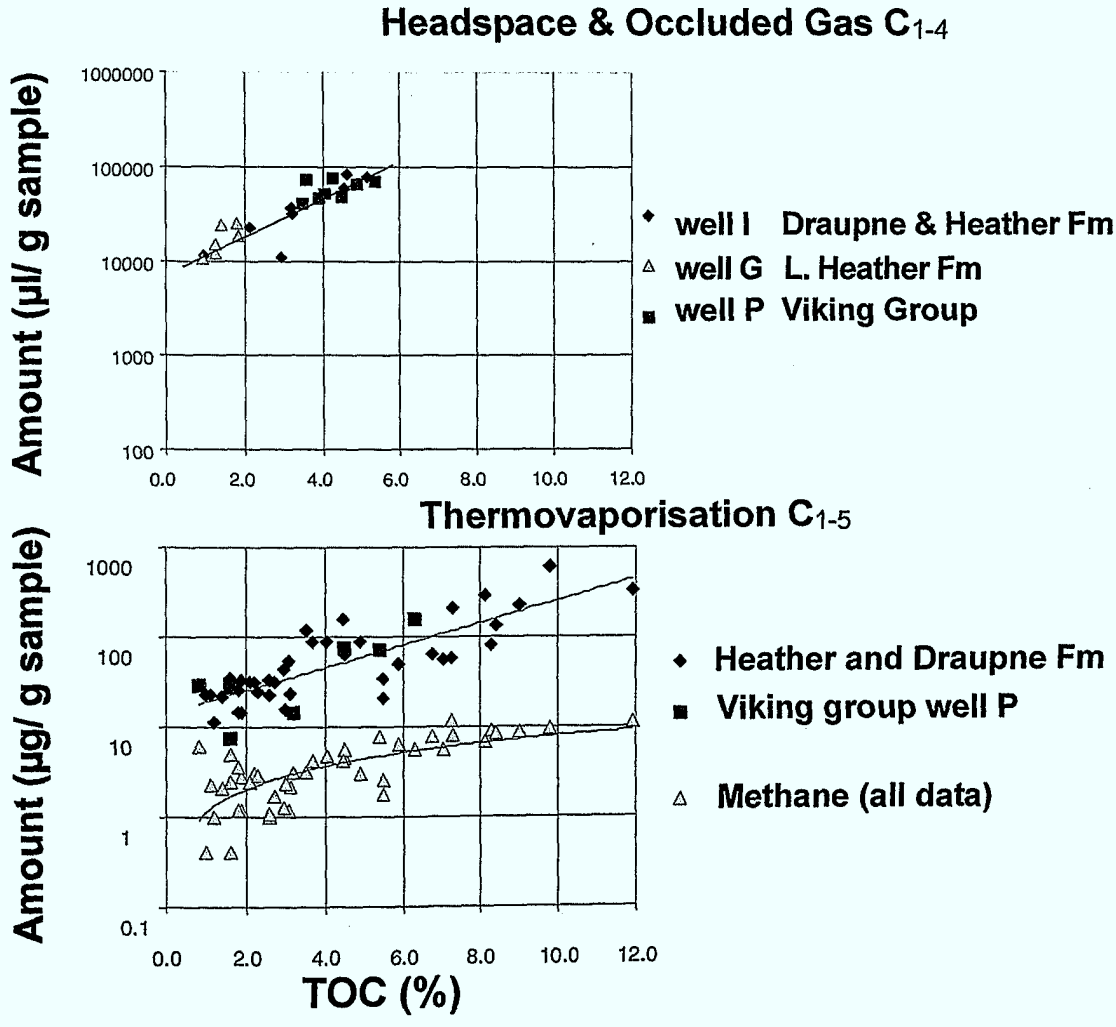


Fig. 58: Retention of gas as a function of TOC. Thermovaporisation and headspace gas data (note different scales).

thermovaporisation show a similar trend as the total gas. A positive correlation of methane and n-butane with TOC was also observed by Pepper & Corvi (1995). Contradictory headspace methane yields do not follow the trend (Table 26) and instead show that methane is present in excess indicating allochtonous or unexpelled gas in quantities exceeding probably the sorption capacities.

Muscio *et al.* (1993) observed the sorption of gas by organic matter for the low maturity Bakken shale (0.3-0.7% R_o). For higher degrees of maturity the Bakken shale lost its retention capability a feature which was not recognised here.

Compositional Features of Light-ends

The C_7 hydrocarbon fraction is believed to be less affected by alterations during sampling and sample storage than C_{1-4} gas components. Several molecular ratios have been developed by different authors (Philippi 1975, Thompson 1979 & 1983, Schaefer *et al.* 1984, Mango 1987 & 1990) in order to relate compositional changes in the light hydrocarbon suite to maturity or source rock quality.

Iso-alkanes

The application of Mango's light-end hydrocarbon parameters was stated to be an excellent tool for the correlation of condensates and oils (ten Haven 1996). The so-called invariance of isoheptanes employs iso-alkanes and is defined as [(2-MH)+(2,3-DMP)/(3-MH)+(2,4-DMP)]. The ratio was tested for MSSV pyrolysates of Draupne Formation sample E 43254 and thermal extracts from two wells shown in Fig. 59. A steady state catalytic process was used to explain why the ratio had a numerical value of approximately one. Ten Haven (1996) observed that this invariance is not universal but is valid for homologous series of petroleum.

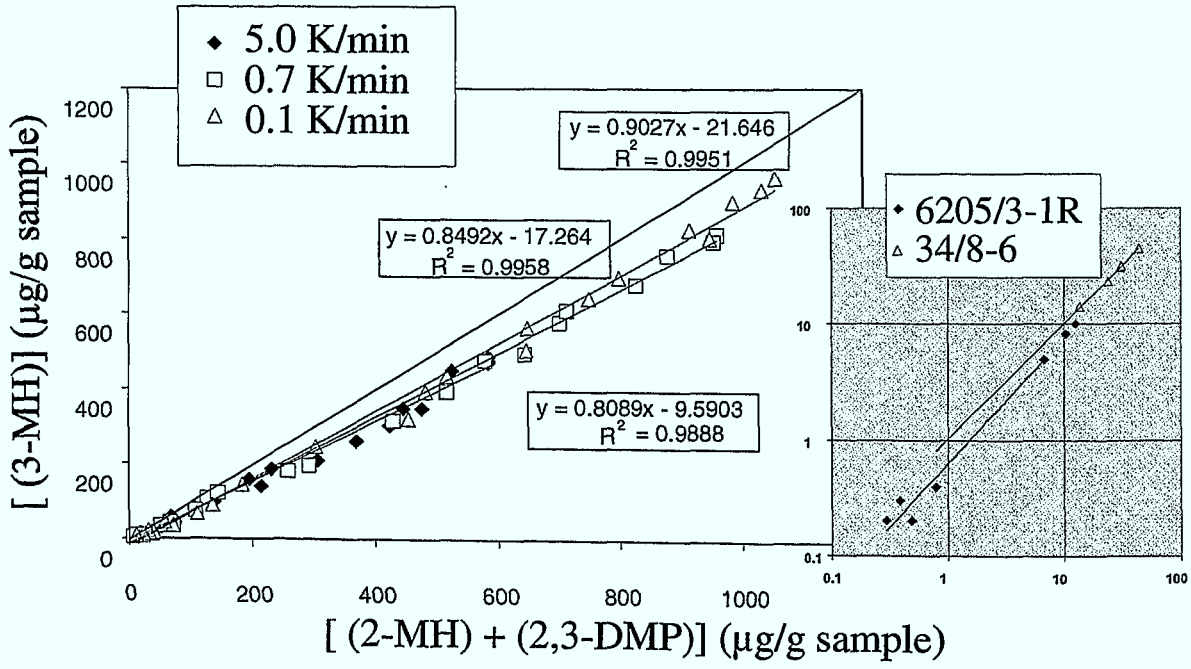


Fig. 59: Molecular ratio [(3-MH)+(2,4-DMP)]/[(2-MH)+(2,3-DMP)] modified after Mango (1987) from MSSV pyrolysis Draupne Formation well B (2764,7m). 2-MH = 2-methylhexane, 3-MH = 3-methylhexane, 2,3- DMP = 2,3-dimethylpentane. 2,4-DMP= 2,4-dimethylpentane is not included (see text).

The ratio originally proposed by Mango (1987) is slightly modified here in that the y-axis does not include the component 2,4-dimethylpentane which co-eluted with other components and was not quantifiable from the gc-traces. However, 2,4-dimethylpentane contributes only small concentrations so that the regression lines in Fig. 59 are still in general agreement with Mango's observation that the ratio of these isoheptanes remains relatively fixed. Moreover the Draupne Formation MSSV products show similar regression lines for all three heating rates. It can be concluded that mechanisms forming isoheptanes in MSSV pyrolysis appear to work essentially identical to those in nature. For the Heather Formation sample MSSV pyrolysis the relationship of these components was not further investigated

because the peaks were too strong disturbed by co-eluting species. The small diagram in Fig. 59 displays thermal extract data for early mature Draupne Formation well I which go in line with the reported mean of 1.06± 0.336 for the invariance ratio. The data from well P represent high maturity thermal extracts and fall below the mean trend indicating a different source type according to the interpretation of ten Haven (1996). This is in accordance with the former assumption that the Viking group kerogen of well P is more similar to Heather Formation.

cyclo-alkanes

Mango (1990) extended his theory of steady state catalytic processes to cyclo-alkanes. He suggested that light cycloalkanes are formed by a steady state processes rather than by decomposition of heavier polycyclic precursors as had been speculated by Thompson (1987). Cycloalkanes can represent high proportions in petroleum. A proportion of 9.5% of the total thermal extract was for instance obtained from Draupne Formation in well I.

The possibility offered by Mango (1990) founds on the cyclisation of alkanes. For example the cyclisation of hexane could yield a methylcyclopentane, whereas the cyclisation of 2-methylhexane could produce for instance 1,3-dimethylcyclopentane. Since both of these reactions are five-ring closures Mango assumed both reaction rates to be proportional for the case that a steady state mechanism is active. To prove this hypothesis Mango plotted the concentrations of the reaction products methylcyclopentane and 1,3-dimethylcyclopentane in a logarithmic diagram using a 2000

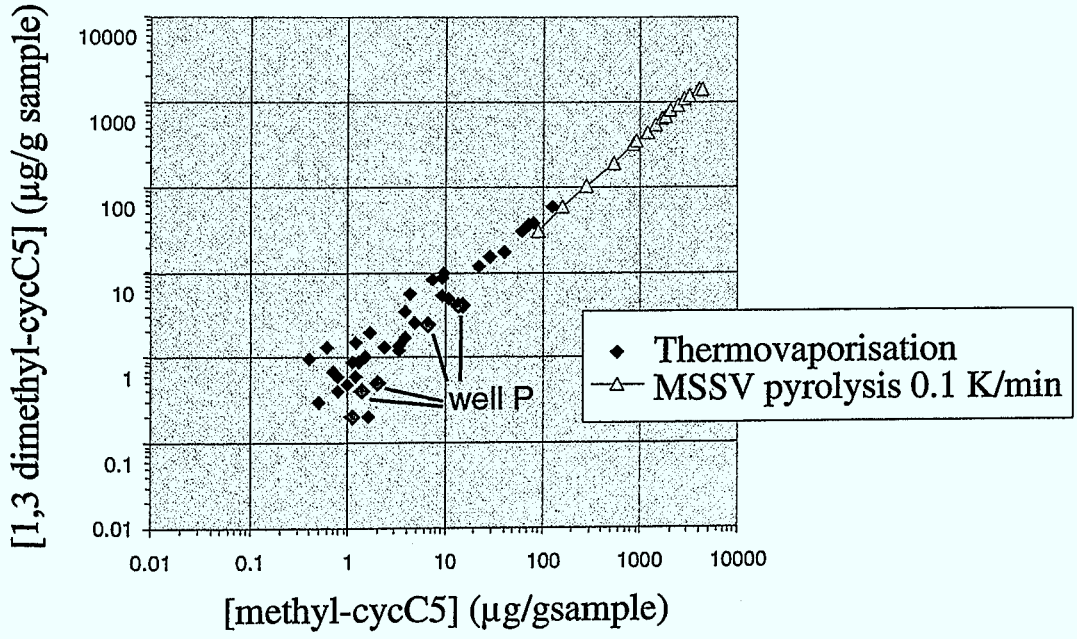


Fig. 60: Concentration-plot modified from Mango (1990) for MSSV pyrolysates of Draupne Formation well B (2764.7m) and all available thermovaporisation data (Table 3). For the case of MSSV pyrolysis only data prior to the onset of secondary cracking are included.

oils database. The relative "invariance" that could be observed was thought to confirm the postulated process. Fig. 60 displays a similar diagram for the here investigated thermal extracts from Heather and Draupne Formation source rocks and Draupne Formation MSSV pyrolysis products at one heating rate. The trend in Fig. 60 becomes broader at lower concentrations. This is probably an effect of the decreasing accuracy of measurements when approaching the limits of detection. Laboratory and

natural cycloalkane compositions turn out to be in good agreement. For the case of secondary cracking in MSSV experiments datapoints shift to higher methylcyclopentane values (not depicted) because the cracking of methylgroups from 1,3 dimethylpentanes reduces their values and at the same time increases the amount of methylcyclopentanes. Thus secondary cracking is likely for data points which come to lie on the lower edge of the trend. Actually the data points of well P can be found in a position relatively enriched in methylcyclopentane. An alternative explanation for data points in this position are migration effects, which might be able to shift data points in this position because methylcyclopentane is the higher volatile compound (delta boiling temp.$\Delta°C_b$= 19.7, Mango 1990).

alkanes / cycloalkanes

Up till now it was shown that iso-alkanes and cyclo-alkanes compared to different species of the same compound-group show regular patterns for both, MSSV pyrolysis and natural petroleums. Philippi (1975) and Thompson (1979,1983) created compound ratios which employ n- and iso-alkanes versus cyclo-alkanes. They correlated changes in the ratios, namely Paraffinicity 1 (2MH+3MH/ sum of DMCP) and Paraffinicity 2 or "V"(n-heptane / methylcyclohexane), with changes in temperatures or maturity.

First of all changes in n-alkane versus cyclo-alkane ratios will be considered. Thompson (1979) suggested that n-alkanes might be thermally more stable than cycloalkanes, so that ratios with n-alkanes in the numerator should increase with maturity. On the contrary Mango (1990) stated that stabilities would behave exactly the other way around. His arguments employed theories from the field of reaction mechanics dealing with the maintenance of orbital symmetry. According to the theory the C-C bond breaking by beta-scission becomes more and more unlikely the higher the

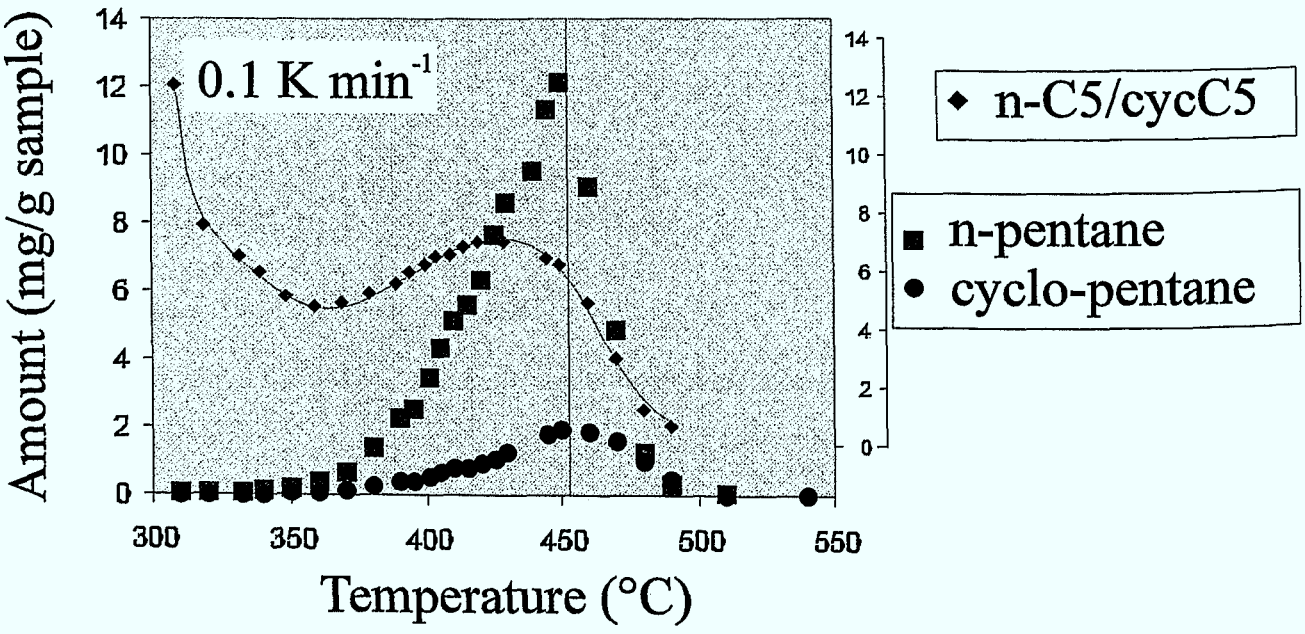


Fig. 61: N-C5 and cyc-C5 as a function of MSSV pyrolysis temperature (left scale) for Draupne Formation sample from well B (2764.7m) and their respective paraffinicity ratio (right scale).

deviation from co-planarity for radical center and breaking bond is. From the results of MSSV-pyrolysis (Fig. 61) no significant differences in apparent thermal stabilities can be observed. The cumulative formation curves for both components start to decrease at 450°C. However, a retardation

of the decrease by cracking of heavier components was shown before to have an impact on the inflexion points (see page 84). The n-C5/cyc-C5 component ratio versus temperature in Fig. 61 shows a complex curvature. In a first part, which can be referred to as early mature, the ratio decreases. Assuming that two gaussian normal-distributions show an interference, a division of the first by the second distribution would lead to values which will show an negative exponential behaviour (Fig. 66, page 100). Translated to the components here this means that the onset of n-alkane formation is at lower temperatures than for the cycloalkane formation.

In a second part, which can be referred to as mature, the ratio increases as postulated by Thompson (1979). This is rather due to different increases in formation rates, than to different thermal stabilities. Finally, in a third stage, which corresponds to "overmature", the ratio decreases as a consequence of faster secondary cracking of n-alkanes. To account for Mango's hypothesis that cycloalkanes are extreme thermally stable, it can be stated that the disappearance of cyclopentane could also be a sign for incorporation of cyclopentane into an inert residue by aromatisation. No matter what is more

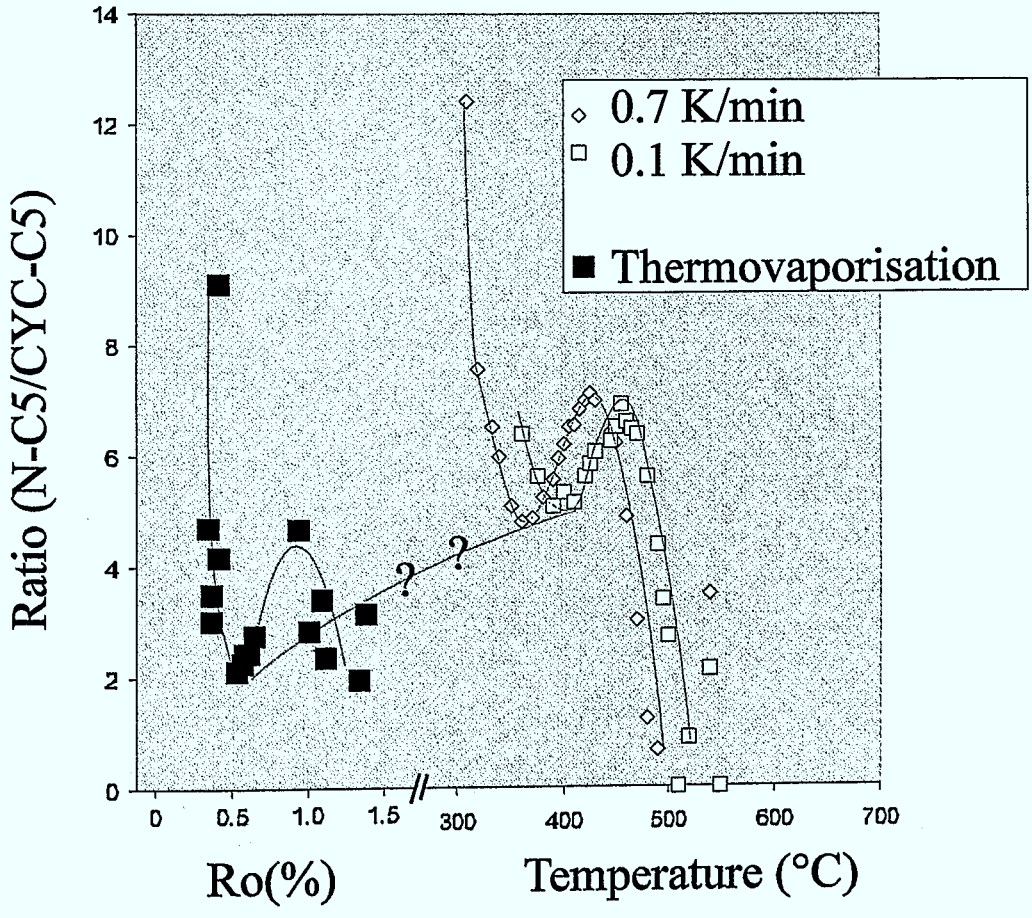


Fig. 62: Molecular ratio of n-C5 versus cyc-C5 (paraffinicity) for two heating rates of MSSV pyrolysis (Draupne Formation well B, 2764.7m) and thermal extract data of selected samples, note the different x-axis scales. Thermal extract data of the wells F and G were excluded because the suspicion of impregnation (see Figure 65).

correct, the observation of paraffinicity-increase and -decrease sections, can also be confirmed from thermal extract data (Fig. 62).

Though the natural samples will neither have suffered a linear heating history nor one which was the same for all locations, reveals the distribution of ratio versus maturity an astonishing similarity to laboratory results. It can be concluded, that the n-alkane vs. cycloalkane paraffinicity, for the case of five carbon atoms follows the increasing trend as proposed by Philippi (1975) and Thompson (1979), only in the boundaries of oil window maturity. For gas and related condensates from overmature settings, which are central to the present study, paraffinicities of this type have to be interpreted with caution and for the case of n-C5/cyc-C5 follow decreasing trends.

Another issue results from Fig. 62. Values of thermal extracts are lower compared to those of MSSV pyrolysates, which is the main deviation of laboratory trends to the natural data. This reflects probably an influence of heating rate on the relative amounts of products. It must be assumed that the formation of cycloalkanes is slow compared to the formation of the bulk of products, supporting the idea that different processes than cracking take place, as for instance cyclisation. This reaction type is likely to follow steady state schemes because it can explain the apparent universal similarities in compositional patterns as outlined above.

A component pair of the same type, namely n-heptane versus methylcyclohexane (V of Philippi 1975, and paraffinicity 2 of Thompson 1979), was investigated in order to check the validity of the findings outlined above. For this molecular ratio experimental data for both source rock formations were

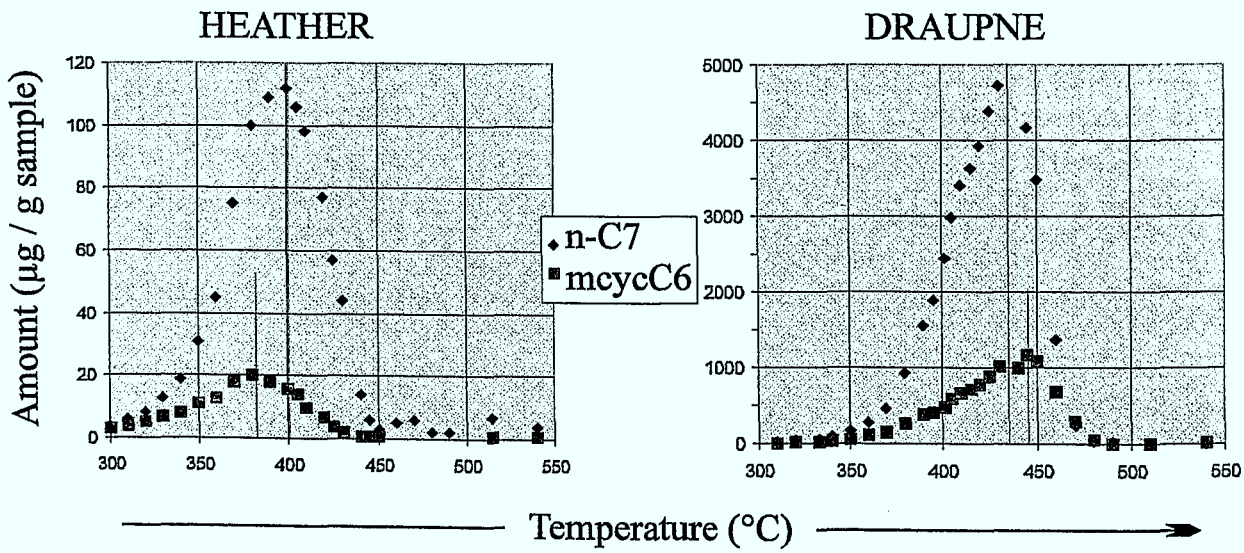


Fig. 63: MSSV pyrolysis formation curves (0.1 $Kmin^{-1}$) for n-heptane and methylcyclohexane for Heather Formation (well G, 2138.75m) and Draupne Formation (well B, 2764.7m). Interest is focused on the different apparent thermal stabilities of both components.

available. Concerning the question of thermal stabilities of n-alkanes and cyclo-alkanes the information from Fig. 63 is similarly ambiguous as observed before. Draupne Formation experimental data are contradictory to those of Heather Formation where methylcyclohexane appears to be less stable than heptane. Nevertheless, the resulting paraffinicity ratios reveal essentially the same features as for the case of pentane and cyclopentane except for the significant decrease in the early mature section.

Two main trends are obvious for both natural and MSSV pyrolysis data from both source rock formations (Fig. 64).

- Increasing values until peak oil window to end of oil-window maturity is reached and

- decreasing values for the overmature section.

Thus, increasing values like reported in literature (Thompson 1979) hold as long as oil window mature samples are concerned. This is due to differences in the formation rates. Differences in thermal stabilities become important for samples, which have experienced overmature conditions. Here the ratio decreases for experimental data as well as for those of the natural system. In terms of

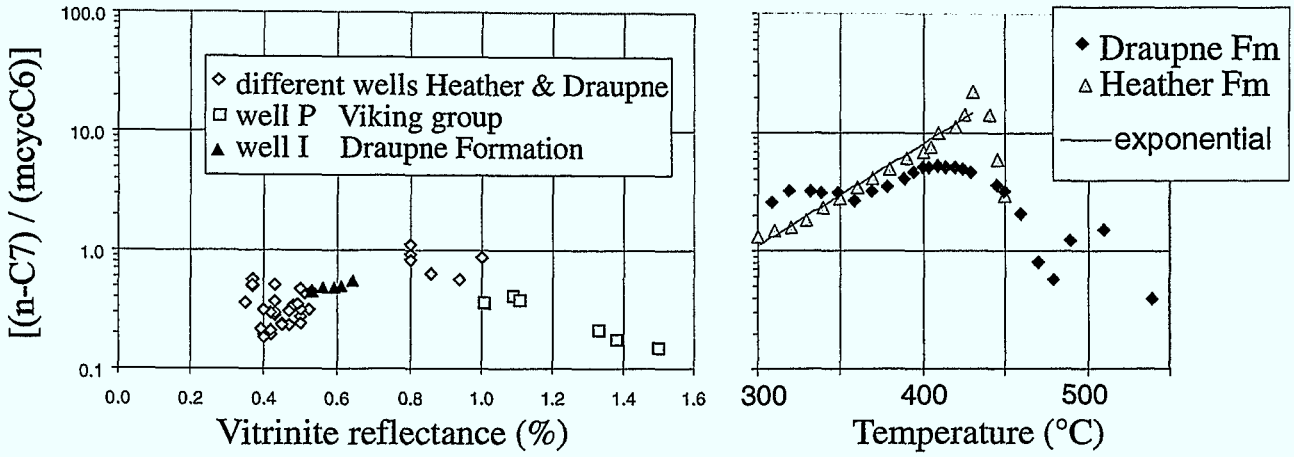


Fig. 64: Paraffinicity 2 (Thompson 1979) for thermal extract data and MSSV pyrolysis (0.1 K/min).

stability, n-alkanes undergo decomposition at a faster rate than do cycloalkanes which actually must not decompose but could alternatively undergo aromatisation. Again ratios from natural samples tend to show about one order of magnitude lower values implying different heating rate dependencies for n-alkanes and cyclo-alkanes in that the latter become quantitative more important for geological heating rates. As a sidebar it results from Fig. 64 that secondary cracking is occurring in well P, which was already inferred from the occurrence of biphenyls in thermal extracts.

After iso-/iso-alkanes, cyclo-/cyclo-alkanes and normal-/cyclo-alkanes were investigated a last combination which was also employed in literature (Thompson 1979, Schaefer & Littke 1988) remains to be discussed. This is the paraffinicity 1 or the modified ratio "J" which employs iso- versus cycloalkanes and which was also suggested to reflect maturity. The molecular ratio PI 1' (Table 5, Appendix) was calculated as a slightly modified version of the "paraffinicity 1" of Thompson (1979) because the 2-methylhexane peak overlaps with dimethylpentane. This should not affect the validity of the ratio because both compounds are isoheptanes and dimethylpentane contributes only minor amounts. The ratio "J" as proposed by Schaefer & Littke (1988) is also a modification of paraffinicity 1 in that 1,cis-2-dimethylcyclopentane is added to the naphthenic fraction. Plotting the PI 1' parameter from thermovaporisation data versus vitrinite reflectance (Fig. 65) shows no clearly situation immediately. By comparing the distribution with the exponential correlation reported by Schaefer & Littke (1988), the most likely explanation for the distribution of thermal extract data seems, that only samples from the wells D, I and P correspond to the source rock maturity, whereas the wells F, G and H contain hydrocarbons that have been generated at higher levels of source rock maturation. In the block 35 a mixing of hydrocarbons from different maturity levels is likely to be caused by the intercalation of source rock intervals with reservoir or carrier units. The following sequence of

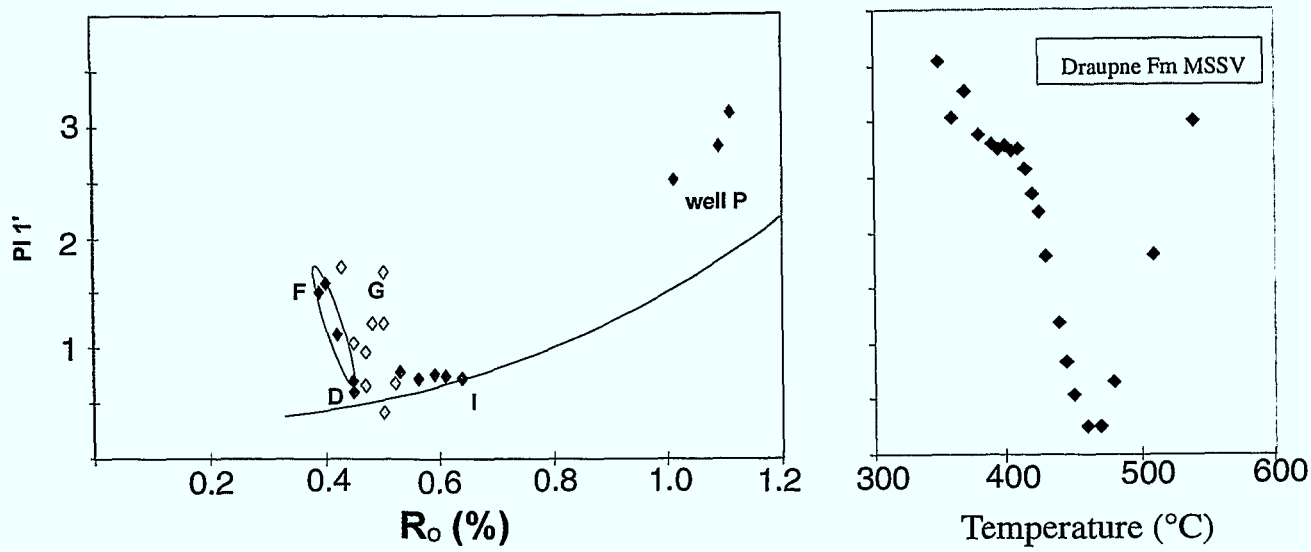
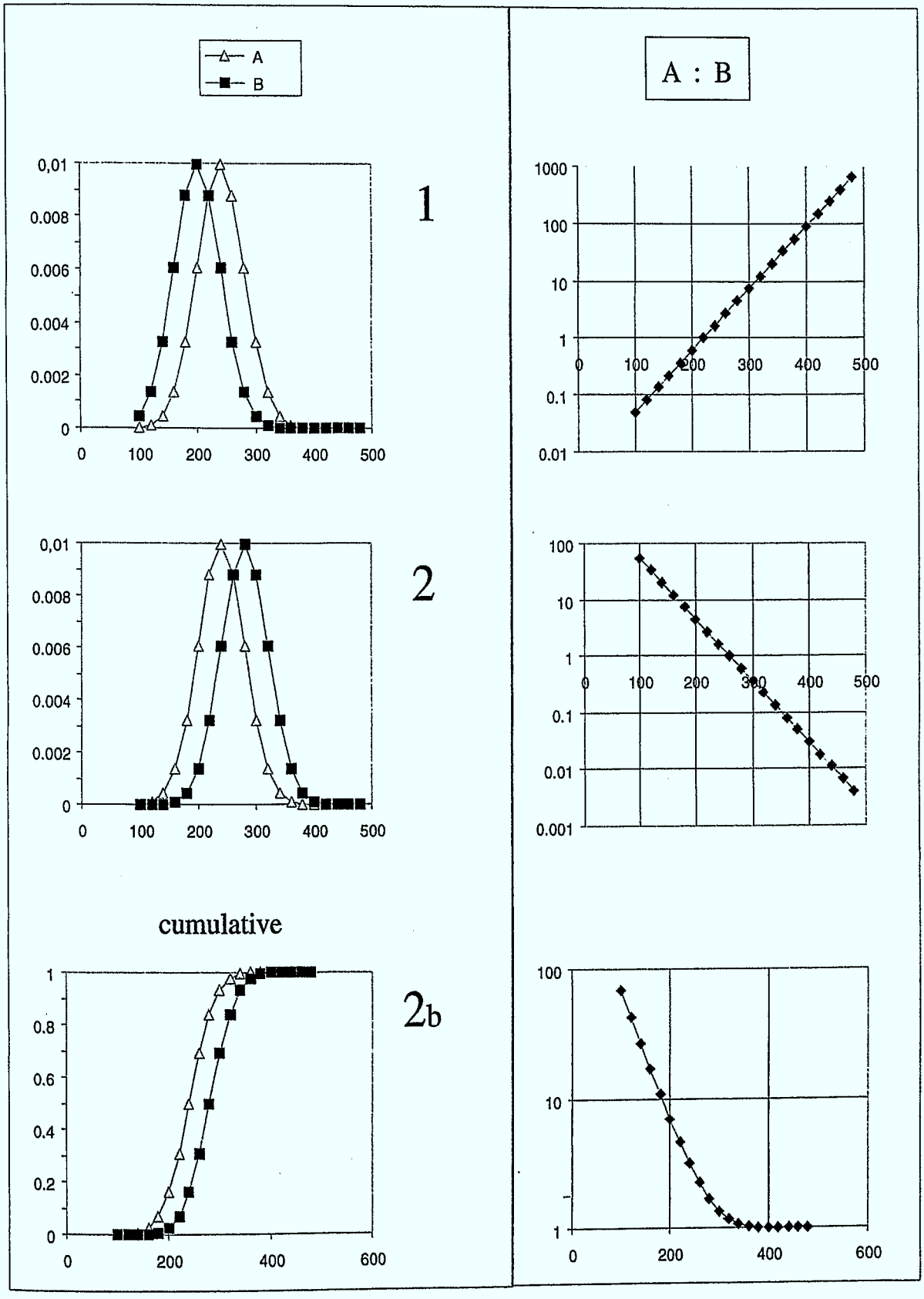


Fig. 65: The modified paraffinicity 1 (for explanation see text) molecular parameter as a function of maturity for thermal extract data and for Draupne formation MSSV pyrolysis data at a heating rate of 0.1 $Kmin^{-1}$ (trendline from Schaefer & Littke 1988).

hydrocarbons results with increasing maturity: well D < I < H < F <G < well P. Interpolation of the PI 1' values of the wells F and G in Fig. 65 indicates a maturity range from 0.5-0.8 R_o(%) for the generation of these hydrocarbons.

In contrast to the reported good agreement of laboratory trends with trends occurring in natural data sets the calculation of the PI 1' from Draupne Formation MSSV pyrolysis data shows a completely different behaviour. These data show by far no simple positive exponential distribution but rather a zonation comprising three stages with different slopes. As an aside it may be remarked that an almost identical distribution was found for the molecular ratio *Methyl Phenanthrene Index 3* by Garrigues *et al.* (1990) during pyrolysis of a Kimmeridge Clay sample. Stage one in the here observed distribution (Fig. 65) comprises a shallow decrease which becomes steeper in zone two. The decrease in zone two can be explained by scenario 2 (2b for cumulative data) in the model in Fig. 66. Translated to the paraffinicity index, isoheptanes form first (A) and dimethylcyclopentanes second (B) in the experiment. In contrast case 1 in Fig. 66 is valid for the natural system, where the ratio is reported to increase exponentially (Schaefer & Littke 1988). The consequence is that, the relative order of component formation for laboratory heating rates is exactly the other way around than for geological heating rates, indicating that different kinetic parameters apply. In a third stage in Fig. 65, values start to increase again. Similar to the observations from the five- and seven- carbon atom system this reflects the relative decomposition rates of iso- and cycloalkanes. This time the compound ratio increases for overmature conditions, indicating that cycloalkanes decompose faster.

Fig. 66 (opposite page): Mathematical model for the explanation of molecular compound ratio behaviour. The cases 1 and 2 show normal distributions with different mean values i.e. interference. The bottom scenario is identical to case 2 but expressed as cumulative distributions. On the right hand side the ratio A : B for the different normal distribution scenarios is depicted. Changes in the standard deviations (broad or narrow normal-distributions), differences in the amplitudes or in the degree of interference have no effect on the sign of the slope, i.e. positive or negative.


A
B
A : B
0,01
0.008
0.006
0.004
0.002
0
0 100 200 300 400 500
1
1000
100
10
1
0.1
0.01
2
0.001
cumulative
2b
1
0.8
0.6
0.4
0.2
0 200 400 600

Concluding remarks, compositional features of light ends

Component ratios based on iso-, cyclo- and n- alkanes provide information about source type and maturity. It turned out, that compositional ratios which employ components from one and the same compound-group have an affinity to yield information on processes with small source related deviations, whereas heterogeneous ratios were shown to be more maturity dependent arising from differences in formation and decompositon rates.

- The so-called "invariance" of isoheptanes holds for MSSV pyrolysis data, regardless of heating rate.
- The isoheptane ratio indicates source differences for thermal extracts of the wells I and P.
- Iso-/iso-alkane and cyc-/cyc-alkane ratios infer that steady state processes are important mechanisms for gas formation, because ratios of isomers show remarkable constance.
- Cyc-/cyc-alkane and n-/cyc-alkane ratios indicated that secondary cracking processes are significant for gas formation in well P.
- Paraffinicity ratios were shown to be behave complex. Especially n-/cyc-alkane ratios were found to decrease in the overmature interval. The quality of the trend in Fig. 64 might allow application for maturity assessments.
- Except for the paraffinicity 1, which is a ratio of iso-/cyc-alkanes, data from thermovaporisation and MSSV pyrolysis revealed similar trends. PI 1' was the only ratio where different kinetic parameters seemed to apply for the formation of the participating components.

Compositional Features of Gas

The compositional information for C_{1-4} gas is mainly restricted to normal alkanes and iso-butane. Besides headspace and occluded gas data also compositional informations from Draupne and Heather Formation MSSV pyrolysis provided valuable informations. Based on the findings from above it can be assumed that comparisons between n- and n- alkanes as well as iso- and n- alkanes should be in good agreement with those from natural data sets.

i/n butane

The i/n butane ratio which is measured today on a routine basis for headspace and occluded gas analyses has already been proposed by Reznikov (1969) as a maturation index for gas. Héroux *et al.* (1979) reported values > 1.0 for shallow gas and decreasing ratios down to 0.7 for the beginning of the oil window. Monnier *et al.* (1981) confirmed decreasing values with depth from observations of single wells. In contrast Savcenko *et al.* (1971) stated that the ratio is independent of stratigraphic level, burial depth and temperature, but reflects the contact of gas with oil. They reported values >0.9

if the gas was never in contact with oil and <0.8 for gas dissolved in oil. Connan & Cassou (1980) go in line with both types of interpretation by reporting i/n C4 > 0.8 for gas produced with condensates which they classify as immature and <0.8 for gas produced with high wax crudes or mature condensates, and come to the conclusion to see a maturity related decrease. Besides maturity or depth the alteration of the ratio by biodegradation must be considered. N-alkanes are preferentially degraded (Connan 1984) and therefore the ratio will increase. This feature was observed for the shallowest Tampen Spur petroleum discovery the, Gullfaks field (Horstad *et al.* 1992). Finally the effect of pressure might have an impact on i/n-butane. Dominé (1991) could show strong variations in the ratio by pyrolysing 1-phenyl-butane to 5% conversion at 357°C and at pressures ranging from 0 to 15Kbar. The i/n-butane ratio decreased from 1.4 at 2Kbar to 0.43 at 15Kbar. All of these interpretations have in common that the reported values are of the same order of magnitude. But it is also fact that most interpretations are restricted to observations form wells which in addition concentrate on relatively shallow samples.

In Fig. 67 a detailed investigation of the development of i- and n-butane during MSSV pyrolysis is compiled taking also account for the differences resulting from ratios calculated from cumulative or differential curves as explained using the model in Fig. 66. That means differentiated curves can be considered as calculated open conditions whereas the cumulative curves represent closed conditions allowing also changes in ratios by secondary reactions. The calculation of i/n-butane by differential curves as shown in Fig. 67 is only reliable in the central part of the distribution because the error becomes extremely large at the low and high temperature edges. In these sections the single component formation rate curves have very low values and in addition come very close together, therefore small deviations result in large errors.

Draupne differential

Most values center around a mean of 0.25 for all heating rates. The curves show a slight decrease at low maturities and an increase at high maturities. It is not clear whether this must be considered an edge-effect or not. The impact of mathematical error caused by edge effects becomes clear as each heating rate shows individual curvature either to higher or to lower values.

Draupne cumulative

The cumulative values center around the same value of 0.25 but they also reveal a slight heating rate dependence in that average values increase for slower heating rates. The strong rise at high temperatures is related to differences in secondary cracking rates.

Heather differential

Contrary to the more or less constant values of Draupne Formation the ratio shows an overall increase, starting at 0.1-0.2 and rising up to values of approximately 1.

Heather cumulative

The cumulative curves have got a shallower slope, but reveal essentially the same trend. The data do not indicate any pronounced dependence of heating rates. The secondary cracking rise is present but less significant than for Draupne Formation.

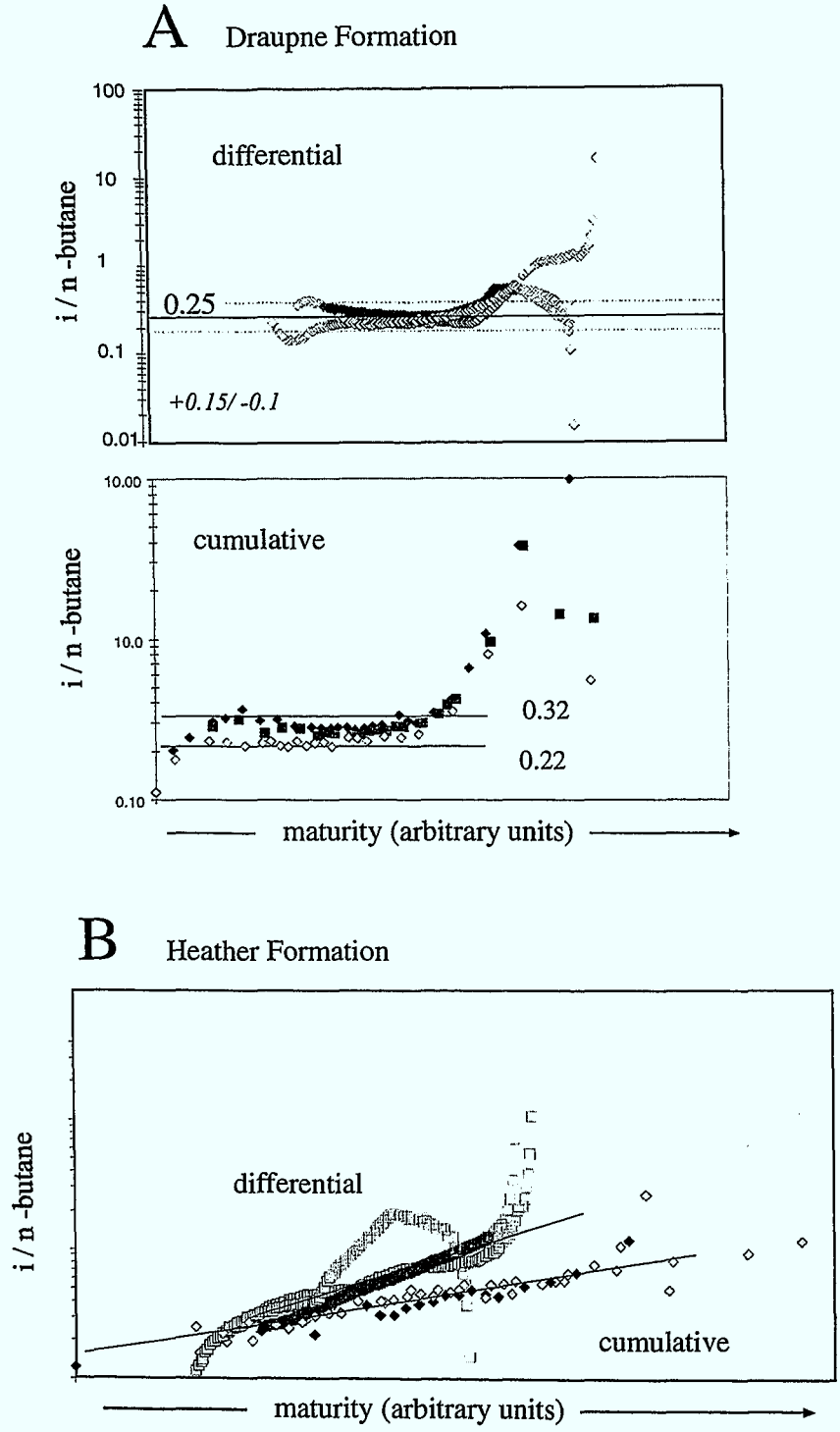


Fig. 67: Molecular ratio i/n butane from MSSV pyrolysis for Draupne and Heather Formation at three heating rates (0.1, 0.7, 5.0 $Kmin^{-1}$). The ratio was calculated from the cumulative MSSV curves i.e. including decrease by secondary cracking at higher temperatures, and from spline approximated and differentiated curves i.e. without regard of secondary cracking. The curves are shifted in temperature direction until best match was obtained.

If assuming heating rate independence for the i/n butane ratio, for which some evidence was provided, the following hypothesis can be summarised:

- Low values centering around 0.2-0.3 might be indicative for Draupne Formation gas whereas values higher 0.4 up to 1.0 signify Heather Formation.

- Experimental Heather Formation values reflect maturity in that i/n butane increases with temperature. Reinterpretation of a diagram by Connan & Cassou (1980) shows lower average values for gas linked to oil and higher average values for gas linked to mature condensates and corroborates these findings.
- Finally, values higher than 1.0 occur for the case of secondary cracking for both source rocks investigated here.

With regard to these hypothesis headspace and occluded gas data are interpreted. The abundance of i/n butane ratios derived from a headspace gas data base depicted as a histogram (Fig. 68) shows two maxima at 0.5 and 2.0. The first maxima at 0.5 holds more than 80% of measurements. Values reported by Larter *et al.* (1990) for oils of the block 7/12 fall also in the range of 0.44 to 0.58.
A similar distribution can be observed by employing thermovaporisation data (Fig. 69). Inspite of gas losses during drilling and storage the same distribution of i-/n-butane ratios seems to be preserved. In this diagram a relation between ratio, maturity and source type becomes visible. Draupne Formation thermal extract data range from less than 0.1 to 0.5 regardless of their respective source rock maturity. The mean value is approximately 0.25 though data are not normal distributed and n = 14 is certainly no reliable data-quantity for statistics. However, 0.25 is exactly the value found from MSSV pyrolysis in Fig. 67. A single value for Heather Formation thermovaporisation can be considered to represent the source rock maturity indicating i-/n-butane to be 0.6-0.7 for low degrees of maturity. Values inscribed as *Heather Formation migrated* stem from wells of quadrant IV and are likely to be influence by migrated hydrocarbons.

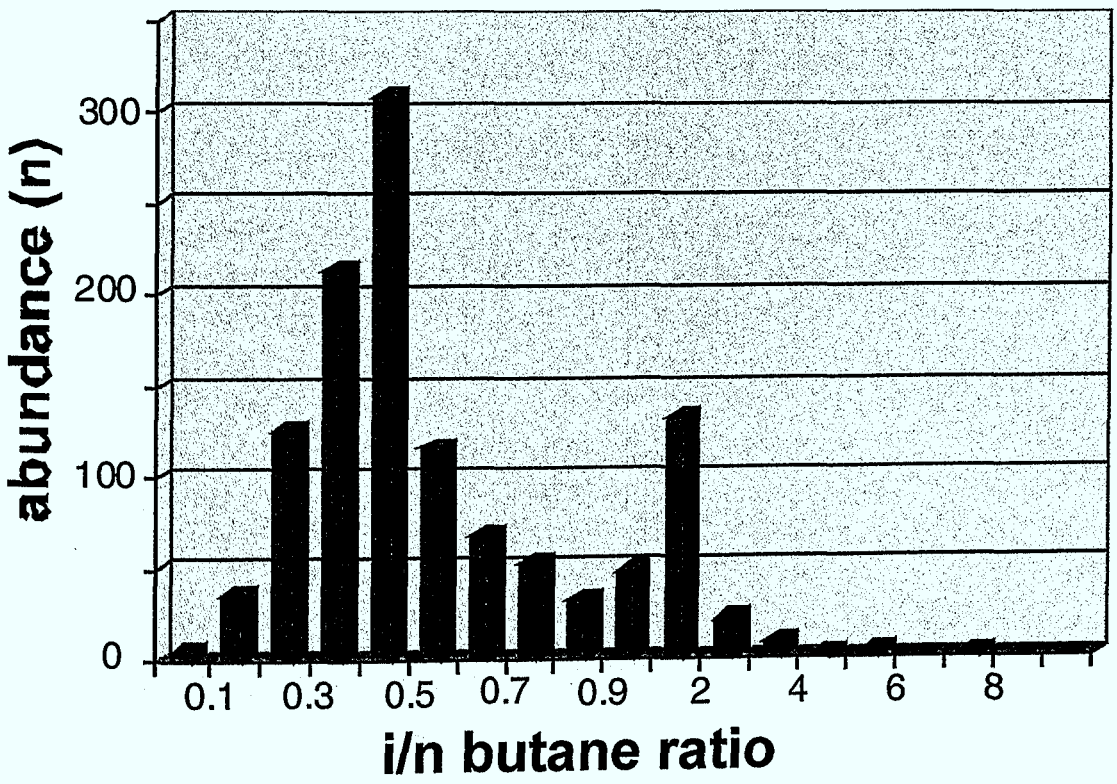


Fig. 68: Headspace and occluded gas data from Norwegian quadrants I, II, III and IV. (Norsk Hydro data base and Table 26).

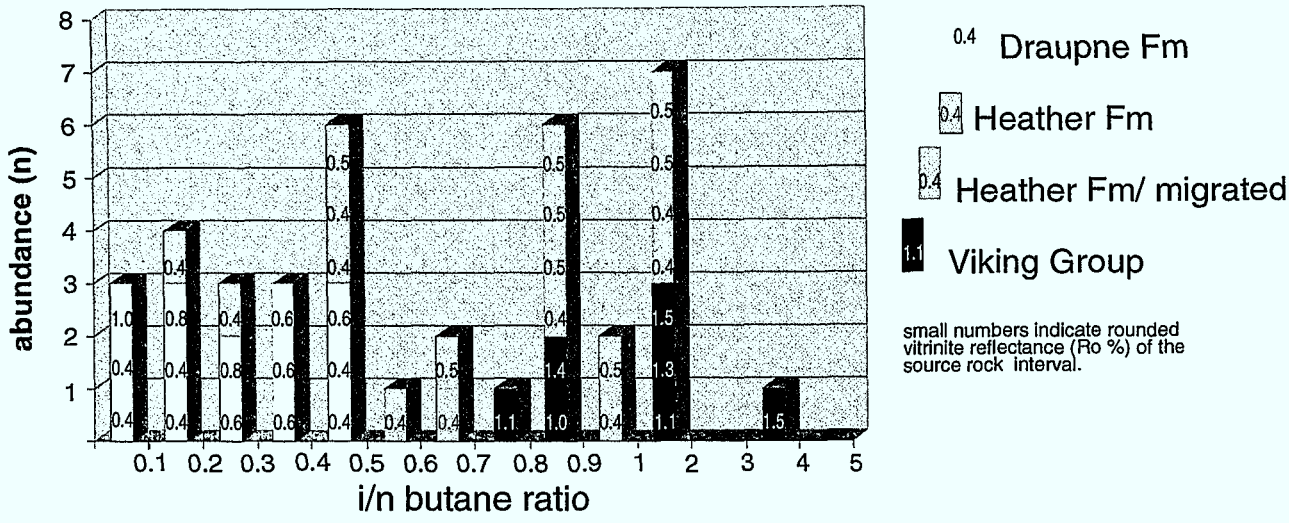


Fig. 69: Thermal extract data for Heather and Draupne Formations (quadrants Vi, I, III and IV) and Viking Group well P, Table 3.

Finally Viking group samples from well P display overall high values corroborating the assumption of values higher 1.0 for overmature conditions. With respect to the findings from MSSV pyrolysis, ratios lower than 0.5 might represent predominantly Draupne Formation gas and values higher 0.5 up to 1.0 should be related to late mature gas formation before the onset of secondary cracking probably derived from Heather Formation. Extremely high values higher than 1.0 might indicate gas from secondary cracking of oil or unexpelled bitumen. This type of gas is indicated by Fig. 68 to be of minor importance in the Viking Graben area. However, gas samples which do not contain i- and n-butanes but only methane, ethane and propane are not included in interpretations based on this ratio.

C_{1-4} compositional patterns

The parameter wetness is often considered to yield valuable information on gas maturity. Wetness is defined as $(C_{2-4}/C_{1-4})*100$ and is an expression of the relative proportion of wet gas and methane. In the following a kind of resolved wetness is investigated by characterising the n-C_{1-4} compositional patterns and finally integrating them in a model using cluster-analysis.

Fig. 70 shows the development of the n-C_{1-4} compositional patterns with increasing temperatures as observed from MSSV pyrolysis for Draupne and Heather Formations at a heating rate of 5.0 $Kmin^{-1}$. The corresponding i/n-butane values are given in brackets. It is not only that the amounts of individual components increase with rising temperature, moreover the relative proportions of the components compared to each other change. These changes can also be expressed in a logarithmic system (Fig. 70) as slopes between C_1 and C_2, C_2 and C_3 and C_3 and C_4 and seem to be significant for both, kerogen-type and maturity. Observed compositional alterations are the same for all three experimental heating rates. Most striking are the changes of compositional patterns with the onset of the secondary cracking of C_{2-4} gas compounds at temperatures higher than 510°C (Heather) or 530°C (Draupne) respectively. This is also the temperature where i/n butane values increase more distinctively.

These compositional patterns show striking similarities to distributions obtained from headspace gas data. Fig. 72 shows some headspace gas data sets for apparently different levels of maturity which correlate well with the experimental compositions.

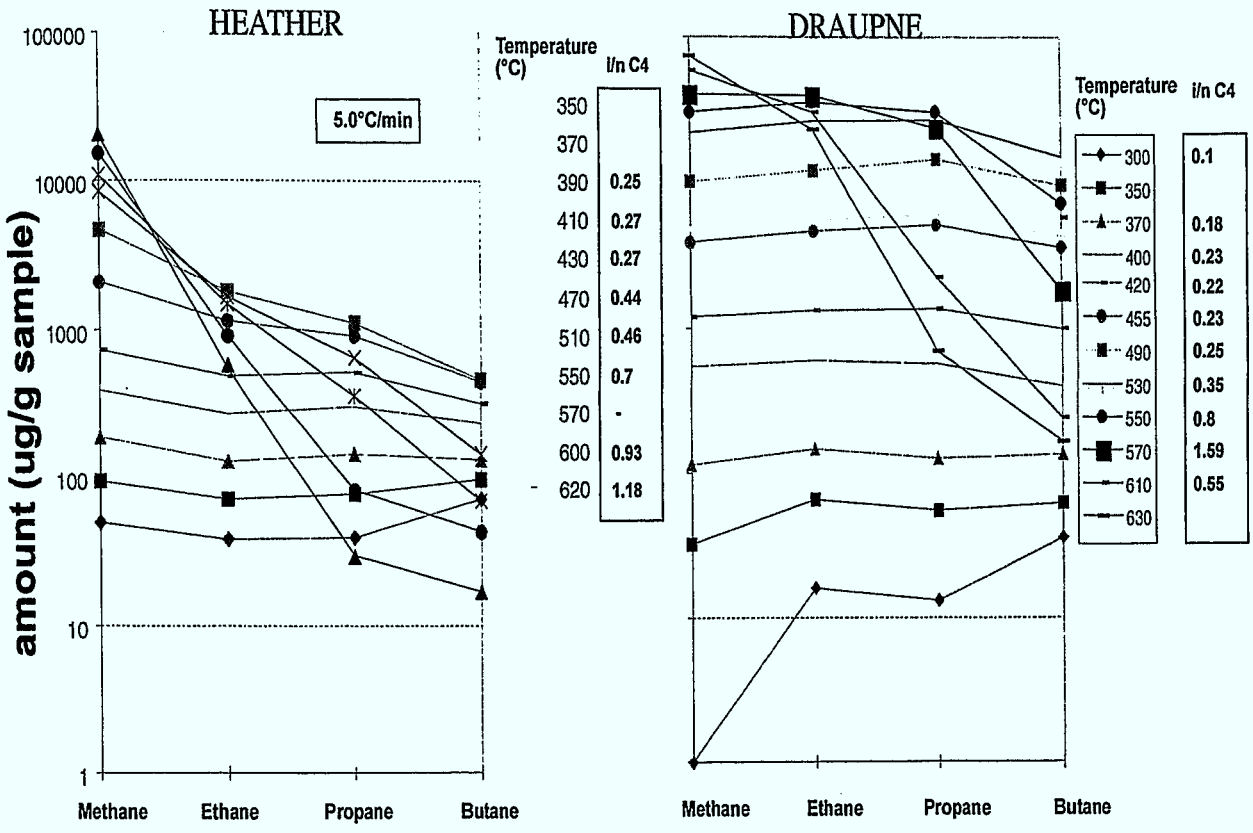


Fig. 70: Compositional evolution of C_{1-4} gas components during MSSV pyrolysis at a heating rate of 5.0 $Kmin^{-1}$ for Heather and Draupne Formation.

Cluster Analyses

On the basis of these observations a cluster-analyses was performed in order to see whether significant patterns can be determined for low or high maturity gases and for gas originating from Heather or Draupne Formation. Moreover it was attempted to see if the experimental distributions fall into clusters together with natural samples so that gas families can be discriminated with respect to their origin.

The cluster analyses is a statistical method which allows similarities or dissimilarities to be expressed in distances. That means samples which fall close together in one and the same branch of the resulting tree-diagram are more similar than those which lie on different distant branches.

In order to describe the C_{1-4} composition the input parameters were chosen to be simply the slopes between two components in a logarithmic system to ensure similar weighting for all components. The parameters were calculated as *ln ([C1]/[n-C2])*, *ln ([n-C2]/[n-C3])* and *ln ([n-C3]/[n-C4])*. Hence, three parameters describe one sample. The obtained range of slopes was transformed to values between 0 and 1. The distances i.e. dissimilarities were calculated as Euclidean distances which is the standard method in cluster analyses. Euclidean distances are the diagonal distances in an n-dimensional system.

where n is the number of parameters employed. Finally the linkage method determines whether two samples, a sample and a cluster or two clusters will be merged in a calculation step.

Fig. 71 shows the result of cluster-analyses using 18 Heather MSSV-, 16 Draupne MSSV- and 30 headspace gas-compositional patterns. The headspace gas data stem from the eastern flank of the

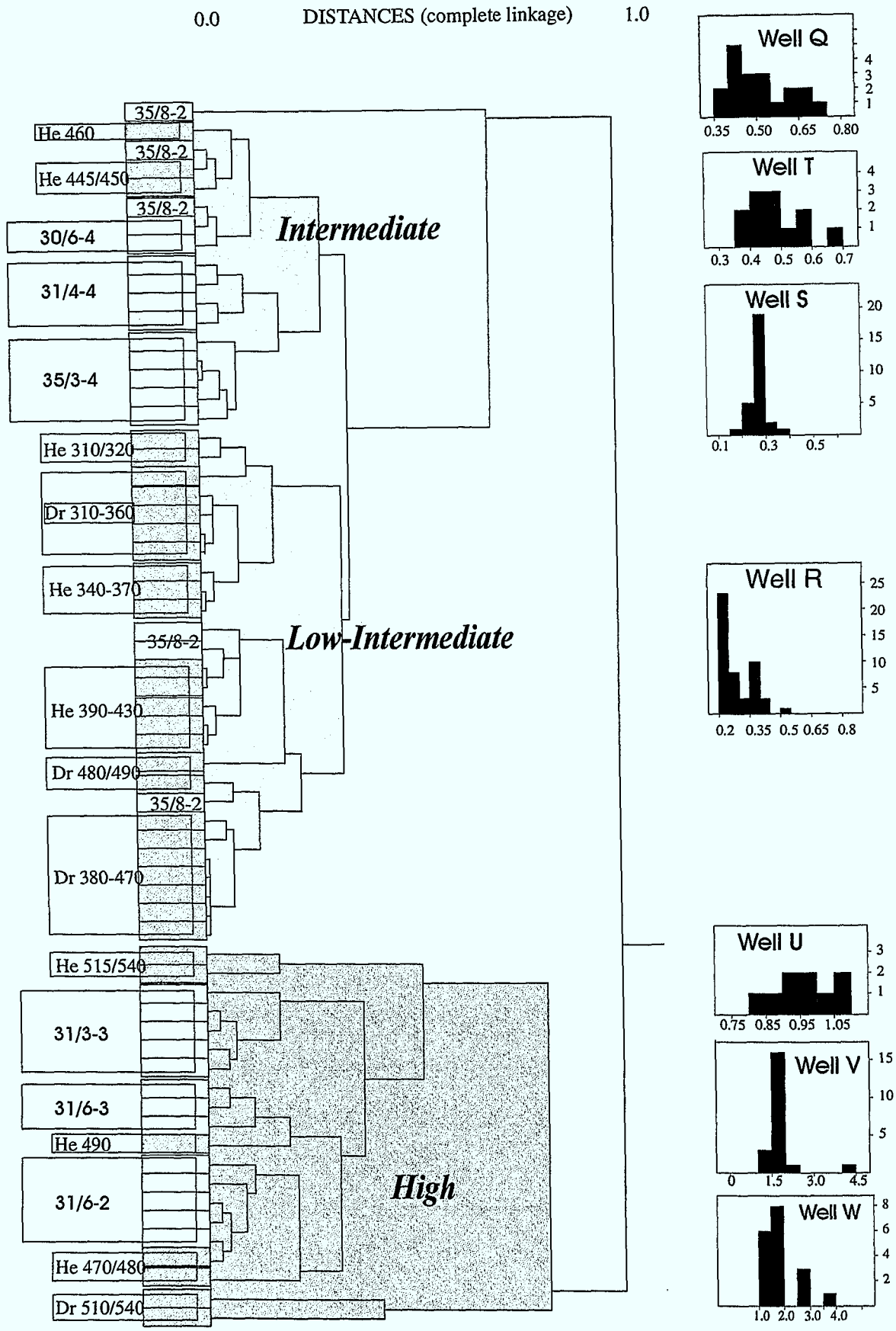


Fig. 71: Result of cluster analyses using headspace and occluded gas data from the eastern Viking Graben flank and experimental MSSV data sets (Heather and Draupne at 0.1 $Kmin^{-1}$). Input parameters are: ln ([n-C_1]/[n-C2]), ln ([n-C2]/[n-C3]), ln ([n-C3]/[n-C4]). The independent i/n-butane distribution is depicted for comparison.

Viking Graben (Norsk Hydro data base). One first order cluster and two third order clusters appear, the first is called *high* and the two latter *intermediate* and *low-intermediate*. Except for the well R the employed gas compositions group together for individual wells indicating very homogeneous gas occurrence. The only sample appearing in a Draupne Formation MSSV cluster is also a sample of well R.

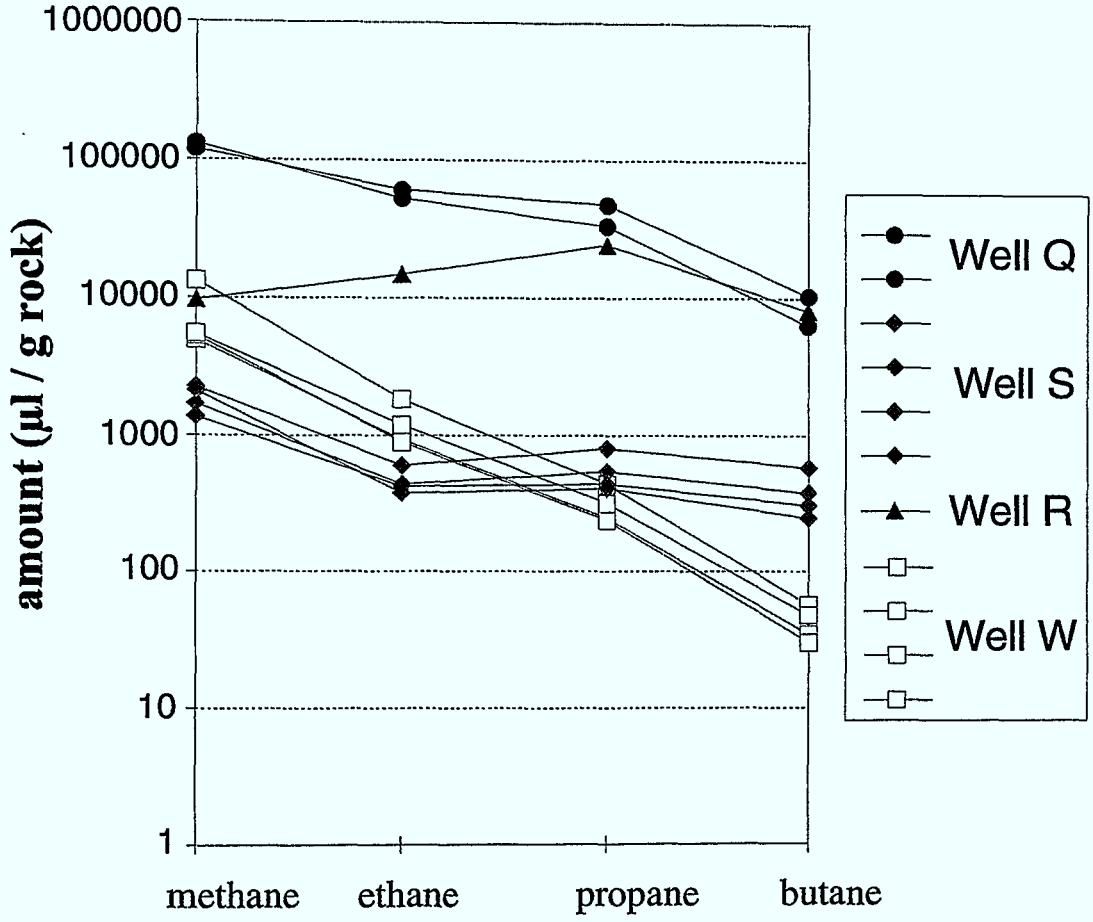


Fig. 72: Headspace and occluded gas compositions. Examples for natural gas compositional patterns. The wells depicted are also part of the cluster analyses in Fig. 71.

As an example the well R gas composition with the lowest apparent maturity is included in Fig. 72. The decrease towards methane causes the grouping in a cluster together with Draupne MSSV gas obtained at 470-480°C (0.1 $Kmin^{-1}$). Independently the distribution of i/n-butane values for well R shows a maximum at 0.2-0.25 matching the value proposed before for typical Draupne gas. In the "intermediate" cluster gas data of wells from different locations group together which correspond to an experimental Heather Formation gas composition obtained at a temperature of 445°C (0.1 $Kmin^{-1}$). Except for well S the i/n-butane distributions are bimodal. These gases might be interpreted as mature gas of mixed origin but probably with significant contributions of Heather Formation. Finally gas obtained from wells in the Troll area correspond to high temperature Heather Formation MSSV gas also confirmed by high i/n-butane values, which indicate contributions from secondary cracking. Because these samples stem from relatively shallow depth an alterations of gas compositions cannot be excluded. These findings are in line with the opinion of Horstad & Larter (1997) that Troll field

gas migrated in a single phase into the structure without associated oil. Moreover the authors argued against a scenario where a charge from the block 35/8 would be responsible for Troll filling.



Concluding remarks, compositional features of gas

- Experimental i/n butane ratios for Draupne Formation were found to center around 0.25, more or less temperature independent except for increasing values at very high temperatures.
- Heather Formation i/n butane ratios increased successively and values higher 1.0 indicated gas formation by secondary cracking.
- Slopes between individual gas component concentrations in a logarithmic calculated as *ln ([C_1]/[n-C2])*, *ln ([n-C2]/[n-C3])* and *ln ([n-C3]/[n-C4])* revealed source and maturity related characteristics in experiments.
- In the experiments significant increases of i/n butane values coincided with secondary cracking related changes in C_{1-4} gas compositions .
- With the help of cluster analysis it was shown that experimental gas compositional features can be related to natural gas and that the results are in accordance with i/n butane values. Interpretations based on these findings were:
  - Well R contains gas from varying degrees of maturity. The gas with the lowest maturity was interpreted to originate from Draupne Formation.
  - Thermal extracts from well P contain gas which is most likely secondary gas. This was already concluded before, based on observations from C7 hydrocarbons and the presence of biphenyls.
  - Quadrant II headspace gas samples seem to be generated from Heather Formation source rocks at very high maturities.

3.5.3 Stable Carbon Isotopes

Some fundamental insights in gas generation were obtained during decades of research from the investigation of ^{12}C to ^{13}C isotope abundances in gas components, which are usually reported as

$$\delta^{13}C\ (‰) = (((^{13}C/^{12}C)\ \text{sample} - (^{13}C/^{12}C)\ \text{standard})/((^{13}C/^{12}C)\ \text{standard}) \quad (8)$$

with the "Peedee Belemnite" as standard.

The relative abundance of carbon isotopes is a function of their abundance in the precursor, i.e. the kerogen, bitumen or oil and fractionation effects accompanying generation. A review of biological fractionation mechanisms in organisms which controls the isotopic composition of such precursors was given by Degens (1989). Generally the ^{12}C isotope is enriched in lipids relative to other plant constituents. Consequently ^{13}C is more abundant in terrestrial derived organic matter which contained low amounts of lipids. When gas is generated from such precursors fractionation effects become important. Silverman (1964) and Sackett *et al.* (1966) demonstrated that C-C bonds of different isotope combinations result in different bond strengths with ^{12}C-^{12}C being the weakest and ^{13}C-^{13}C the strongest bonds. Thus it was concluded that the thermal cracking of petroleum and gas precursors would result in fractionation of both isotope species in that in early stages of maturation predominantly ^{12}C would be released and later more and more heavier ^{13}C. Tang & Jenden (1995) performed *ab initio* quantum chemistry calculations on the C-C bond strengthening by ^{13}C. They reported a bond strengthening of 20-60 cal/mol by ^{13}C. These consideration also imply differences in kinetic parameters for the formation of gas components with or without incorporated ^{13}C. It was therefore suggested by Cramer *et al.* (1997) that heavy and light gas components of one species as for instance ^{12}C methane and ^{13}C methane, should have slightly different activation energy distributions, if the frequency factor is defined to be equal. The differences in bond strength caused by ^{13}C are most pronounced for methane, diminishing for longer chains. Consequently methane is assumed to have the highest differences in activation energy distributions for light and heavy species. For larger molecules, generation processes have less isotopic generation effects and result in an isotopic signature similar to the source material.

Isotope compositions were determined for 12 MSSV pyrolysis temperatures (6 for each source rock sample) at a heating rate of 0.7 $Kmin^{-1}$ (Fig. 73). The temperatures were selected in that they cover the whole temperature interval measured during MSSV pyrolysis. This should enable the observation of isotopic changes during primary as well as secondary processes. Molecular species that were measured include methane and C_2 to C_5 alkanes, ethene, propene, i-butane and CO_2 (Table 27, Appendix). The isotope differences could not always be determined for all of these components, for example, propene and propane were sometimes integrated together and the accuracy of ^{13}C determination of butane was disturbed by an unidentified shoulder.

The trends present in Fig. 73 are essentially the same for both source rock formations. Generally the values for different molecular species diverge with increasing temperature, corroborating observations reported by James (1983). The effect is small for ethane and propane and even not present for both components for Heather Formation at intermediate temperatures. In contrast the divergence becomes more pronounced with very high temperatures where severe secondary cracking takes place. Isotopic compositions for gas components especially for propane and butane become extremely heavy with

values up to -2 ‰. The overall isotopic compositions are heavier for the Heather Formation which is in accordance with the above stated dependence of the precursor isotope composition.

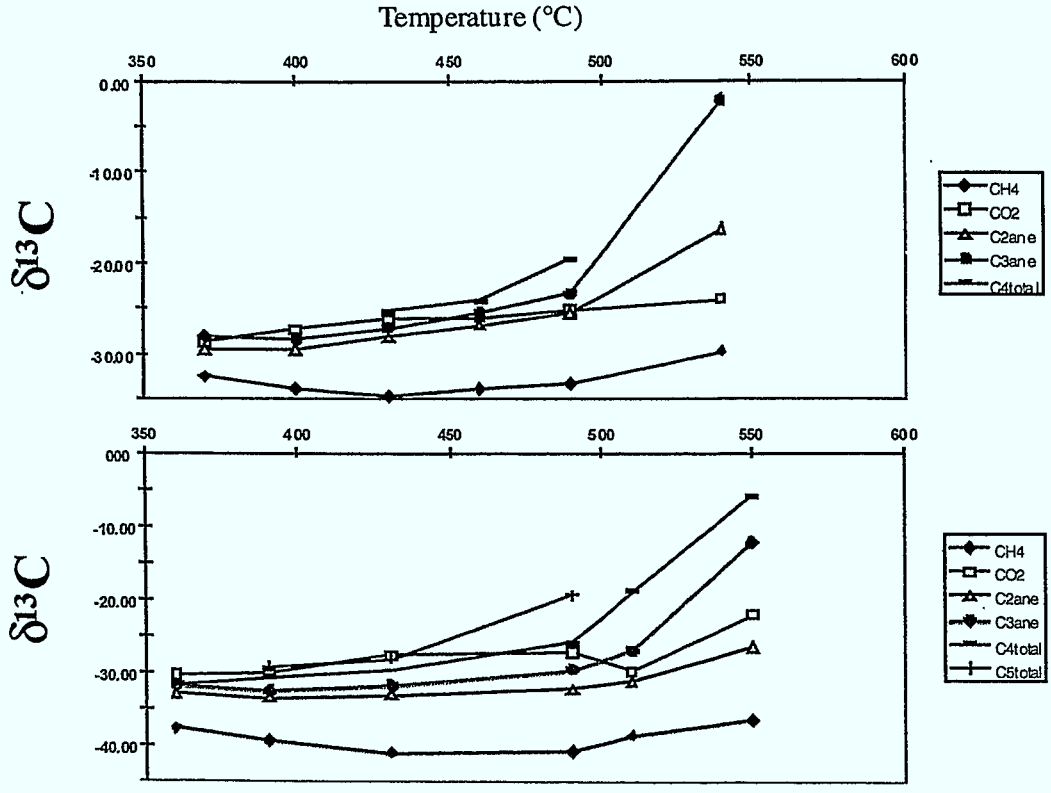


Fig. 73: $\delta^{13}C$ isotope compositions as a function of MSSV pyrolysis temperature at a heating rate of 0.7 K/min. Top, Heather Formation and bottom Draupne Formation.

An attempt was made to model the isotopic compositional development observed in the experiment using the approach of Cramer et al. (1997) which assumes that two activation energy distributions with small differences in the main energy for light and heavy species govern the isotope composition. Kinetic parameters for ethane and propane from Heather and Draupne Formations (Table 28) were employed. The problem that single component kinetic parameters derived from closed system devices are problematic because they are likely to have inherited errors due to merging of primary and secondary generations, must be kept in mind. Additional input data are the $\delta^{13}C$ values of ethane and propane (Table 27). Firstly a second activation energy distribution for the generation of the heavy molecule is created, it is the same distribution as for the light molecule but shifted to higher energies. The difference between both distributions, called $\Delta E(a)$, can be considered as an optimisation parameter. Using different values of $\Delta E(a)$, a calculated $\delta^{13}C$ ethane versus temperature curve is iterative approximated to the measured data set.

The result of modelling for ethane generation from Draupne Formation is depicted in Fig. 74. The modelled curve is a cumulative curve of isotopic changes during heating and shows a good fit for values between 400 and 500°C. The deviation to measured values above 500°C can be explained to result from the cracking of propane and ethane. Whereas in an open system gas can become successively heavier this is not the case for cumulative closed system gas because the amounts of this heavier gas are small compared to light gas produced before. In Fig. 74 for example appr. 80% of ethane are already produced before $\delta^{13}C$ values increase. The increase can alternatively be explained

by two processes. The first is the cracking of propane (starting at 500°C) which will preferentially happen at ^{12}C-^{12}C bonds, yielding ^{12}C methane and heavy ethane. The second process is the cracking of ethane itself, starting at least at 540°C, which will result in a concentration of heavy ethane due to preferential

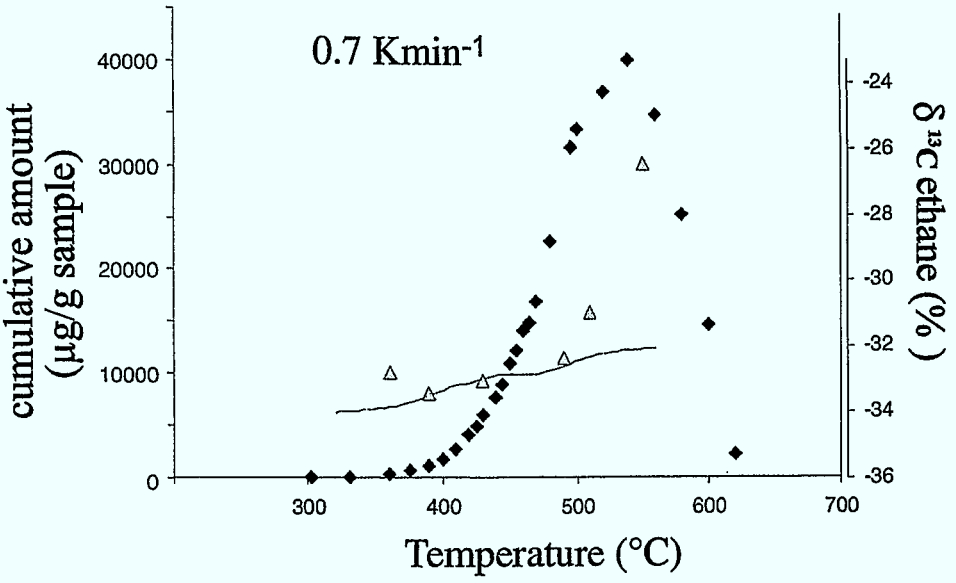


Fig. 74: Measured $\delta^{13}C$ versus temperature for ethane of Draupne Formation (triangles) and modelled cumulative development (thin line). Rhomboids are measured MSSV pyrolysis amounts.

cracking of the lighter molecule. However for temperatures lower 500°C the model shows good results. The Δ Ea values for Heather and Draupne Formations were for ethane 2.34 and 2.05 (cal/mol) and for propane 4.72 and 3.24 cal/mol. The latter values are in the range of observed values from Cramer (1997) and calculated values from Tang & Jenden (1995).

Two conclusions can be drawn. Methane should become isotopically lighter at high temperatures, which is actually not the case in the experiment, but might be counterbalanced by high temperature ^{13}C methane production. And secondly experimental propane and ethane isotopic compositions can be assumed to be similar to values obtained from natural systems because of the small differences in activation energy distributions.

These hypothesis was tested using headspace gas isotope data from the Viking Graben quadrants I, II, V, III and IV (Norsk Hydro data). In Fig. 75 the hypothesis seems to be confirmed that ethane and propane values are comparable to natural system data, except for the values obtained at very high pyrolysis temperatures. Draupne Formation experimental values group together with two measurements (headspace gas data) from quadrant I and values from block III/4 and III/7. These data are also signified by low i/n butane values and might be interpreted as oil window mature Draupne Formation gas. In contrast most of the quadrant I headspace gas isotope values fall close to Heather Formation experimental data. Well Q data were said before to be of intermediate maturity Heather Formation origin. Finally quadrant II headspace gas data which were assumed before to represent very high maturity Heather Formation gas shift into the heavy propane direction similar to the trend observed from the experiments.

Experimental methane $\delta^{13}C$ values are significantly heavier than those of natural system gases (Fig. 76) and not suitable for direct comparisons. The relative light character of quadrant II headspace methane might however be interpreted by an origin from high temperature cracking of gas.

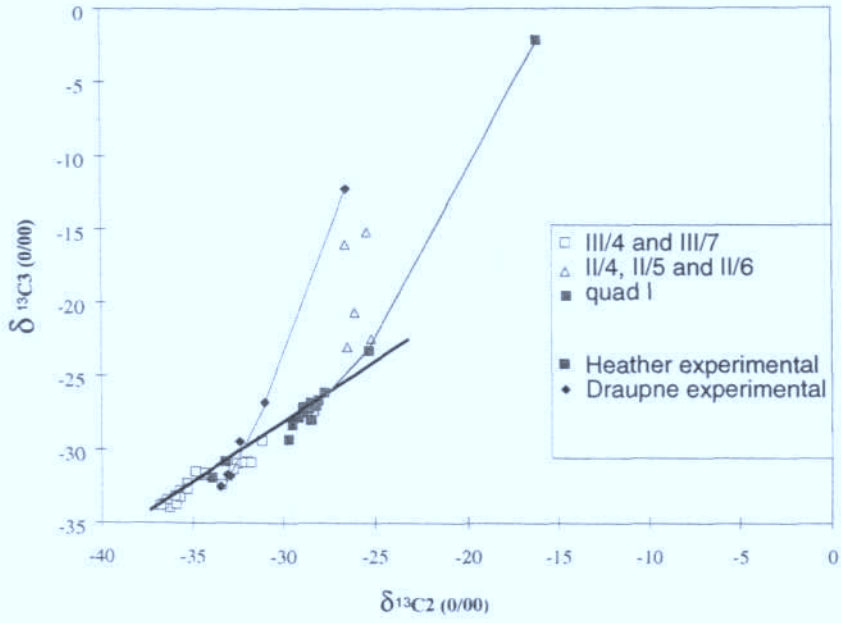


Fig. 75: Experimental ethane versus propane $\delta^{13}C$ values compared to headspace gas data from the Viking Graben.

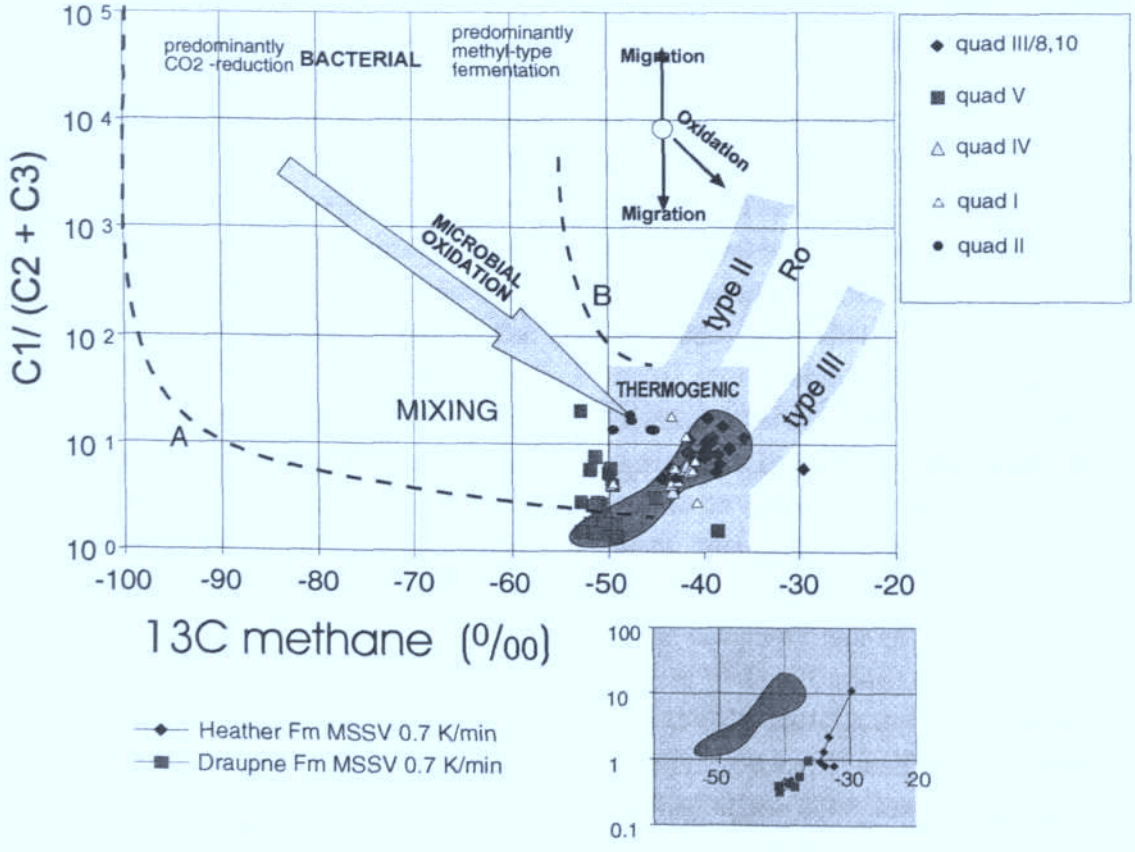


Fig. 76: Bernard plot (Bernard 1978) for Northern North Sea headspace gas data. The small diagram depicts the experimental MSSV values for Heather and Draupne Formation.

4 CONCLUSIONS

It was concluded from predictions using the determined kinetic parameters that the temperature ranges for the different types of gas generation are the following (linear geological heating rate of 5.3 K/ma):

- Primary gas generation covers a broad temperature interval of approximately 110-230°C, with a maxium at 195°C for Heather Formation and a slightly less broad range of approximately 120-220°C, and a maximum at 180°C for the Draupne Formation.

- Secondary gas generation occurs at higher temperatures (approximately 175-260°C with maxima ranging between 205-220°C) for both source rock units.

- A high temperature secondary gas formation from neoformed bitumen was detected for the Heather Formation. This is outstanding and was inferred to occur at very high temperatures (max appr. 250°C) for geological heating rates.

The overall results were found to be in accordance with oil generation and bulk product generation.
With regard to the relative importance of these processes it is the main outcome of the project that from the two investigated source rock formations preferentially the Heather Formation can be considered to be important for gas generation in overmature settings.

- It was found from MSSV pyrolysis and confirmed by different experiments as well as from literature findings that recombination of first formed products results in the formation of a residue, which undergoes secondary cracking at very high maturities. As the formation of gas from this process was assessed to occur at maturities, exceeding R_o >3.0% and depth of more than 7000m, this process might be of increased importance for the Sogn Graben and the Møre Basin.

- A method to prove the validity of this process for the natural system was introduced. Bulk kinetic analyses for samples of comparable kerogen type covering a broad maturity range can show the evolution of new activation energies upon maturation and thus the formation of recombination residues. Heterogeneities in kerogen types of samples used to perform this investigation prohibited the finding of clear evidence that the process occurs in nature.

- The application of kinetic parameters to linear geological heating rates indicated primary gas from Heather Formation to form at slightly higher temperatures compared to Draupne Formation. Secondary gas generation via thermal degradation (secondary cracking) of unexpelled petroleum takes place at higher temperatures compared to primary generation and in a similar temperature interval for both source rock units.

- The application of kinetic parameters using basin modelling revealed that secondary gas formation from cracking of unexpelled oil is likely to occur for the Heather

Formation. It was not detected for the Draupne Formation where oil was predicted to be efficiently expelled. This observation confirms the initial hypothesis that Heather Formation as a bad expeller would generate gas from residual bitumen and oil, whereas for the Draupne Formation kerogen the primary cracking of gas from the kerogen would be more important.

- In this regard a migra- or pyrobitumen was detected in the well P which provides microscopic evidence for the presence of a source for secondary cracking processes. Parts of the Viking Group source rocks in well P are likely to be equivalent to Heather Formation.

- Molecular parameters such as paraffinicity indices as well as high i/n butane ratio, high maturity gas C_{1-4} compositions and the presence of high amounts of biphenyls underlined the importance of secondary cracking in this well.

- For the case of the Viking Graben the interpretation of gas range molecular ratios and compositional features as well as isotope compositions confirmed the importance of Heather Formation source rocks for high maturity secondary gas formation.

- The quantitative contributions of Heather and Draupne Formation gases to reservoirs in the Viking Graben area could not be answered unambiguously. Results from basin modelling indicated the possibility of dominance for Heather gas for the case that preferential Draupne gas losses to the atmosphere are reasonable. Even for the most disadvantageous scenario for Heather Formation the respective contributions were still 1:4.

- Finally the i/n butane ratio and methane, ethane and propane carbon isotopes indicated that in the drilled areas gas from overmature settings is present but less abundant than "oil window – mature" gas.

Important processes for gas generation from overmature source rocks have been recognised and discussed. For different processes like primary and different types of secondary cracking kinetic parameters were determined and tested. These results will help to improve predictions for exploration purposes.

5 REFERENCES

ALLEN, P.A. & ALLEN, J.R. (1995): Basin analyses: principles and applications. Blackwell, Oxford, p. 1-451.

ANDRESEN,P.; MILLS,N.; SCHENK,H.J. & HORSFIELD,B. (1993): The importance of kinetic parameters in modelling generation by cracking of oil to gas - a case study in 1D from well 2/4-14. In: DORÉ *et al.* (eds.): Basin Modelling: Advances and Applications. NPF Special Publication **3**, p. 563-571.

ASINGER,F. (1971): Die Petrolchemische Industrie. Akademie Verlag. Berlin.

BAKKEN,K.A. (1993): Comparison of commonly used maturity parameters with temperature and quantitative hydrocarbon generation in source rocks, North Viking Graben. In: ØYGARD (ed): Organic Geochemistry. Poster sessions from the 16th Intern. Meet. on Org. Geochem., Stavanger.

BARTH,T; NIELSEN,S.B. & SCHMIDT,B.J. (1996): Do kinetic parameters from open pyrolysis describe petroleum generation by simulated maturation? Bull. of Canad. Petrol. Geol. **44**, no.3, p. 446-457.

BARTON,D.C. (1937): Evolution of Gulf Coast Crude Oil. AAPG Bull. **21**, no.7, p.914-946.

BASKIN,D.K. & PETERS,K.E. (1992): Early generation characteristics of a sulphur-rich Monterey Kerogen. AAPG Bull. **76**, No.1, p. 1-13.

BÉHAR,F. & PELET,R. (1988): Hydrogen-transfer reactions in the thermal cracking of asphaltenes. Energy & Fuels **2**, p. 259-264.

BÉHAR,F.; UNGERER,P.; KRESSMANN,S. & RUDKIEWICZ,J.L. (1991): Thermal evolution of crude oils in sedimentary basins: experimental simulation in a confined system and kinetic modelling. Rev. Inst. Fr. Pét. **44**, p. 387-397.

BÉHAR,F.; KRESSMANN,S.; RUDKIEWICZ,J.L. & VANDENBROUCKE,M. (1992): Experimental simulation and kinetic modelling of kerogen and oil cracking. Org. Geochem. **19**, no.1-3, p. 173-189.

BÉHAR,F.; VANDENBROUCKE,M.; TEERMANN,S.C.; HATCHER,P.G.; LEBLOND,C. & LERAT,O. (1995): Experimental simulation of gas generation from coals and a marine kerogen. Chem. Geol. **126**, p. 247-260.

BÉHAR,F. & VANDENBROUCKE,M. (1996): Experimental determination of the rate constants of the n-C_{25} thermal cracking at 120, 400, and 800 bar: Implications for high-pressure/ high-temperature prospects. Energy & Fuels **10**, p. 932-940.

BERNER,U.; FABER,E.; SCHNEIDER,G. & PANTEN,D. (1995): Primary cracking of algal and landplant kerogens: kinetic models of isotope variations in methane, ethane and propane. Chem. Geol. **126**, p. 233-245.

BOSTICK,N.H. (1973): Time as a factor in thermal metamorphism of phytoclasts (coaly particles): 7th Cong. Internat. Stratigraphie et Géologie Carbonifère, Krefeld 1971, Compte Rendu, **2**, p. 183-193.

BOUCHER,R.J.; STANDEN,G.; PATIENCE,R.L. & EGLINTON,G. (1990): Molecular characterisation of kerogen from the Kimmeridge clay formation by mild selective chemical degradation and solid state ^{13}C -NMR. Org. Geochem. **16**, nos 4-6, p. 951-958.

BRAUN,R.L.; BURNHAM,A.K.; REYNOLDS,J.G. & CLARKSON,J.E. (1991): Pyrolysis kinetics for lacustrine and marine source rocks by programmed micropyrolysis. Energy & Fuels **5**, p. 192-204.

BRAUN,R.L.; BURNHAM,A.K. & REYNOLDS,J.G. (1992): Oil and gas evolution kinetics for oil shale and petroleum source rocks determined from pyrolysis-TQMS data at two heating rates. Energy & Fuels **6**, p. 468-474.

BRAUN,R.L. & BURNHAM,A.K (1992): PMOD: a flexible model of oil and gas generation, cracking and expulsion. Org. Geochem. **19**, no. 1-3, p. 161-172.

BUISKOOL TOXOPEUS,J.M.A. (1983): Selection criteria for the use of vitrinite reflectance as maturity tool. In BROOKS,J. (ed.): Petroleum Geochemistry and Exploration in Europe. Blackwell, Oxford, p. 295-307.

BURNHAM,A.K (1989): A simple model of petroleum formation and cracking. Lawrence Livermore National Laboratory, Rep. UCID 21665, March.

BURNHAM,A.K. & BRAUN,R.L. (1990): Development of a detailed model of petroleum formation, destruction and expulsion from lacustrine and marine source rocks. In: DURAND,B. & BÉHAR,F. (eds.): Advances in Organic Geochemistry 1989. Org. Geochem. **16**, nos. 1-3, p. 27-39.

CHUNG ,H.M.; WINGERT,W.S. & CLAYPOOL,G.E. (1992): Geochemistry of oils in the Northern Viking Graben. In: HALBOUTY,M.T. (ed.): Giant oil and gas fields of the decade 1978-1988. AAPG Memoir **54**, p. 277-296.

CHUNG ,H.M. CLAYPOOL,G.E. & WALTERS (1995): Multiple origins of petroleum in the Viking Graben. 17th Intern. Meet. on Org. Geochem., San Sebastian. p.505.

CONNAN,J.; Le TRAN,K & van der WEIDE,B.M. (1975): Alteration of petroleum in reservoirs. Proc. Eighth World Petr. Congr., p.171-178.

CONNAN,J. & CASSOU,A.M. (1980): Properties of gases and petroleum liquids derived from terrestrial kerogen at various maturation levels. Geochim. et Cosmochim. Acta **44**, p.1-23.

CONNAN,J. (1984): Biodegradation of crude oils in reservoirs. In: BROOKS,J. & WELTE,D.H. (eds.): Advances in Petroleum Geochemistry, Academic Press, London, p.299-335.

COOLES,G.P.; MACKENZIE,A.S. & QUIGLEY,T.M. (1986): Calculation of petroleum masses generated and expelled from source rocks. Org. Geochem. **10** , p. 235-245.

COOPER,B.S. & BARNARD,P.C. (1984): Source Rocks and Oils of the Central and Northern North Sea. In: DEMAISON,G. & MURRIS,R.J. (eds.): Petroleum Geochemistry and Basin evaluation. AAPG Mem. **35**, p. 303-314.

COOPER,B.S.; BARNARD,P.C & TELNÆS,N. (1995): The Kimmeridge Clay Formation if the North Sea. In: KATZ,B. (ed.): Petroleum Source Rocks. Springer Verlag, p. 89-110.

CRAMER,B.; KROOSS,B.M. & LITTKE,R. (1997): Modelling isotope fractionation during primary cracking of natural gas: a reaction kinetic approach. Chemical Geology **149**, p.235-250.

DAHL,B.; NYSAETHER,E.; SPEERS,G.C. & YUKLER,A. (1987): Oseberg Area - integrated basin modelling. In: BROOKS,J. & GLENNIE,K. (eds.): Petroleum Geology of North West Europe. p. 1029-1038.

DAHL,B.; REIN,E.; AAKVAAG,L.; BOCKELIE,T. & SAUAR,B.E. (1992): PL120 special geochemical study. Norsk Hydro Report.

DAHL,B. & AUGUSTSON,J.H. (1993): The influence of tertiary and quarternary sedimentation and erosion on hydrocarbon generation in Norwegian offshore basins. In: DORÉ et al. (eds.): Basin modelling: Advances and applications. NPF Special Publication **3**, Elsevier, Amsterdam, p. 419-431.

DEGENS,E.T. (1989): Perspectives on Biogeochemistry. Springer, Berlin, 423pp.

DEMBICKI,H. Jr (1992): The effects of the mineral matrix on the determination of kinetic parameters using modified Rock Eval pyrolysis. Org. Geochem. **18**, no.4, p.531-539.

DIECKMANN,V.; SCHENK,H.J.; HORSFIELD,B. & WELTE,D.H. (1997): Kinetics of petroleum generation and cracking by programmed-temperature closed-system pyrolysis of Toarcian Shales. submitted to Energy & Fuels.

DOMINÉ,F. (1991): High pressure pyrolysis of n-hexane, 2,4-dimethylpentane and 1-phenylbutane. Is pressure an important geochemical parameter? Org. Geochem. **16**, p. 259-266.

DURAND,B. (ed.): Kerogen, insoluble organic matter from sedimentary rocks. Editions Technip, Paris 1980.

DURAND,B. & NICAISE,G. (1980): Procedures for kerogen isolation. In: DURAND,B. (ed.): Kerogen, insoluble organic matter from sedimentary rocks. Editions Technip, Paris, p.35-53.

EGLINTON,T.I.; SINNINGHE DAMSTE,J.S.; KOHNEN,E.L. & de LEEUW,J.W. (1990): Rapid estimation of the sulphur content of kerogens, coals and asphaltenes by pyrolysis-gas chromatography. FUEL **69**, nov., p. 1394-1404.

ENGLAND,W.A.; MACKENZIE,A.S.; MANN,D.M. & QUIGLEY,T.M. (1987): The movement and entrapment of petroleum fluids in the subsurface. Journal of the Geological Society, London, **144**, p. 327-347.

ENGUEHARD,F.; KRESSMANN,S. & DOMINÉ,F. (1990): Kinetics of dibutylether pyrolysis at high pressure: Experimental study. Org. Geochem. **16**, no.1-3, p. 155-160.

ERDMAN,J.G. (1961): Some chemical aspects of petroleum genesis as related to the problem of source bed recognition. Geochim. et Cosmochim. Acta **22**, p.16.

ERDMAN,J.G. (1967): Geochemical origins of the low molecular weight hydrocarbon constituents of petroleum and natural gases. In: 7th World Petroleum Congress Proceedings **2**, p. 13-24.

ERDMANN,M. (1995): Gas generation from overmature source rocks, Northern Viking Graben. First Progress Report, KFA /ICG-4 Interner Bericht 501095.

ERDMANN,M. (1995): Gas generation from overmature source rocks, Northern Viking Graben. Second Progress Report, KFA /ICG-4 Interner Bericht 501396.

ESPITALIÉ,J.; LAPORTE,J.L.; MADEC,M.; MARQUIS,F.; LEPLAT,P.; PAULET,J. & BOUTEFEU,F. (1977): Méthode rapide de caractérisation des roches mères de leur potentiel petrolier et de leur degré d'évolution. Rev. Inst Fr. Petr. **32**, p. 23-42.

ESPITALIÉ,J.; MADEC,M & TISSOT,B. (1980): Role of Mineral matrix in Kerogen pyrolysis: Influence on Petroleum generation and migration. AAPG Bull. **64**, no.1, p.59-66.

ESPITALIÉ,J.; DEROO,,G. & MARQUIS,F. (1985): La pyrolyse Rock-Eval et ses applications. Deuxième partie: Interprétation des paramèters. Rev. Inst. Fr. Pét. **40**, p.755-784.

ESPITALIÉ,J.; UNGERER,P.; IRWIN,I. & MARQUIS,F. (1988): Primary cracking of kerogens. Experimenting and modeling C1, C2-C5, C6-C15 and C15+ classes of hydrocarbons formed. Org. Geochem. **13**, nos.4-6, p. 893-899.

ESPITALIÉ,J.; LAFARGUE,E. & EGGEN,S. (1991): Petroleum potential of terrestrial and marine organic matter in Jurassic sequences of the northern North Sea and offshore mid-Norway. In: SPENCER,A.M. (ed.): Generation, accumulation and production of Europe's hydrocarbons. Special Publication of the European Association of Petroleum Geoscientists **1**, p. 49-63.

ESPITALIÉ,J.; MARQUIS,F. & DROUET,S. (1993): Critical study of kinetic modelling parameters. In: DORÉ et al. (eds.): Basin modelling: Advances and applications. NPF Special Publication **3**, p. 233-242.

EVANS,C.R.; ROGERS,M.A. & BAILEY,N.J.L (1971): Evolution and alteration of petroleum in western Canada. Chem. Geol. **8**, p.147-170.

FABER,E. GERLING,P. & DUMKE,I. (1988): Gaseous hydrocarbons of unknown origin found while drilling. Org. Geochem. **13**, no.4-6, p. 875-879.

FABUSS,B.M.; DUNCAN,D.A.; SMITH,J.O. & SCATTERFIELD,C.N. (1965): Effect of organosulphur compounds on the rate of thermal decomposition of selected saturated hydrocarbons. I&EC Process design & Development **4**, no.1, p. 17-122.

FIELD,J.D. (1985): Organic geochemistry in exploration of the Northern North Sea. In: THOMAS,B.M. et al. (eds.): Petroleum Geochemistry in Exploration of the Norwegian Shelf. Norwegian Petroleum Society, Graham & Trotman, p. 39-57.

GALIMOV,E.M. (1975): Carbon isotopes in oil-gas geology. National Aeronautics and Space Administration, NASA TT F-682.

GARRIGUES,P; OUDIN,J.L.; PARLANTI,E.; MONIN,J.C.; ROBCIS,S. & BELLOCQ,J. (1990): Alkylated phenanthrene distribution in artificially matured kerogens from Kimmeridge clay and the Brent Formation (North Sea). Org. Geochem. **16**, nos. 1-3, p.167-173.

GOFF,J.C. (1983): Hydrocarbon Generation and Migration from Jurassic Source Rocks in the East Shetland Basin and Viking Graben of the Northern North Sea. Journal of the Geological Society of London, **140**, p. 445-473.

GREENSFELDERB.S.; VOGE,H.H. & GOOD,G.M. (1949): Catalytic and thermal cracking of pure hydrocarbons. Ind. Eng. Chem. **41**, p.2573.

GUTJAHR,C.C.M. (1983): Introduction to incident-light microscopy of oil and gas source rocks. Geologie en Mijnbouw, **62**, p.417-425.

HALL,P.B.; SCHOU,L. & BJORØY,M. (1985): Aromatic hydrocarbon variations in North Sea wells. In: THOMAS,B.M. et al. (eds.): Petroleum Geochemistry in Exploration of the Norwegian Shelf. Norwegian Petroleum Society, Graham & Trotman, p.293-301.

HANBABA,P. (1967): Reaktionskinetische Untersuchungen zur Kohlenwasserstoffentbindung aus Steinkohlen bei niedrigen Aufheizgeschwindigkeiten (10-3 bis 1 grd/min). Thesis RWTH Aachen, 107p.

HANSFORD,R.C. (1953) In: Physical chemistry of hydrocarbons. FARKAS,A.(ed.), Academic press, New York, p. 224-226.

HEEK,K.H. van & JUENTGEN,H. (1968): Bestimmung reaktions-kinetischer Parameter aus nicht isothermen Messungen. Ber. Bund.ges Phys Chem **72**, p. 1223-1231.

HÉROUX,Y.; CHAGNON,A. & BERTRAND,R. (1979): Compilation and Correlation of Major Thermal Maturation Indicators. AAPG Bull. **63**, no.**12**, p. 2128-2144.

HOERING,T.C. & ABELSON,P.H. (1963): Hydrocarbons from kerogen. Carnegie Institut, Washington Yearbook **62**, p. 229-234.

HOERING,T.C. (1984): Thermal reactions of kerogen with added water, heavy water and pure organic substances. Org. Geochem. **5**, no.4, p. 267-278.

HORSFIELD,B. & DOUGLAS,A.G. (1980): The influences of minerals on the pyrolysis of kerogen. Geochim. Cosmochim. Acta **44**, p. 1119-1131.

HORSFIELD,B. (1984): Pyrolysis Studies and Petroleum Exploration. Advances in Petroleum Geochemistry **1**, p. 247-298.

HORSFIELD,B (1989): Practical criteria for classifying kerogens: some observations from pyrolysis-gas chromatography. Geochim. et Cosmochim. Acta **53**, p. 891-901.

HORSFIELD,B.; DISKO,U. & LEISTNER,F. (1989): The microscale simulation of maturation: Outline of a new technique and its potential applications. Geologische Rundschau **78**, p. 361-374.

HORSFIELD,B. & DÜPPENBECKER,S.J (1991): The decomposition of Posidonia shale and Green River Shale kerogens using microscale sealed vessel (MSSV) pyrolysis. J. of Anal. and Appl. Pyrolysis **20**, p. 107-123.

HORSFIELD, B.; SCHENK,H.J.; MILLS,N. & WELTE,D.H. (1992): An investigation of the in-reservoir conversion of oil to gas: compositional and kinetic findings from closed-system programmed-temperature pyrolysis. Org. Geochem. **19**, nos. 1-3, p. 191-204.

HORSFIELD,B. (1997): The bulk composition of first-formed petroleum in source rocks. In: WELTE,D.H. HORSFIELD,B. & BAKER,D.R. (eds.): Petroleum and basin evolution. Springer, Berlin, p.335-401.

HORSTAD,I.; LARTER,S. & MILLS,N. (1992): A quantitative model of biodegradation within the Brent group reservoir in the Gullfaks field, Norwegian North Sea. Org. Geochem. **19**, no.1-3, p. 107-117.

HORSTAD,I. LARTER,S.R. & MILLS,N. (1995): Migration of hydrocarbons in the Tampen Spur area, Norwegian North Sea; A reservoir geochemical evaluation. In: CUBITT,J.M. & ENGLAND,W.A.(eds.): The Geochemistry of reservoirs. Geol. Soc. Spec. Publ.**86**, p. 159-183.

HORSTAD,I. & LARTER,S. (1997): Petroleum migration, alteration and remigration within Troll-Field, Norwegian North Sea. AAPG Bull. **81**, no.2, p. 222-248.

HUC,A.Y. & HUNT,J.M. (1980): Generation and migration of hydrocarbons in offshore South Texas Gulf Coast sediments. Geochim. et Cosmochim. Acta **10**, p.1081-1089.

HUNT,J.M. (1963): Geochemical data on organic matter in sediments. In: BESE,V. (ed.), Vorträge der 3. int. wiss. Konferenz für Geochemie, Mikrobiologie und Erdölchemie, Budapest,. p.394.

HUNT,J.M. (1984): Generation and Migration of light Hydrocarbons. Science **226**, no.4680, p. 1265-1270.

HUNT,J.M. (1996): Petroleum Geochemistry and Geology. (Sec. Edition), Freeman & Company, U.S.A.

ISHIWATARI,R.; ISHIWATARI,M.; KAPLAN,I.R. & ROHRBACK,B.G. (1976): Thermal alteration of young kerogen in relation to petroleum genesis. Nature **264**, no. 5584, p. 347-349.

JACKSON,K.J.; BURNHAM,A.K.; BRAUN,R.L. & KNAUSS,K.G (1995): Temperature and pressure dependence of n-hexane cracking. Org. Geochem. **23**, no. 10, p. 941-953.

JACOB,H. (1989): Classification, structure, genesis and practical importance of natural solid bitumen („migra-bitumen"). International Journal of Coal Geology, **11**, p. 65-79.

JAMES,A.T. (1983): Correlation of natural gas by use of carbon isotopic distribution between hydrocarbon components. AAPG Bull. **67**, no.7, p. 1176-1191.

JONATHAN,D, L'HOTE,G. & DU ROCHET,J. (1975): Analyse géochimique des hydrocarbures légers par thermovaporisation. Rev. Inst. Fr. Pet. **30**, p. 65.

JÜNTGEN,H. (1964): Reaktionskinetische Überlegungen zur Deutung von Pyrolyse-Reaktionen. Erdöl und Kohle-Erdgas-Petrochemie **17**, p. 180-186.

JÜNTGEN,H. & VAN HEEK,K.H. (1968): Gas Release from Coal as a Function of the Rate of Heating. FUEL **47**, p. 103-117.

JÜNTGEN,H. & VAN HEEK,K.H. (1970): Reaktionsabläufe unter nicht-isothermen Bedingungen. In: Davison,A. Dewar,M.J.S. Hafner,K. Heilbronner,E. Hofmann,U. Niedenzu,K. Schaefer,K. & Wittig,G. (eds.): Fortschritte der chemischen Forschung. Topics Curr. Chem. **13**, p. 601-699.

JÜNTGEN,H. & KLEIN,J. (1975): Entstehung von Erdgas aus kohligen Sedimenten. Erdöl und Kohle - Erdgas - Petrochemie vereinigt mit Brennstoffchemie, Bd. **28**, Heft **2** , p. 65-73.

JURG,J.W. & EISMA,E. (1964): Petroleum hydrocarbons: generation from fatty acids. Science **144**, p.1451.

KARLSSON,W. (1986): The Snorre, Statfjord and Gullfaks oilfields and the habitat of hydrocarbons on the Tampen Spur, offshore Norway. In: SPENCER,A.M. et al. (eds.): Habitat of Hydrocarbons on the Norwegian Continental Shelf. Norwegian Petroleum Society, Graham & Trotman, p.181-197.

KARWEIL,J. (1955): Aktuelle Probleme der Geochemie der Kohle. Mittelung aus der Bergbau-Forschung GmbH, Forschungsinstitut des Steinkohlebergbauvereins Essen-Kray.

KHORASANI,G.K. & MICHELSEN,J.K. (1992): Primary alteration - oxidation of marine algal matter from oil source rocks of the North Sea and Norwegian Arctic: new findings. Org. Geochem. **19**, no.4-6, p. 327-343.

KISSIN,Y.V. (1987): Catagenesis and compositions of petroleum: origin of n-alkanes and iso-alkanes in petroleum crudes. Geochim. et Cosmochim. Acta **51**, p. 2445-2457.

KNUDSEN,K.; LEYTHAEUSER,D.; DALE,B.; LARTER,S.R. & DAHL,B. (1988): Variation in organic matter quality and maturity in Draupne Formation source rocks from the Oseberg field region, offshore Norway. Org. Geochem. **13**, nos 4-6, p.1051-1060.

KOSSIAKOFF,A. & RICE,F.O. (1943): Thermal decomposition of hydrocarbons, resonance stabilization and isomerisation of free radicals. J. of Americ. Chem. Soc. **65**, p. 590-595.

KRESSMANN,S,; DOMINÉ,F.; ENGUEHARD,F,; BÉHAR,F.; UNGERER,P.; BILLAUD,F. & GOFFE,B. (1990): Secondary cracking of crude oils: experimental simulation and kinetic interpretation on model compounds. Presented at the Proc. of the 14th Intern. Meet. on Org. Geochem., Paris.

KUO,L.-C. & MICHAEL,G.E. (1994): A multicomponent oil-cracking kinetic model for modelling preservation and composition of reservoired oils. Org. Geochem. **21**, p. 911-925.

LAFARGUE,E. & BÉHAR,F. (1989): Application of a new preparative pyrolysis technique for the determination of source rock types and oil/source rock correlations. Geochim. et Cosmochim. Acta **53**, p. 2973-2983.

LALLIER-VERGÈS,E. & BERTRAND,P. (1993): Control of the preservation of organic matter by productivity and sulphate reduction in Kimmeridge shales from Dorset. Marine and Petroleum Geology **10**, dec., p. 600-605.

LANDES,K.K. (1967): Eometamorphism, and oil and gas in time and space. AAPG Bull. **51**, no.6, p.828-841.

LANGFORD,F.F. & BLANC-VALLERON,M.-M. (1990): Interpreting Rock-Eval data using graphs of pyrolizable hydrocarbons vs. total organic carbon. AAPG Bull. **74**, No.6, p.799-804.

LARTER,S.R. (1985): Integrated kerogen typing in the recognition and quantitative assessment of petroleum source rocks. In: THOMAS,B.M. et al. (eds.): Petroleum Geochemistry in Exploration of the Norwegian Shelf. Norwegian Petroleum Society, Graham & Trotman, p. 269-286.

LARTER,S.R. & SENFTLE,J.T. (1985): Improved kerogen typing for petroleum source rock analysis. Nature **318**, p. 277-280.

LARTER,S.R. (1989): Chemical models of vitrinite reflectance evolution. Geol. Rundsch. **78**, p.349-359.

LARTER,S.R.; BJØRLYKKE,K.O.; KARLSEN,D.A.; NEDKVITNE,T.; EGLINTON,T.I.; JOHANSEN,P.E.; LEYTHAEUSER,D.; MASON,P.C.; MITCHELL,A.W. & NEWCOMBE,G.A. (1990): Determination of petroleum accumulation histories: examples from the Ula field, Central Graben, Norwegian North Sea. In: BULLER,A. (ed.): North Sea oil and gas reservoirs, **2**. Graham & Trotman, London, p.319-330.

LARTER,S.R. & HORSFIELD,B. (1993): Determination of structural components of kerogens by the use of analytical pyrolysis methods. In: ENGEL,M.H. & MACKO,A. (eds.): Organic Geochemistry; Plenum Press, New York, p.271-287.

LEADHOLM,R.H.; THOMAS,T.; HO,Y. & SAHAI,S.K. (1985): Heat flow, geothermal gradients and maturation modelling on the Norwegian continental shelf using computer methods. In: THOMAS,B.M. et al. (eds.): Petroleum Geochemistry in Exploration of the Norwegian Shelf. Norwegian Petroleum Society, Graham & Trotman, p. 131-143.

LEISCHNER,K.; WELTE,D.H. & LITTKE,R. (1993): Fluid inclusions and organic maturity parameters as calibration tools in basin modelling. In: DORÉ,A.G. et al. (eds.): Basin modelling: advances and applications. NPF Spec. Publ. **3**, Elsevier, Amsterdam, p. 161-172.

LEITH,T.L; KAARSTAD,I.; CONNAN,J.; PIERRON,J. & CAILLET,G. (1993): Recognition of caprock leakage in the Snorre field, Norwegian North Sea. Marine and Petroleum Geology **10**, feb., p.29-41.

LEWAN,M.D. (1994): Assessing natural oil expulsion from source rocks by laboratory pyrolysis. In: MAGOON,L.B. & DOW,W.G.(eds.): The petroleum system - from source to trap. AAPG Mem. **60**, p. 201-210.

LEYTHAEUSER,D.; SCHAEFER,R.G. & WEINER,B. (1979): Generation of low molecular weight hydrocarbons from organic matter in source beds as a function of temperature and facies. Chem. Geol. **25**, p. 95-108.

LILLACK,H. (1992): Untersuchungen zur Beeinflussung der pyrolytischen Gasbildung aus Kerogenen durch Muttergesteinsmineralien. Diss. RWTH Aachen.

LIN,R. & WANG,P. (1988): PAH in fossil fuels and their geochemical significance. Journal of Southeast Asian Earth Sciences, Oxford, **5**, p.257-262.

LITTKE, R. & LEYTHAEUSER, D. (1993): Migration of oil and gas in coals. In: Law, B.E. & Rice,D.D. (eds.): Hydrocarbons from coal. AAPG Studies in Geology 38. American Association Petroleum Geologist, Tulsa, p. 219-236.

LOPATIN,N.V. (1971): Temperature and geologic time as factors in coalification. Acad Nauk SSSR Izv Ser Geol. **3**, p.95-106. (in Russian).

LOUIS,M.C. & TISSOT,B.P. (1967): Influence de la temperature et de la pression sur la formation des hydrocarbures dans les argiles a kerogen. In: Proc. 7th World Petroleum Congr., Mexico. Elsevier, London, p.47-60.

MACKENZIE,A.S & QUIGLEY,T.M. (1988): Principles of geochemical Prospect Appraisal. AAPG Bull. **72**, no.4, p. 399-415.

MALHOTRA,R. MCMILLEN,D.F. TSE,D.S. & ST.JOHN,G.A. (1989): Relative importance of thermolysis and hydrogenolysis processes: Liquefaction of a Bibenzyl polymer. Energy & Fuels **3**, p. 465-468.

MANGO,F.D. (1987): An invariance in the isoheptanes of petroleum. Science **237**, p. 514-517.

MANGO,F.D. (1990): The origin of light cycloalkanes in petroleum. Geochim. et Cosmochim. Acta **54**, p. 54.

MANGO,F.D. (1990): The origin of light hydrocarbons in petroleum: A kinetic test of the steady-state catalytic hypothesis. Geochim. et Cosmochim Acta **54**, p. 1315-1323.

MANGO,F.D. (1991): The stability of hydrocarbons under the time temperature conditions of petroleum genesis. Nature **352**, no.11, p. 146-148.

MANGO,F.D. (1992): Transition metal catalysis in the generation of petroleum and natural gas. Geochim. et Cosmochim. Acta **56**, p.553-555.

MANGO,F.D. (1994): The origin of light hydrocarbons in petroleum: ring preference in the closure of carbocyclic rings. Geochim. et Cosmochim. Acta **58**, no.2, p. 895-901.

MARCHAND,A. & CONARD,J. (1980): Electron paramagnetic resonances in kerogen studies. In: DURAND,B. (ed.): Kerogen, insoluble organic matter from sedimentary rocks. Editions Technip, Paris, p.243-270.

MCKIRDY & KANTSLER (1980): Oil-geochemistry and potential source rocks of the Officer Basin, south Australia. Aust. Petr. Explor. Assoc. J. **20**, p. 68-86.

MICHELS,R.; LAMDAIS,P.; TORKELSON;B.E. & PHILIP,R.P. (1995): Effects of effluents and water pressure on oil generation during confined pyrolysis and high-pressure hydrous pyrolysis. Geochim. et Cosmochim. Acta **59**, no.8, p.1589-1604.

MONIN,J.C.; CONNAN,J.; OUDIN,J.L. & DURAND,B. (1989): Quantitative and qualitative experimental approach of oil and gas generation: Application to the North Sea source rocks. Org. Geochem. **16**, nos.1-3, p. 133-142.

MONNIER,F.; POWELL,T.G. & SNOWDON,L.R. (1981): Qualitative and quantitative aspects of gas generation during maturation of sedimentary organic matter. Examples from Canadian frontier basins. In: BJORØY,M. (ed.): Advances in Organic Geochemistry 1981, p. 487-495.

MONTEL,F.; CAILLET,G.; PUCHEU,A. & CALTAGIRONE,J.P. (1992): Diffuson model for predicting reservoir gas losses. Marine and Petroleum Geology **10**, feb. p. 51-57.

MONTHIOUX,M. & LANDAIS;P. (1988): Natural and artificial maturations of a coal series: Infrared spectrometry Study. Energy & Fuels **67**, no.2, p. 794-801.

MONTHIOUX,M. (1988): Expected mechansims in nature and confined-system pyrolysis. FUEL **67**, p. 843-847.

MUSCIO,G.P.A.; HORSFIELD,B. & WELTE,D.H. (1994): Occurrence of thermogenetic gas in the immature zone - Implications from the Bakken in- source reservoir system. Org. Geochem. **22**, nos.3-5, p. 461-476.

NORSK HYDRO REPORT (1992) unpublished, see DAHL,B et al.

ORR,W.L. (1986): Kerogen/ asphaltene / sulphur relationships in sulphur rich Monterey oils. In: LEYTHAEUSER & RULLKÖTTER (eds.): Advances in Organic Geochemistry 1985. Pergamon Journals, Oxford, p.499-516.

PELET,R.; BÉHAR,F. & MONIN,J.C. (1986): Resins and asphaltenes in the generation and migration of petroleum. Org. Geochem. **10**, p.551-562.

PEPPER,A.S. & CORVI,P.J. (1995): Simple kinetic models of petroleum formation. Part I: oil and gas generation from kerogen. Marine and Petr. Geol. **12**, no.3, p.291-319.

PEPPER,A.S. & DODD,T.A. (1995): Simple kinetic models of petroleum formation. Part II: oil-gas cracking. Marine and Petr. Geol. **12**, No.3, p.321-340.

PEPPER,A.S. & CORVI,P.J. (1995): Simple kinetic models of petroleum formation. Part III: Modelling an open system. Marine and Petr. Geol. **12**, No.4, p.417-452.

PHILIPPI,G.T. (1965): On the depth, time and mechanism of petroleum generation. Geochim. et Cosmochim. Acta **29**, p. 1021-1049.

PHILIPPI,G.T. (1975): The deep subsurface temperature controlled origin of the gaseous and gasoline-range hydrocarbons of petroleum. Geochimica et Cosmochimica Acta **39**, p. 1353-1373.

PILAWA,B. WIECKOWSKI,A.B. & LEWANDOWSKI,M. (1996): E.p.r. studies of thermal decomposition of exinite and inertinite. FUEL **75**, no.10, p. 1181-1185.

PILLING,M.J. (1980): Hydrocarbon cracking. In: PILLING &SMITH (eds.): Modern gas kinetics. Blackwell scientific publications.

POELCHAU,H.S. BAKER,D.R. HANTSCHEL,T. HORSFIELD,B. & WYGRALA,B. (1997): Basin simulation and the design of the conceptual basin model. In: WELTE,D.H. HORSFIELD,B. & BAKER,D.R. (eds.): Petroleum and basin evolution. Springer, Berlin, p.3-70.

POLLACK,H.N. & CERCONE K.R. (1994): Anomalous thermal maturities caused by carbonaceous sediments. Basin Research **6**, p. 47-51.

POUTSMA,M.L. (1990): Free radical thermolysis and hydrogenolysis of model hydrocarbons relevant to processing of coal. Energy & Fuels **4**, no.2, p.113-131.

PRICE,L.C. (1982): Organic Geochemistry of core samples from an ultadeep hot well (300°C, 7 km). Chem. Geol. **37**, p. 215-228.

PRICE,L.C. & BARKER,C.E. (1985): Suppression of vitrinite reflectance in amorphous rich kerogen- a major unrecognised problem. Journal of Petroleum Geology, **8**, no.1, p. 59-84.

PRICE, L.C. & WENGER, L.M.(1992): The influence of pressure on petroleum generation and maturation as suggested by aqueous pyrolysis. Org. Geochem. **19**, nos **1-3**, p.141-159.

QUIGLEY,T.M. & MACKENZIE,A.S. (1988): The temperatures of oil and gas formation in the subsurface. Nature **333** , No.6173, p.549-552.

RADKE,M.; HORSFIELD,B.; LITTKE,R. & RULLKÖTTER,J. (1997): Maturation and petroleum Generation. In: WELTE,D.H. HORSFIELD,B. & BAKER,D.R. (eds.): Petroleum and basin evolution. Springer, Berlin, p.169-229.

RAWSON,P.F. & RILEY,L.A. (1982): Latest Jurassic - Early Cretaceous Events and the „Late Cimmerian Unconformity" in North Sea Area. AAPG Bull. **66**, p. 2628-2648.

REEDER,M.L. & SCOTSMAN,I.C. (1985): Hydrocarbon generation- central and northern north sea. Oil & Gas Journal **25**, mar, p. 137-144.

REYNOLDS,J.G. & BURNHAM,A.K. (1995): Comparison of kinetic analyses of source rocks and kerogen concentrates. Org. Geochem. **23**, no.1, p. 11-19.

REZNIKOV,A.N. (1969): On the geochemical significance of the n-butane/ isobutane ratio in petroleum gases. Geol. Nefti Gaza **4**, p.43-47.

RITTER,U.; MYHR,M.B.; VINGE,T. & AARESKJOLD,K. (1995): Experimental heating and kinetic models of source rocks: comparison of different methods. Org. Geochem. **23**, no.1, p.1-9.

ROBINSON,W.E.; HEADY,H.H. & HUBBARD,A.B. (1953): Alkaline permanganate oxidation of oil shale kerogen. Ind. Eng. Chem. **45**, april, p.788-791.

ROBINSON,R. (1966): The origin of petroleum. Nature **212**, p. 1291-1295.

RØNNING,K.; JOHNSTON,C.D.; JOHNSTAD,S.E. & SONGSTADP.(1986): Geology of the Hild Field. In: SPENCER,A.M. (ed.): Habitat of Hydrocarbons on the Norwegian Continental Shelf. Norwegian Petroleum Society (Graham & Trotman), p. 199-206.

RULLKÖTTER,J. & MICHAELIS,W. (1989): The structure of kerogen and related materials. A review of recent progress and future trends. Org. Geochem. **16**, no.4-6, p. 829-852.

SACKETT,W.M.; NAKAPARKSIN,S. & DALRYMPLE,D. (1966): Carbon isotope effects in methane production by thermal cracking. Third Intern. Meet. Org. Geochem., London.

SAGA REPORT (1994) Geomechanics and stress regimes, Norwegian North Sea. 940331.

SANDERSON,R.T. (1976): Chemical bonds and bond energy. Academic Press, New York.

SAVAGE,P.E. & KLEIN,M.T. (1988): Asphaltene reaction pathways. 4. Pyrolysis of Tridecylcyclohexane and 2-Ethyltetralin. Ind. Eng. Chem. Res. **27**, p. 1348-1356.

SAVCENKO,J.P.; KARPAR,A.K. & BERETO,J.A. (1971): De l'interêt en prospection, de la valeur du rapport de l'isobutane au butane normal dans les gaz d'hydrocarbures. Centre Recherche Pau, Gas. Prom. **4**, p. 2-5.

SCHAEFER,R.G.; WELTE,H.D. & POOCH,H. (1984): Geochemistry of low molecular weight hydrocarbons in two exploration wells of the Elmworth gas field (western Canada Basin). Org. Geochem. **6**, p. 695-701.

SCHAEFER,R.G. & LITTKE,R. (1988): Maturity-related compositional changes in the low-molecular-weight hydrocarbon fraction of Toarcian shales. Org. Geochem. **13**, nos. 4-6, p. 887-892.

SCHAEFER,R.G.; SCHENK,H.J.; HARDELAUF;H. & HARMS,R. (1990): Determination of gross kinetic parameters for petroleum formation from Jurassic source rocks of different maturity levels by means of laboratory experiments. Org. Geochem. **16**, nos.1-3, p. 115-120.

SCHENK,H.J; WITTE,E.G.; LITTKE,R. & SCHWOCHAU,K (1986): Infrared estimates of aliphatic kerogen carbon in sedimentary rocks. In: LEYTHAEUSER,D. & RULLKÖTTER,J. (eds.): Advances in Organic Geochemistry 1985. Org. Geochem. **10**, p. 1099-1104.

SCHENK,H.J. & HORSFIELD,B. (1993): Kinetics of petroleum generation by programmed-temperature closed- versus open-system pyrolysis. Geochim. et Cosmochim. Acta **57**, p. 623-630.

SCHENK,H.J. & HORSFIELD,B. (1996): Kinetics of petroleum generation: applications and limitations. Zbl. Geol. Paläont. (in press).

SCHENK,H.J.; HORSFIELD,B; KROOSS,B.; SCHAEFER,R.G. & SCHWOCHAU,K (1997): Kinetics of Petroleum Formation and cracking. In: WELTE,D.H.; HORSFIELD,B. & BAKER,D.R. (eds.): Petroleum and basin evolution. Springer, Berlin, p.231-269.

SCHLOEMER,S. & KROOSS,B.M. (1996): Hydrocarbon migration and trapping- experiments and theory. Experimental investigation of the sealing efficiency of cap rock. In: Norweg. Petrol. Soc., Hydrocarbon seals- importance for exploration and production, Conf., Trondheim, p.21.

SEEWALD,J.S. (1994): Evidence for metastable equilibrium between hydrocarbons under hydrothermal conditions. Nature **370**, no.28, p.285-287.

SILSBY,R.I. & SAWYER,E.W. (1956): The dealkylation of alkyl aromatic hydrocarbons. The kinetics and mechanism of toluene decomposition in the presence of hydrogen. J. Appl. Chem. **6**, aug., p. 347-356.

SILVERMAN,S.R. (1967): Carbon isotopic evidence for the role of lipids in petroleum. J. Am. Oil Chem. Soc. **44**, p. 691-695.

SKÅLNES,E.; PATIENCE,R.L.; BJØRLYKKE,K. & KARLSEN,D.A. (1993): Petroleum geochemistry and filling history of the Hild field, Norwegian Continental Shelf. In: ØYGARD (ed): Organic Geochemistry. Poster sessions from the 16th Intern. Meet. on Org. Geochem., Stavanger, p.51-55.

SKJERVØY,A. & SYLTA,Ø. (1993): Modelling of expulsion and secondary migration along the southwest margin of the Horda Platform. In: DORÉ,A.G. et al. (1993): Basin Modelling: Advances and Applications. NPF Special Publication **3**, p. 499-537.

SKJEVRAK,I.; LARTER,S.; van GRAAS,G.; JONES,M. & BERGE,E. (1994): A practical approach to quantitative group type analysis of kerogens using non-dedicated pyrolysis-mass spectrometry equipment: applications and comparison with other Methods. Org.Geochem. **22** , nos.3-5, p. 873-883.

SNOWDON,L.R (1979): Errors in extrapolation of experimental kinetic parameters to organic geochemical systems. AAPG Bull. **63**, no.7, p. 1128-1138.

SOLOMON,D.H. & ROSSER,M.J. (1965): Reactions catalysed by minerals. Part 1: polymerization of styrene. J. of appl. polymer scie. **9**, p. 1261-1271.

SOKOLOV,V.A.; GEODEKYAN,A.A.; GRIGORYEV,C.G.; KREMS,,A.Y.; STROGANOV,V.A.; ZORKIN,L.M.; ZEIDELSON,M.I. & VAINBAUM,S.J. (1971): The new methods of gas surveys, gas investigations of wells and some practical results. In: BOYLE,R.W. (ed.): Geochemical Exploration. Can Inst. Min. and Met. **11**, p.538-544.

SPEERS,G.C. & WHITEHEAD,E.V. (1969): Crude petroleum. In: EGLINGTON,G. & MURPHY,M.T.J. (eds.): Organic Geochemistry. Springer, p. 638-675.

STAHL,W. (1975): Kohlenstoff-Isotopenverhältnisse von Erdgasen. Erdöl, Kohle-Erdgas-Petrochem. **18**, no.4, p. 188-191.

SWEENEY,J.J.; BURNHAM,A.K. & BRAUN,R.L. (1987): A model of hydrocarbon generation from type I kerogen: Application to Uinta Basin, Utah. Am. Assoc. Petrol. Geol. Bull. **71**, p.967-985.

SWEENEY,J.J (1990): BASINMAT - Fortran program calculates oil and gas generation using a distribution of discrete activation energies. Geobyte, april, p.37-43.

SWEENEY,J.J. & BURNHAM,A.K. (1990): Evaluation of a simple model of vitrinite reflectance based on chemical kinetics. Am. Assoc. Petrol. Geol. Bull. **74**, p.1559-1570.

TAKACH,N.E.; BARKER,C. & KEMP,M.K. (1987): Stability of natural gas in the deep surface: Thermodynamic calculation of equilibrium composition. Am. Assoc. Petrol. Geol. Bull. **71**, p. 322-333.

TANG,Y. & JENDEN,P.D. (1995): Theoretical meodeling of carbon and hydrogen isotope fractions in natural gas. 17th Intern. Meet. on Org. Geochem., San Sebastian. p.1067-1069.

TANG,Y. & STAUFFER,M. (1993): Multiple cold trap pyrolysis gas chromatography: a new technique for modeling hydrocarbon generation. Org. Geochem. **22**, no.3-5, p. 863-872.

TAYLOR, G.H.; TEICHMÜLLER, M.; DIESSEL, CFK.; LITTKE,R. & ROBERT, P. (1998): Organic Petrology. Gebr. Bortraeger, Stuttgart, 784 p.

TEGELAAR,E.W. & NOBLE,R.A. (1993): Kinetics of hydrocarbon generation as a function of the molecular structure of kerogen as revealed by pyrolysis -gas chromatography. Org. Geochem. **22**, n.3-5, p. 543-574.

TEICHMÜLLER,M. (1974): Über neue Macerale der Liptinit-gruppe und die Entstehung des Micrinites. Fortschr. Geol. Rheinld. Westf. **24**, p. 37-64.

TEICHMÜLLER,M. (1986): Organic Petrology of source rocks, history and state of the art. Org. Geochem. **10**, p. 581-599.

TEN HAVEN,H.L. (1996): Applications and limitations of Mango's light hydrocarbon parameters in petroleum correlation studies. Org. Geochem. **24**, no.10/11, p.957-976.

THOMAS,B.M.; MØLLER-PEDERSEN,P.; WHITAKER,M.F. & SHAW,N.D. (1985): Organic facies and hydrocarbon distributions in the Norwegian North Sea. In: THOMAS,B.M. et al. (eds.): Petroleum Geochemistry in Exploration of the Norwegian Shelf. Norwegian Petroleum Society, Graham & Trotman, p. 3-26.

THOMPSON,K.F.M. (1979): Light hydrocarbons in subsurface sediments. Geochim. et Cosmochim. Acta **43**, p. 657-672.

THOMPSON,K.F.M. (1983): Classification and thermal history of petroleum based on light hydrocarbons. Geochim. et Cosmochim. Acta **47**, p. 303-316.

THOMPSON,K.F.M. (1987): Gas-condensate migration and oil fractionation in deltaic systems. Mar. Petrol. Geol. **5**, no. 3, p.237-246.

TISSOT,B.P. (1969): Premières données sur les mécanismes et la cinétique de la formation du pétrole dans les sédiments. Simulation dùn schéma réactionnel sur ordinateur. Rev. Inst. Fr. Pét. **24**, p.470-501.

TISSOT,B.P.; DURAND,B.; ESPITALIÉ,J. & COMBAZ,A. (1974): Influence of the nature and diagenesis of organic matter in the formation of petroleum. Am. Assoc. Pet. Geol. Bull. **58**, p.499-506.

TISSOT,B.P. & WELTE,D.H. (1984): Petroleum Formation and Occurrence. Springer Verlag, Berlin Heidelberg New York Tokyo.

TISSOT,B.P.; PELET,R. & UNGERER, P. (1987): Thermal history of sedimentary basin, maturation indices, and kinetics of oil and gas generation. AAPG Bull. **71**, no.12, p. 1445-1466.

UNGERER,P. & PELET,R. (1987): Extrapolation of the kinetics of oil and gas formation from laboratory experiments to sedimentary basins. Nature **327** ,p. 52-54.

UNGERER,P.(1990): State of the art of research in kinetic modelling of oil formation and expulsion. Org. Geochem. **16**, nos 1-3, p. 1-25.

VAN KREVELEN.D.W.; VAN HEERDEN,C. & HUNTJENS,F.J. (1951): Physicochemical aspects of the pyrolysis of coal and related organic compounds. FUEL **30**, p. 253-259.

VOLLSET,J & DORÉ,A.G. (1984): A revised Triassic and Jurassic lithostratigraphic nomenclature for the Norwegian North Sea. NPD Bull. **3.**

WEI,H.; BJOROY,M. & ROALDSET,E. (1994): Multicomponent generation kinetics of source rocks and coals from norwegian North Sea. 6th Conf. of Europ. Assoc. of Petrol. Geosciences & Eng., Ext. Abstr. P532.

WELTE,D.H.; SCHAEFER,R.G.; STOESSINGER,W. & RADKE,M. (1984): Gas Generation and Migration in the Deep Basin of Western Canada. In: MASTERS,J.A. (ed.): Elmworth: Case study of a deep basin gas field. Am. Assoc. Petrol. Geol. Mem. **38**, p. 35-47.

WERES,O.; NEWTON,A.S. & TSAO,L. (1988): Hydrous pyrolysis of alkanes, alkenes, alcohols and ethers. Org. Geochem. **12**, no.5, p.433-444.

WHELAN,J.K.; CARANGELO,R.; SOLOMON,P.R. & DOW,W.G. (1990): TG/plus- a pyrolysis method for following maturation of oil and gas generation zones using Tmax of methane. Org. Geochem. **16**, nos. 4-6, p.1187-1201.

WITTE,E.G.; SCHENK,H.J.; MÜLLER,P.J. & SCHWOCHAU,K. (1988): Structural modifications of kerogen during natural evolution as derived from 13CP/MAS NMR, IR spectroscopy and Rock Eval pyrolysis ofToarcian shales. Org. Geochem. **13**, p. 1039-1044.

WYGRALA,B.P. (1989): Integrated study of an oil field in the southern Po basin, northern Italy. Diss, Univ. Koeln. Berichte Kernforschungsanlage Juelich, no.2313, 217pp.

YALCIN,M.N. LITTKE,R. & SACHSENHOFER,R.F. (1997): Thermal history of sedimentary basins. In: WELTE,D.H. HORSFIELD,B. & BAKER,D.R. (eds.): Petroleum and basin evolution. Springer, Berlin, p.71-168.

YÜKLER,M.A. (1979): Sensitivity analysis of groundwater flow systems and an application to a real case. In: GILL,D. & MERRIAM,D.F. (eds.): Geomathematical and petrophysical studies in sedimentology, computery and geology. Pergamon Press, Oxford, p.33-49.

ZIEGLER,W.H. DOERY,R. & SCOTT,J. (1986): Tectonic habitat of norwegian oil and gas. In: SPENCER,A.M. (ed.): Habitat of hydrocarbons on the norwegian continental shelf. Graham & Trotman, London, p.3-20.

6 APPENDIX

List of contents:

Table 1: Sample set for the project. (page 7)
Table 2: Data provided by Norsk Hydro and Sage Petroleum.
Table 3: Sample-numbers, well-numbers and depth. Rock Eval screening data, TOC and vitrinite reflectance. (page 19)
Table 4: Thermovaporisation gas chromatography. Individual component yields.
Table 5: Ratios calculated from thermovaporisation (PI 1', GOR, wetness, i/n butane).
Table 6: Open pyrolysis (300-600°C at 60 $Kmin^{-1}$). Total yields.
Table 7: Open pyrolysis (300-600°C at 60 $Kmin^{-1}$). Individual component yields.
Table 8: Open pyrolysis (300-600°C at 60 $Kmin^{-1}$). Aliphatic fraction boiling range compositions.
Table 9: Closed pyrolysis (0.7 K/min -520°C), total yields.
Table 10: Bulk reaction kinetic parameters. Samples of different maturities, Heather and Draupne Formation.
Table 11: Reaction kinetic parameters reported in literature. (page 29)
Table 12: Hydrogen Index from Rock Eval and MSSV and open system pyrolysis equivalents. (page 37)
Table 13: Peak Identification, light hydrocarbons. Open and closed pyrolysis gc-ms, Draupne and Heather Formation. (page 39)
Table 14: MSSV pyrolysis hydrocarbon boiling ranges, totals. Heather Fm well G, 2138.75m.
Table 15: MSSV pyrolysis hydrocarbon boiling ranges, resolved. Heather Fm well G, 2138.75m.
Table 16: MSSV pyrolysis hydrocarbon boiling ranges, totals. Draupne Fm well B, 2764.7m.
Table 17: MSSV pyrolysis hydrocarbon boiling ranges, resolved. Draupne Fm well B, 2764.7m.
Table 18: MSSV pyrolysis individual components. Heather Formation well G, 2138.75m.
Table 19: MSSV pyrolysis individual components. Draupne Formation well B, 2764.7m.
Table 20: Multistep open system pyrolysis, totals. Heather Formation well G, 2138.75m.
Table 21: Multistep open system pyrolysis, totals. Draupne Formation well B, 2764.7m.
Table 22: Heather Formation compositional kinetic parameters.
Table 23: Draupne Formation compositional kinetic parameters.
Table 24: Stratigraphy for the investigated section, basin modelling. (page 70)
Table 25: Modified kinetic parameters for basin modelling. (on request from the author or supervisor available)
Table 26: Headspace and occluded gas.
Table 27: Stable carbon isotopes.
Table 28: Kinetic parameters for ethane and propane, from MSSV pyrolysis used for modelling of isotopic compositional changes.

Photoplates

Table 2: Data provided by Norsk Hydro and Saga Petroleum

gechem. data	number of wells
vitrinite reflectance	56
headspace and occluded gas	40
gas isotope data	35
Rock Eval screening parameter	25
EOM extractable organic matter	19
Iartroscan group type analyses	10

Table 4: Thermovaporisation gas chromatography	amounts in (µg/g rock).																						
well	P	P	P	P	P	P	P	G	G	G	G	G	G	G	G	G	H	H	H	I	I	I	I
E-nr.	E41699	E41700	E41701	E41702	E41703	E41705	E41706	E41714	E41715	E41716	E41718	E41719-D1	E41720	E41721	E41722	E41723	E41695	E41696	E41697	E41690	E41691	E41692	E41693
C1	5.6	7.7	4.6	6.2	3.1	5.0	0.4	1.0	2.6	6.3	2.2	3.0	1.2	1.7	1.0	2.8	5.6	4.2	2.5	7.0	8.7	9.6	3.0
N-C2	2.5	2.6	1.8	1.7	0.6	10.1	0.3	1.0	2.6	4.8	2.1	2.3	0.9	1.4	1.2	1.8	5.7	4.2	1.9	6.4	16.8	19.9	3.0
N-C3	26.4	7.4	2.9	4.7	1.4	4.1	0.4	2.6	2.4	8.3	3.5	3.4	1.4	2.3	1.5	6.9	4.8	6.1	2.2	42.1	26.0	131.1	10.6
I-C4	32.2	16.0	11.3	4.9	3.7	3.1	1.6	3.5	2.8	4.1	4.1	5.2	2.5	4.9	1.6	3.2	13.7	26.2	9.1	23.9	22.1	46.2	7.6
N-C4	37.4	13.2	14.4	6.1	2.8	2.4	0.5	4.3	3.5	8.3	4.0	4.6	2.9	7.6	1.7	7.6	23.0	30.9	8.8	79.6	54.3	181.5	23.0
I-C5	33.2	16.5	24.7	4.0	2.1	2.1	3.1	6.7	5.5	12.5	6.4	10.3	4.3	9.8	3.2	7.4	6.6	13.5	5.5	59.0	52.2	98.7	21.5
N-C5	19.2	9.6	14.5	1.9	0.8	0.9	1.1	4.1	1.7	4.4	1.8	3.4	1.1	3.5	1.3	2.7	3.8	4.3	2.2	68.0	50.1	129.9	20.9
neo pentane																							
CY-C5	6.7	2.8	6.1	0.6	0.4			2.1	1.1	3.2	1.1	1.9	0.5	0.9		0.9	2.0	2.2		27.8	23.0	47.2	8.5
2-M-C5	13.6	7.3	19.2	0.4	0.5	0.4	1.2	3.1	1.8	4.9	2.6	4.3	1.5	3.7	1.4	2.3	2.6	5.5	1.4	35.9	34.4	58.4	15.2
3-M-C5	7.6	4.4	8.3	0.3	0.2	0.2		2.0	1.0	3.4	1.2	3.0	0.8	1.5	0.5	1.0		3.1	0.7	27.8	23.5	43.4	10.6
N-C6	13.5	7.2	12.3	0.8	0.9	0.2	0.8	5.7	2.1	7.3	2.2	3.5	0.8	1.5	0.3	1.0	1.2	5.7	0.9	54.1	41.7	93.3	18.8
M-CY-C5	15.4	6.7	13.3	2.0	1.4	1.1		6.6	3.3	10.6	3.3	9.3	2.4	4.8	0.8	3.8		5.9	1.0	80.0	72.0	128.9	28.5
benzene	68.7	28.1	35.4	21.8	10.5	8.7	0.7	6.4	3.4	8.2	3.2	6.1	2.2	3.4	1.2	4.6	5.8	10.2	3.4	13.3	21.9	34.7	5.9
CY-C6	26.7	12.9	21.9	4.7	3.8	2.7	0.9	11.4	7.2	24.4	7.0	8.0	2.2	3.3	0.7	3.3	3.5	14.1	2.6	59.7	58.5	92.7	24.4
2MC6+DMC5	10.3	6.8	12.7	0.8	0.4	0.3	0.5	2.6	2.8	5.4	1.6	3.6	1.1	2.3	1.8	3.5	2.7	5.0	1.3	30.3	30.9	44.9	13.8
DM-CY-C5	1.9	1.0	1.7	0.2	0.2	0.2	0.1	0.8	0.5	1.9	0.6	0.3	1.0		0.1	0.4	0.7	1.4	0.4	7.3	9.6	10.9	3.7
3-M-C6	8.3	5.0	10.1	0.4	0.3	0.2	0.2	2.8	1.5	5.0	1.4	3.5	0.8	4.1	0.4	1.6	1.2	5.1	2.9	30.5	31.5	45.2	14.1
1Cis-3DM-CY-C5	2.0	1.1	1.9	0.3	0.2	0.1		1.1	0.6	2.5	0.7	2.9	0.7	1.3	0.3	1.7	0.4	1.7	0.9	18.8	18.8	28.1	7.5
1Trans-3DM-CY-C5	2.1	1.3	2.2	0.2	0.2	0.1		1.2	0.6	2.3	0.7	2.5	0.6	1.2	0.3	1.7				18.9	17.6	29.6	7.9
1Trans-2DM-CY-C5	3.3	1.8	3.2	0.5	0.4	0.3	0.1	2.1	1.3	5.3	1.7	5.3	1.5	2.7	0.7	8.6	17.2		6.7	45.0	43.7	65.0	20.6
N-C7	11.9	7.7	12.7	0.8	0.6	0.3	0.3	5.6	2.7	9.3	3.1	4.0	1.2	2.2	0.6	1.6	3.2	9.7	1.6	54.0	44.8	87.1	22.6
M-CY-C6	32.9	18.5	33.6	4.5	2.8	2.0	0.2	16.5	9.5	38.7	10.1	17.2	3.8	7.9	1.9	6.6	9.1	22.5	3.4	107.7	98.9	158.4	46.4
toluene	167.9	79.0	109.9	40.6	17.7	12.7	0.9	18.1	8.7	32.9	8.9	13.9	3.0	7.2	2.3	5.7	19.6	23.1	4.4	37.4	38.9	82.7	15.1
DM-CY-C6	17.6	12.0	22.0	0.5				8.5	4.9	26.3	5.7	8.5	2.0	4.6	1.1	3.7	12.5	15.2	3.0	120.3	108.8	170.4	57.6
N-C8	11.0	7.2	12.8	0.8	0.5	0.1	0.0	6.1	3.5	15.1	4.0	3.9	1.0	3.2	1.1	2.7	13.3	10.8	2.6	59.8	53.8	87.7	27.5
ethylbenzene	8.2	4.3	6.1	2.0	0.8	1.6	0.0	5.2	3.2	18.8	3.3	6.3	1.7	3.7	1.1	3.5	4.5	4.1	1.5	30.9	31.0	49.0	15.3
m,p-xylene	72.0	36.2	54.8	13.4	5.8	8.9	0.1	18.2	10.2	64.3	11.1	9.3	2.3	5.6	1.9	4.8	25.7	21.6	6.1	45.6	42.5	72.8	22.0
I-C9?	20.1	12.4	22.3		0.3												10.5	5.9	2.6	44.4	44.1	58.3	22.6
o-xylene	16.9	8.3	12.5	2.5	1.1	2.8		8.7	4.9	31.3	5.6	5.7	1.5	3.7	1.3	2.8	13.8	12.4	3.6	31.5	30.6	50.3	14.7
N-C9	10.2	6.1	10.9	0.4	0.3			5.6	3.6	24.9	4.0	3.3	0.9	1.8	0.7	2.1	19.3	10.3	5.1	55.6	51.0	73.6	28.7
sum C3-benzene	23.8	12.8	20.3	3.0	1.4			28.3	17.6	136.2	24.9	21.0	5.5	13.7	4.0	11.2	27.9	22.3	9.1	105.1	99.0	131.5	57.3
N-C10	9.5	6.1	10.3	0.3	0.4			5.9	4.9	34.5	6.3	2.3	0.6	1.7	0.5	2.1	20.8	11.7	4.3	50.8	47.7	66.2	32.8
N-C11	9.0	6.1	9.8	0.5	0.4			6.3	6.2	34.8	8.7	1.9	0.7	1.7	0.6	2.0	19.0	11.7	4.4	58.1	47.3	64.8	44.2
naphthalene	8.6	4.0	6.3	4.3	2.1			18.5	14.3	82.4	20.1	14.6	5.9	11.5	3.2	9.9	23.0	21.3	6.8	32.4	31.8	42.3	20.8
N-C12	8.0	5.8	8.7	0.8	0.6			6.6	7.3	26.2	9.0	1.9	0.7	1.6	0.5	2.5	14.2	10.5	3.5	49.8	41.4	51.2	41.0
I-C13																	5.9	3.2	1.1	24.4	21.0	24.9	22.0
2-M-naphthalene	14.0	6.0	10.6	4.8	1.9			26.8	22.8	114.7	30.2	14.2	4.2	9.3	2.3	9.1	12.8	13.6	3.8	43.2	42.8	56.3	28.9
1-M-naphthalene	5.7	2.7	4.7	1.8	0.9			19.7	17.1	83.9	23.2	10.3	3.8	7.2	2.2	6.4	12.9	11.3	4.2	54.3	48.7	65.9	35.0
N-C13	7.7	6.5	8.4	2.5	1.5			7.6	9.4	25.0	13.0	2.8	1.4	1.7	1.0	3.6	12.9	11.2	3.8	57.3	47.9	57.4	49.2
biphenyl	13.3	6.2	9.5	5.9	2.0			6.7	6.5	26.7	8.3	2.7	1.0	1.3		1.6	4.9	4.7		7.1	8.2	7.3	6.0
D-M-naphthalene	6.4	2.7	5.0	1.4				40.3	23.2	162.9	34.5	10.9	2.0	12.6	3.2	20.3	2.9	1.9	0.9	19.7	15.7	19.3	17.9
N-C14+DMN	11.6	9.0	10.5	4.7	2.1			10.0	29.3	59.3	14.1	3.4	5.5	2.3	0.5	2.4	16.3	14.0	4.5	94.9	83.9	106.2	73.7
M-biphenyl	18.3	8.1	13.9	5.4	1.3																		
N-C15	6.7	5.4	7.1	2.6	0.7			7.8	10.6	20.8	9.0	3.1	4.1	4.1	0.9	3.2	7.5	3.4	1.6	55.1	45.2	53.1	49.4
T-M-naphthalene																				15.4	11.6	14.6	11.3
N-C16	4.7	3.5	5.6	0.9				5.8	7.8	16.1	6.2	2.2	2.2	3.2	0.3	2.2	5.1	2.5	0.6	50.4	37.9	40.6	41.0
Isoprenoid C-18																	3.1	1.2	0.8	32.8	25.3	26.8	29.7
N-C17	4.3	2.7	4.7					3.1	4.5	9.6	4.2	1.5	0.5	1.8		1.7	4.3	0.8	0.4	42.4	32.9	35.5	38.8
pristane	1.9	1.5	3.8					3.4	5.7	8.8	4.7	2.9	1.3	5.7		3.4	6.3	1.1	1.2	44.7	32.0	32.5	38.1
phenanthrene	5.4	2.0	4.1	4.6	0.9			6.6	4.8	26.1	7.3	3.4		2.0		2.1	0.8	2.1	0.2	12.1	11.6	13.6	4.7
N-C18	3.6	2.0	4.8					2.0	2.8	5.3	2.8	1.0		0.7		0.7	2.7	0.4	0.1	33.5	25.9	27.0	30.8
phytane	0.6	0.4	1.2					1.5	2.1	3.0	1.7	0.6		0.7		0.5	1.3		0.0	30.9	22.4	20.9	26.1
sum M-phenanthrene	8.9	3.0	6.1	3.2				7.0	5.5	31.8	8.1	2.5											
N-C19																	3.2		0.1	42.8	33.8	34.3	34.1
M-P+NC19	4.2	2.2	5.4					3.9		14.7	4.6	2.6				1.9		2.3					
N-C20	3.1	1.3	3.6													0.3	1.1		0.0	25.6	18.9	18.0	23.9
N-C21	1.9	0.8	2.5													0.6	0.7		0.0	21.6	16.2	13.4	18.8
N-C22	1.4	0.6	2.1													0.7	0.4		0.0	21.7	15.7	14.0	19.2
N-C23	0.8	0.4	1.2													0.4	0.3		0.0	17.9	13.3	9.8	15.8
N-C24			0.7													0.3				17.7	12.2	9.7	15.1
N-C25																0.3				15.5	10.3	8.0	12.5
N-C26																0.3				14.1	9.1	7.0	11.4
N-C27																				12.0	8.0	5.4	9.8
N-C28																				9.4	6.3	4.6	7.8
N-C29																				10.2	7.1	4.4	8.0
N-C30																				6.9	4.5	3.3	5.5
Summe	888.7	452.9	691.0	174.7	80.0	70.6	13.4	381.4	301.9	1317.5	348.1	264.3	87.2	184.6	51.2	190.0	442.3	436.1	139.7	2452.4	2131.3	3319.3	1422.2

Table 4, continued: Thermovaporisation gas chromatography	amounts in (µg/g rock).																				
well	I	F	F	F	F	F	F	F	D	A	A	A	J	J	J	B	B	C	C	L	K	K
E-nr.	E41694	E41707	E41708	E41709	E41710	E41711	E41712	E41713	E42180	E43249	E43250	E43251	E43252	E43253	E41746	E43254	E43255	E43256	E43257	E43284	E41739	E41725
C1	8.0	2.5	1.2	2.9	3.6	2.4	2.3	2.1	11.6	9.4	5.7	1.2	7.7	1.8	4.6	11.4	8.6	4.3	3.1	0.4	1.1	1.3
N-C2	8.2	1.9	1.2	3.0	3.7	2.4	2.9	1.9	9.5	6.8	5.4	2.9	9.3	4.6	3.4	12.6	8.6	6.9	3.7	1.1	2.6	1.4
N-C3	23.9	2.7	1.8	4.3	4.2	2.3	2.7	1.7	8.8	9.6	5.7	4.1	10.7	4.0	2.9	59.4	11.6	18.7	15.9	1.6	1.9	4.5
I-C4	18.9	3.7	2.3	2.3	2.5	1.9	3.6	1.5	2.5	2.9	0.9	1.3	3.2		5.3	39.0	14.3	34.8	23.8	0.3	0.6	4.9
N-C4	56.4	16.7	2.4	4.3	5.1	2.2	3.1	10.3	13.2	26.8	16.1	13.7	18.8	13.5	50.8	85.5	35.0	34.4	37.5	11.8	15.8	17.8
I-C5	46.4	5.6	4.0	5.5	4.9	3.1	5.6	2.8	7.2	7.3	16.3	10.0	5.7	3.7	13.2	55.4	28.0	44.8	27.7	3.4	6.1	6.7
N-C5	48.5	1.6	1.6	2.2	1.9	1.5	2.1	1.1	5.2	17.0	6.3	20.1	8.0	7.4	8.4	58.6	24.9	10.5	8.0	3.8	4.7	6.6
neo pentane										1.3	1.0	1.0	0.8	1.1	1.6	2.5	1.9	1.4	0.8	0.4	0.9	0.6
CY-C5	21.3							0.3	1.7	3.6	1.5	2.2	1.7		0.5	16.6	8.2					1.1
2-M-C5	28.3	2.1	1.3	1.4	0.9	0.9	2.4	0.6	3.7	7.2	4.6	6.9	4.7	6.6	3.2	31.1	22.2	31.0	20.0	2.6	3.9	6.5
3-M-C5	22.0	1.0	0.4	0.7	0.5			0.7	2.6	5.4	4.3	3.4	3.0	2.4	5.3	17.8	12.8	13.1	9.8	1.2	1.4	2.1
N-C6	39.9	0.6	0.5	0.7	0.8	0.4	0.6	0.5	7.3	2.8	3.5	4.7	6.6	2.2	1.7	49.9	27.2	5.9	6.4	1.6	2.1	1.9
M-CY-C5	62.9	1.2	0.7	1.1	0.8	0.5	1.3	0.8	9.2	1.7	1.2	4.3	3.8	1.6	0.6	41.3	22.2	9.6	7.3	1.0	0.4	1.5
benzene	13.6	2.4	2.4	2.9	2.6	1.9	4.2	1.3	19.6	14.2	5.5	5.0	12.7	4.7	5.5	33.0	14.7	13.8	12.7	4.2	3.0	2.9
CY-C6	48.9	3.2	2.6	3.0	3.5	1.7	2.3	2.5	11.0	4.8	2.6	6.2	9.9	3.3	1.6	67.1	36.2	4.8	5.0	1.4	1.3	1.6
2MC6+DMC5	23.9	1.7	0.9	2.1	1.3	0.2	1.1	0.6	5.9	2.4	2.1	2.2	2.9	3.1	0.8	21.6	15.7	26.3	20.8	1.2	3.4	3.6
DM-CY-C5	6.2	3.9	0.4	1.0	0.6	0.7		0.2	0.9	1.7	1.0	0.9	1.0		0.8	5.6	3.7	1.1	1.2	0.1	0.2	
3-M-C6	23.5		6.1	3.2	0.8	0.3	12.5	0.4	6.4	1.4	0.8	3.9	2.9	5.2	1.1	19.4	13.7	16.6	13.3	0.5	1.0	2.0
1Cis-3DM-CY-C5	14.9	0.4	0.4	0.4	0.3	0.2	0.5	0.2	4.3	0.8	0.3	4.6	0.8	0.2	1.3	8.3	5.6	4.9	3.8	0.2	1.0	0.3
1Trans-3DM-CY-C5	15.1	1.1	0.3	0.5	0.3	0.1	0.4	0.2	4.2	1.2	0.3	0.9	0.9			8.7	5.9	5.0	4.4	0.3		0.7
1Trans-2DM-CY-C5	35.9		1.0	0.1	0.8	0.4	1.2	0.6	12.0	4.8	1.6	2.4	2.2	1.2		19.4	13.9	7.1	7.0	0.7		1.4
N-C7	41.6	0.8	0.7	1.3	1.1	0.5	0.9	0.7	14.3	2.7	1.7	1.3	7.6	2.4	1.4	49.1	29.9	7.4	9.0	1.5	1.1	2.1
M-CY-C6	86.3	4.1	3.6	4.3	5.0	2.1	3.0	3.3	25.0	7.5	5.4	7.1	13.4	3.8	1.7	99.1	59.0	20.2	17.5	1.7	1.2	1.9
toluene	36.5	2.0	2.0	3.5	3.1	1.5	2.3	1.9	86.0	6.4	4.8	9.9	24.1	5.5	2.2	89.1	37.6	11.7	10.4	5.9	2.1	1.8
DM-CY-C6	98.4	2.6	1.1	1.8	1.9	1.2	1.0	1.1	18.7	10.5	5.9	4.3	8.9	3.5	2.1	64.4	45.7	57.2	46.3	2.4	1.8	3.9
N-C8	48.8	2.3	1.6	2.0	1.9	0.9	1.7	0.9	14.2	6.8	5.5	4.3	9.6	4.4	2.5	44.3	32.9	25.2	20.0	3.4	2.6	2.9
ethylbenzene	27.1	1.2	1.3	1.9	2.0	0.7	0.8	0.6	27.5	10.0	5.1	3.6	5.4	2.0	1.1	22.5	15.9	5.9	5.0	0.8	1.0	1.1
m,p-xylene	39.4	3.2	3.8	5.6	5.5	2.3	2.0	1.9	56.9	14.2	9.3	8.7	18.4	4.5	2.0	68.0	41.5	10.3	10.2	3.9	2.6	2.5
I-C9?	36.3								7.0	5.7	2.2	7.1	5.8	8.9	1.5	31.0	27.9	40.1	33.5	5.8	7.9	6.2
o-xylene	27.1	2.2	2.5	3.6	3.7	1.5	1.2	1.3	29.5	5.7	4.3	3.7	8.2	2.1	1.1	33.7	21.2	8.0	8.6	1.2	1.1	1.0
N-C9	45.0	2.0	2.5	3.2	3.6	1.1	1.1	0.8	11.0	9.0	4.4	0.6	10.0	2.0	0.7	34.9	26.7	14.4	13.1	0.8	1.3	0.5
sum C3-benzene	77.5	12.4	15.2	20.3	25.5	11.1	4.9	4.7	44.0	21.4	22.3	10.9	18.4	7.8	4.8	66.7	45.3	31.8	27.1	2.1	4.3	3.7
N-C10	38.4	4.2	7.6	9.8	14.0	4.8	1.7	1.8	7.8	8.2	6.7	0.8	11.2	2.4	0.5	25.0	19.6	16.7	13.1	0.8	2.6	1.2
N-C11	40.9	7.3	12.0	16.0	26.3	11.7	3.3	4.3	6.4	10.7	9.5	1.2	18.7	5.8	0.8	23.3	19.9	22.4	16.3	1.3	5.6	1.9
naphthalene	23.3	9.3	11.9	16.3	22.4	10.8	4.5	5.3	11.5	12.9	17.1	7.4	11.6	6.8	1.0	30.9	21.1	16.5	12.5	1.3	2.2	1.1
N-C12	34.7	10.1	11.0	15.7	23.1	14.0	6.1	7.3	5.1	12.6	11.3	2.7	25.0	16.7	1.2	18.7	17.4	23.0	15.8	2.6	14.6	3.4
I-C13	17.7									5.7	4.9	0.9	4.5	4.3	0.2	6.6	5.4	12.0	8.6	0.3	2.4	0.4
2-M-naphthalene	31.8	14.4	15.0	21.2	29.3	12.8	6.1	7.2	7.9	18.3	29.2	10.0	24.6	23.6	1.6	44.8	30.5	20.4	16.0	1.2	3.6	1.3
1-M-naphthalene	39.8	14.3	14.2	20.4	27.0	14.0	6.9	9.4	12.3	12.7	19.9	6.6	17.0	18.7	1.6	34.1	24.0	16.6	14.1	0.7	2.7	0.8
N-C13	41.1	16.1	13.9	20.4	27.3	17.0	11.0	15.1	6.1	18.8	16.7	6.2	33.1	51.0	4.5	22.3	21.7	30.2	21.3	4.4	30.0	6.0
biphenyl	4.5	5.1	4.3	6.2	8.4	4.0	1.8	1.4		5.0	6.9	3.3	10.3	16.6	2.4	13.6	10.4	9.7	7.4	1.5	5.5	1.9
D-M-naphthalene	13.2	18.1	5.7	8.1	10.6	16.2	2.5	3.5	3.0	17.4	27.7	12.3	38.4	64.8	11.1	53.3	40.8	47.3	35.7	2.3	18.3	2.5
N-C14+DMN	68.1	29.8	6.2	9.0	11.6	25.6			10.7	17.8	15.0	10.7	39.6	98.2	18.3	27.5	25.2	34.4	24.4	4.8	27.1	9.4
M-biphenyl										6.0	1.6	2.6	25.5		5.2	2.9	2.7	13.3	9.9	0.8	4.6	1.2
N-C15	37.6	11.6	8.6	11.6	13.6	8.7	6.9	11.9	6.7	17.4	16.5	10.2	48.6	117.2	36.5	34.7	36.9	39.4	30.1	3.5	15.0	9.0
T-M-naphthalene	9.1									4.1	3.9	1.9	11.8	27.7	8.9	10.1	9.2	11.1	30.1	0.6	3.1	1.1
N-C16	30.2	9.2	7.1	10.5	10.5	6.3	5.1	7.7	4.0	10.6	9.7	4.7	38.3	99.0	43.5	24.1	32.4	31.9	26.7	2.3	10.1	6.6
Isoprenoid C-18	20.6								3.2	9.2	9.1	9.6	17.3	46.9	20.7	8.0	11.6	16.0	15.6	0.6	4.1	1.2
N-C17	26.7	6.4	4.8	6.7	7.0	5.2	3.6	4.3	3.7	11.7	10.0	2.1	37.2	85.5	35.2	12.6	19.6	22.5	20.0	1.4	8.2	4.1
pristane	24.5	4.5	3.3	4.6	4.9	3.3	2.6	3.7	7.2	17.1	15.1	5.6	26.9	64.0	20.7	10.2	13.4	18.7	19.3	0.5	4.9	0.9
phenanthrene	6.9	3.4	2.7	4.5	6.1	3.1	0.4	0.5		3.8	2.7	0.6	10.1	21.7	6.6	4.0	5.0	5.5	5.2	0.1	1.6	0.5
N-C18	20.0	4.6	3.9	5.2	6.1	3.4	2.2	2.9	2.4	6.2	4.8	0.9	35.4	67.3	18.6	8.9	12.4	14.3	11.8	0.8	4.9	2.2
phytane	15.4	1.8	1.3	1.8	2.2	1.7	1.2	1.5	6.7	9.5	8.0	0.9	19.4	33.3	9.4	5.2	6.4	8.7	8.1	0.1	1.9	0.5
sum M-phenanthrene		1.5	1.6	1.9			0.0	0.2			4.8	2.4	35.7			23.3						
N-C19	24.6								4.1	4.2	3.7	0.5	38.7	60.7	19.2	6.8	7.6	14.0	12.7	0.5	3.9	1.1
M-P+NC19		6.1	4.8	8.2	8.1	6.9	3.6	4.7														
N-C20	13.1	3.1	2.7	3.8	4.1	2.5	1.6		1.9	3.3	2.4	0.3	40.2	55.3	17.5	8.9	8.2	11.1	10.2	0.2	3.2	0.4
N-C21	10.7	2.5				1.7			1.6	2.9	1.8	0.2	30.0	39.9	11.6	3.6	3.6	7.1	6.9	0.1	1.9	0.1
N-C22	10.3	3.9				2.0			2.0	2.1	1.4	0.1	28.1	35.7	10.4	2.9	3.1	5.5	5.7	0.1	1.2	0.1
N-C23	8.0	2.1				1.0			1.7	1.8	1.3	0.2	25.2	32.1	8.5	2.0	2.3	3.7	4.2	0.0	0.6	
N-C24	7.5	1.8								1.5	1.0	0.1	23.3	29.2	7.5	1.6	1.9	2.8	3.2		0.3	
N-C25	6.3	1.5								1.0	0.9	0.1	23.4	28.1	5.9	1.2	1.6	2.0	2.3		0.1	
N-C26	5.6	1.3								0.6	0.4	0.0	18.2	20.6	4.4	0.8	1.0	1.0	1.3		0.1	
N-C27	4.2	1.3								0.3	0.3	0.1	15.0	15.5	2.8	0.5	0.7	0.6	0.7			
N-C28	3.0	0.9								0.1	0.2	0.1	11.9	10.4	1.8	0.2	0.5	0.3	0.4			
N-C29	3.4	0.9									0.2	0.3	9.3	6.8	1.2	0.6	0.7	0.2	0.2			
N-C30	2.2										0.0				0.7	0.4	0.7	0.1	0.1			
Summe	1774.1	282.2	208.4	291.0	355.0	222.7	138.8	140.2	596.9	486.4	421.7	269.0	1050.6	1319.3	473.8	1741.5	1136.0	1006.2	842.8	100.1	262.7	155.9

Table 5: Ratios calculated from Thermovaporisation.					
sample	**GOR (kg/kg)**	**Ro (%)**	**PI'**	**i/n C4**	**wetness**
E41699	0.10	1.01	2.00	0.86	94.62
E41700	0.10	1.09	2.27	1.21	83.58
E41701	0.07	1.11	2.53	0.78	86.86
E41702	0.11	1.38	1.00	0.80	73.73
E41703	0.11	1.33	0.70	1.32	73.28
E41705	0.88	1.50	0.71	1.29	79.76
E41706	0.16	1.45		3.20	87.50
E41714	0.03	0.48	1.04	0.81	91.94
E41715	0.02	0.43	1.43	0.80	81.29
E41716	0.01	0.45	0.87	0.49	80.19
E41718	0.02	0.47	0.81	1.03	86.16
E41719	0.05	0.47	0.65	1.13	83.78
E41720	0.05	0.52	0.50	0.86	86.52
E41721	0.06	0.50		0.64	90.50
E41722	0.08	0.50	1.57	0.94	85.71
E41723	0.06	0.50	0.41	0.42	87.44
E41695	0.07	0.49		0.60	89.39
E41696	0.13	0.51		0.85	94.13
E41697	0.13	0.50		1.03	89.80
E41690	0.03	0.61	0.68	0.30	95.60
E41691	0.03	0.53	0.70	0.41	93.20
E41692	0.06	0.64	0.67	0.25	97.53
E41693	0.01	0.59	0.70	0.33	93.64
E41694	0.04	0.56	0.66	0.34	93.07
E41707	0.05	0.42		0.22	90.91
E41708	0.02	0.40	3.33	0.96	86.52
E41709	0.03	0.43	2.65	0.53	82.74
E41710	0.02	0.39	1.05	0.49	81.15
E41711	0.03	0.45	0.36	0.86	78.57
E41712	0.07	0.42		1.16	84.25
E41713	0.05	0.42	0.83	0.15	88.00
E 43249	0.05	0.35	0.45	0.11	83.06
E 43250	0.05	0.40		0.06	83.14
E 43251	0.11	0.40	0.69	0.09	94.83
E 43252	0.02	0.94	1.20	0.17	84.51
E 43253	0.01	0.86		0.00	92.47
E 43254	0.09	0.37	0.98	0.46	94.52
E 43255	0.05	0.37	1.01	0.41	88.99
E 43256	0.07	0.43	2.37	1.01	95.66
E 43257	0.06	0.43	2.08	0.63	96.31
E 42384	0.17	1.00	1.31	0.03	97.37
E 41739	0.05	0.80		0.04	95.00
E 41725	0.21	0.80		0.28	95.65
E 41746	0.05	0.80		0.10	92.86

PI 1' (mod. after Thompson 1979)
2,methylhexane+3,methylhexane / sum (dimethylcyclopentane)
GOR - Gas - Oil - Ratio (unresolved) C_{1-5} / C_{5+}.
Wetness (C2-4 / C1-4)*100.

Table 6: Open pyrolysis (300-600°C at 60 K/min), total yields.

		mg/g TOC				
	TOC	C1-5	C6-14	C15+	sum	hump (%)
E41690PA2-S2	8.12	57.30	111.39	195.43	**364.12**	27.1
E41692PA2-S2	9.8	47.14	98.94	137.10	**283.19**	28.2
E41694PA2-S2	7.3	43.81	93.05	141.40	**278.26**	28.3
E41695PA2-S2	4.5	50.69	112.90	123.69	**287.27**	30.5
E41697PA2-S2	2.1	23.85	43.73	24.86	**92.44**	36.8
E41701PA1-S2	4.5	19.90	17.54	11.89	**49.33**	37.7
E41703PA1-S2	3.2	6.61	2.28	0.03	**8.92**	81.3
E41711PA2-S2	3	28.24	53.81	40.30	**122.35**	33.4
E41715PA1-S2	5.5	19.00	29.51	33.82	**82.33**	31.0
E41721PA1-S2	2.7	33.69	54.59	45.59	**133.87**	35.9
E43249PA1-S2	8.28	45.90	125.12	186.18	**357.20**	26.3
E43251PA1-S2	3.07	17.85	23.05	4.53	**45.43**	48.9
E43253PA1-S2	5.47	28.34	54.95	78.15	**161.45**	31.7
E43254PA1-S2	11.9	50.88	124.94	221.61	**397.42**	25.6
E43256PA1-S2	4.45	35.00	77.60	100.47	**213.07**	26.7
E42383D1-S2	6.5	49.30	111.52	191.05	**351.86**	28.3
E42384D1-S2	1	43.85	44.62	15.70	**104.17**	41.7
E41725D1-S2	2.93	3.83	2.47	0.20	**6.51**	69.5
E41739D1-S2	2.58	27.05	34.77	19.84	**81.66**	43.8
E41746D1-S2	4.07	31.88	55.57	32.60	**120.05**	40.5
E41748D1-S2	2.96	18.46	28.08	7.23	**53.77**	42.4
E42180PA1-S2	7.25	56.82	146.02	232.97	**435.81**	24.7
E41695MK-S2	38.3	45.36	89.26	139.84	**274.46**	27.9
E41711MK-S2	23.9	20.76	38.65	43.30	**102.71**	32.7
E41715MK-S2	47.6	29.95	40.73	67.41	**138.09**	30.1
E41721MK-S2	30.8	11.15	21.59	19.86	**52.60**	34.6
E41699MK-S2	37.5	6.10	24.11	25.99	**56.21**	70.7
E41701MK-S2	45.2	5.89	12.86	15.67	**34.43**	22.9
E41703MK-S2	32.1	2.45	8.84	12.38	**23.67**	10.8
E41706MK-S2	36.8	0.95	0.60	11.00	**12.56**	7.7

PA=whole rock, D1=whole rock manually crushed, MK=kerogen concentrate

Table7: Open system pyrolysis (300-600°C at 60 K/min). Single compound yields (µg/g sample).

Whole rock samples (PA) and kerogen concentrates (MK).

well	I			H			P						F	
E nr	41690	41692	41694	41695	41695	41697	41699	41701	41701	41703	41703	41706	41711	41711
PA2/MK	PA2	PA2	PA2	PA2	MK	PA2	MK	PA2	MK	PA2	MK	MK	MK	PA
fm	dr	dr	hea	dr	dr	hea	vik	vik	vik	vik	vik	vik	hea	hea
compound														
µg/g rock														
N-C1	1234.1	1216.1	793.9	539.8	5629.8	97.5	1289.7	369.2	1508.6	131.5	417.5	123.5	1559.4	255.7
N-C2	961.6	957.9	693.1	452.2	4006.3	89.1	316	178.4	467	39.3	139.4	66.4	1052.5	147.3
N-C3	722.1	611.9	386.1	342.4	1824.5	92.9	206.6	112.7	167.5	17.2	37.9	18.7	567.4	164.1
N-C4	772.8	761.8	610.9	405	2390	99.7	164.3	61.6	175.7	10.6	36	20	729.2	123.9
N-C5:1	184.1	217.6	150.2	106.2	621.8	14.3	24.8		32.6	4.5	9.4	4.6	177.7	32.7
N-C5	328.5	307.4	236.8	114.1	734.8	28.8	24.5	52.5	28	3.1	8.4	4.3	197.8	27.7
2-Pentene	78.5	157.8	108.5	84.4	515.2	15.9	21.2	18.6	16.1	1.9	7.5	7.9	122.6	13.8
?	61.8	74.8	45.8	40.6	150	12.4		14.4	88.4	1.1	41.6	68	80.3	20.1
N-C6:1	193.2	172.5	139.3	86.6	656.8	13.1	30.5	9.2	28	0.3	13.1	17.2	133.5	24.8
N-C6	152.4	130.4	111.7	66.9	502.1	17.8	29.4	6.3	32.1	0.5	7.5	8	129.5	16.2
2-Hexene	86.4	59.7	64.4	53	197.5	15.2		5.7	16.4	0.4			80.1	15.6
?M-Cyclopentene	54.8	76.5	49.4	34.1	104.1	4.2		5.3					57.5	10.9
Benzene (z.T. + Thiophen)	124.5	140.4	98.9	76	507.4	28.2	132.3	29	149.6	11.2	51.9	13.4	211.7	19.9
Thiophen			7.8	16.7	138.3		47.8		43.2	2.4		15.5	40.6	
C6H10 cyc-alkene	33.1	40.9	27.1	20.8	144.5	7.5		8.6	31.6	0.3			61.7	13.7
N-C7:1	137.5	127	102.3	66.3	513.6	5.9	23.6	6.8	23.4				102.1	17
N-C7	174.2	138	127.4	72.1	533.1	7.6	34.2	5	21.5	0.5			131	16.6
Pyridin??	46.9	50.2	35.6	20	167.1	14.7	26.7	5.7	16.2	0.5			40.7	5.1
Pyrrol	58.6	67	44.5	28.4		3		6.3		0				9.8
Toluene+2-M-Thiophen	94.1	162.5	88.7	83.8	940.3	26.1	137.9	47.2	245.3	9.6	52.2		337.9	29.6
2-M-Thiophen	55	57.1	41.5			9.4				0				
3-M-Thiophen	54.5	84.1	37.6	26.6	148.9	5.8	27.9	5.9	34.7	0			62.8	9.4
I-C8	51.8	58.8	38.4	19.9	163.7	4.3				0			26.3	3.6
N-C8:1	116.4	115.6	84.7	57.7	418.4	5.6		3.6	20.1				73.2	12.6
N-C8	116.4	97.6	85.2	57.9	393.2	10.1		4.4	17.2				90.4	10.6
2-Octene	34.9	35.9	24.5	61.3	104.7	5.5							28.6	4.1
M-Pyrrol						6.7								
E-Benzene+E-Thiophen	69	79.7	57.2	42.7	294.7	14.8		4	27.4				96.3	7.8
2,5 DM Thiophen + M,P Xylene	122.7	138.3	97.4	63.1	601.9	3.7		24.4	91.4				190.5	17.3
2,4 DM Thiophen	26.3	32.2	24.4	15	106.6	2.3							25.2	4.3
2,3 DM Thiophen				10.9										
O Xylene	63.8	68.2	45.9	43.3	265.5	10.9		6.3	37.1				90.7	9.6
N-C9:1	87.4	79.1	64.3	41.1	316.6	3.2		2	11.5				44.2	8.6
N-C9	92.7	74.9	66.4	38.6	314.5	6.2		3.7	11.3				60.9	7.5
Phenol?														
C3 Benzene	21.6	25.2	15.9	11.3	114.5	3.9		1.8	9.7				34.1	2.3
C3 Benzene	40.1	54.7	31.4	32.1	256.8	5.2		2.8	15.1				139.3	14.5
N-C10:1	77.4	68.9	57.7	35	267.6	1.5		1.1	2				39	7.8
N-C10	78.2	61.9	55.7	32.2	250.7	4.7		1.4	7.9				49.9	6
N-C11:1	79.7	77.7	55.4	34.3	294.6				3.8				43	8
N-C11	67.9	56.6	48.7	31.3	244.3				9.4				47.7	4.6
Naphthalin									21.8					
N-C12:1	58.2	53.5	41.5	24.6	224.1				1.7				33.4	6.4
N-C12	62.8	60.2	44.1	26.6	233.1				4.6				47.5	6.2
2-M-Naphthalin	33	36.7	30.6	19.9	162.8				12				104	6.6
1-M-Naphthalin				12.8					27.7				73.4	
N-C13:1	63.1	55	44.9	26.7	339.8									6.1
N-C13	66.5	54.6	48.1	29.9	226.6				11				64	7.2
N-C14:1	60.1	55	43.4	23.5	221.5								29.6	7
DMN									24					
N-C14	92.7	67.3	55.3	35	361.1								99.6	9.6
N-C15:1	41.8	44.2	32.2	19.1	183								25.8	3.8
N-C15	52.7	48.8	40	30.2	203				6.8				55.6	6.2
N-C16:1	32.9	33.1	24.5	12.4	112.7								20.4	2.7
N-C16	45.9	42	33.4	21.6	152.5				1				57	4
IP 18?	18.8	21.3	14.6	7.7	74.3									0.8
N-C17:1	40.6	42.2	31.1	18.5	152.5								33.8	4
N-C17	45.9	39.4	31.8	21.8	155.1				4.1				41.1	4.6
Prist-1-ene	12.7	14.2	9.1	3.3	51.6				3.1					1.1
N-C18:1	26.7	26.9	19.6	11.2	103.8								16.8	2.1
N-C18	35.1	30.5	24.1	16	133.9				10.2				42.4	3
N-C19:1	24	24.9	17.8	10	108.1								18.1	1.9
N-C19	39.2	30.5	26.5	16.8	152.9				18.3				52.4	4.4
N-C20:1	20.7	21.1	16.4	7.5	77.1								13.2	1.2
N-C20	28.7	24	20.1	12.9	100				6.4				22.7	2.4
N-C21:1	16.7	15.2	12.6	6.3	71.4								5.2	1.3
N-C21	21.9	18.9	17	9.9	82.7				9.7				18.4	2.5
N-C22:1	14.6	13.1	10.5	5.3	65.3								8.7	1.2
N-C22	19.4	16.5	13.1	7.9	69.2				3.1				19.7	2.5
N-C23:1	11.3	11.7	9.2	3.9	48								6.9	0.8
N-C23	15.1	12.9	11.5	6	54.8				7.9				14.7	2
N-C24:1	9.4	9.1	6.5	2.6	38.4								6.8	0.7
N-C24	17.5	14.2	11.6	5.5	55.1				6				16.1	2
N-C25:1	9.9	9.7	7.3	2.4	34.9								4.2	0.4
N-C25	15.6	13.2	11.1	5	48.7				1.1				16.8	1.7
N-C26:1	9.5	9.4	6.7	1.5	28.1								4.6	0.3
N-C26	13.4	11	9.7	3.3	41				0.2				13.2	1.4
N-C27:1	7.3	6.2	3.6	1.1	19.3									0
N-C27	11.4	10.5	8.7	2.4	32								11.7	0
N-C28:1	6.9	5.6	4.3	0.7	12.3								2.8	0
N-C28	11.6	10.2	7.1	1.7	25.7								8.8	0
N-C29:1	4.6	5.1	3.7	0.8	13.9				0.1				2.6	0
N-C29	10.7	9.3	7.5	1.9	24.7								5.7	0
N-C30:1	3.6	6.7	3.1	0.5	12.6				1				0.7	0
N-C30	9.7	8.7	7.4	1.6	18.9				1.1				3.2	0
N-C31	8.5	7.5	6.5	0.7	15.1				0.3				1.5	0
N-C32	7.9	8.2	6.5	0.5	19.9								0.9	0

Table 7 continued: Open system pyrolysis 300-600°C at 60 K/min. Single compound yields (µg/g sample).
Whole rock samples (PA) and kerogen concentrates (MK).

well	G				K		J		
E nr	41715	41715	41721	41721	41725	41739	41746	41748	43253
PA2/MK	PA	MK	MK	PA	D	D	D	D	PA
fm	hea	hea	hea	hea	dr	hea	dr	dr	hea
compound									
µg/g rock									
N-C1	386.1	7435.2	1132.1	310.3	70.4	264.9	275	132.4	468.5
N-C2	210.1	2814.8	712.9	176.9	8.2	125.8	201	87.1	315.8
N-C3	173.1	1011.5	329.5	153.5	8	107	242.6	107	179.9
N-C4	123.2	1169.3	522.5	118.4	2	82.9	209.4	61.1	268
N-C5:1	22.7	260.8	109.7	25.1	8.2	16	78.9	10-15	66.5
N-C5	30.8	262.2	133.7	32.3	2	33.6	84	34.5	94.8
2-Pentene	15.6	214.5	90.2	12.8	1.3	20.8	53.3	33.1	52.2
?	18.8	180.5	53.9	17.2			19.9		23.5
N-C6:1	17.3	213.1	93.4	21.8	0.7	14.4	43.7	11.5	54.1
N-C6	14.4	152.4	78.4	16	1.3	13.4	38.3	15.6	44
2-Hexene	5.9	94	28.2	9	0.8	13.1	33.5	19.3	12.1
?M-Cyclopentene	10.3	63.3	26.3	11.2		4.3			15.1
Benzene (z.T. + Thiophen)	24.2	426.5	192.5	19.2	12.2	25.4	77.6	25.2	52.9
Thiophen	9.6	83.2	35.3	6.8	3.6	5.5		5.1	17.4
C6H10 cyc-alkene	11.8	109.2	44.5	9.8	0.3	7.1	15.3	3.6	23.6
N-C7:1	11	160.3	71.1	15	0.2	8.5	28.9	6.2	43.3
N-C7	10.3	151.6	84.3	15.1	1.3	11.3	34.9	11	43.6
Pyridin??	6.1	54.1	29.5	4.8	0.3	5	8.5	3.3	15.1
Pyrrol	4.4								
Toluene+2-M-Thiophen	33.4	963	362.1	35.8	7.1	25.4	73.9	23.7	67.7
2-M-Thiophen	10								
3-M-Thiophen	8.7	110.5	33.4	8.3	0.7	6	13	5.7	19.4
I-C8		51.9	27.1	4.8		4	10.9	6.2	11.3
N-C8:1	8.8	120.7	52.9	11.8	0.1	6.4	21.2	4.2	34.8
N-C8	5.8	109	59.2	10.9	0.7	8.8	28.8	10	34.6
2-Octene	1.9	35.5	14.8	3.9		3	7.9	3.3	12.1
M-Pyrrol		24.1							
E-Benzene+E-Thiophen	7.5	180.1	71.2	8.8	0.2	5.5	20.6	6.3	18.6
2,5 DM Thiophen + M,P Xylene	24.5	541.8	142.5	19.7	1.6	13.8	37.9	13.9	43.2
2,4 DM Thiophen	4.8	87	12.6	2.8		2.2	4.9	2.2	5.9
2,3 DM Thiophen	2.1	43.3							
O Xylene	9.8	170.2	78	9.8	1.2	6.9	22	8.7	18.2
N-C9:1	5.3	82.5	34	8.1		3.7	14.5	2.7	24.6
N-C9	4.4	78.6	40.8	7.4	0.3	5.3	18.8	5.9	24
Phenol?		152.4							
C3 Benzene	1.6	52.6	26.6	3.8		2.6	13	5	7.9
C3 Benzene	17.4	286	129.1	6.8		5.4	14.7	7.4	15.7
N-C10:1	6.8	86.3	33.4	10.3		1.7	10.9	1.2	19.35
N-C10	4.5	68.6	34.9	6.8		3.4	14.9	3.8	20.4
N-C11:1	6.7	113.4	38.4	9.5		3.5	13		22.5
N-C11	3.1	66	30.1	5.3		4.4	12.9		16.9
Naphthalin	9.3	308.3							10.3
N-C12:1	4.5	95.6	27.3	6.4		2.7	10.1		16.5
N-C12	4.1	69.8	34.9	6.7		4.4	10.9		18.2
2-M-Naphthalin	7.9	318.2	57.2	8.2			9		13.9
1-M-Naphthalin	6	187.5	48.4				10.7		10.4
N-C13:1	6	70	21	6.8		5	9.3		18.1
N-C13	5.5	109.5	37	7.1		5.6	14		21.3
N-C14:1	6.1	90.2	19.4	6.2		2.4	6.7		16.8
DMN	4.3	252.7							8.6
N-C14	9.5	179.1	57	8.6		9	15.9		27.8
N-C15:1	3	65.7	13.5	4.1		1.5	4.4		11
N-C15	4.5	120.6	40.6	5.8		3.3	10.1		16.7
N-C16:1	1.7	43.3	10.7	2.7		0.5	3.2		9
N-C16	2.9	145.8	33.2	4.7		2.6	8.2		16.7
IP 18?			9.7	1.9		0.9	2.5		4.9
N-C17:1	4	53.9	18.6	4.5		0.3	4.3		15
N-C17	3.8	83.4	25.3	5.2		3.2	8.1		14.5
Prist-1-ene	3.2	55.5		2.2					2.5
N-C18:1	2.1	25.5	9.2	2.4			1.4		7.3
N-C18	2.7	106.5	22.1	3.8		2.1	6.5		14.1
N-C19:1	2.2	57.1	7	2.4			1.4		7.3
N-C19	3.9	67.1	29.8	4.7		1.7	8.1		19.8
N-C20:1	1.4	36.5		1.7			0.8		5.2
N-C20	2.1	45.3	12.7	2.8		1.1	5		11.1
N-C21:1	1.3	28.5	6	1.5			0.3		3.3
N-C21	1.4	48.8	11.9	2.4		0.01	2.9		12.1
N-C22:1	1.3	102.3	6.3	1.5					3
N-C22	1.6	60.6	10.2	2.2		0.001	1.9		13.3
N-C23:1	0.8	25.6		0.9		0.02			2.7
N-C23	1.2	29.7	6.8	1.8		0.03	0		16
N-C24:1	0.8	30		0.8		0.05	0.5		1.4
N-C24	1.3	42.7	7.5	1.9		0.05	0		20.8
N-C25:1	0.7	23.3		0.7		0.02	0		1.3
N-C25	1.2	40	7.8	1.8		0.02	0		25.3
N-C26:1	0.6	20.7		0.6			0		2
N-C26	1	30.1	1.6	1.6		0.03	0		23.2
N-C27:1	0.5	22.7		0.2			0		
N-C27	0.7	9.5	3.4	1		0.002	0		24
N-C28:1		5.4	0.1	0.3			0		
N-C28	0.7	16	2.2	0.9		0.004	0		21.1
N-C29:1		8.6	0.1	0.2			0		1.8
N-C29	0.8	18.3	0.1	0.6		0.07	0		19.1
N-C30:1		6.3		0.2			0		0.9
N-C30	0.2	12.4	0.09	0.8		0.3	0		14.9
N-C31	0.09	10.7	0.06	0.3		0.1	0		12.6
N-C32	0.07	8.2	0.7	0.1		0.04	0		8.7

Table 7 continued: Open system pyrolysis 300-600°C at 60 K/min. Single compound yields (µg/g s
Whole rock samples (PA) and kerogen concentrates (MK).

well	E	L	A		B	C	D
E nr	42383	42384	43249	43251	43254	43256	42180
PA2/MK	D	D	PA	PA	PA	PA	D
fm	dr	dr	dr	hea	dr	hea	dr
compound							
µg/g rock							
N-C1	799.7	182.5	773.9	189.3	1500.7	306.4	1099.3
N-C2	655.8	69.4	769.4	104.6	1294.8	0	925.5
N-C3	527.5	61.9	674.9	102.1	753.5	347.9	517.7
N-C4	606.8	55.6	644.6	67.1	1090.9	273.4	736.8
N-C5:1	131.9		175.9	10.2	252.7	67	156.8
N-C5	226	20.8	198.9	17.9	454.5	81.4	279.9
2-Pentene	107.6	19.6	156.8	7.4	213.1	58.8	138.2
?	46.9	3.4	71.5	9.3	80	28.5	54
N-C6:1	137.3	5.7	164.7	9.1	259	71.2	152.8
N-C6	113.2	9	125.2	11.3	244.2	48.3	139.8
2-Hexene	64.1	14.4	88.9	7.6	130.2	25.9	87.4
?M-Cyclopentene	49	1.8	74.3	3.2	94.5	23.3	62.9
Benzene (z.T. + Thiophen)	103.8	14.1	145	22.9	194.8	55.6	137.9
Thiophen	23.6	3.1	33.3	6.5	30.4	8.9	21.1
C6H10 cyc-alkene	27.2	1.8	52.8	6.4	74.5	17.7	36.8
N-C7:1	107.1	2.8	120.3	6	188.8	52	112.2
N-C7	118.8	7.3	138.7	6.9	241.2	47.8	146.6
Pyridin??	30	1.4	34.6	3.7	72.2	16.1	32.8
Pyrrol	49.9	1.8	58.8		96.8	25.4	59.3
Toluene+2-M-Thiophen	114.2	16.2	165	28.3	182	51.2	121.1
2-M-Thiophen	58.8		149.9		160.6		101
3-M-Thiophen	36.2	2.6	67.1	4.6	85.2	21.9	55.9
I-C8	40.1	1.8	42.5	3.9	66.3	16.8	44.9
N-C8:1	92.8	1.7	120.2	5.1	166.6	44	91.2
N-C8	99.8	6.1	102.1	4.5	176.7	38.6	104.9
2-Octene	27.7	2.2	39.3	1.8	58.8	10.4	40.6
M-Pyrrol							
E-Benzene+E-Thiophen	67	3.5	112	4.5	130.4	26.3	94.1
2,5 DM Thiophen + M,P Xylene	124.7	12.2	206	11.4	250.4	47.6	174.8
2,4 DM Thiophen	32.8		69.8	2.8	79.3	11.9	56.6
2,3 DM Thiophen	19.1		54.3	1.4	58.1		44.7
O Xylene	50.5	5.3	80.2	6.6	91.8	24.7	58.1
N-C9:1	72.2	1.2	76.6	2	116.6	33.3	71
N-C9	75.4	3.4	78.7	2.7	135.5	28.9	81.8
Phenol?			63.3		77.2		
C3 Benzene	24.3	2.2	49.9	2	70.8	8.8	48.7
C3 Benzene	40.8	4.9	59	4.2	79	21.8	51.2
N-C10:1	68.6	1.4	71.6	1	110.5	28.3	67.4
N-C10	66.3	2.8	69.7	1.6	121.4	24.5	79.3
N-C11:1	74.3	1.1	74.3		114	31.1	74.1
N-C11	62.3	2.4	63.2		107.2	22.2	67.3
Naphthalin			31.3		54.4	11.4	
N-C12:1	56.4	0.7	53.4		81.1	23.1	54.8
N-C12	63.2	2.5	62.7		99.2	21.6	72
2-M-Naphthalin	28	5.7	55.6		89.6	13.1	58.5
1-M-Naphthalin		3.7				9.1	
N-C13:1	58.7		82.7		123.9	23.8	78.8
N-C13	66.9	3	67.4		113	23.8	74.5
N-C14:1	61.8		66.3		110.5	24.1	66
DMN						7.4	
N-C14	77.7	6.3	83.6		163.1	27	87.1
N-C15:1	49.4	0.4	57.1		90.8	20.7	64
N-C15	64.1	4.1	63.5		92.5	19.4	62.2
N-C16:1	41.5		31.6		52.6	14	32.9
N-C16	58.5	5	54.5		84	17.5	53.1
IP 18?	25.3	0.9	22.6		36.8	6.9	25.7
N-C17:1	51.9	1.2	49.2		70.8	17.1	42.9
N-C17	57.3	4.5	52.7		77.8	16.9	52.8
Prist-1-ene	17.2	0.4	16.3		24.8	3.2	27.9
N-C18:1	33.6		31.5		48.4	10.2	27.3
N-C18	42.4	3.6	41.5		60	12.8	36.2
N-C19:1	28.7		25.8		44.4	9.9	25.7
N-C19	43.5	3	42.8		76.3	12.7	43.7
N-C20:1	26.4		24.1		40.3	8.3	19.7
N-C20	35.4	1.5	33.5		53.7	10.4	32.1
N-C21:1	25.6		19.6		39.2	6.3	17.7
N-C21	29.2	0.9	25.9		44.3	8.6	23.3
N-C22:1	19.7		20.7		31.9	5.4	15.7
N-C22	25.7	0.3	25		40.6	6.9	27.1
N-C23:1	16.5		15.3		23.7	4.9	12.4
N-C23	22.6	0.1	20.9		35.3	5.8	20
N-C24:1	12.7	0	11.9		21.7	3.3	11
N-C24	22.7	0	20		35	5.8	20.9
N-C26:1	12.6	0	8.8		19.5	3.9	8.3
N-C25	20.1	0	16.6		30.4	6.2	16.8
N-C26:1	11.2	0	8.5		23.2	2.9	8.6
N-C26	18.4	0	14.1		26.9	4.9	14.7
N-C27:1	8.7	0	5.9		11.7	3.7	6
N-C27	16.2	0	10.2		23.7	0.03	13
N-C28:1	7.5	0	4		9.1	1.6	5.4
N-C28	14.2	0	6.4		18.1	3.3	10
N-C29:1	6.5	0	2.5		11.1	1.5	5.2
N-C29	14.6	0	7.5		16.5	3	9.9
N-C30:1	6	0	3.2		5.7	1.9	1.5
N-C30	12	0	6.4		15.1	3.3	7.6
N-C31	10.8	0	5		8.4	2	6.3
N-C32	8.9	0	4.5		8.9	2.2	6.8

Table 8: Open pyrolysis (300-600°C at 60 $Kmin^{-1}$). Aliphatic fraction boiling range compositions.

Well	E-no.		fm		Aliphatic fraction (µg HC/ g TOC)				Aliphatic fraction (% of sum aliphatics)			
					1-5	6-14	15+	sum	1-5 %	6-14 %	15+ %	sum
I	41690	Pa	dr	1	52976.6	24013.5	8886.7	85876.8	61.7	28.0	10.3	100
	41692	Pa	dr	1	42818.8	17103.2	6820.9	66742.9	64.2	25.6	10.2	100
L	42384	Pa	dr	1	29482.0	5453.2	1863.3	36798.6	80.1	14.8	5.1	100
A	43249	Pa	dr	1	40922.7	21631.6	9777.8	72332.1	56.6	29.9	13.5	100
B	43254	Pa	dr	1	46724.4	24519.3	11363.0	82606.7	56.6	29.7	13.8	100
D	42180	Pa	dr	1	53160.0	24667.6	11093.8	88921.4	59.8	27.7	12.5	100
K	41725	Pa	dr	2	3416.4	184.3	0.0	3600.7	94.9	5.1	0.0	100
J	41746	Pa	dr	2	28113.0	9828.0	1710.1	39651.1	70.9	24.8	4.3	100
	41748	Pa	dr	2	15378.4	3408.8	0.0	18787.2	81.9	18.1	0.0	100
E	42383	Pa	dr	2	45466.2	24595.4	14116.9	84178.5	54.0	29.2	16.8	100
I	41694	Pa	hea	3	40927.2	19277.5	7201.9	67406.6	60.7	28.6	10.7	100
H	41695	Pa	hea?	3	45525.6	20550.1	6247.2	72322.9	62.9	28.4	8.6	100
	41695	MK	hea?	3	40894.0	17670.5	6768.9	65333.4	62.6	27.0	10.4	100
	41697	Pa	hea	3	21067.3	4841.3	0.0	25908.7	81.3	18.7	0.0	100
F	41711	MK	hea	3	18437.7	5659.0	2399.6	26496.2	69.6	21.4	9.1	100
	41711	Pa	hea	3	25571.9	6859.5	1943.1	34374.6	74.4	20.0	5.7	100
G	41715	Pa	hea	3	17515.5	2584.7	979.2	21079.4	83.1	12.3	4.6	100
	41715	MK	hea	3	25264.9	4230.1	2874.5	32369.5	78.1	13.1	8.9	100
	41721	MK	hea	3	9839.6	2972.7	965.1	13777.4	71.4	21.6	7.0	100
	41721	Pa	hea	3	31154.1	7424.8	2676.7	41255.6	75.5	18.0	6.5	100
A	43251	Pa	hea	3	16247.6	2068.4	0.0	18316.0	88.7	11.3	0.0	100
C	43256	Pa	hea	3	25503.4	14982.0	6009.7	46495.1	54.9	32.2	12.9	100
K	41739	Pa	hea	4	25232.6	5193.8	695.6	31122.0	81.1	16.7	2.2	100
J	43253	Pa	hea	4	26795.2	9805.3	6884.8	43485.4	61.6	22.5	15.8	100
P	41699	MK	vik	5	32086.2	1829.2	0.0	33915.4	94.6	5.4	0.0	100
	41701	Pa	vik	5	14604.1	942.9	0.0	15547.0	93.9	6.1	0.0	100
	41701	MK	vik	5	5277.7	477.4	164.6	5919.7	89.2	8.1	2.8	100
	41703	Pa	vik	5	6419.8	52.5	0.0	6472.2	99.2	0.8	0.0	100
	41703	MK	vik	5	2040.8	64.2	0.0	2105.0	97.0	3.0	0.0	100
	41706	MK	vik	5	666.6	68.5	0.0	735.1	90.7	9.3	0.0	100

Legend: 1= Draupne immature (R_o=0.3%-0.6%), 2= Draupne mature (R_o=>0.6%), 3= Heather immature (R_o=0.3%-0.6%), 4= Heather mature (R_o=>0.6%), 5= Viking Group.

Table 9: Closed pyrolysis (0.7°C/min - 520°C), total yields

	TOC	C1-5	C6-14	C15+	sum
42384PA-S1	1	33.38	3.49	0	36.87
42383PA-S1	6.5	133.48	36.64	8.77	178.89
41692MK-S1	41.6	62.47	24.52	4.75	91.74
41695MK-S1	38.3	80.63	17.7	5.26	103.59
41701MK-S1	45.2	11.96	1.43	0.67	14.06
41703MK-S1	32.1	5.35	0.82	0.47	6.64
41706MK-S1	36.8	11.45	1.98	1.18	14.61
41711MK-S1	23.9	124.11	26.97	6.06	157.14
41715MK-S1	47.6	20.28	3.05	0.95	24.28

Table 10: Bulk reaction kinetic parameters. Samples of different maturities, Heather and Draupne Formation

			Heather Formation				marine kerogen	Viking Group		Draupne Formation				
	well		G	G	G	G	I	P	P	D	D	I	B	L
	depth	(m)	2138.75	2138.75	2138.75	2553.95	3583.55	4449.33	5253.85	3115	3115	3573.75	2764.7	4478
	sample type		whole rock	kerogen konc.	k.konc. extracted	whole rock	whole rock	whole rock	whole rock	whole rock	whole rock extracte	whole rock	kerogen extracted	whole rock
	E-number		41716	41716MK	41716MK E1	41723	41694	41700	41705	42180	42180E1	41690	43254	42384
	freq.factor A	1/min	1.91E+18	1.21E+17	1.68E+17	7.63E+16	5.21E+16	2.61E+18	1.86E+18	6.75E+16	5.90E+16	1.83E+16	2.88E+16	5.49E+18
activation energy		1/sec	3.18333E+16	2.01667E+15	2.8E+15	1.27167E+15	8.68333E+14	4.35E+16	3.1E+16	1.125E+15	9.83333E+14	3.05E+14	4.8E+14	9.15E+16
kcal/mol	kJ/mol		Anfangspotentiale (mg/g)											
40	167.5											0.22		
41	171.7		0.004	0.209			0.32			0.15		0.31		
42	175.8			0.367			0.05			0.05		0.34		
43	180.0		0.014	0.628			0.3			0.19		0.31		
44	184.2		0.050	0.628			0.1	0.01		0.16		0.34		
45	188.4		0.068	0.719			0.23	0.02		0.19		0.29		0.01
46	192.6		0.077	0.605	0.19	0.03	0.11	0.02		0.22	0.11	0.38	0.46	0.01
47	196.8		0.074	0.643			0.2	0.02		0.17	0.01	0.2		0.01
48	201.0		0.071	0.585	0.10	0.01	0.1	0.01		0.34		0.62	0.64	0.01
49	205.2		0.074	0.619	0.11	0.01	0.22	0.02		0.08	0.15			0.01
50	209.3		0.056	0.624	0.14	0.02	0.11	0.02		0.52		0.85	1.61	0.02
51	213.5		0.071	0.719	0.18	0.02	0.21	0.01		0.15		0.39		0.01
52	217.7		0.069	0.871	0.24	0.03	0.33	0.02					0.77	0.04
53	221.9		0.051	0.928	0.28	0.02		0.01		0.62	0.81		4.18	0.01
54	226.1		0.091	1.537	0.55	0.04		0.02		4.43	5.22		11.57	0.01
55	230.3		0.077	1.823	0.79	0.04		0.02		5.83	6.8	16.03	87.11	0.03
56	234.5		0.022	3.061	1.26		8.52	0.02		11.11	11.35	13.22	30.70	0.01
57	238.6		0.208	5.679	2.86	1.26	7.55	0.02		8.74	6.85	4.82	20.86	0.03
58	242.8		0.109	5.774	3.15	0.58	3.26	0.02		5.92	4.99	3.2	11.05	0.01
59	247.0		0.214	5.674	3.00	0.57	2.79	0.02	0.01	3.39	2.56	0.69	3.80	0.01
60	251.2		1.058	3.546	3.53	0.14		0.04		1.59	0.9	0.65	2.29	0.02
61	255.4		1.142	2.561	0.85	0.26	0.5	0.02	0.01	0.62	0.49		1.04	0.01
62	259.6		1.254	1.214	0.64			0.08	0.01	0.66	0.21			0.02
63	263.8		0.856	0.295	0.33	0.07		0.06	0.02		0.03		0.30	
64	268.0		0.797	0.190	0.28	0.05		0.18	0.02	0.17	0.06		0.01	0.06
65	272.1		0.259	0.148			0.05	0.2	0.03	0.03		0.16	0.14	0.08
66	276.3		0.388	0.081	0.07	0.02		0.41	0.07				0.15	0.2
67	280.5		0.281	0.176	0.17	0.01		0.41	0.09	0.08	0.01			0.18
68	284.7			0.052				0.2	0.09	0.01			0.02	0.12
69	288.9		0.040	0.167				0.17	0.07				0.10	0.06
70	293.1		0.162		0.21	0.01		0.02		0.03				0.09
71	297.3			0.167				0.06	0.06					0.03
72	301.4			0.052				0.07	0.04					0.05
73	305.6		0.080					0.02	0.02					0.03
74	309.8							0.06	0.07					
75	314.0		0.031	0.105				0.04						0.04
76	318.2		0.022					0.12	0.05					0.02
77	322.4		0.035						0.05					
78	326.6							0.04						0.03
79	330.8							0.09	0.06					0.01
80	334.9		0.042											
81	339.1								0.03					
82	343.3								0.02					
83	347.5													
84	351.7								0.02					
85	355.9								0.02					
86	360.1													
87	364.3													
88	368.4								0.01					

Table 14: MSSV pyrolysis hydrocarbon boiling ranges totals (µg/g sample)

E 41716MK EC
well G
2138.75m

heating rate																										
0.1°C / min	temperature	300	310	320	330	340	350	360	370	380	390	400	405	410	420	425	430	440	445	450	460	470	480	490	515	540
	C1	3	29	58	113	181	279	417	628	888	1227	1718	1921	2262	3164	3578	4251	5004	5718	6382	7841	9144	11551	12716	17569	21568
	C2-4total	172	192	240	323	411	611	806	1211	1607	2083	2579	2790	3025	3692	3772	4101	3962	3998	3954	3634	2926	2550	1573	512	342
	C5	175	199	206	239	241	305	366	432	567	481	529	510	478	481	407	381	247	204	149	98	54	39	45	76	59
	C1-5total	350	420	504	675	833	1195	1589	2271	3062	3791	4826	5221	5765	7337	7757	8733	9213	9920	10485	11573	12124	14140	14334	18157	21969
	C6-14total	595	715	894	1287	1548	2282	2796	3683	4470	4118	3981	3986	3846	4057	3699	3719	3039	3220	3035	3035	2611	2490	2012	1910	1462
	C15-25total	73	112	152	286	395	589	748	871	903	623	403	407	416	456	412	363	202	302	297	304	262	252	96	115	82
	C1+	1018	1247	1550	2248	2776	4066	5133	6825	8435	8532	9210	9614	10027	11850	11868	12815	12454	13442	13817	14912	14997	16882	16442	20182	23513

0.7°C / min	temperature	300	325	350	370	380	390	400	410	415	420	425	430	435	440	445	450	455	460	470	480	490	510	530	560
	C1	8	27	88	227	334	469	681	918	1091	1182	1350	1582	1804	2169	2444	2731	3131	3522	4699	5656	6450	9168	11303	16742
	C2-4total	183	211	318	505	746	956	1302	1636	1956	1988	2135	2412	2547	2924	3051	3252	3453	3438	3872	3912	3428	2420	1406	668
	C5	209	257	285	388	425	541	569	602	647	571	537	569	544	570	528	514	526	407	322	203	97	40	36	49
	C1-5total	400	495	691	1120	1505	1966	2552	3156	3694	3741	4022	4563	4895	5683	6023	6497	7110	7367	8893	9771	9975	11628	12745	17459
	C6-14total	689	882	1264	2097	2915	3520	3899	4495	5314	4539	4366	4336	4438	4719	4394	4225	4637	3519	3725	3403	2865	2520	2207	2119
	C15-25total	140	185	275	542	788	670	901	883	963	721	605	501	518	579	480	414	453	217	293	258	156	153	98	67
	C1+	1229	1562	2230	3759	5208	6156	7352	8534	9971	9001	8993	9400	9851	10981	10897	11136	12200	11103	12911	13432	12996	14301	15050	19645

5.0°C / min	temperature	350	370	390	400	410	420	425	430	435	440	445	450	460	465	470	475	480	490	500	510	530	550	570	600	620
	C1	6	1	2	145	260	346	491	601	642	752	854	1050	1348	1427	1858	2060	2259	2992	3828	4541	6231	8377	10915	15273	20425
	C2-4total	259	420	669	805	1076	1227	1425	1610	1820	2012	2170	2222	2533	2304	2928	3062	3081	3474	3567	3787	3324	2644	2013	1155	690
	C5	243	309	339	399	475	453	528	579	578	608	619	607	605	483	610	599	571	505	457	411	186	109	94	93	29
	C1-5total	508	730	1010	1349	1811	2026	2444	2790	3040	3372	3643	3879	4486	4214	5396	5721	5911	6971	7852	8739	9741	11130	13022	16521	21144
	C6-14total	1239	1782	2237	2469	3772	4143	4641	5306	4414	5223	5350	5317	5364	3793	5473	5450	5153	4910	4186	4525	3793	3619	3166	3005	2370
	C15-25total	430	576	671	526	1069	1082	1323	1473	778	1045	1025	947	752	294	603	576	638	541	256	382	293	297	138	190	108
	C1+	2177	3088	3918	4344	6652	7251	8408	9569	8232	9640	10018	10143	10602	8301	11472	11747	11702	12422	12294	13646	13827	15046	16326	19716	23622

Table 15: MSSV pyrolysis hydrocarbon boiling ranges resolved (µg/g sample)	E 41716MK EC well G 2138.75m

heating rate																										
0.1	temperature	300	310	320	330	340	350	360	370	380	390	400	405	410	420	425	430	440	445	450	460	470	480	490	515	540
	C1-5	348	419	503	673	789	1192	1560	2270	3060	3789	4825	5219	5762	7335	7755	8732	9212	9919	10485	11572	12123	14137	14333	18156	21966
	C6-14	335	414	580	818	1093	1672	2141	2928	3671	3508	3474	3503	3398	3577	3310	3341	2746	2911	2720	2719	2336	2236	1839	1688	1234
	C15-25	20	34	68	96	175	252	365	421	484	350	214	234	253	251	250	214	132	187	183	193	162	150	59	60	26
	hump	315	380	399	661	719	950	1057	1206	1220	885	697	658	614	687	553	528	364	425	429	428	376	359	211	278	287
	hump %	30.94	30.47	25.74	29.40	25.90	23.36	20.79	17.67	14.46	10.37	7.57	6.84	6.12	5.80	4.66	4.12	2.92	3.16	3.10	2.87	2.51	2.13	1.28	1.38	1.22
	GOR	0.98	0.94	0.78	0.74	0.62	0.62	0.62	0.68	0.74	0.98	1.31	1.40	1.58	1.92	2.18	2.46	3.20	3.20	3.61	3.97	4.85	5.92	7.55	10.39	17.43

0.7	temperature	300	325	350	370	380	390	400	410	415	420	425	430	435	440	445	450	455	460	470	480	490	510	530	560
	C1-5	399	495	688	1117	1504	1964	2551	3154	3691	3739	4019	4550	4894	5680	6021	6494	7099	7364	8890	9768	9974	11627	12744	17457
	C6-14	320	533	848	1567	2269	2822	3200	3791	4397	3882	3765	3761	3901	4156	3948	3737	4078	3228	3406	3070	2626	2275	1982	1883
	C15-25	30	61	121	255	401	349	486	517	522	424	375	286	308	336	306	244	282	140	181	142	90	88	76	44
	hump	480	473	573	820	1034	1021	1115	1072	1361	956	834	803	748	809	622	661	741	371	434	452	306	311	248	261
	hump %	39.06	30.28	25.70	21.81	19.85	16.59	15.17	12.56	13.65	10.62	9.27	8.54	7.59	7.37	5.71	5.94	6.07	3.34	3.36	3.37	2.35	2.17	1.65	1.33
	GOR	1.14	0.83	0.71	0.61	0.56	0.62	0.69	0.73	0.75	0.87	0.97	1.12	1.16	1.26	1.42	1.63	1.63	2.19	2.48	3.04	3.67	4.92	6.19	9.06

5.0	temperature	350	370	390	400	410	420	425	430	435	440	445	450	460	465	470	475	480	490	500	510	530	550	570	600	620
	C1-5	506	729	1006	1346	1808	1884	2351	2787	3038	3368	3641	3876	4464	4164	5480	5719	5909	6969	7849	8738	9738	11127	13019	16518	21141
	C6-14	674	1101	1538	1800	2832	3132	3659	4229	3617	4307	4452	4499	4587	3287	4717	4796	4488	4354	3727	4034	3400	3167	2793	2649	2152
	C15-25	74	147	250	204	459	453	622	665	342	496	497	455	348	133	305	341	357	298	137	221	160	132	57	75	11
	hump	923	1111	1124	994	1553	1782	1776	1888	1235	1469	1428	1311	1183	717	970	891	948	801	581	653	529	620	457	474	318
	hump %	42.40	35.98	28.69	22.88	23.35	24.58	21.12	19.73	15.00	15.24	14.25	12.93	11.16	8.64	8.46	7.58	8.10	6.45	4.73	4.79	3.83	4.12	2.80	2.40	1.35
	GOR	0.68	0.58	0.56	0.67	0.55	0.53	0.55	0.57	0.77	0.70	0.74	0.78	0.91	1.22	1.09	1.11	1.22	1.50	2.03	2.05	2.74	3.37	4.57	6.06	9.77

Table 16: MSSV pyrolysis	E43254
hydrocarbon boiling ranges	well B
totals (µg/g sample)	2764.7m

heating rate (K/min)

0.1	temperature	300	310	320	333	340	350	360	370	380	390	395	401	405	410	415	420	425	430	440	445	450	460	470	480	490	510	540
	C1	46	82	137	271	365	586	885	1345	2161	3284	3992	4871	5701	6709	7201	8428	9660	11330	12895	15863	18431	21442	26604	31806	34374	50756	73494
	C2-4	98	232	359	656	935	1583	2821	4429	7880	12901	14818	18833	23666	28481	29485	34094	41561	47978	43733	74211	89882	100280	115374	101304	90098	63734	29970
	C5	162	166	247	393	487	768	1105	1835	3041	4255	4535	5960	7387	8921	9362	10576	12771	14383	15384	18664	19652	15202	8650	2798	800	284	92
	C1-5	306	480	743	1320	1787	2937	4811	7609	13082	20440	23345	29664	36754	44111	46048	53098	63992	73691	72012	108738	127965	136924	150628	135908	125272	114774	103556
	C6-14	1135	1891	3339	5398	7332	11724	18032	25637	39748	54745	58686	67766	77716	88384	89356	90868	95687	99378	83918	85683	78497	56364	45074	36584	29962	23546	16080
	C15+	335	1131	2736	5688	6994	14486	24118	30286	47294	58760	44804	50513	54121	49769	41537	31660	26229	22036	11880	11623	9488	6682	5298	4742	3106	2038	854
	C6+	1470	3022	6075	11086	14326	26210	42150	55923	87042	113505	103490	118279	131837	138153	130893	122528	121916	121414	95798	97306	87985	63046	50372	41326	33068	25584	16934
	C1+	1776	3502	6818	12406	16113	29147	46961	63532	100124	133945	126835	147943	168591	182264	176941	175626	185908	195105	167810	206044	215950	199970	201000	177234	158340	140358	120490

0.7	temperature	302	330	360	375	390	400	410	420	425	430	440	445	450	455	460	465	470	480	490	495	500	520	540	560	580	600	620
	C1	1	82	306	619	1000	1543	2212	3206	3964	4863	6461	7425	8726	9721	11110	12212	13554	18180	22940	24429	24768	34577	44980	57073	73480	85966	100706
	C2-4	117	229	840	1856	3271	5537	8710	12439	15255	18507	25027	28639	35658	40102	46445	52006	57207	78419	101803	95787	103391	87047	66600	43857	27532	15591	2850
	C5	101	192	470	929	1411	2294	2944	4586	4925	6361	7607	9180	11379	12985	14293	14407	15167	16287	12346	9190	6879	996	394	199	111	79	44
	C1-5	219	503	1616	3404	5682	9374	13866	20231	24144	29731	39095	45244	55763	62808	71848	78625	85928	112886	137089	129406	135038	122620	111974	101129	101123	101636	103600
	C6-14	800	2178	6805	13353	20371	31831	42773	55381	64055	74571	82319	90507	99545	97640	96505	86448	82596	69034	57454	48867	44457	34232	27899	18894	13103	10415	4074
	C15+	0	378	5493	15202	22953	40506	51533	56039	65100	64713	48422	40965	34755	29349	22900	14265	13950	10859	9606	7592	6250	5527	4336	2682	2051	1833	1252
	C6+	800	2556	12298	28555	43324	72337	94306	111420	129155	139284	130741	131472	134300	126989	119405	100713	96546	79893	67060	56459	50707	39759	32235	21576	15154	12248	5326
	C1+	1019	3059	13914	31959	49006	81711	108172	131651	153299	169015	169836	176716	190063	189797	191253	179338	182474	192779	204149	185865	185745	162379	144209	122705	116277	113884	108926

5.0	temperature	300	350	370	390	400	410	420	425	430	435	440	445	450	455	460	470	475	480	490	500	510	530	550	570	610	630
	C1	1	32	113	349	546	813	1177	1376	1659	2101	2440	2729	3419	3894	4489	6381	7095	7942	10081	11455	14740	22325	30831	40443	59137	74145
	C2-4	125	267	493	1141	1865	2855	4191	5096	6113	7921	9165	10383	12917	14855	17534	24239	26389	30475	39350	44684	55419	74450	79029	68310	34028	24171
	C5	0.9	168	247	457	788	1108	1509	1856	2133	2731	3103	3508	4164	4770	5555	7196	8669	9852	11132	11686	11875	7837	1586	725	230	181
	C1-5	126.9	465	853	1947	3199	4776	6877	8328	9905	12753	14708	16620	20500	23519	27578	37816	42153	48269	60563	67825	82034	104612	111446	109478	93395	98497
	C6-14	1173	2082	3788	7542	12600	18788	24293	29427	31975	40730	44393	48083	54007	60757	66897	76090	73912	77233	74224	71385	61594	51676	40253	33441	19321	16524
	C15+	1020	1298	2426	4929	11709	19647	26046	32244	31663	43504	46022	47602	45320	52356	49288	38000	28865	26686	19274	12454	11045	11069	8382	6821	2700	3526
	C6+	2193	3380	6214	12471	24309	38435	50339	61671	63638	84234	90415	95685	99327	113113	116185	114090	102777	103919	93498	83839	72639	62745	48635	40262	22021	20050
	C1+	2319.9	3845	7067	14418	27508	43211	57216	69999	73543	96987	105123	112305	119827	136632	143763	151906	144930	152188	154061	151664	154673	167357	160081	149740	115416	118547

Table 17: MSSV pyrolysis	E43254
hydrocarbon boiling ranges	well B
resolved & hump (µg/g sample)	2764.7m

heating rate (K/min)

0.1	temperature	300	310	320	333	340	350	360	370	380	390	395	401	405	410	415	420	425	430	440	445	450	460	470	480	490	510	540
	C1-5	305	476	739	1314	1781	2929	4801	7594	13065	20423	23330	29649	36739	44096	46027	53098	63992	73670	72001	108725	127951	136911	150613	135895	95264	114767	103554
	C6-14	594	946	1859	3342	4761	7833	12408	18274	29514	42591	45949	55575	65032	74736	77117	79596	85854	89810	77895	80072	74195	53687	42949	34539	28299	11053	14994
	C15+	66	163	535	1054	1599	2418	3975	5779	9124	12589	12841	14525	15796	16551	15954	14229	12438	10860	7458	6418	5446	3935	2999	2578	1895	1015	446
	hump	811	1917	3685	6696	7972	15967	25777	31885	48421	58342	48811	48194	51024	46881	37843	28703	23624	20765	10456	10829	8358	5437	4439	4222	32882	13523	1496
	hump %	45.66	54.74	54.05	53.97	49.48	54.78	54.89	50.19	48.36	43.56	37.28	32.58	30.26	25.72	21.39	16.34	12.71	10.64	6.23	5.26	3.87	2.72	2.21	2.38	20.77	9.63	1.24
	Sec gas c6+res																			10721.9	9926	14720.3	30133.6	38305.4	44487.1	49333.2	62021.4	59661
	Sec gas c6+hump											6670.3	7102.2	5121.2	8021.3	14352.1	20735.4	24290.7	26306.7	33516	33256.3	34986.7	37030.7	37730.7	37881.2	38915.7	31366.3	39781.7
	prim gas	305	476	739	1314	1781	2929	4801	7594	13065	20423	16659.7	22546.8	31617.8	36074.7	31674.9	32362.6	39701.3	47363.3	27763.1	65542.7	78244	69746.7	74576.9	53526.7	7115.1	21379.3	4111.3
	GOR	0.46	0.43	0.31	0.30	0.28	0.29	0.29	0.32	0.34	0.37	0.40	0.42	0.45	0.48	0.49	0.57	0.65	0.73	0.84	1.26	1.61	2.38	3.28	3.66	3.16	9.51	6.71

0.7	temperature	302	330	360	375	390	400	410	420	425	430	440	445	450	455	460	465	470	480	490	495	500	520	540	560	580	600	620
	C1-5	212	490	1576	3325	5856	9168	13846	20214	24128	29712	38298	45218	55763	62808	71848	78611	85917	112876	137083	129249		122611	111968	101125	101111	101636	103492
	C6-14	354	1209	4214	8682	13842	22074	31165	42419	50381	60308	67356	78062	87239	87067	87830	79581	76192	64770	54765	46851		32700	26334	17829	11933	9063	3373
	C15+	61	263	1185	2627	4015	6575	9180	12125	14006	16202	15486	15189	14106	12872	10904	7614	7288	5969	5812	4950		3693	2455	1333	979	814	400
	hump	392	1097	6939	17325	25293	43894	53981	56893	64784	62793	48696	38247	32955	27050	20671	13532	13077	9164	6489	4815		3375	3452	2418	2254	2371	1661
	hump %	38.47	35.86	49.87	54.21	51.61	53.72	49.90	43.22	42.26	37.15	28.67	21.64	17.34	14.25	10.81	7.55	7.17	4.75	3.18	2.59		2.08	2.39	1.97	1.94	2.08	1.52
	Sec gas c6+res														984.2	1827.7	9905	12505.5	21424.2	28537.6	34680.8		45466.4	50789.2	57528.1	61903.1	64027.6	68300.4
	Sec gas c6+hump										1395.8	11808.3	18582.9	22269.1	26402.6	30867.9	35875	36191.4	38929.8	40799.5	42077		42981.4	42925.4	43647.8	43768.2	43677.9	44250.5
	prim gas	212	490	1576	3325	5856	9168	13846	20214	24128	28316.2	26489.7	26635.1	33493.9	35421.2	39152.4	32831	37220.1	52522	67745.9	52491.2		34163.2	18253.4	-50.9	-4560.3	-6069.5	-9058.9
	GOR	0.51	0.33	0.29	0.29	0.33	0.32	0.34	0.37	0.37	0.39	0.46	0.48	0.55	0.63	0.73	0.90	1.03	1.60	2.26	2.50		3.37	3.89	5.28	7.83	10.29	27.43

5.0	temperature	300	350	370	390	400	410	420	425	430	435	440	445	450	455	460	470	475	480	490	500	510	530	550	570	610	630
	C1-5	233	462	850	1942	3199	4765	6862	8317	9890	12736	14692	16604	20411	23499	27560	37787	41794	47859	60057	67815	82024	104309	111441	109470	93383	98482
	C6-14	416	1075	2376	5063	8553	12659	17113	20568	22788	29761	32749	35816	41175	47322	53198	64062	63838	66709	65662	65599	57057	48642	38733	32001	18012	15109
	C15+	129	223	741	1272	2394	3631	5004	6268	6657	8742	9725	10805	11196	12624	13496	13500	11378	10981	8684	7011	6265	6879	6030	4437	2022	2071
	hump	1541.9	2085	3100	6141	13362	22156	28237	34846	34208	45748	47957	49080	47045	53187	49509	37157	27920	26639	19658	11239	9327	7527	3877	3832	1999	2885
	hump %	66.46	54.23	43.87	42.59	48.57	51.27	49.35	49.78	46.51	47.17	45.62	43.70	39.26	38.93	34.44	24.36	19.26	17.50	12.76	7.41	6.03	4.50	2.42	2.56	1.73	2.43
	sec gas C6+res																			2340.6	3556	10057.6	15518.3	23048.9	28876.4	40359.2	42357
	sec gas C6+hump															2573.2	11227.3	17924.2	18856.6	23810.5	29356.6	30695	32160.1	34506.5	34540.1	35826	35207.9
	prim gas	233	462	850	1942	3199	4765	6862	8317	9890	12736	14692	16604	20411		24986.8	26559.7	23869.8	29002.4	33905.7	34902.4	41271.4	56630.6	53885.6	46053.5	17197.8	20917.1
	GOR	0.43	0.36	0.27	0.31	0.29	0.29	0.31	0.31	0.34	0.33	0.35	0.36	0.39	0.39	0.41	0.49	0.56	0.62	0.81	0.93	1.30	1.88	2.49	3.00	4.66	5.73

Table 18 : Heather formation well G, 2138m. 0.1°C /min heating rate.

temperature (°C)	300	310	320	330	340	350	360	370	380	390	400	405
C1	41	58	82	146	170	311	429	653	908	1227	1720	1943
N-C2	25	34	49	75	112	166	251	379	589	787	1009	1199
N-C3	27	39	55	91	133	200	287	422	556	712	875	891
i-C4	63	10	13	17	25	40	61	95	122	168	210	198
N-C4	12	66	70	89	94	142	170	244	320	352	440	437
Neopentane					11	21	27	23	23	13	15	16
i-C5	78	92	98	110	111	134	147	172	195	183	193	186
N-C5	30	30	28	31	34	55	71	105	153	192	218	222
2MC5	7	11	13	19	17	34	32	41	61	54	53	51
N-C6	7	9	11	16	21	33	49	72	103	126	137	137
McycC5	2	3	4	5	6	9	11	16	20	20	22	15
Benzene	33	30	34	39	44	55	67	93	121	143	210	225
Thiophen		6	8	10	12	16	20	25	30	32	39	42
cycC6	7	9	10	13	14	15	18	22	25	23	22	20
2MC6	3	2	3	4	5	8	10	14	17	14	14	14
DMcycC5	3	4	4	6	6	9	10	13	15	12	11	10
N-C7	4	6	8	13	19	31	45	75	100	109	112	106
McycC6	3	4	5	7	8	11	13	18	20	18	16	14
Toluene	20	26	39	60	92	138	196	272	354	455	581	634
3 M-Thiophen	2	3	4	6	8	12	14	20	23	21	21	20
N-C8	3	4	6	9	13	22	32	50	68	77	76	70
TMcycC6	4	4	2	3	3	5	6	8	9	9	7	6
E-Benzene	4	6	10	15	24	37	51	71	89	93	87	84
M,P-Xylene	19	22	19	29	56	76	110	150	200	231	259	268
2,4 DM Thiophen			6	8	7	11	14	19	20	17	12	15
2,3 DM Thiophen	1	2	2	3	5	8	10	13	15	12	8	7
O-Xylene	6	9	13	18	27	37	50	70	94	115	134	139
N-C9	2	2	3	5	8	13	21	33	47	54	49	43
Propyl-Benzene	2	2	3	4	6	10	14	20	26	28	24	22
C3 Benzene	4	3	5	6	11	17	23	32	41	41	35	33
C3 Benzene	3	3	5	7	10	15	20	27	31	29	22	22
C3 Benzene	3	3	5	5	8	10	13	17	19	20	19	20
Phenol	4	8	11	17	15	33	47	69	92	83	87	87
C3 Benzene	5	7	12	15	22	29	38	50	60	64	60	60
N-C10	1	2	3	4	6	10	16	25	35	40	33	28
C3 Benzene	3	5	7	11	16	22	26	36	41	40	35	33
Cresol			2	5	7	17	24	37	52	39	34	32
Cresol	1	1	1	2	9	28	38	50	79	57	55	50
N-C11	1	2	3	5	8	12	18	28	37	38	28	21
C2-Phenol						1	2	5	9	3	3	3
C2-Phenol	1	1	1	2	3	9	12	10	15	14	5	4
Naphthalin	8	10	11	16	22	31	39	50	62	71	84	90
N-C12	1	2	3	4	7	10	15	24	32	30	21	16
2M-Naphthalin	7	10	17	25	38	54	67	83	99	97	88	91
1M- Naphthalin	5	8	13	19	28	39	49	60	73	76	72	75
N-C13	1	2	2	4	6	10	15	22	30	26	14	10
Biphenyl	4	3	3	4	6	10	13	16	23	24	29	33
E-Naphthalin	1	2	3	5	8	12	16	18	21	15	9	9
DMN	3	3	5	8	9	12	17	19	25	20	11	12
DMN	2	5	10	13	21	30	38	43	51	45	34	35
DMN	4	5	9	14	19	29	37	40	49	42	29	29
N-C14	1	3	3	4	6	10	14	22	28	25	14	12
DMN	2	4	7	10	15	21	27	30	35	30	23	23
DMN	1	1	3	4	7	10	13	14	16	13	9	8
M-Biphenyl	1	2	3	4	7	10	13	15	20	18	14	15
C3-Naphthalin	1	2	3	5	5	9	15	18	25	18	6	4
N-C15		1	2	3	6	9	11	11	13	10	6	6
C3-Naphthalin		1	1	2	5	8	10	12	15	11	6	7
C3-Naphthalin		1	3	5	8	13	16	18	21	14	8	7
C3-Naphthalin	1	3	4	7	13	19	25	29	32	21	11	10
C3-Naphthalin	1	1	2	2	4	6	10	13	18	13	5	4
N-C16				1	4	5	8	9	11	10	8	8
N-C17			1	1	3	4	7	9	11	7	2	2
Pristene			1	2	3	5	8	9	8	4	2	2
C4 Naphthalin				3	5	7	10	12	13	16	14	16
Phenanthrene					2	3	4	5	5	5	3	4
N-C18				1	2	3	6	8	9	5	2	2
MP					1	2	4	5	4	4	3	3
MP					2	2	4	5	5	4	3	3
MP					2	2	4	4	4	4	3	3
MP					3	4	7	7	6	6	6	6
N-C19			1		1	2	5	6	6	3	1	
N-C20						2	4	5	5	1		
N-C21							2	2	2			
N-C22							1	1	1			
N-C23												
N-C24												
sum C1+(µg/g sample)	478	597	767	1096	1474	2255	3047	4238	5612	6453	7530	7972

Table 18 continued (0.1 K/min)

temperature (°C)	410	420	425	430	440	445	450	460	470	480	490	515	540
C1	2290	3197	3613	4291	5038	5752	6425	7879	9208	11610	12766	17630	21774
N-C2	1272	1652	1754	1957	2142	2244	2252	2287	2063	1934	1310	371	215
N-C3	1018	1220	1223	1319	1147	1122	1143	940	616	436	151	35	38
i-C4	231	259	257	271	211	202	194	149	87	66	25		
N-C4	444	494	477	486	398	359	304	198	84	25	31	26	17
Neopentane	10	14	9		7			5					
i-C5	173	165	97	93	59	50	35	17	14	8	8	11	7
N-C5	229	232	212	203	123	101	70	21	11	10	13	20	13
2MC5	47	45	32	29	8	12	9	12	10	5	1	10	7
N-C6	133	124	101	85	36	22	12	3	4	2	1	2	5
McycC5	13	10	7	6	3	2	1	1	1				
Benzene	224	264	274	298	348	375	382	461	536	660	781	1061	934
Thiophen	38	42	39	39	41	34	33						
cycC6	17	14	10	9	5	5	4	5	6	6	6	6	7
2MC6	13	10	8	6	3	7	6	6	6	8	6	4	4
DMcycC5	7	6	5	2	2	2	2	2	1	1	2	3	2
N-C7	98	77	57	44	14	6	3	5	6	2	2	7	4
McycC6	10	7	4	2	1	1	1					1	1
Toluene	677	804	802	861	856	879	872	892	801	760	528	232	98
3 M-Thiophen	19	21	18	19	19	20	15	13	9	8		6	3
N-C8	60	42	28	19	5	4							
TMcycC6	6	3	2	2	2	2	1	1	2	1		2	
E-Benzene	84	82	71	68	43	37	29	21	12	9	5	3	1
M,P-Xylene	286	325	326	349	307	314	295	254	176	133	60	14	2
2,4DM Thiophen	13	12	11	11	8	9	8	8	1	1	1	1	
2,3 DM Thiophen	7	7	6	6	4	3	3	2					
O-Xylene	140	144	133	130	91	78	62	36	16	10	6	1	3
N-C9	35	21	13	9	2	1							
Propyl-Benzene	20	15	11	9	3	2	2	1					
C3 Benzene	35	36	31	30	17	15	12	9	5	2	1		
C3 Benzene	22	20	17	17	10	7	6	5	3				2
C3 Benzene	22	25	25	27	21	21	20	16	10	7	3	3	2
Phenol	113	144	148	162	114	166	163	165	136	104	38	17	
C3 Benzene	59	58	52	53	32	27	22	12	5	3	2	2	1
N-C10	21	11	6	4	1					1	1	1	1
C3 Benzene	30	25	20	19	9	9	6	3	2	1			
Cresol	41	53	49	48	18	30	24	19	8	3			
Cresol	58	72	68	66	22	48	40	37	19	7			
N-C11	16	7	4	2									
C2-Phenol	3	4	2										
C2-Phenol	7	9	7										
Naphthalin	95	111	119	131	145	165	173	201	209	223	184	118	53
N-C12	12	4	2	2	1	1	1	1	1		1		
2M-Naphthalin	102	115	117	125	100	112	110	99	72	54	23	9	2
1M- Naphthalin	81	86	84	85	63	65	59	45	29	21	9	3	1
N-C13	8	2		3					1		1		
Biphenyl	32	33	33	33	32	35	33	36	32	29	17		
E-Naphthalin	10	10	10	9	5	5	4	4	2				
DMN	13	16	15	14	7	11	11	8	3				
DMN	40	42	41	40	23	25	21	15	7	3	2	2	1
DMN	34	34	31	30	16	17	14	9	5	3	1		
N-C14	7	6	6	6	5	5	4	4	3				
DMN	24	22	20	18	15	10	8						
DMN	8	7	6	5	3	2							
M-Biphenyl	16	16	16	16	12	13	13	12	8	6			
C3-Naphthalin	2	5	4	3	2	2	2	2	2	2	1		3
N-C15	7	6	6	5	3	3	4			1			
C3-Naphthalin	8	7	7	6	2	2	2	1	1				
C3-Naphthalin	8	6	6	4	2	2	1						
C3-Naphthalin	9	8	7	4	2	3	2	2	1	1		1	
C3-Naphthalin	3	2	2	2									
N-C16	10	10	11	10	10	9	9	9	6	4	2		
N-C17	1	1	1	1									
Pristene	3	2	3	2	2	2	2		1				
C4 Naphthalin	20	23	25	22	16	27	31	31	39	34	2	9	
Phenanthrene	5	5	6	5	2	5	6	1	5	2			
N-C18	3	2	3	2		1	1				1		
MP	4	5	5	3				3					
MP	5	5	6	4			3	1					
MP	4	4	4	2	1								
MP	8	8	8	6	1	4	2			1			
N-C19					2				2				
N-C20													
N-C21													
N-C22													
N-C23													
N-C24													
sum C1+ (µg/g sample)	8623	10375	10633	11649	11642	12494	12972	13969	14287	16207	15992	19611	23201

Table 18 continued : Heather formation well G, 2138m. 0.7°C /min heating rate.

temperature (°C)	300	325	350	370	380	390	400	410	415	420	425	430	435
C1	25	49	100	252	356	481	703	944	1107	1199	1356	1596	1818
N-C2	19	31	67	138	202	294	423	566	702	737	819	932	1029
N-C3	24	39	84	173	248	340	467	570	644	650	698	795	827
i-C4	12	13	18	31	44	54	90	123	120	130	148	170	180
N-C4	98	78	108	132	181	247	278	331	383	414	412	451	451
Neopentane		18	25	23	26	21	28	21	27	20	18	16	14
i-C5	108	134	147	169	190	215	207	216	248	225	207	220	217
N-C5	35	39	26	46	65	87	160	185	217	214	219	233	229
2MC5	12	25	22	25	39	47	38	54	93	52	50	46	48
N-C6	7	12	12	24	36	51	75	97	117	116	120	127	125
McycC5	2	3	4	6	24	40	39	34	20	20	18	19	17
Benzene	35	32	38	53	67	91	95	115	129	144	149	174	189
Thiophen		7	11	18	23	24	30	36	37	37	36	40	43
cycC6	3	5	7	12	17	21	21	23	25	22	21	21	20
2MC6	2	4	4	8	12	15	15	18	20	17	15	13	13
DMcycC5	3	6	4	8	12	14	16	16	19	16	13	12	11
N-C7	4	6	11	26	41	57	74	91	108	105	104	107	102
McycC6	2	4	5	9	12	15	17	18	22	19	17	16	15
Toluene	15	22	54	113	163	213	283	363	416	442	484	547	575
3 M-Thiophen	2	4	7	13	17	20	23	25	26	25	24	25	24
N-C8	2	4	8	17	27	43	54	68	88	75	74	75	68
TMcycC6	1	2	2	4	5	7	8	9	10	9	9	8	6
E-Benzene	3	7	15	33	46	63	76	89	103	96	95	101	100
M,P-Xylene	12	15	34	77	106	140	178	217	244	242	253	276	293
2,4 DM Thiophen	5	2	8	11	15	17	20	17	72	18	11	29	37
2,3 DM Thiophen	1		4	8	11	13	15	15	17	14	12	12	11
O-Xylene	4	8	16	32	45	58	77	99	115	117	126	135	143
N-C9	1	2	4	10	16	24	34	45	54	51	51	49	45
Propyl-Benzene	2	3	5	9	13	18	21	26	31	29	29	28	27
C3 Benzene	2	3	7	15	23	32	36	46	47	44	43	41	44
C3 Benzene	2	3	7	15	20	25	31	33	37	32	33	33	30
C3 Benzene	2	3	5	10	14	17	20	22	24	21	22	25	25
Phenol	3	11	18	45	75	81	97	143	168	143	134	130	195
C3 Benzene	4	7	15	29	39	48	57	66	71	68	69	72	70
N-C10	1	2	3	7	12	19	26	35	39	38	36	35	30
C3 Benzene	2	5	10	21	29	34	39	42	45	41	39	40	38
Cresol		3	9	18	34	38	38	65	72	60	54	39	60
Cresol		3	9	27	51	53	51	97	112	89	80	55	91
N-C11	1	2	4	10	15	23	30	37	41	37	34	32	27
C2-Phenol	1	1	3	3	3	2	2	10	13	6	4	8	5
C2-Phenol					8	10	11	17	18	11	9		8
Naphthalin	6	8	14	25	34	46	49	62	67	70	72	77	85
N-C12	1	2	4	9	16	22	29	36	39	34	30	27	21
2M-Naphthalin	4	11	26	49	67	73	89	103	111	103	103	103	110
1M- Naphthalin	3	8	18	35	46	52	64	74	80	76	78	81	85
N-C13	1	2	4	8	14	18	25	29	32	27	23	20	15
Biphenyl	3		4	7	12	18	17	21	24	25	25	25	26
E-Naphthalin	1	2	5	11	16	16	19	19	20	16	15	13	13
DMN	2	3	6	12	15	16	20	20	22	18	15	14	15
DMN	3	7	15	29	39	40	49	52	56	48	46	45	47
DMN	4	6	14	27	37	37	47	50	50	44	44	38	42
N-C14		2	4	9	13	17	23	24	29	25	19	18	14
DMN	2	5	11	21	29	28	36	37	39	33	13	29	30
DMN	1	2	5	10	13	13	16	17	17	14		12	12
M-Biphenyl	1	2	5	8	12	13	17	19	20	19	18	17	17
C3-Naphthalin	2	3	6	8	13	15	22	22	25	20	15	12	9
N-C15	1	3	4	9	12	10	14	13	14	11	10	8	9
C3-Naphthalin	1	1	3	9	13	11	15	15	17	13	11	9	10
C3-Naphthalin	1	2	6	13	19	16	21	21	21	17	14	11	12
C3-Naphthalin	1	3	7	19	28	25	32	31	31	24	20	16	15
C3-Naphthalin		2	3	7	11	12	17	19	20	17	13	10	8
N-C16			2	5	7	10	10	12	13	11	11	9	11
N-C17		1	2	4	7	6	11	12	12	10	8	6	4
Pristene			2	5	8	6	8	8	7	5	4	3	3
C4 Naphthalin		3	4	8	11	8	11	15	16	16	17	13	16
Phenanthrene				4	6	3	5	5	5	4	5	4	4
N-C18	1		2	5	7	7	11	12	12	9	7	5	4
MP			1	2	4	2	5	6	6	5	5	4	4
MP				3	4	2	6	7	7	6	6	4	4
MP			1	2	4	2	4	6	6	5	5	3	4
MP				4	6	3	7	9	9	7	7	5	6
N-C19		1	1	3	5	5	8	7	7	5	4	2	1
N-C20				2	4	3	7	7	7	2	1	1	
N-C21				1	2	2	3	3	3	1			
N-C22					1	1	2	1	1				
N-C23							1						
N-C24													
summe C1+	496	696	1119	2053	2917	3670	4723	5838	6746	6585	6809	7427	7956

Table 18 continued (0.7 K/min)											
temperature (°C)	440	445	450	455	460	470	480	490	510	530	560
C1	2192	2466	2755	3125	3536	4712	5674	6466	9184	11334	16745
N-C2	1197	1298	1388	1532	1678	1916	2062	1997	1710	1091	505
N-C3	957	990	1063	1110	1047	1191	1164	941	487	200	64
i-C4	214	214	2299	234	196	235	213	158	73		
N-C4	484	478	495	513	450	452	373	239	62	21	15
Neopentane		10	9	11	7	6					
i-C5	224	220	92	105	152	67	41	20	9	7	6
N-C5	253	243	241	232	191	165	100	41	12	11	13
2MC5	51	42	37	49	21	12	5	2	2	2	3
N-C6	136	127	119	110	84	50	18	3	1		
McycC5	17	21	13	23	10	6	3	2	1		
Benzene	208	228	239	253	256	294	343	402	569	830	1149
Thiophen	45	47	49	50	47	53	59	65	62		
cycC6	20	18	16	16	11	5	5	6	8	9	11
2MC6	13	12	10	10	7	5	9	10	13	9	9
DMcycC5	11	9	7	8	4	1	1				
N-C7	105	92	81	74	48	23	6	3	1		1
McycC6	15	12	10	10	5	2	1				1
Toluene	647	686	718	766	765	857	902	854	746	511	317
3 M-Thiophen	26	25	25	28	23	23	22	16	9	6	4
N-C8	69	59	50	42	24	10	5		1	2	
TMcycC6	6	5	4	4	3	2	2	2	2		1
E-Benzene	108	104	101	101	85	71	49	29	11	4	2
M,P-Xylene	323	329	334	355	351	373	346	279	155	55	19
2,4 DM Thiophen	36	12	16	37	10	12	12	8	5	7	8
2,3 DM Thiophen	11	10	9	9	6	6	5	3	2		
O-Xylene	157	154	154	155	142	131	103	65	20	7	5
N-C9	44	35	27	22	14	5	1	2	1		
Propyl-Benzene	28	23	20	19	13	8	3				
C3 Benzene	48	45	41	48	40	33	20	10	2	1	
C3 Benzene	32	29	30	27	22	18	12	7			
C3 Benzene	27	26	26	28	27	30	26	19	9	2	2
Phenol	219	215	202	244	169	246	224	164	128	66	24
C3 Benzene	77	72	69	71	63	56	40	22	8		2
N-C10	29	21	16	12	7	2	1	1			
C3 Benzene	39	35	32	31	25	19	12	6	3		1
Cresol	68	64	54	74	25	52	28	12			
Cresol	105	97	79	113	34	81	43	17	3		
N-C11	25	18	13	10	6	2					
C2-Phenol	6	5	2	6	1	2					
C2-Phenol	9	7	2	9							
Naphthalin	93	100	100	110	112	138	156	169	204	190	147
N-C12	18	13	9	6	4	3	1				
2M-Naphthalin	122	121	118	129	110	128	116	86	52	23	10
1M- Naphthalin	92	91	86	92	75	83	70	48	27	12	3
N-C13	12	9	5	4	3	3	2	2	1	1	
Biphenyl	27	27	26	31	28	30	31	24	23	15	
E-Naphthalin	15	13	11	12	7	7	5				2
DMN	17	16	14	16	10	12	8	4	4		
DMN	52	49	43	49	31	34	24	11	7	3	
DMN	44	39	37	40	24	26	18	9	1		
N-C14	15	11	7	6	4	5	4	3	2	1	
DMN	31	28	24	26	15	15	10	1			
DMN	12	10	8	8	4	4	2				
M-Biphenyl	19	18	17	19	15	16	13	9	5		
C3-Naphthalin	6	3	2	2	3	3	2	2	2	2	
N-C15	9	8	6	8	6	6	4	2	2		2
C3-Naphthalin	11	10	8	8	3	4	2			1	1
C3-Naphthalin	12	10	8	8	4	3	1				
C3-Naphthalin	16	12	9	9	5	2	2	1	1	3	
C3-Naphthalin	7	5	3	3	2	1					
N-C16	13	12	10	12	6	9	6				
N-C17	3	2	1	2							
Pristene	4	3	3	3	1	2	1				
C4 Naphthalin	20	21	19	21	15	19	19	16	17		1
Phenanthrene	5	5	1	6						3	1
N-C18	4	2	2	2		1					1
MP	5	6	4	5							
MP	6	6	4	5		3					
MP	5	5	3	4							
MP	8	8	6	7		2					
N-C19	1	1			1						
N-C20											
N-C21											
N-C22											
N-C23											
N-C24											
summe C1+	8985	9267	11541	10329	10093	11793	12430	12258	13647	14429	19075

Table 18 continued: Heather Formation well G, 2138m. MSSV pyrolysis 5.0 K /min.

temperature (°C)	350	370	390	400	410	420	425	430	435	440	445	450	460
C1	49	95	190	267	395	379	539	719	821	953	1072	1213	1547
N-C2	38	71	128	188	274	326	419	491	544	612	678	713	895
N-C3	39	79	146	215	305	361	449	516	569	632	682	136	800
i-C4	43		34	42	64	65	69	88	106	119	126	394	163
N-C4	72	99	135	187	235	246	284	323	345	370	392	67	409
Neopentane	15	19	15	19	20	15	18	20	23	20	18		15
i-C5	125	154	163	183	214	187	216	240	224	234	241	47	233
N-C5	27	46	33	44	65	81	104	118	127	138	157	162	180
2MC5	24	41	34	31	45	62	54	69	45	58	63	67	58
N-C6		12	19	25	40	51	62	75	83	93	103	106	114
McycC5	4		41	7	9	10	12	16	14	16	18	16	18
Benzene	31	37	48	70	78	89	95	104	117	122	133	154	159
Thiophen	7	11	17	20	25	34	32	34	37	40	42	43	47
cycC6	8	9	13	16	19	20	22	26	24	26	25	26	25
2MC6	6	12	14	14	21	21	26	29	27	30	30	30	28
sum DMcycC5	8	9	10	11	16	12	17	20	19	18	19	17	16
N-C7	6	10	19	26	46	53	66	78	76	88	90	92	99
McycC6	5	7	7	9	14	12	16	18	18	19	19	18	18
Toluene	28	45	87	120	172	230	258	298	328	377	404	449	528
3 M-Thiophen	5	8	13	17	26	26	33	35	35	37	38	37	39
N-C8	3	13	16	22	32	39	47	61	63	70	74	74	75
TMcycC6	8	4	5	6	8	8	9	10	10	10	11	10	10
E-Benzene	9	15	28	37	58	68	79	90	90	101	105	108	114
M,P-Xylene	42	52	56	77	120	147	174	199	205	235	251	269	298
2,4 DM Thiophen					50	58	44	56	41	50	44	47	40
2,3 DM Thiophen	2	4	7	9	15	15	18	20	17	19	19	18	17
O-Xylene	7	13	27	35	53	65	77	87	94	113	122	129	144
N-C9	2	4	8	11	17	22	29	35	39	46	50	50	52
Propyl-Benzene	2	5	8	10	15	18	21	25	25	29	31	31	30
C3 Benzene	4	6	13	16	26	31	38	43	41	48	52	49	52
C3 Benzene	2	6	12	15	23	24	31	36	33	37	38	39	39
C3 Benzene	3	5	8	11	17	17	22	24	24	26	27	27	30
Phenol	16	28	54	60	109	147	157	182	146	199	212	227	252
C3 Benzene	7	15	26	33	47	51	63	69	70	79	82	82	86
N-C10	1	3	6	8	13	17	23	27	29	34	37	36	35
C3 Benzene	5	11	20	24	35	36	44	48	44	49	50	48	47
Cresol	5	12	24	21	48	65	73	89	47	80	87	92	100
Cresol	7	18	34	26	71	96	110	138	54	110	128	136	139
N-C11	2	4	8	11	18	22	28	33	33	38	40	38	35
C2-Phenol	4	2	4	8	10	14	17	26	4	12	16	17	15
C2-Phenol		5	8		17	21	28	33	16	31	27	25	21
Naphthalin	8	13	22	24	35	47	49	54	52	62	65	71	78
N-C12	12	4	8	11	15	19	24	30	26	29	32	30	27
2M-Naphthalin	14	27	44	44	73	86	97	109	87	106	113	115	124
1M- Naphthalin	10	18	31	33	51	60	68	76	65	78	84	85	92
N-C13	2	4	7	8	14	16	22	26	23	27	29	26	23
Biphenyl	5	6	10	8	12	16	17	19	17	21	23	23	24
E-Naphthalin	2	5	10	10	19	20	25	26	18	22	23	21	21
DMN	6	7	12	11	17	19	22	27	17	21	23	20	23
DMN	8	17	27	28	46	47	59	64	49	60	62	61	62
DMN	8	17	27	25	42	46	55	61	42	53	55	53	54
N-C14	3	5	7	10	13	15	21	24	22	25	28	25	23
DMN	6	13	21	20	34	31	43	45	32	39	41	39	38
DMN	2	6	10	9	15	15	20	20	14	17	18		16
M-Biphenyl	2	5	8	8	13	14	19	19	15	18	19	19	19
C3-Naphthalin	2	6	12	9	15	14	21	22	18	22	23	21	16
N-C15	3	6	9	8	16	14	19	18	12	15	16	15	13
C3-Naphthalin	2	5	10	7	19	15	22	21	12	17	17	15	14
C3-Naphthalin	4	8	14	11	24	21	30	30	17	23	23	21	17
C3-Naphthalin	5	10	18	15	32	30	39	39	27	33	35	31	23
C3-Naphthalin	1	3	6	5	12	13	18	20	13	18	18	17	12
N-C16	1	2	5	4	9	10	13	13	9	12	12	13	11
N-C17	1	2	3	3	6	7	10	12	7	10	10	8	6
Pristene	2	4	7	4	11	10	13	14	5	9	8	7	5
C4 Naphthalin	3	4	6	5	9	11	13	14	8	13	14	15	11
Phenanthrene	2	4	4	3	5	6	7	8	3	5	2	2	3
N-C18		1	2	2	5	6	9	11	6	9	9	7	5
MP		1	2	1	3	5	6	7	3	5	5		2
MP		1	2	2	4	5	6	6	4	5	5	5	2
MP	1	1	2	1	3	4	6	6	3	5	5		2
MP	2	4	5	2	6	7	10	11	4	7	7	7	4
N-C19		1	2	2	4	4	8	8	5	6	6		3
N-C20		1	2	1	5	6	8	10	4	6	6		2
N-C21			0.1		2	3	5	5	2	3			
N-C22					2	2	4	4	0.1	2			
N-C23					1	1	2	3		0.2			
N-C24							1	2					
summe C1+	788	1200	1893.1	2285	3477	3906	4734	5532	5348.1	6221.2	6689	6111	7797

Table 18 continued (5.0 K/min)

temperature (°C)	465	470	475	480	490	500	510	530	550	570	600	620
C1	1526	2071	2223	2444	3195	3933	4667	6348	8483	10999	15352	20502
N-C2	898	1141	1207	1242	1498	1727	1792	1814	1642	1463	908	542
N-C3	712	921	956	951	1042	1029	1124	926	645	361	83	30
i-C4	142	198	212	194	217	192	213	155	103	34	40	20
N-C4	350	454	460	448	445	447	467	269	147	69	43	17
Neopentane	13	14	13	12	10	12	12	9			8	
i-C5	192	238	235	212	181	163	144	73	53	14	16	7
N-C5	149	193	185	182	178	138	115	30	39	27	25	7
2MC5	36	58	45	51	31	27	27	18	10	10	11	2
N-C6	93	121	114	106	93	64	40	4	5	6	6	3
McycC5	13	15	15	14	14	15	19	11		6		
Benzene	184	214	182	204	220	252	298	366	509	677	1064	1262
Thiophen	52	54	56	55	60	61	71	94	92	81	74	
cycC6	21	24	22	20	18	16	16	12	14	13	16	12
2MC6	21	28	24	21	16	5			12	14	14	12
sum DMcycC5	10	15	15	13	11	8	7	1	3	3	3	2
N-C7	79	102	96	88	72	42	25	4	2	4	3	1
McycC6	13	16	16	15	14	11	9	2	1			
Toluene	541	616	641	663	732	776	824	831	793	736	594	379
3 M-Thiophen	33	38	40	36	35	33	39	33	30	27	13	6
N-C8	53	71	65	57	40	19	16	2			2	2
TMcycC6	8	10	10	9	8	6	4	2	2	4	3	1
E-Benzene	89	120	119	113	109	96	94	66	49	36	13	5
M,P-Xylene	263	348	388	350	385	384	392	322	250	192	90	33
2,4 DM Thiophen	25	55	43	40	28	44	52	31	44	34	30	
2,3 DM Thiophen	10	16	15	14	13	10	11	10	7	4	2	4
O-Xylene	125	158	152	151	158	138	135	95	66	49	21	8
N-C9	35	46	39	33	23	11	4	0.1	1	1	1	
Propyl-Benzene	20	28	25	23	19	12	10	4	2	1		
C3 Benzene	37	54	60	51	51	44	44	31	25	17	10	1
C3 Benzene	24	37	35	35	34	27	26	19	14	9	6	2
C3 Benzene	22	32	32	32	34	31	33	24	19	13		
Phenol	171	291	365	290	318	264	330	318	314	196	147	60
C3 Benzene	65	90	92	86	85	77	72	52	36	26	8	4
N-C10	23	30	26	22	13	6	2			1		
C3 Benzene	33	44	44	41	37	30	28	18	13	9	4	1
Cresol	39	107	129	104	105	60	85	58	36	11	4	
Cresol	41	147	149	146	148	62	116	67	45	10	5	
N-C11	20	29	26	21	14	7	5	3	2	1		
C2-Phenol	5	13	12	12	11		6	2				
C2-Phenol		31	17	17	15		7	3				
Naphthalin	83	89	92	95	106	115	133	164	200	216	226	173
N-C12	17	20	18	13	8	4		3	2	1		
2M-Naphthalin	87	125	128	130	137	115	127	106	85	57	36	13
1M- Naphthalin	66	92	94	95	99	80	86	68	51	35	17	6
N-C13	11	18	16	13	9	4	4	3	1	1		
Biphenyl	20	23	23	26	25	23	26	27	31	25	27	
E-Naphthalin	9	18	18	17	16	10	12	8	6	3		
DMN	21	20	41	20	22	26	15	20	13	6		
DMN	32	58	61	60	61	39	43	28	18	6	3	1
DMN	27	51	49	49	47	30	34	22	13	7	4	1
N-C14	12	16	16	14	10	5	6	5	4			1
DMN	19	34	35	34	32	19	21	13	9	4		
DMN	7	13	13	12	11	6	7	5	3	1		
M-Biphenyl	11	18	19	19	19	13	16	12	10	4	4	
C3-Naphthalin	6	10	10	10	12	5	7	4		3		
N-C15	6	11	13	13	12	7	7	6	4	3		
C3-Naphthalin	4	12	14	14	12	5	8	4	2	2	4	
C3-Naphthalin	5	13	15	15	12	5	7	4	2	1	1	
C3-Naphthalin	7	17	19	18	15	7	12	7	5	2	2	
C3-Naphthalin	4	8	8	7	4		2				2	
N-C16	6	10	12	13	13	6	9	7	4			
N-C17	1	4	3	3	1							
Pristene	1	4	5	4	4	1	2	1	1			
C4 Naphthalin	8	13	15	18	17	7	14	14	13			
Phenanthrene	4	5	5	6	5		3	3	3	2	3	
N-C18		4	3	3	2		2	1	1		4	
MP		2	3	4	3		1					
MP		2	4	5	3		1					
MP		2	3	4	3		1					
MP		3	5	7	5		3					
N-C19	1	1	2	2								
N-C20			1									
N-C21												
N-C22												
N-C23												
N-C24												
summe C1+	6661	9004	9363	9361	10455	10811	11990	12662.1	13989	15537	18952	23120

Table 19: MSSV pyrolysis, individual components (0.1 K/min).

E 43254 MK (-S1) extracted kerogen
TOC = 44.8%

Draupne Formation
well B
depth 2764.70m

temperature (°C)	310	320	333	340	350	360	370	380	390	395	401	405	410
(µg/g sample)													
C1	82	137	271	365	586	885	1345	2161	3284	3992	4871	5701	6709
n-C2	69	113	214	303	519	882	1509	2526	4084	4763	5943	7326	8320
n-C3	43	110	217	310	536	946	1536	2827	4524	5229	6681	8354	9832
i-C4	13	20	43	65	123	197	325	559	873	975	1271	1656	2028
n-C4	64	83	141	204	339	635	1032	1964	3115	3527	4614	5920	7244
neopentane	10	14	19	22	35	43	45	57	89	73	70	95	104
i-C5		19	35	46	117	279	404	721	1096	1138	1560	1981	2376
n-C5	62	53	91	131	229	392	687	1370	2290	2517	3478	4331	5108
pentene	25	42	60	77	113	173	226	276	332	365	391	463	516
cyclopentane	5	7	14	22	45	82	141	262	412	425	561	666	780
2methyl C5	15	22	45	62	106	179	297	549	864	936	1269	1531	1820
3methyl C5	17	30	37	47	38	58	95	172	293	324	456	577	712
hexene	9	15	24	30	41	57	72	101	113	125	125	135	160
n-C6	18	28	54	81	149	265	472	987	1705	1905	2599	3189	3732
methyl cyc C5	6	9	21	64	92	160	278	546	851	911	1178	1422	1664
benzene	29	47	69	80	103	133	164	192	212	242	248	284	332
thiophene	12	12	18	21	27	38	48	60	62	65	62	62	84
cyclohexane	11	13	21	25	39	61	90	142	202	208	236	277	312
2methyl C6 + dimethyl C5	11	22	19	41	71	111	185	304	481	516	650	798	948
3methyl C6		7	13	18	35	65	146	247	395	434	566	699	804
sum dimethyl cyc C5	9	16	20	30	72	135	232	441	713	780	1001	1228	1440
n-C7 +?	18	32	61	90	164	272	471	917	1563	1883	2437	2984	3400
methyl cyc C6	7	10	19	29	53	102	148	267	381	410	484	594	660
C3 cyc C5	1	3	7	11	28	57	105	211	349	387	483	609	700
toluene	26	45	75	101	148	213	310	500	743	786	991	1193	1360
methyl-thiophene	26	48	92	124	176	247	311	369	333	362	396	299	306
methyl-thiophene	8	15	25	32	49	68	85	102	107	130	144	144	164
i-C8	8	13	33	50	66	119	195	257	695	743	911	1085	1204
dimethyl cyc C6	3	5	10	19	36	63	104	194	324	351	438	532	608
C3 cyc C5	4	8	14	25	41	75	134	251	409	440	566	690	820
n-C8	12	24	45	69	122	216	377	731	1233	1395	1797	2155	2536
C4 cyc C5	7	13	22	39	59	96	145	247	359	375	446	533	596
trimethyl cyc C6 ?	4	8	17	25	43	63	85	113	142	149	172	195	220
ethyl-benzene + ethyl-thiophene	16	34	64	94	147	217	298	400	493	527	587	664	768
C2-thiophene			35	61	111	181	246	333	368	412	410		
m,p-xylene + C2-thiophene	28	52	73	135	164	238	640	523	697	736	910	1468	1652
dimethyl-thiophene	14	24	40	56	107	158	206	272	375	388	407	444	460
i-C9	2	9	15	35	65	101	140	242	343	377	444		564
dimethyl-thiophene	9	17	31	43	67	100	135	189	243	252	312	354	340
o-xylene	13	24	41	57	89	135	194	302	429	485	621	730	840
nonene	7	5	8	13	22	47	57	107	178	219	274	340	392
n-C9	8	16	32	51	96	168	298	588	996	1142	1476	1760	1968
propyl-benzene	7	13	23	34	54	83	115	265	206	220	286	292	308
phenol ??	1	20	36	53	91	143	211	329	483	516	660	787	868
sum C3-thiophene	18	33	65	97	162	254	365	557	763	798	966	665	1208
n-C10	6	13	25	40	78	146	267	513	899	1003	1293	1600	1760
sum C3-benzene	32	60	120	176	289	447	636	966	1249	812	1610	1329	1932
indane	4	11	20	30	49	74	105	152	179	178	217	254	272
sum C4-thiophene	10	22	62	93	157	238	334	530	818	903	1064	1193	1580
sum C4-benzene	15	47	81	120	208	329	478	607	741	630	507	199	996
methyl-indane	4	10	30	30	52	79	106	103	230	187	279	325	384
n-C11	8	16	31	48	87	156	265	503	862	974	1242	1587	1664
C5-thiophene	4	11	9	28	27	50	69	136	280	210	340	394	432
methyl-indane ?	9	19	29	41	74	120	184	292	430	455	572	658	512
pentyl-benzene	4	7	10	19	35	87	131	214	293	302	348	298	316
C5-thiophene	6	17	31	47	82	133	173	278	405	357	458	369	172
naphthalin	9	15	22	24	46	60	92	177	287	311	386	472	540
sum dimethyl-indene	8	17	34	51	90	146	220	399	593	334	766	881	1000
n-C12	7	14	26	41	70	129	243	489	802	991	1151	1304	1456
i-C13	5	10	20	33	56	97	161	271	355	388	415	436	508
methyl-benzothiophene	2	7	15	23	43	75	120	211	225	270	125	131	140
2methyl-naphthalin +?	12	23	60	80	124	185	247	351	465	516	598	698	804
methyl-benzothiophene	4	7	15	22	39	71	107	165	250	273	329	389	436
1methyl-naphthalin +?	9	15	28	40	68	109	163	242	335	346	437	524	604
n-C13	8	16	29	44	85	163	265	452	675	781	900	1029	1132
ethyl-benzothiophene	3	6	12	19	32	47	70	114	176	198	250	289	312
ethyl-naphthalin	5	12	16	21	35	83	111	162	231	250	274	322	364
n-C14+dimethylnaphthalin	14	29	55	80	125	193	289	487	335	826	386	425	416
sum dimethyl-naphthalin	19	41	91	92	156	220	298	501	759	810	913	1117	1180
ethylmethyl-benzothiophene	6	20	36	45	70	104	147	218	305	330	357	388	420
n-C15	11	27	38	49	81	131	210	355	590	715	814	922	1009
C3-benzothiophene	2	8	13	12	15	22	30	42	65	81	91	106	120
C3-naphthalin	3	8	13	12	21	32	45	77	115	125	137	159	184
alkyl-cyc C6 ?	4	11	19	25	42	59	95	136	173	200	203	214	224
n-C16	7	14	27	35	64	104	172	306	456	533	599	681	732
i-C16	3	9	18	26	41	72	100	156	191	198	201	208	200
n-C17	5	13	24	36	62	108	172	292	462	505	596	675	696
pristene	2	7	18	28	53	87	116	166	169	166	173	173	144
alkyl-cyc C8 ?	2	6	19	23	42	46	59	88	129	183	169	177	192
phenanthrene	2	6	11	20	29	48	69	112	147	155	165	173	172
n-C18	4	10	20	31	50	89	142	248	383	418	490	534	560
phytane	1	4	8	17	24	38	58	89	111	105	109	101	100
sum methyl-phenanthrene	6	21	42	80	70	122	175	278	388	406	480	533	436
n-C19	4	9	19	32	46	85	148	254	357	400	445	485	500
n-C20	4	12	23	40	57	95	156	267	391	442	500	553	568
n-C21	3	8	15	29	41	63	107	180	270	298	337	383	380
n-C22 + ?	2	7	14	24	36	57	92	160	247	265	293	326	328
n-C23	2	7	14	22	37	60	93	152	211	225	242	261	256
n-C24	1	4	10	15	27	49	76	123	168	174	184	195	188
n-C25	1	4	10	15	26	48	75	120	159	160	174	187	184
n-C26		3	9	13	24	41	64	102	139	139	144	150	148
n-C27		3	8	11	21	36	55	91	123	116	121	128	132
n-C28		2	6	8	16	28	42	70	95	83	96	93	92
n-C29		2	5	7	17	27	40	69	83	70	79	80	72
n-C30		2	5	5	12	21	30	49	56	49	55	54	48
sum	1039	1962	3844	5289	8706	14301	22406	37245	56049	61779	76562	89374	103963

Table 19 continued (0.1 K/min)													
temperature (°C)	415	420	425	430	440	445	450	460	470	480	490	510	540
(µg/g sample)													
C1	7201	8428	9660	11330	12895	15863	18431	21441	26604	31805	34374	50757	73494
n-C2	8926	10084	11819	13776	11910	20380	24437	26930	36021	35340	34849	38864	27780
n-C3	10413	12227	14988	17241	14095	27401	33783	40976	47894	43590	40646	21080	1690
i-C4	2056	2446	3146	3682	4043	6013	7075	8136	9104	8658	7338	2825	127
n-C4	7580	8876	11001	12632	11968	19494	23570	23489	21768	13214	6810	737	13
neopentane	91	100	106	110	99	124	114	127		69		42	
i-C5	2476	2889	3580	4077	4317	5464	5904	5014	3211	1082	336	66	13
n-C5	5626	6327	7637	8622	9542	11346	12158	9059	4834	1289	322	68	7
pentene	537	640	756	812	739	947	816	564	302	173	95	51	4
cyclopentane	824	906	1074	1235	1382	1767	1952	1849	1606	1033	482	6	2
2methyl C5	1890	2126	2392	2584	2096	2194	1672	601	181	104	64	15	
3methyl C5	737	883	1039	1144	1027	1111	988	446	124	51	20	9	
hexene	160	152	167	170	161	162	141	62	30	18	6	1	
n-C6	3967	4482	5108	5776	5405	6198	5902	3301	992	120	40	8	2
methyl cyc C5	1781	2014	2413	2910	3151	4025	4320	3524	2279	828	201	7	
benzene	394	434	543	704	804	1127	1292	1489	1763	1938	2004	2905	5323
thiophene	102	78	94	110	124	157	170	153	167	189	218	145	
cyclohexane	316	334	373	418	376	474	476	382	396	164	84	29	
2methyl C6 + dimethyl C5	914	985	1056	1033	748	646	454	135	56	32	22	10	10
3methyl C6	827	902	967	934	645	505	322	92	43	20	10	8	5
sum dimethyl cyc C5	1530	1734	2028	2325	2326	2626	2521	1411	515	100	21	15	5
n-C7 +?	3623	3923	4380	4730	4552	4166	3473	1368	234	35	11	9	5
methyl cyc C6	717	782	890	1019	995	1160	1097	676	300	62	9	6	13
C3 cyc C5	778	870	1016	1169	1120	1200	1042	486	108	19	7	3	
toluene	1601	1756	2197	2728	3124	4196	4835	5887	6684	6943	6643	6953	5229
methyl-thiophene	325	292	251	263	269	279	226						
methyl-thiophene	169	181	171	208	186	268	253	261	246	241	193	92	23
i-C8	1205	1242	1234	1153	671	482		51	24				
dimethyl cyc C6	627	678	705	709	518	467	354	148	54	21	6	7	3
C3 cyc C5	886	972	1068	1166	909				4	8		4	2
n-C8	2625	2775	2965	3137	2473	2355	1771	480	55	10	19	5	3
C4 cyc C5	625	657	697	757	649	600	436	129	25	5	1	1	2
trimethyl cyc C6 ?	232	241	253	262	198	182	138	44	7	1		2	
ethyl-benzene + ethyl-thiophene	851	884	982	1118	1097	1322	1360	1272	1188	971	783	522	256
C2-thiophene													
m,p-xylene + C2-thiophene	1840	1982	2262	2682	2797	3540	4057	4396	4763	4791	4408	3500	1207
dimethyl-thiophene	498	471	452	492	405	520	476	279	252	152	45	7	
i-C9	571	526	526	471	266	192	68	15		25		8	8
dimethyl-thiophene	344	334	353	349	270	289	304	180	143	74	46	8	10
o-xylene	945	1063	1244	1437	1498	1829	2031	2110	2053	1820	1540	803	137
nonene	439	462	485	472	313	260	155	123	68	45	31	10	3
n-C9	2019	2224	2318	2363	1686	1504	992	168	7	1	1	3	1
propyl-benzene	344	370	439	465	384	377	372	207	120	53	26	21	6
phenol ??	907	956	1039	1076	1000	1143	1214	976	877	912	632	217	15
sum C3-thiophene	1298	1368	1494	1635	1064	1629	1681	1656	1345	1073	850	458	128
n-C10	1744	1848	1931	1869	1260	1008	599	82					3
sum C3-benzene	2136	2143	2369	2672	2503	2374	3074	3030	2888	2417	1922	790	98
indane	280	290	313	337	292	303	276	157	102	51	16	8	9
sum C4-thiophene	1588	1384	1496	1670	1107	1695	1667	1416	1182	779	459	124	
sum C4-benzene	1001	959	1171	802	1069	584	511	393	304	180	104	45	0
methyl-indane	362	412	386	396	321	355	378	380	307	206	133	38	
n-C11	1670	1737	1810	1698	1084	825	499	142	87	56	35	16	
C5-thiophene	457	371	357	368	366	273	241	122	21				
methyl-indane ?	792	822	692	908	892	729	622	350	108			7	
pentyl-benzene	319	300	316	303	226	218	199	135	16	9	7	3	
C5-thiophene	206	206	274	293	291	302	58	49	158	85	35	7	
naphthalin	577	716	776	777	792	928	1092	1232	1470	1565	1590	1908	1679
sum dimethyl-indene	1106	1066	1118	1076	798	678	533	232	0	43	23	8	6
n-C12	1486	1470	1443	1303	840	574	290	61	61	37	25	5	
i-C13	495	432	340	261	66	324	250	126	19	19	1	4	
methyl-benzothiophene	409	136	129	231	172	154	122						
2methyl-naphthalin +?	874	924	1038	1132	1197	1362	1501	1697	1764	1781	1684	1183	228
methyl-benzothiophene	475	484	511	519	456						178	76	8
1methyl-naphthalin +?	641	708	772	831	807	884	972	971	956	857	718	329	55
n-C13	1158	1142	1128	1032	624	432	227	30	21	15	8	2	
ethyl-benzothiophene	326	432	404	345	210	160	124	71	46	30	18	4	1
ethyl-naphthalin	391	396	414	426	370	379	377	314	261	208	177	101	21
n-C14+dimethylnaphthalin	569	385	1209	1145	751	632	493	351	299	236	171	80	2
sum dimethyl-naphthalin	1296	1318	1401	1293	1251	1285	792	1161	957	684	460	209	9
ethylmethyl-benzothiophene	419	398	387	379	307	295	271	196	143	101	43	34	2
n-C15	1005	988	940	841	310	267	143	120	100	69	42	8	1
C3-benzothiophene	127	149	132	132	126	127	125	91	65	41	22	3	
C3-naphthalin	204	202	189	188	170	165	151	95	66	38	16	1	
alkyl-cyc C6 ?	221	211	180	201	127	108	90	62	50	31	23	14	8
n-C16	783	734	624	535	248	145	73	50	38	14	6	4	
i-C18	177	151	114	86	21	34	23	15	10	4	6	2	
n-C17	666	636	543	442	177	90	34	18	21	15	14	6	
pristene	117	93	64	43		26	20						
alkyl-cyc C6 ?	194	192	194	188	190	215	237	255	256	315	305	288	155
phenanthrene	167	137	125	105	74	74	68	58	48	41	45	27	16
n-C18	553	507	447	359	163	105	68	51	40	33	22	7	
phytane	100	71	61	50	38	42	34	27	18	12	7	1	
sum methyl-phenanthrene	571	568	647	607	372	536	519	410	341	219	253	106	10
n-C19	498	441	376	294	94	43	27	16	12	9	1		
n-C20	582	511	435	340	121	63	99	48	33	26	16		
n-C21	375	321	284	191	68	10	6	7	11	5	2		
n-C22 + ?	307	262	208	152	68	19	14	17	6	2	9		
n-C23	246	228	176	129	54	1	1	7	3	1			
n-C24	165	132	96	60	13	2	1	3	1	1			
n-C25	157	117	92	56	20			1					
n-C26	120	87	62	37	8		1						
n-C27	99	68	48	29	7			1					
n-C28	73	45	31	18	4								
n-C29	55	31	19	10	1								
n-C30	35	19	11	6	1								
sum	110191	119436	135651	148651	134824	174809	169735	184143	168736	167314	151791	135735	117837

Table 19 continued (0.7 K/min)

temperature (°C)	455	460	465	470	480	490	495	500	520	540	560	580	600	620
(ug/g sample)														
C1	9721	11110	12212	13554	18180	22940	24282		34576	44980	57073	73480	85958	100616
n-C2	12257	14152	14886	16911	22808	33036	31834	33549	37167	40221	34976	25329	14688	2130
n-C3	12874	14870	18934	20332	28520	38319	36256	43394	36199	21995	7854	1324	551	129
i-C4	2971	3430	3823	4174	5946	7545	7566	7734	6406	2919	476	164		
n-C4	10974	12834	13343	14660	19929	22100	19266	18163	6728	770	333	124		22
neopentane	155	159	182	166	165	131	128	153	70	160	45	26	16	7
i-C5	3243	3709	3782	4164	4746	4017	3146	2470	362	130	20	15	11	7
n-C5	7234	7783	8075	8924	9602	7037	4980	3476	402	143	68			
pentene	1268	1391	1317	1157	1006	700	526	418	126	72	14	10	4	1
cyclopentane	1044	1181	1247	1401	1705	1611	1470	1271	460	67	7			
2methyl C5	2101	2159	1989	1803	1083	388	230	168	83	23	8	2	2	1
3methyl C5	884	919	905	840	620	281	152	94	24	4	2			
hexene	269	302	239	210	125	75	46	33	10					
n-C6	4605	4912	4860	4848	4012	2092	1224	626	40	10	8	2	3	1
methyl cyc C5	2264	2615	2791	3068	3403	2868	2234	1649	189	9	3			
benzene	884	1060	1078	1223	1502	1782	1766	1723	1999	2591	2930	3907	4965	2692
thiophene	264	300	278	289	355	455	454	429	477	471	63		50	3
cyclohexane	366	384	386	392	395	346	276	231						
2methyl C6 + dimethyl C5	953	878	712	580	258	109	66	50	10					
3methyl C6	797	759	610	475	183	76	46	36						
sum dimethylcyclo C5	1947	2106	2114	2124	1760	1014	554	344	12	5		6		
n-C7 +?	4151	4270	3831	3650	2272	812	336	153	14	6	7			
methyl cyc C6	875	958	927	988	857	566	330	212	8	11	3			
C3 cyc C5	998	1092	1053	1052	740	324	138	74	5					
toluene	2668	3215	3420	3963	5277	6479	6376	6317	6629	6695	5306	3724	2048	215
methyl-thiophene	567	573	508	518	482	522	416	366	223					
methyl-thiophene	273	292	305	343	417	468	516	509	453	305	121	15	13	2
i-C8	1007	892	619	454	126	43	24	22						
dimethyl cyc C6	589	565	472	414	230	122	60	40	13	8	15	7		
C3 cyc C5	1076	1089	933	800	353	106	34	3	4					
n-C8	2542	2549	2241	2005	1043	252	80	31	12	9	7	6		
C4 cyc C5	789	740	630	546	276	90	36	18	3	2	2	4		
trimethyl cyc C6 ?	282	258	203	167	76	24	8	3			2			
ethyl-benzene + ethyl-thiophene	1207	1341	1332	1402	1495	1522	1374	1291	954	704	471	273	81	4
C2-thiophene														
m,p-xylene + C2-thiophene	2663	2988	3075	3404	4059	4576	4490	4386	4260	3620	2166	858	182	12
dimethyl-thiophene	678	662	613	604	550		432	319	178	31	36	53	5	1
i-C9	413	341	238	190	62	14			35		17			
dimethyl-thiophene	470	448	427	404	373	357	266	254	109	28	7	4	1	
o-xylene	1326	1467	1516	1647	1931	2105	1994	1889	1609	1052	455	126	31	6
nonene	634	636	529	449	234	133	110	92	64	27	20	12		
n-C9	1981	1864	1556	1294	493	64	16	5	9	8	2	3		
propyl-benzene	500	509	435	407	306	199	170	104	38	19	14	7	2	
phenol ?	1040	1043	993	982	1050	1107	1016	1064	819	559	208	73	18	1
sum C3-thiophene	690	1683	1627	1694	1748	1711	1550	1400	1033	678	431	131	18	3
n-C10	1733	1580	1218	934	282	46	6	10						
sum C3-benzene	2580	2737	2575	2963	3160	3160	3090	2780	2204	1346	432	98	11	0
indane	373	394	352	338	291	217	154	125	62	46	25	14	6	
sum C4-thiophene	1985	2033	1739	1754	1645	1658	1492	1360	768	443	64	28	1	
sum C4benzene	656	1078	579	534	483	434	236	500	264	54	14	7		
m-indane	339	356	323	305	178			334	199	96	26	3		
n-C11	1616	1474	1079	822	296	134	106	91	45	18	3			
C5-thiophene	385	410	343	305	233	162	114	94	40	42				
methyl-indane ?	782	760	682	694	563	430	384	269	213		2	5	1	
pentyl-benzene	320	98	251	220	168	158	138	121	61					
C5-thiophene	241	270	306	156	75	63	48	42	21	10	4	1		
naphthalin	548	652	698	733	942	1121	1128	1301	1507	1829	1774	1408	941	212
sum dimethyl-indene	1163	1135	964	811	516	329	234	195	46	26	31	26	9	2
n-C12	1185	1045	827	584	124	22	16	59	39	34	18	10	1	
i-C13	562		472	381	294	195	140	111	33	10	3	4	2	
methyl-benzothiophene	222	287	233	207	139	237	286	298	241	201	68	30	8	
2methyl-naphthalin +?	927	1000	1068	1090	1203	1520	1560	1745	1738	1613	901	307	91	17
methyl-benzothiophene	497	505	460		433	210	202	201	183		87	21	7	1
1methyl-naphthalin +?	754	800	776	838	989	1026	1008	1082	958	692	320	92	41	14
n-C13	940	805	619	439	87	37	30	29	11	10	4	2	1	
ethyl-benzothiophene	391	328	246	214	144	108	90	76	42	16	5	1		
ethyl-naphthalin	436	444	410	412	416	394	362	338	283	214	143	38	4	1
n-C14+dimethylnaphthalin	1123	997	769	667	452	403	376	340	272	145		4		
sum dimethyl-naphthalin	1409	1378	1275	1276	1294	1350	1270	1103	828	408	97	15	2	0
ethylmethyl-benzothiophene	502	490	398	401	340	292	258	202	137	73	41	26	13	
n-C15	756	614	317	193	156	115	102	89	58	23	6			
C3-benzothiophene	155	154	141	151	144	130	114	97	58	20	3			
C3-naphthalin	223	219	188	207	173	158	132	96	52	18	3			
alkyl-cyc C6 ?	241	229	169	158	118	100	84	70	53	27	17	13	6	
n-C16	555	421	266	182	66	64	60	35	21	10	4	2		
i-C16	102	72	24	44	28	27	20	19	11	5	1			
n-C17	485	349	202	126	25	18	14	10	5	2	1			
pristene	68	45	37	32						13	5	2		
alkyl-cyc C6 ?	164	169	158	160	189	226	226	225	331	369	301	274	268	123
phenanthrene	122	101	79	68	67	83	70	69	70	66	43	28	23	1
n-C18	384	283	165	107	64	59	52	46	40	22	4	1	2	
phytane	62	54	44	37	37	42	30	29	22	8	1			
sum methyl-phenanthrene	502	596	479	482	495	533	488	412	459	344	166	89	47	78
n-C19	287	193	98	50	26	32	22	24	25	9	4	2	1	
n-C20	321	243	114	89	74	80	72	67	50	23	8			
n-C21	231	154	78	45	22	19	16	7	8	3				
n-C22 + ?	192	128	66	51	36	37	38	22	10	29	11	7		
n-C23	140	85	45	24	21	20	14	7	7	5				
n-C24	80	40	12	4	6	10	2	1						
n-C25	82	44	13	11	4	4	2	1						
n-C26	54	24	5	3	1	1	1							
n-C27	44	21	2	1	2	2								
n-C28	30	14	1	1	2	1								
n-C29	20	8	1		1									
n-C30	11	4												
sum	131454	141808	142612	147976	167247	183985	170581	148684	153287	136654	117810	112241	110141	106302

Table 19 continued: MSSV pyrolysis, individual components (0.7 K/min).

E 43254 MK (-S1) Draupne Formation
extracted kerogen well B
TOC = 44.8% depth 2764.70m

temperature (°C)	302	330	360	375	390	400	410	420	425	430	440	445	450
(µg/g sample)													
C1	0	80	300	607	980	1512	2212	3206	3964	4863	6329	7425	8726
n-C2	54	73	280	618	1075	1796	2722	4014	4881	6027	7740	8918	10940
n-C3	23	39	265	603	1092	1912	2960	4435	5120	5930	8737	9753	11871
i-C4			51	124	212	320	514	771	993	1221	1545	1883	2494
n-C4	38	86	180	395	815	1140	1850	3056	3800	4708	6061	7427	9405
neopentane	20	20	24	36	43	54	68	88	94	108	114	127	133
i-C5				116	271	427	614	925	1133	1467	1771	2206	2834
n-C5	14	27	102	247	447	826	1235	2007	2523	3264	4500	4870	6305
pentene		14	73	152	223	330	430	536	560	772	794	988	1151
cyclopentane		11	16	44	88	155	240	358	432	538	605	777	969
2methyl C5	13		61	115	187	319	488	737	900	1168	1340	1650	1991
3methyl C5	9	22	46	45	56	92	145	235	302	403	493	636	809
hexene				57	87	122	165	180	191	225	242	257	295
n-C6	7	17	64	157	300	572	935	1496	1851	2418	2936	3521	4323
methyl cyc C5	2	5	23	87	160	285	438	679	845	1077	1297	1650	2034
benzene	20	35	89	141	189	240	292	321	339	423	490	607	777
thiophene	4	11	21	34	45	62	77	90	117	149	137	200	258
cyclohexane	4	8	21	40	64	97	133	177	201	239	255	299	357
2methyl C6 + dimethyl C5	5	11	38	71	127	145	291	427	516	645	701	825	959
3methyl C6	2	6	14	36	108	124	197	315	396	496	576	678	813
sum dimethylcyclo C5	6	15	32	78	145	258	397	609	756	959	1192	1475	1821
n-C7 +?	7	23	72	169	325	584	1073	1632	1970	2485	2930	3462	4093
methyl cyc C6	3	8	22	44	86	143	231	319	376	465	564	662	834
C3 cyc C5	1	3	8	26	56	107	180	293	367	472	609	732	937
toluene	18	29	89	156	232	357	561	773	945	1206	1526	1949	2413
methyl-thiophene		29	101	199	281	375	432	480	471	522	545	534	624
methyl-thiophene	4	11	35	33	50	82	111	134	149	196	201	222	250
i-C8	2	7	26	69	159	226	342	601	607	864	908	1007	1099
dimethyl cyc C6	1	3	11	34	65	111	166	259	322	400	460	534	616
C3 cyc C5	2	6	16	47	83	145	223	367	464	586	746	922	1081
n-C8	4	17	58	129	244	443	717	1118	1373	1700	1941	2295	2599
C4 cyc C5	2	7	31	62	100	158	217	301	358	444	630	717	795
trimethyl cyc C6 ?	1	7	27	51	75	108	136	162	185	225	239	273	298
ethyl-benzene + ethyl-thiophene	5	20	73	155	246	336	442	552	618	750	859	1005	1153
C2-thiophene		18	42	120	203	297	399	476	462	600	443		
m,p-xylene + C2-thiophene	15	33	89	190	279	406	555	720	875	1029	1417	2174	2536
dimethyl-thiophene	7	18	48	126	182	249	328	385	454	514	580	627	713
i-C9	1	5	18	33	57	166	225	302	361	428	403	462	485
dimethyl-thiophene	3	12	42	78	114	161	212	267	314	368	378	435	488
o-xylene	4	13	44	98	151	227	328	453	552	694	851	1049	1241
nonene	2	8	12	26	71	113	173	254	321	411	495	590	724
n-C9	3	9	38	95	191	341	561	896	1098	1374	1568	1810	1995
propyl-benzene	2	8	30	61	96	138	181	232	272	328	375	438	489
phenol ?	3	7	52	106	44	248	344	471	599	718	771	902	998
sum C3-thiophene	5	18	78	172	280	424	578	772	907	1066	1186	1380	1545
n-C10	1	7	29	78	163	306	506	790	1004	1231	1398	1594	1722
sum C3-benzene	9	39	145	321	563	763	1016	1331	1524	1755	1976	2299	2560
indane	1	6	28	58	88	128	166	215	234	273	287	336	359
sum C4-thiophene	4	17	77	171	231	401	572	788	997	1140	1288	1468	1917
sum C4benzene	6	25	101	226	367	542	746	829	816	415	474	1140	1226
m-indane	1	5	39	60	87	135	103	160	215	266	253	291	332
n-C11	2	8	37	93	175	322	514	794	983	1202	1345	1532	1638
C5-thiophene	1	2	14	35	54	80	139	212	126	292	173	376	396
methyl-indane ?	2	10	36	79	133	218	338	434	513	623	757	615	757
pentyl-benzene	1	6	12	39	98	160	223	299	327	381	417	316	332
C5-thiophene	2	10	45	97	134	221	332	379	480	535		182	231
naphthalin	3	8	19	40	59	101	161	242	305	356	452	554	639
sum dimethyl-indene	1	8	43	101	161	281	424	617	731	888	1073	1209	1261
n-C12	2	9	28	76	140	282	563	827	931	1069	1170	1244	1279
i-C13	1	5	25	64	114	263	261	418	404	418	436	634	628
methyl-benzothiophene		2	19	30	47	95	218	129	142	107	128	225	258
2methyl-naphthalin +?	4	14	47	134	194	283	360	451	510	591	702	809	907
methyl-benzothiophene	1	4	18	41	75	116	173	245	289	344	418	473	505
1methyl-naphthalin +?	3	9	32	68	113	182	239	409	369	525	610	694	746
n-C13	3	8	34	88	178	308	446	631	727	838	930	1009	1017
ethyl-benzothiophene	1	2	11	23	48	76	106	188	198	254	292	436	440
ethyl-naphthalin	1	6	18	26	49	123	171	223	276	314	357	420	431
n-C14+dimethylnaphthalin	4	15	66	125	204	329	484	693	830	975	1026	1131	1154
sum dimethyl-naphthalin	6	24	106	152	221	344	517	777	942	1091	1057	1273	1329
ethylmethyl-benzothiophene	1	8	35	79	116	183	254	357	410	469	470	519	526
n-C15	3	13	40	83	142	242	359	529	627	754	787	834	814
C3-benzothiophene	1	3	11	21	23	37	50	69	96	119	127	143	152
C3-naphthalin	1	5	11	24	33	57	80	116	140	179	179	213	226
alkyl-cyc C6 ?	1	6	21	44	75	117	168	205	233	270	249	264	249
n-C16	2	7	28	68	122	216	308	435	518	611	630	653	621
i-C18	1	3	19	47	77	113	146	181	192	222	177	150	128
n-C17	2	5	27	66	115	194	287	450	522	613	672	621	587
pristene	1	2	19	48	80	118	137	159	175	173	133	112	88
alkyl-cyc C6 ?	2	6	23	34	42	65	102	121	153	176	186	168	171
phenanthrene	1	3	15	22	51	76	111	144	164	197	173	156	138
n-C18	1	5	23	50	92	165	248	354	419	491	490	490	457
phytane		2	12	25	39	60	80	101	105	105	94	80	68
sum methyl-phenanthrene	3	14	61	72	148	154	303	352	386	469	563	591	598
n-C19	1	5	24	51	89	164	233	339	376	422	436	398	359
n-C20	2	6	27	60	100	176	265	351	379	433	519	427	386
n-C21	1	4	19	43	75	126	181	253	286	340	341	334	280
n-C22 + ?	1	3	16	39	62	107	162	233	249	306	286	279	227
n-C23		3	16	41	63	109	154	200	221	245	226	207	198
n-C24		2	12	29	50	88	114	161	185	196	155	137	105
n-C25		2	11	27	49	81	119	158	170	183	152	127	99
n-C26		1	10	26	44	72	101	128	143	154	118	90	72
n-C27		1	9	23	38	64	89	109	119	130	105	76	62
n-C28			7	17	29	50	71	84	93	98	73	53	41
n-C29			6	16	26	46	63	76	83	84	58	40	29
n-C30			4	12	19	33	44	56	60	58	38	24	17
sum	401	1157	4297	9374	15879	25705	38135	54683	64721	78325	92934	107798	126031

Table 19 continued (0.7 K/min)

temperature (°C)	455	460	465	470	480	490	495	500	520	540	560	580	600	620
(pg/g sample)														
C1	9721	11110	12212	13554	18180	22940	24282		34576	44980	57073	73480	85966	100616
n-C2	12257	14152	14886	16911	22808	33036	31834	33549	37167	40221	34976	25329	14688	2130
n-C3	12874	14870	18934	20332	28520	38319	36256	43394	36199	21995	7854	1324	551	129
i-C4	2971	3430	3823	4174	5946	7545	7566	7734	6406	2919	476	164		
n-C4	10974	12834	13343	14660	19929	22100	19266	18163	6728	770	333	124		22
neopentane	155	159	182	166	165	131	128	153	70	160	45	26	16	7
i-C5	3243	3709	3782	4164	4746	4017	3146	2470	362	130	20	15	11	7
n-C5	7234	7783	8075	8924	9602	7037	4980	3475	402	143	68			
pentene	1268	1391	1317	1157	1006	700	526	418	126	72	14	10	4	1
cyclopentane	1044	1181	1247	1401	1705	1611	1470	1271	460	67	7			
2methyl C5	2101	2159	1989	1803	1083	388	230	168	83	23	8	2	2	1
3methyl C5	884	919	905	840	620	281	152	94	24	4	2			
hexene	269	302	239	210	125	75	46	33	10					
n-C6	4605	4912	4860	4848	4012	2092	1224	626	40	10	8	2	3	1
methyl cyc C5	2264	2615	2791	3068	3403	2868	2234	1649	189	9	3			
benzene	864	1060	1078	1223	1502	1782	1768	1723	1999	2591	2930	3907	4965	2692
thiophene	264	300	278	289	355	455	454	429	477	471	63		50	3
cyclohexane	366	384	386	392	395	346	276	231						
2methyl C6 + dimethyl C5	953	878	712	580	258	109	66	50	10					
3methyl C6	797	759	610	475	183	76	46	36						
sum dimethylcyclo C5	1947	2106	2114	2124	1760	1014	554	344	12	5		6		
n-C7 +?	4151	4270	3831	3650	2272	812	336	153	14	6	7			
methyl cyc C6	875	958	927	988	857	566	330	212	8	11	3			
C3 cyc C5	998	1092	1053	1052	740	324	138	74	5					
toluene	2668	3215	3420	3963	5277	6479	6376	6317	6629	6695	5306	3724	2048	215
methyl-thiophene	567	573	508	518	482	522	416	366	223					
methyl-thiophene	273	292	305	343	417	468	516	509	453	305	121	15	13	2
i-C8	1007	892	619	454	126	43	24	22						
dimethyl cyc C6	589	565	472	414	230	122	60	40	13	8	15	7		
C3 cyc C5	1076	1089	933	800	353	106	34	3	4					
n-C8	2542	2549	2241	2005	1043	252	80	31	12	9	7	6		
C4 cyc C5	789	740	630	546	276	90	36	18	3	2	2	4		
trimethyl cyc C6 ?	282	258	203	167	76	24	8	3			2			
ethyl-benzene + ethyl-thiophene	1207	1341	1332	1402	1495	1522	1374	1291	954	704	471	273	81	4
C2-thiophene														
m,p-xylene + C2-thiophene	2663	2988	3075	3404	4059	4576	4490	4386	4260	3620	2166	858	182	12
dimethyl-thiophene	678	662	613	604	550		432	319	178	31	36	53	5	1
i-C9	413	341	238	190	62	14			35		17			
dimethyl-thiophene	470	448	427	404	373	357	266	254	109	28	7	4	1	
o-xylene	1326	1467	1516	1647	1931	2105	1994	1889	1609	1052	455	126	31	6
nonene	634	636	529	449	234	133	110	92	64	27	20	12		
n-C9	1981	1864	1556	1294	493	64	16	5	9	8	2	3		
propyl-benzene	500	509	435	407	306	199	170	104	38	19	14	7	2	
phenol ?	1040	1043	993	982	1050	1107	1016	1064	819	559	208	73	18	1
sum C3-thiophene	690	1683	1627	1694	1748	1711	1550	1400	1033	678	431	131	18	3
n-C10	1733	1580	1218	934	282	46	6	10						
sum C3-benzene	2580	2737	2575	2963	3160	3160	3090	2780	2204	1346	432	98	11	0
indane	373	394	352	338	291	217	154	125	62	46	25	14	6	
sum C4-thiophene	1985	2033	1739	1754	1645	1658	1492	1360	768	443	64	28	1	
sum C4benzene	656	1078	579	534	483	434	236	500	264	54	14	7		
m-indane	339	356	323	305	178			334	199	96	26	3		
n-C11	1616	1474	1079	822	296	134	106	91	45	18	3			
C5-thiophene	385	410	343	305	233	162	114	94	40	42				
methyl-indane ?	782	760	682	694	563	430	384	269	213		2	5	1	
pentyl-benzene	320	98	251	220	168	158	138	121	61					
C5-thiophene	241	270	306	156	75	63	48	42	21	10	4	1		
naphthalin	548	652	698	733	942	1121	1128	1301	1507	1829	1774	1408	941	212
sum dimethyl-indene	1163	1135	964	811	516	329	234	195	46	26	31	26	9	2
n-C12	1185	1045	827	584	124	22	16	59	39	34	18	10	1	
i-C13	562		472	381	294	195	140	111	33	10	3	4	2	
methyl-benzothiophene	222	287	233	207	139	237	286	298	241	201	68	30	8	
2methyl-naphthalin +?	927	1000	1068	1090	1203	1520	1560	1745	1738	1613	901	307	91	17
methyl-benzothiophene	497	505	460		433	210	202	201	183		87	21	7	1
1methyl-naphthalin +?	754	800	776	838	989	1026	1008	1082	958	692	320	92	41	14
n-C13	940	805	619	439	87	37	30	29	11	10	4	2	1	
ethyl-benzothiophene	391	328	246	214	144	108	90	76	42	16	5	1		
ethyl-naphthalin	436	444	410	412	416	394	362	338	283	214	143	38	4	1
n-C14+dimethylnaphthalin	1123	997	769	667	452	403	376	340	272	145		4		
sum dimethyl-naphthalin	1409	1378	1275	1276	1294	1350	1270	1103	828	408	97	15	2	0
ethylmethyl-benzothiophene	502	490	398	401	340	292	258	202	137	73	41	26	13	
n-C15	756	614	317	193	156	115	102	89	58	23	6			
C3-benzothiophene	155	154	141	151	144	130	114	97	58	20	3			
C3-naphthalin	223	219	188	207	173	158	132	96	52	18	3			
alkyl-cyc C6 ?	241	229	169	158	118	100	84	70	53	27	17	13	6	
n-C16	555	421	266	182	66	64	80	35	21	10	4	2		
i-C16	102	72	24	44	28	27	20	19	11	5	1			
n-C17	485	349	202	126	25	18	14	10	5	2	1			
pristene	68	45	37	32						13	5	2		
alkyl-cyc C6 ?	164	169	158	160	189	226	226	225	331	369	301	274	268	123
phenanthrene	122	101	79	68	67	83	70	69	70	66	43	26	23	1
n-C18	384	283	165	107	54	59	52	46	40	22	4	1	2	
phytane	62	54	44	37	37	42	30	29	22	8	1			
sum methyl-phenanthrene	502	596	479	482	495	533	488	412	459	344	166	89	47	78
n-C19	287	193	98	50	26	32	22	24	25	9	4	2	1	
n-C20	321	243	114	89	74	60	72	57	50	23	8			
n-C21	231	154	78	45	22	19	16	7	8	3				
n-C22 + ?	192	128	66	51	36	37	38	22	10	29	11	7		
n-C23	140	85	45	24	21	20	14	7	7	5				
n-C24	80	40	12	4	6	10	2	1						
n-C25	82	44	13	11	4	4	2	1						
n-C26	54	24	5	3	1	1	1							
n-C27	44	21	2	1	2	2								
n-C28	30	14	1	1	2	1								
n-C29	20	8	1		1									
n-C30	11	4												
sum	131454	141808	142612	147976	167247	183985	170581	148684	153287	136654	117810	112241	110141	106302

Table 19 continued: MSSV pyrolysis, individual components (5.0 K/min).

E 43254 MK (-S1) Draupne Formation
extracted kerogen well B
TOC = 44.8% depth 2764.70m

temperature (°C)	300	350	370	390	400	410	420	425	430	435	440	445	450
(µg/g sample)													
C1	1	32	113	349	546	813	1177	1376	1659	2101	2440	2729	3353
n-C2	16	66	148	366	595	905	1325	1615	1925	2529	2878	3243	4026
n-C3	13	55	125	336	568	902	1351	1629	2028	2615	3074	3545	4421
i-C4	4	11	24	55	91	135	221	240	315	407	516	549	697
n-C4	36	63	136	239	399	625	985	1048	1461	1909	2221	2532	3102
neopentane	14	17	22	33	44	54	64	86	94	114	124	131	124
i-C5	15	21	42	49	156	150	302	345	396	526	605	648	798
n-C5	26	34	43	113	202	336	496	616	780	1045	1230	1445	1765
pentene	8	20	39	89	143	219	296	372	411	495	527	611	661
cyclo pentane	1	5	8	20	36	60	98	115	141	172	205	227	270
2methyl C5	22	55	64	72	117	182	217	278	317	413	470	529	658
3methyl C5	6	12	21	32	25	41	62	73	90	118	142	154	201
hexene	6	10	18	33	56	89	104	138	143	171	181	212	215
n-C6	5	14	28	74	132	216	338	426	534	728	895	1032	1323
methyl cyc C5	2	4	10	41	78	113	172	195	241	329	384	421	530
benzene	30	39	67	130	169	218	247	293	310	373	382	418	438
thiophene	5	13	21	29	42	53	69	78	85	103	112	116	126
cyclo hexane	3	7	16	36	53	57	77	89	101	114	124	134	154
2methyl C6 + dimethyl C5	3	8	17	38	51	73	108	138	142	195	233	305	369
3methyl C6		6	10	16	31	44	82	100	120	159	188	208	260
sum dimethyl cyclo C5	6	12	54	43	78	121	180	217	254	342	390	431	526
n-C7 +?	6	12	35	92	158	238	382	471	564	784	895	1003	1241
methyl cyc C6		6	13	25	42	61	90	104	121	158	172	225	256
C3 cyc C5		3	4	12	22	36	62	73	92	132	153	176	234
toluene	14	26	49	106	160	217	271	352	408	524	636	720	821
methyl-thiophene			56	127	190	248	338	373	407	481	486	492	521
methyl-thiophene	2	10	13	26	38	53	74	85	95	126	141	148	163
i-C8		5	11	33	55	87	140	170	200	277	312	352	425
dimethyl cyc C6		3	5	13	23	35	62	70	85	119	141	153	191
C3cyc C5		7	11	22	44	71	102	132	153	201	220	250	322
n-C8	11	24	37	68	122	196	290	373	445	609	712	808	989
C4 cyc C5			16	40	58	88	117	130	146	182	191	211	248
trimethyl cyc C6 ?			54	45	51	86	96	114	113	144	152	158	168
ethyl-benzene + ethyl-thiophene	4	16	38	94	155	222	300	353	393	481	527	563	632
C2-thiophene				54	100	165	234	285	325	405	436	476	530
m,p-xylene + C2-thiophene	26	53	49	109	166	247	324	390	427	514	576	634	712
dimethyl-thiophene	3	13	28	65	45	196	211	262	255	308	293	31	388
i-C9	1	2	5	20	33	54	94	102	117	154	230	248	278
dimethyl-thiophene	2	8	22	50	78	111	141	161	178	219	239	252	276
o-xylene	2	9	21	53	83	123	169	199	246	313	355	396	466
nonene	1	4	8	14	26	35	52	59	60	75	164	186	231
n-C9	3	6	17	43	83	137	219	270	335	456	531	610	764
propyl-benzene	2	6	15	38	63	91	122	138	160	196	208	227	257
phenol ??	2	7	15	34	62	88	127	152	177	340	373	399	470
sum C3-thiophene	2	10	32	86	156	238	320	375	434	549	591	644	744
n-C10	1	6	15	34	66	117	194	238	306	428	496	560	714
sum C3-benzene	4	27	76	177	342	482	666	764	881	1065	1172	1214	1525
indane		4	15	38	60	84	115	123	143	178	189	186	230
sum C4-thiophene		12	32	84	156	229	314	350	393	659	615	755	917
sum C4-benzene		13	46	117	154	272	395	531	513	741	710	870	841
methyl-indane		3	17	36	59	82	116	129	148	188	213	228	248
n-C11		6	17	44	81	133	210	261	317	428	507	563	689
C5-thiophene		2	8	20	35	52	78	85	99	142	166	168	184
methyl-indane ?		6	23	46	75	113	168	190	222	290	324	352	410
pentyl-benzene		4	12	21		86	121	142	159	206	229	239	275
C5-thiophene		5	19	47	88	129	174	222	221	305	329	337	412
naphthalin		6	13	19	31	47	67	75	89	130	150	162	190
sum dimethyl-indene		8	21	55	41	139	207	248	271	402	458	498	603
n-C12		7	22	46	83	99	212	260	314	392	544	593	702
i-C13		3	12	31	56	83	136	152	171	262	282	300	451
methyl-benzothiophene		1	7	20	32	47	80	95	146	162	253	271	195
2 methyl-naphthalin + ?		8	21	43	76	103	232	163	284	220	221	410	472
methyl-benzothiophene					43		99	110	133	187	206	225	238
1 methyl-naphthalin + ?		6	17	35	64	94	138	165	186	248	271	290	339
n-C13		6	18	42	78	128	216	265	322	425	475	512	604
ethyl-benzothiophene		1	7	14	26	48	53	68	76	106	114	117	131
ethyl-naphthalin		3	7	18	50	49	50	76	102	173	192	215	168
n-C14+dimethylnaphthalin		10	31	76	136	190	249	300	142	237	235	268	349
sum dimethyl-naphthalin		16	55	74	212	258	334	373	423	519	556	647	772
ethylmethyl-benzothiophene		4	20	53	86	142	167	196	213	242	295	336	357
C15		8	27	57	92	139	198	233	249	313	392	441	488
C3-benzothiophene		3	7	10	19	26	37	31	49	53	56	63	88
C3-naphthalin		4	12	16	22	39	52	67	68	86	93	109	114
alkyl-cyc C6 ?		2	12	24	44	66	94	110	126	159	184	199	239
n-C15		5	14	31	58	90	149	176	196	265	298	330	382
i-C16		3	9	23	37	62	79	107	108	131	139	152	157
n-C17		5	14	32	58	89	137	161	191	252	292	321	397
pristene		2	7	24	42	55	82	84	97	125	120	134	133
alkyl-cyc C6 ?		6	16	20	33	46	53	103	62	90	86	133	97
phenanthrene		4	10	11	20	32	61	76	82	99	112	138	139
n-C18		6	13	24	45	69	107	134	154	199	234	263	302
phytane		3	8	12	21	32	48	62	59	76	83	89	92
sum methyl-phenanthrenes		3	20	53	104	126	206	246	160	216	329	322	461
n-C19		3	11	23	44	67	107	128	153	205	236	268	304
n-C20		4	13	29	54	82	117	146	166	222	256	302	319
n-C21		2	9	21	37	60	90	109	123	162	176	201	228
n-C22 + ?		2	7	18	33	50	72	93	104	138	163	175	194
n-C23		2	6	17	32	51	74	94	100	134	141	163	179
n-C24		2	5	14	25	39	59	74	84	110	120	126	135
n-C25		3	5	14	23	39	57	70	81	103	119	118	123
n-C26		1	4	12	23	37	50	61	71	90	101	103	109
n-C27			3	10	20	33	43	53	63	80	93	88	95
n-C28			3	8	16	26	34	39	47	59	66	70	69
n-C29			2	6	14	24	31	37	43	53	66	59	61
n-C30			2	5	12	17	23	30	30	37	40	42	43
sum	308	974	2350	5164	8681	13131	19158	22783	26423	34499	39234	43698	52308

Table 19 continued (5.0 K/min)

temperature (°C)	455	460	470	475	480	490	500	510	530	550	570	610	630
(µg/g sample)													
C1	3894	4489	6381	7037	7878	10000	11455	14740	22045	30831	40443	59137	74145
n-C2	4641	5479	7725	8405	9594	12188	13623	18115	26233	35197	39251	30988	22982
n-C3	5101	6076	8464	9569	10978	14544	15529	18906	26942	30473	24026	2251	701
i-C4	823	917	1421	1529	1774	2368	2716	3512	5271	5856	2920	134	
n-C4	3640	4310	5860	6453	7666	9648	11270	13709	15044	7278	1838	242	166
neopentane	135	150	139	159	165	163	166	184	182	124	132	110	63
i-C5	935	1057	1579	1744	1965	2427	2750	2981	2399	498	185	100	25
n-C5	2135	2460	3567	3830	4422	5340	6035	6313	3765	413	255	14	8
pentene	745	899	964	1066	1237	1230	1460	1309	800	211	124		
cyclo pentane	315	335	470	513	579	717	895	1104	1280	664	114	2	5
2methyl C5	767	847	1152	1218	1315	1355	1280	805	242	84	41		
3methyl C5	243	263	415	456	490	567	559	415	136	26	10		2
hexene	244	289	293	293	342	267	268	130	68	18		6	
n-C6	1572	1821	2506	2649	3014	3260	3483	2921	940	66	20	2	2
methyl cyc C5	633	701	1032	1138	1305	1630	1998	2300	1954	332	21	14	25
benzene	483	572	637	652	828	957	1242	1490	1865	1914	2361	3588	4986
thiophene	171	158	201	180	205	235	336	368	588	694	831	507	372
cyclo hexane	162	188	199	202	225	231	270	279	231	64			
2methyl C6 + dimethyl C5	423	476	583	583	584	524	444	216	69	11			
3methyl C6	300	350	484	474	475	449	346	142	58	9	6	4	3
sum dimethyl cyclo C5	619	700	1010	1066	1195	1355	1429	1212	486	32	9	8	4
n-C7 +?	1587	1932	2579	2747	2994	2965	2833	1904	305	18	9	5	4
methyl cyc C6	288	338	423	464	536	614	669	638	307	12	2	19	21
C3 cyc C5	273	326	499	545	612	734	740	603	150	18	4		6
toluene	1022	1228	1702	1798	2146	2702	3196	4285	5851	6296	6627	5336	4435
methyl-thiophene	540	646	581	530	577	516	573	616	705	683	322		
methyl-thiophene	181	190	242	206	256	260	322	463	587	589	577	145	59
i-C8	474	533	756	710	587	525	346			5			
dimethyl cyc C6	217	253	337	364	370	351	294	183	56			10	2
C3cyc C5	394	460	665	699	770	745	615			2	4	4	3
n-C8	1147	1314	1664	1678	1744	1679	1496	855	117	21	31	21	17
C4 cyc C5	279	317	407	522	516	486	426	251	44	11	10		3
trimethyl cyc C6 ?	194	216	229	211	229	188	148	74	9	2	1		3
ethyl-benzene + ethyl-thiophene	705	774	939	949	1053	1144	1285	1443	1531	1321	961	382	214
C2-thiophene	612	646	702	738	633								
m,p-xylene + C2-thiophene	771	914	1189	1192	1583	2424	2804	3376	4084	4152	3824	1730	833
dimethyl-thiophene	400	476	569	483	578	518	595	546	556	389	165	31	18
i-C9	292	319	315	288	301	175	120	75	43	19			
dimethyl-thiophene	318	342	426	442	407	450	435	392	365	257	118	9	12
o-xylene	548	633	861	917	1029	1202	1372	1552	1803	1709	1341	292	101
nonene	282	322	436	451	469	416	338	206	145	97	70	13	8
n-C9	896	1026	1302	1317	1325	1221	996	433	19	9	9	5	2
propyl-benzene	295	328	392	391	420	414	433	313	177	79	32	8	5
phenol ??	560	623	768	758	787	909	906	898	1000	832	539	271	175
sum C3-thiophene	860	953	1120	1123	1253	1269	1341	1459	1669	1577	936	217	0
n-C10	837	942	1194	1148	1143	1004	761	274					4
sum C3-benzene	1574	1755	2097	2298	2525	2642	2779	2872	2934	2485	1833	310	123
indane	241	261	308	298	331	345	365	355	283	146	81	21	16
sum C4-thiophene	972	1094	1245	999	1052	1093	1788	1719	1544	1394	901	68	5
sum C4-benzene	1098	1033	1061	1026	1028	852	524	459	382	216	93	36	15
methyl-indane	315	325	413	417	644	654	412	279	320	283	166	12	2
n-C11	797	909	1129	1101	1046	919	680	283	118	118	70	2	1
C5-thiophene	235	256	355	350	338	360	346	293	211	183	206	6	
methyl-indane ?	621	704	749	907	947	997	1007	894	432	103	48		
pentyl-benzene	299	329	249	369	329	283	227	152	141				
C5-thiophene	421	452	425		526	200	92	243	240	201	100	6	
naphthalin	226	266	417	496	475	504	574	653	974	1428	1720	1729	1670
sum dimethyl-indene	707	816	1101	1056	1075	972	963	616	361	0	11	8	6
n-C12	816	920	1112	1007	852	758	510	122	84	76	41	32	6
i-C13	375	405	459	367	318	505	412	246	33	31	15	5	
methyl-benzothiophene	346	377	477	347	339	502	311	206					
2 methyl-naphthalin + ?	519	579	715	741	759	845	975	1053	1461	1734	1808	943	484
methyl-benzothiophene	308	244	302	324	318	433	464	405	418	390	324		
1 methyl-naphthalin + ?	381	401	535	602	581	680	730	757	1004	1067	997	336	145
n-C13	672	741	845	824	760	604	462	73	23	6			
ethyl-benzothiophene	193	304	352	358	362	354	220	157	125	78	42	6	72
ethyl-naphthalin	258	290	357	261	195		391	392	502	433	365		
n-C14+dimethylnaphthalin	703	756	873	838	800	1074	590	422	414	334			
sum dimethyl-naphthalin	836	852	1072	1013	799	427	1095	1114	1329	1577	832	304	90
ethylmethyl-benzothiophene	431	423	477	448	480	427	419	386	371	256	80	41	33
C15	596	605	639	596	539	422	310	99	114	87	49	4	1
C3-benzothiophene	83	94	125	133	132	135	139	126	137	93	48	2	1
C3-naphthalin	141	148	193	176	182	189	189	172	169	112	51	2	1
alkyl-cyc C6 ?	245	248	266	238	226	190	180	148	135	88	54	14	13
n-C16	426	458	492	445	411	290	167	76	43	31	47	2	2
i-C16	156	156	123	102	88	57	43	32	29	20	11		1
n-C17	443	490	476	425	387	245	119	39	28	18	5		
pristene	128	128	103	39	59	42	38	37	30	22	18		10
alkyl-cyc C6 ?	145	139	139	156	139	133	124	145	202	274	373	446	476
phenanthrene	150	146	140	104	98	70	69	69	95	105	88	62	59
n-C18	343	372	384	343	308	231	95	47	55	51	34	5	1
phytane	98	96	83	56	58	36	38	37	43	36	18		
sum methyl-phenanthrenes	341	462	530	456	476	413	427	438	412	426	369	254	199
n-C19	326	365	354	277	233	110	54	7	2		2		
n-C20	376	365	360	269	236	131	80	42	40	28	14		
n-C21	255	277	269	216	183	101	45	33	25	18	8		
n-C22 + ?	205	214	239	154	131	68	42	35	46	55	66	33	29
n-C23	182	196	181	122	99	51	21	11	18	22			
n-C24	148	149	120	87	67	27	4	1	0.2				
n-C25	138	143	115	84	67	31	8	6	11				
n-C26	118	117	82	55	40	13	2	1	2				
n-C27	106	102	68	44	32	10	1	0	2				
n-C28	82	80	51	32	23	8	0	2					
n-C29	68	63	38	22	16	5	1						
n-C30	46	45	25	12	8	2	1						
sum	60642	68738	88099	90977	99671	111804	119131	127744	145463.2	146918	139157	110294	112875

Table 20: Multistep open system pyrolysis, Heather Formation well G 2138,75m (5.0 K/min)											
temperature (°C)	**350**	**370**	**390**	**410**	**430**	**450**	**470**	**490**	**510**	**540**	**570**
totals	µg/g sample										
C2-5	406	508	1015	1536	2682	3968	4919	6191	6726	7433	7438
C1	0	2	92	275	554	1043	1447	2513	3234	4095	4552
C1-5	406	508	1107	1811	3236	5011	6366	8704	9960	11528	11990
C6-14	715	603	1789	3148	6088	8946	8883	11447	12612	14094	13356
C15-32	0	0	330	1100	2850	5000	3750	6500	7260	8631	7300
C6+	715	603	2119	4248	8938	13946	12633	17947	19872	22725	20656
C1+	1121	1111	3226	6059	12174	18957	18999	26651	29832	34253	32646

Table 21: Multistep open system pyrolysis Draupne Formation well B 2764,7m (5.0 K/min)										
temperature (°C)	**370**	**400**	**410**	**420**	**430**	**440**	**450**	**470**	**490**	**530**
totals (µg/g sample)										
C1	111	409	509	798	1238	1751	2209	3181	4487	7398
C2-4	481	1568	2238	3646	5457	7607	9862	12770	17159	17784
C5	276	771	1054	1582	2410	2983	3507	4104	5197	5713
C1-5	868	2748	3801	6026	9105	12341	15578	20055	26843	30895
C6-14	2520	9405	12954	21420	26885	35488	41910	47685	54561	55710
C15+	2025	8790	14003	29310	36840	56014	59798	68072	67500	75502
C6+	4545	18195	26957	50730	63725	91502	101708	115757	122061	131212
C1+	5413	20943	30758	56756	72830	103843	117286	135812	148904	162107

Table 22: Compositional Kinetic Parameters.

Heather Formation
well: G
depth: 2138,75m

MSSV pyrolysis

boiling range	C6-14		C2-5		C1-5 primary		C1-5 secondary A (C6+)	
error/ least square	0.014966194		0.000924036		0.02128119		0.004529774	
freq. factor (1/min)	*		*		*		*	
	Akt. energy (kcal/mol)	potential (mg/g)	Akt. energy (kcal/mol)	potential (mg/g)	Akt. energy (kcal/mol)	potential (mg/g)	Akt. energy (kcal/mol)	potential (mg/g)
	46	0	46	0	46	0	46	0
	47	0	47.4	0	47	0	47.4	0
	48	0	48.8	0	48	0	48.8	0
	49	0	50.2	0	49	0	50.2	0
	50	0	51.6	0	50	0	51.6	0
	51	0	53	0	51	0	53	0
	52	0	54.5	0	52	0	54.5	0
	53	0	55.9	0	53	0.39	55.9	0
	54	0	57.3	0.01	54	0.01	57.3	0
	55	0	58.7	0	55	0.68	58.7	0
	56	0.21	60.1	0	56	0.1	60.1	0
	57	0	61.5	0.16	57	1.18	61.5	0.04
	58	0.83	63	0.18	58	0	63	0.4
	59	1.01	64.4	0.33	59	1.43	64.4	0.36
	60	1.61	65.8	0.42	60	0.55	65.8	0.55
	61	0	67.2	0.74	61	1.43	67.2	0.32
	62	0.26	68.6	0.94	62	1.6	68.6	0.29
	63	0.22	70	0.71	63	1.46	70	0.31
	64	0	71.5	0.44	64	0.78	71.5	0.05
	65	0	72.9	0.31	65	0.99	72.9	0
	66	0	74.3	0.03	66	0.08	74.3	0
	67	0	75.7	0	67	0	75.7	0
	68	0	77.1	0.03	68	0	77.1	0
	69	0	78.5	0.01	69	0	78.5	0
	70	0	80	0.01	70	0	80	0

* Frequency factors can be requested from the author or the supervisor. For resons of confidentiality they are not included here.

Table 23: Compositional Kinetic parameters

Draupne Formation
well: B
depth: 2764,7m

MSSV pyrolysis

boiling range	C6+		C1-5		C1-5 primary		C1-5 secondary A (C6+resolved)		C1-5 secondary B (C6+hump)	
error/ least square	11.06106		9.887239		1.50672		13.42117		3.436199	
freq. factor (1/min)	*		*		*		*		*	
	Akt. energy (kcal/mol)	potential (mg/g)	Akt. energy (kcal/mol)	potential (mg/g)	Akt. energy (kcal/mol)	potential (mg/g)	Akt. energy (kcal/mol)	potential (mg/g)	Akt. energy (kcal/mol)	potential (mg/g)
	46	0	46	0	46	0.56	46	0	46	0
	47	0	47	0	47	2.2	47	0	47	0
	48	0	48	0	48	2.28	48	0	48	0
	49	0	49	0	49	6.43	49	0	49	0
	50	0	50	0	50	1.71	50	0	50	0
	51	0	51	0	51	11.05	51	0	51	0
	52	0	52	0	52	5.4	52	0	52	0
	53	0	53	1.11	53	0	53	0	53	0
	54	0	54	0	54	25.49	54	0	54	0
	55	0	55	0.05	55	10.59	55	0	55	0
	56	18.49	56	1.49	56	8.13	56	0	56	0
	57	0	57	0	57	3.3	57	0	57	0
	58	0	58	6.68	58	0	58	0	58	0
	59	78.29	59	3.15	59	0	59	0	59	0
	60	0.98	60	10.11	60	0	60	0	60	0
	61	43.5	61	20.49	61	0	61	0	61	0
	62	14.83	62	0	62	0	62	42.6	62	0
	63	6.02	63	21.33	63	0	63	0	63	0
	64	0	64	64.79	64	0	64	0	64	0
	65	0	65	0	65	0	65	0.56	65	0
	66	0	66	31.29	66	0	66	17.13	66	0
	67	0	67	3.53	67	0	67	0	67	0
	68	0	68	0	68	0	68	0	68	0
	69	0	69	0	69	0	69	2.49	69	0
	70	0	70	0	70	0	70	0	70	28.29
									71	8.82
									72	0
									73	5.7
									74	0
									75	1.61
									76	1.06
									77	0.08
									78	0
									79	0
									80	1.64

* frequency factors can be requested from the author or supervisor. For reasons of confidentiality they are not included here.

Table 26: Headspace gas (µl gas / kg rock)

Well	Depth (m)	TOC (%)	C1	C2	C3	C4	C5-7	Sum C1-C4	Sum C2-C4	% wet	iC4/nC4	C1/C2	iC4	nC4
K	4180	2.10	2876	5375	15859	22752	34563	46862	43986	93.9	0.33	0.54	5608	17144
I	3485	0.94	786	967	4144	3216	2026	9113	8327	91.4	0.27	0.81	679	2537
	3500	2.90	196	370	1834	1701	1251	4101	3905	95.2	0.28	0.53	367	1334
	3515	4.55	4377	5483	15184	9342	5189	34386	30009	87.3	0.27	0.80	1973	7369
	3545	5.16	7221	7633	20069	12034	6130	46957	39736	84.6	0.25	0.95	2430	9604
	3560	4.64	7853	8191	22630	14623	8224	53297	45444	85.3	0.25	0.96	2906	11717
	3635	3.19	5463	4111	9216	5238	2738	24028	18565	77.3	0.28	1.33	1147	4091
	3650	2.10	3481	2717	7191	5024	2956	18413	14932	81.1	0.28	1.28	1102	3922
	3665	3.21	9883	4765	7459	4081	2159	26188	16305	62.3	0.29	2.07	918	3163
F	2067	0.72	15309	4558	13502	28342	47358	61711	46402	75.2	0.35	3.36	7277	21065
	2085	0.96	25280	12982	43233	71668	74770	153163	128000	83.5	0.37	1.95	19475	52193
	2160	0.99	21650	8828	24002	31203	32322	85683	64033	74.7	0.41	2.45	9103	22100
	2175	1.04	45722	20941	60249	70004	54420	196916	151000	76.8	0.42	2.18	20580	49424
	2220	1.36	30126	20854	31714	16394	7069	99088	68962	69.6	0.49	1.44	5401	10993
G	2065	1.52	9286	5573	14240	13837	9265	42936	33650	78.4	0.43	1.67	4192	9645
	2080	2.33	58883	28052	51781	31665	16021	170381	111000	65.4	0.49	2.10	10458	21207
	2170	2.75	4948	7423	13422	8956	5248	34749	29801	85.8	0.48	0.67	2920	6036
	2200	2.67	22776	16637	32461	26973	17781	98847	76071	77	0.5	1.37	8966	18007
	2245	1.75	15913	10968	27477	28883.9	21958		67328.9	90.5	0.47	1.45	9283.9	19600
	2260	1.62	19279	9345	21224	22012	16791	71860	52581	73.2	0.47	2.06	7011	15001
	2425	1.37	4187	3275	7547	8690	10807	23699	19512	82.3	0.44	1.28	2647	6043
	2440	1.24	1506	1258	4049	5078	5831	11891	10385	87.3	0.39	1.20	1417	3661
	2455	0.92	585	980	3950	4564	7332	10079	9494	94.2	0.37	0.60	1241	3323
	2560	1.23	4542	2349	4048	3233	2370	14172	9630	68	0.62	1.93	1233	2000
	2575	1.83	7054	3719	4222	2184	929	17179	10125	58.9	0.81	1.90	976	1208
	2605	1.80	7627	7990	5448	2888	1632	23953	16326	68.2	0.83	0.95	1310	1578
P	4660	4.90	45967	4115	530	123	34	50735	4768	9.4	1.32	11.17	70	53
	4675	5.37	48924	3888	447	81	14	53340	4416	8.3	1.89	12.58	53	28
	4795	4.06	28554	1680	197	39	4	30470	1916	6.3	2	17.00	26	13
	4825	4.50	35276	2437	286	61	8	38060	2784	7.3	2.21	14.48	42	19
	4870	3.48	28872	3260	365	86	17	32583	3711	11.4	3.1	8.86	65	21
	4900	3.56	58196	3243	231			61705	3509	5.7		17.95	35	
	5065	4.25	60326	3415	368	82	8	64191	3865	6	2.9	17.67	61	21
	5080	3.89	33199	1810	178	30	4	35217	2018	5.7		18.34	30	0

Table 26 continued: Occluded gas (µl gas / kg rock)

Well	Depth (m)		TOC (%)	C1	C2	C3	C4	C5-7	Sum C1-C4	Sum C2-C4	% wet	iC4/nC4	C1/C2	iC4	nC4
K	4180	c	2.10	861	205	757	2616	13780	4439	3578	80.6	0.2	4.20	431	2185
I	3485	c	0.94	50	34	517	1487	4220	2088	2038	97.6	0.15	1.47	191	1296
	3500	c	2.90	49	94	1823	4650	8940	6616	6567	99.3	0.17	0.52	677	3973
	3515	c	4.55	105	767	8403	14958	21417	24233	24128	99.6	0.19	0.14	2337	12621
	3545	c	5.16	187	1311	11570	18826	23353	31894	31707	99.4	0.18	0.14	2821	16005
	3560	c	4.64	164	1163	10739	19123	25281	31189	31025	99.5	0.18	0.14	2874	16249
	3635	c	3.19	183	531	4528	7690	12322	12932	12749	98.6	0.17	0.34	1091	6599
	3650	c	2.10	80	99	1177	2520	4906	3876	3796	97.9	0.15	0.81	329	2191
	3665	c	3.21	163	561	2282	2094	2452	5100	4937	96.8	0.17	0.29	309	1785
F	2067	c	0.72	131	62	355	1170	5773	1718	1587	92.4	0.19	2.11	185	985
	2085	c	0.96	182	26	87	313	2822	608	426	70.1	0.14	7.00	38	275
	2160	c	0.99	163	57	319	1015	4110	1554	1391	89.5	0.2	2.86	168	847
	2175	c	1.04	144	74	509	1520	5491	2247	2103	93.6	0.2	1.95	255	1265
	2220	c	1.36	70	137	740	1026	1324	1973	1903	96.5	0.21	0.51	179	847
G	2065	c	1.52	118	121	755	1719	5280	2713	2595	95.7	0.25	0.98	343	1376
	2080	c	2.33	233	330	1769	3247	6318	5579	5346	95.8	0.28	0.71	702	2545
	2170	c	2.75	312	884	4168	6192	9870	11556	11244	97.3	0.28	0.35	1344	4848
	2200	c	2.67	433	877	3978	7341	13510	12629	12196	96.6	0.26	0.49	1532	5809
	2245	c	1.75	355	374	2052	4599	9662	7380	7025	95.2	0.24	0.95	887	3712
	2260	c	1.62	289	297	1603	3796	9530	5985	5696	95.2	0.23	0.97	710	3086
	2425	c	1.37	145	24	135	430	1763	734	589	80.3	0.12	6.04	45	385
	2440	c	1.24	78	11	54	165	630	308	230	74.7	0.15	7.09	22	143
	2455	c	0.92	77	17	166	353	742	613	536	87.4	0.19	4.53	56	297
	2560	c	1.23	116	46	195	313	699	670	554	82.7	0.23	2.52	59	254
	2560	s	1.83	4658	2395	4243	3546	3069	14842	10184	68.6	0.57	1.94	1292	2254
	2575	c	1.80	94	151	527	546	711	1318	1224	92.9	0.3	0.62	126	420
	2605	c	4.90	76	129	472	456	625	1133	1057	93.3	0.35	0.59	117	339
P	4660	c	5.37	7736	6219	1509	344	108	15808	8072	51.1	1.77	1.24	220	124
	4675	c	4.06	9536	6422	1300	227	39	17485	7949	45.5	2.24	1.48	157	70
	4795	c	4.50	13242	6378	1494	323	80	21437	8195	38.2	2.05	2.08	217	106
	4825	c	3.48	6173	2759	889	249	64	10070	3897	38.7	1.93	2.24	164	85
	4870	c	3.56	3495	2735	747	191	47	7168	3673	51.2	2.6	1.28	138	53
	4900	c	4.25	6491	3586	672	151	36	10900	4409	40.5	3.08	1.81	114	37
	5065	c	3.89	6652	2889	844	220	47	10605	3953	37.3	2.33	2.30	154	66
	5080	c		6577	2878	817	223	47	10495	3918	37.3	2.23	2.29	154	69

Table 26 continued: Sum Headspace and Occluded Gas (µl gas / kg rock)

Well	Depth (m)	TOC (%)	C1	C2	C3	C4	C5-7	Sum C1-C4	Sum C2-C4	% wet	iC4/nC4	iC4	nC4
K	4180	2.10	3737	5580	16616	25368	48343	51503	47564	92.7	0.31	6039	19329
I	3485	0.94	836	1001	4661	4703	6246	11201	10365	92.5	0.23	870	3833
	3500	2.90	245	464	3657	6351	10191	10717	10472	97.7	0.2	1044	5307
	3515	4.55	4482	6250	23587	24300	26606	58619	54137	92.4	0.22	4310	19990
	3545	5.16	7408	8944	31639	30860	29483	78851	71443	90.6	0.21	5251	25609
	3560	4.64	8017	9354	33369	33746	33505	84486	76469	90.5	0.21	5780	27966
	3635	3.19	5646	4642	13744	12928	15060	36960	31314	84.7	0.21	2238	10690
	3650	2.10	3561	2816	8368	7544	7862	22289	18728	84	0.23	1431	6113
	3665	3.21	10046	5326	9741	6175	4611	31288	21242	67.9	0.25	1227	4948
F	2067	0.72	15440	4620	13857	29512	53131	63429	47989	75.7	0.34	7462	22050
	2085	0.96	25462	13008	43320	71981	77592	153771	128426	83.4	0.37	19513	52468
	2160	0.99	21813	8885	24321	32218	36432	87237	65424	75	0.4	9271	22947
	2175	1.04	45866	21015	60758	71524	59911	199163	153103	77	0.41	20835	50689
	2220	1.36	30196	20991	32454	17420	8393	101061	70865	70.1	0.47	5580	11840
G	2065	1.52	9404	5694	14995	15556	14545	45649	36245	79.4	0.41	4535	11021
	2080	2.33	59112	28382	53550	34912	22339	175960	116346	66.4	0.47	11160	23752
	2170	2.75	5260	8307	17590	15148	15118	46305	41045	88.6	0.39	4264	10884
	2200	2.67	23209	17514	36439	34314	31291	111476	88267	79.2	0.44	10498	23816
	2245	1.75	16268	11342	29529	33482	31620		157909	90.7		10170	23312
	2260	1.62	19568	9642	22827	25808	26321	77845	58277	74.9	0.43	7721	18087
	2425	1.37	4332	3299	7682	9120	12570	24433	20101	82.3	0.42	2692	6428
	2440	1.24	1548	1269	4103	5243	6461	12199	10615	87	0.38	1439	3804
	2455	0.92	622	997	4116	4917	8074	10692	10030	93.8	0.36	1297	3620
	2575	1.23	7148	3870	4749	2730	1640	18497	11349	61.4	0.68	1102	1628
	2605	1.83	7703	8119	5920	3344	2257	25086	17383	69.3	0.74	1427	1917
P	4660	1.80	53703	10334	2039	467	142	66543	12840	19.3	1.64	290	177
	4675	4.90	58460	10310	1747	308	53	70825	12365	17.5	2.14	210	98
	4795	5.37	41796	8058	1691	362	84	51907	10111	19.5	2.04	243	119
	4825	4.06	41449	5196	1175	310	72	48130	6681	13.9	1.98	206	104
	4870	4.50	32367	5995	1112	277	64	39751	7384	18.6	2.74	203	74
	4900	3.48	64687	6829	903	186	36	72605	7918	10.9	4.03	149	37
	5065	3.56	66978	6304	1212	302	55	74796	7818	10.5	2.47	215	87
	5080	4.25	39776	4688	995	253	51	45712	5936	13	2.67	184	69

Table 27: Stable Carbon Isotopes

	Sample no.	Temp		CH4	CO2	C2ene	C2ane	C2total	C3ene	C3ane	C3total	iC4	nC4	C4total	
Heather Fm	ME01	**370C**	aver	-32.49	-28.62		-29.49	-26.93	-25.95	-28.09	-27.26				
well G	ME02	**400C**	aver	-33.81	-27.29		-29.49	-28.42	-24.56	-28.27	-27.05				
2138.75m	ME03	**430C**	aver	-34.57	-26.11		-28.22	-27.90	-20.82	-27.06	-26.02	-25.83	-18.66	-25.21	
E 41716MK EC	ME04	**460C**	aver	-33.88	-25.84		-26.77			-25.42	-25.06	-23.80	-18.73	-24.16	
	ME05	**490C**	aver	-33.24	-25.15		-25.35			-23.21	-23.05	-20.17	-18.24	-19.43	
	ME06	**540C**	aver	-29.66	-23.93		-16.19			-2.16	-0.79				

	Sample no.	Temp		CH4	CO2	C2ene	C2ane	C2total	C3ene	C3ane	C3total	iC4	nC4	C4total	C5total
Draupne Fm	ME07	**360.00**	aver	-37.73	-30.50	-27.39	-32.88	-30.92	-30.47	-31.87			-31.11	-31.69	
well B	ME08	**390.00**	aver	-39.25	-30.12	-24.34	-33.50	0.47	-30.56	-32.53	0.47	0.47	-31.05	-30.69	-29.19
2764.7m	ME09	**430.00**	aver	-40.90	-27.68		-33.12	-32.90	-26.99	-31.76	0.47	-32.11	-30.18	-29.69	-28.08
E43254 MK EC	ME10	**490.00**	aver	-40.73	-27.15		-32.41	-32.41	-22.07	-29.48	-28.68	-27.89	-25.62	-25.87	-19.61
	ME11	**510.00**	aver	-38.44	-29.77		-31.04	-31.04	-18.55	-26.81	-26.73	-24.23	-16.16	-18.86	
	ME12	**550.00**	aver	-36.39	-22.10		-26.55	-26.55	-11.61	-12.23	-12.26	-5.12		-6.00	

aver= two or three runs

Table 28: Kinetic parameters for ethane and propane, from MSSV pyrolysis used for modelling of isotopic compositional changes.

Draupne Formation				Heather Formation			
E 43254 MK EC				E 41716 Mk EC			
A (1/min)= 4.92E+14	A (1/sec)= 8.2E+12	A (1/min)= 7.37E+16	A (1/sec)= 1.2283E+15	A (1/min)= 2.45E+17	A (1/sec)= 4.0833E+15	A (1/min)= 1.18E+19	A (1/sec)= 1.9667E+17
Ethane		**Propane**		**Ethane**		**Propane**	
E(a) (kcal/mol)	potential (mg/g sample)	E(a) (kcal/mol)	potential (mg/g sample)	E(a) (kcal/mol)	pot (mg/g sample)	E(a) (kcal/mol)	pot (mg/g sample)
49	0.89	49		49		49	
50		50	0.01	50		50	
51	1.75	51	0.02	51		51	
52	3.47	52		52		52	
53		53		53		53	
54		54	0.02	54	0.03	54	
55	9.53	55	0.4	55	0.03	55	
56	9.56	56	1.13	56	0.07	56	
57	8.57	57		57	0.13	57	0.02
58	6.59	58	2.79	58	0.1	58	0.02
59	0.5	59	4.56	59	0.32	59	0.03
60		60		60		60	0.07
61		61		61	0.42	61	0.07
62		62		62	0.49	62	0.1
63		63	36.02	63	0.36	63	0.16
64		64	0.72	64	0.2	64	0.15
65		65	6.54	65	0.23	65	0.16
66		66	0.44	66	0.05	66	0.17
67		67		67		67	0.17
68		68		68		68	0.13
69		69		69		69	0.04
70	2.28	70		70		70	0.02

Captions to Photo-Plates

Plate 1

Picture 1: sample E 41714. Heather Formation (well G). The brown fluorescing bituminite in the centre of the picture exhibits inclusions of yellow fluorescing liptodetrinite. 50X, 1cm ≅ 15 µm.

Picture 2: sample E 41714. Upper Heather Formation (well G). Identical section as shown in pic.2. Reflectance mode. Unfortunately section is reversed from top to bottom. The bituminite in the centre reveals lower reflectance values compared to the over- and underlying vitrinites. 50X, 1cm ≅ 15 µm.

Picture 3: sample E 42180. Draupne Formation (well D). Adjacent to the altered bituminite in the center is an overlying poly- organic detritic component that includes reworked vitrinite and inertinite. Underlying the bituminite a low reflecting liptinite can be recognised. 50X, 1cm ≅ 15 µm.

Plate 2

Picture 1: sample E 41714. Upper Heather Formation (well G). Thin streaks of low reflecting bituminite intercalate with layers of inertinite and vitrinite. The inertinite is unfocused because of its higher relief. 50X, 1cm ≅ 15 µm.

Picture 2: sample E 41692, Draupne Formation (well I). Strong yellow fluorescing Tasmanites algae. The finely disseminated yellow fluorescing organic matter is hardly visible due to very short exposure time. 50X, 1cm ≅ 15 µm.

Picture 3: sample E 41695, Draupne Formation (well H). Strong yellow fluorescing algal bodies and miscellaneous yellow fluorescing fragments. 20X, 1cm ≅ 37.5 µm.

Plate 3

Picture 1: sample E 41707. Heather Formation (well F). Yellow fluorescing organic matter surrounds grain boundaries of several grains. Lithology: Sandy siltstone with minor amounts of clay. 10X, 1cm ≅ 75 µm.

Picture 2: sample E 41698. Heather Formation (well H). Yellow fluorescing cellular structure. Fragments of this structure are common constituents of the Heather formation samples. 100X, 1cm ≅ 7.5 µm.

Picture 3: sample E 41709. Heather Formation (well F). Yellow to golden fluorescing component showing a high relief and internal cellular structure. 50X, 1cm ≅ 15 µm.

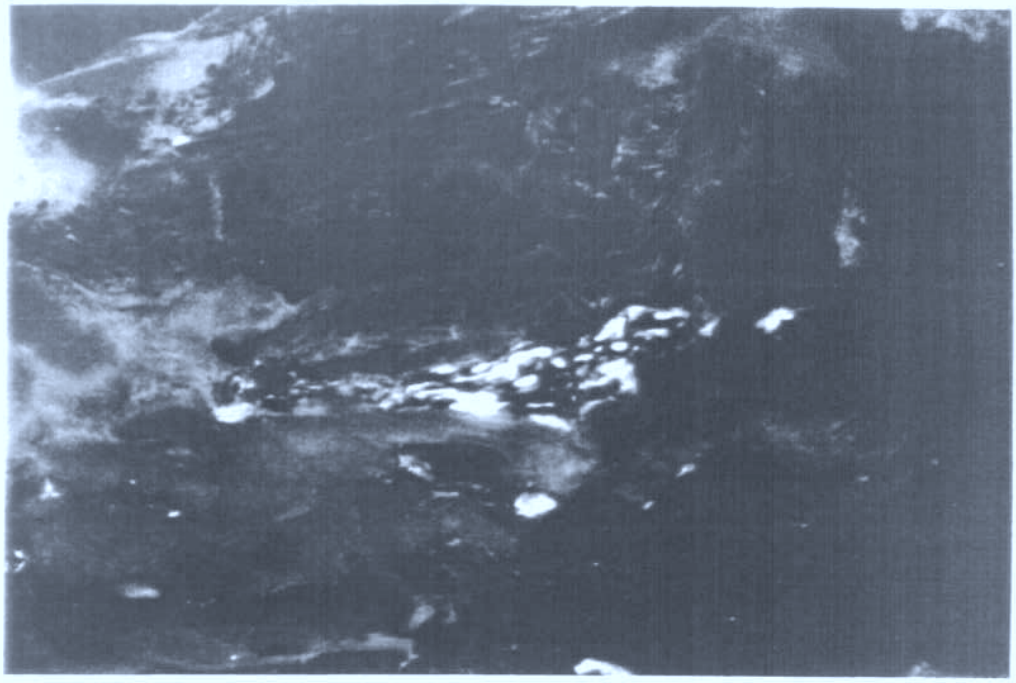
Plate 4

Picture 1: sample E 41721 (well G). Lower Heather Formation. Yellow fluorescing sporinite, surrounded by vitrinite. 100X, 1cm ≅ 7.5 µm.

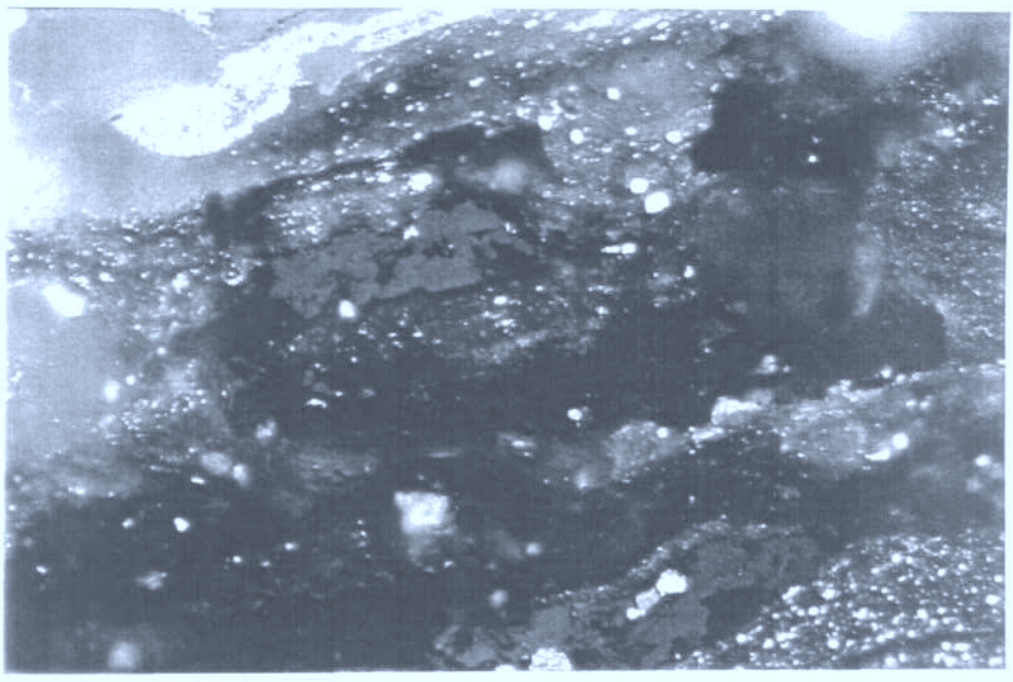
Picture 2: sample E 41711. Heather Formation (well F). Cutinite with dark grey reflectance shows internal layers. It is connected to light grey reflecting, reworked and oxidised vitrinite. 100X, 1cm ≅ 7.5 µm.

Picture 3: sample E 41701. Viking group (well P). Finely disseminated pyro-/ migra-bitumen occurs as a three dimensional web and also as cavity fillings. 50X, 1cm ≅ 15 µm.

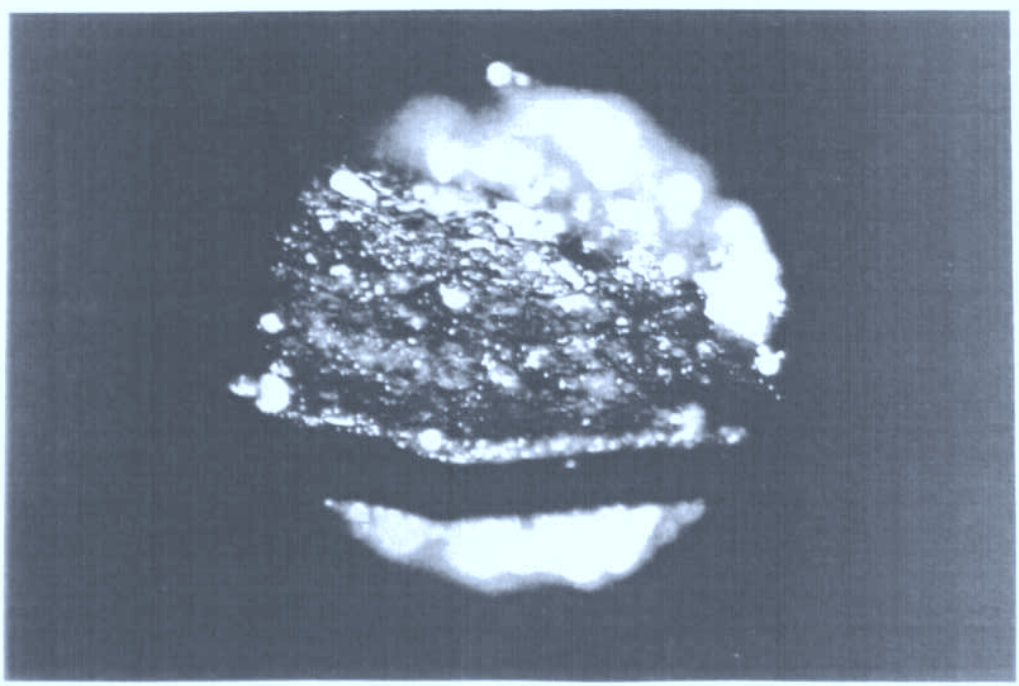
Plate 1



1

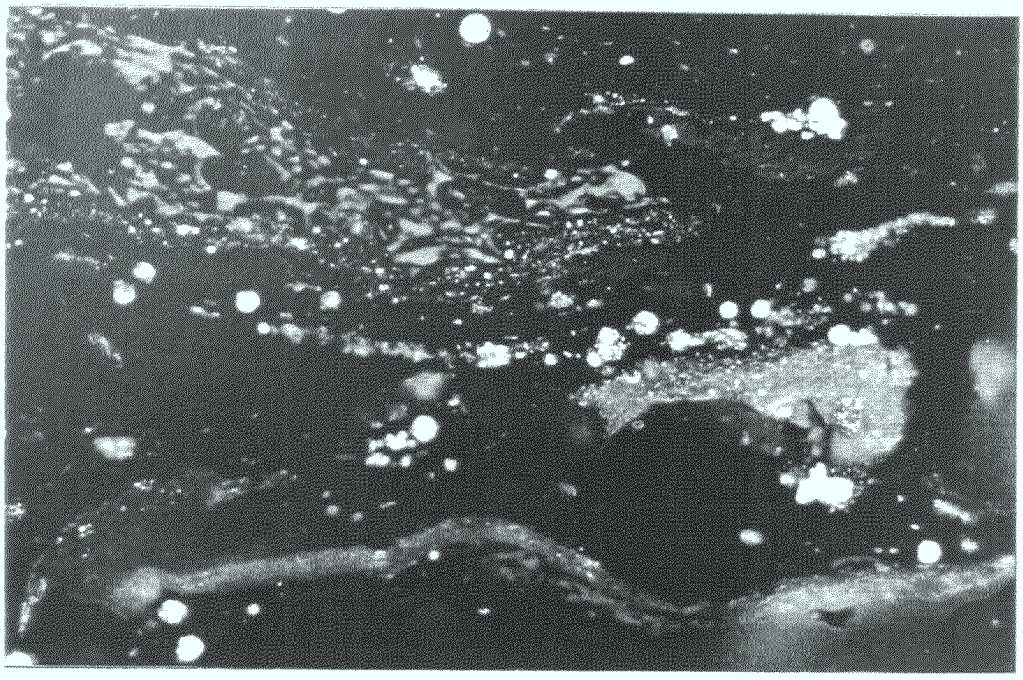


2

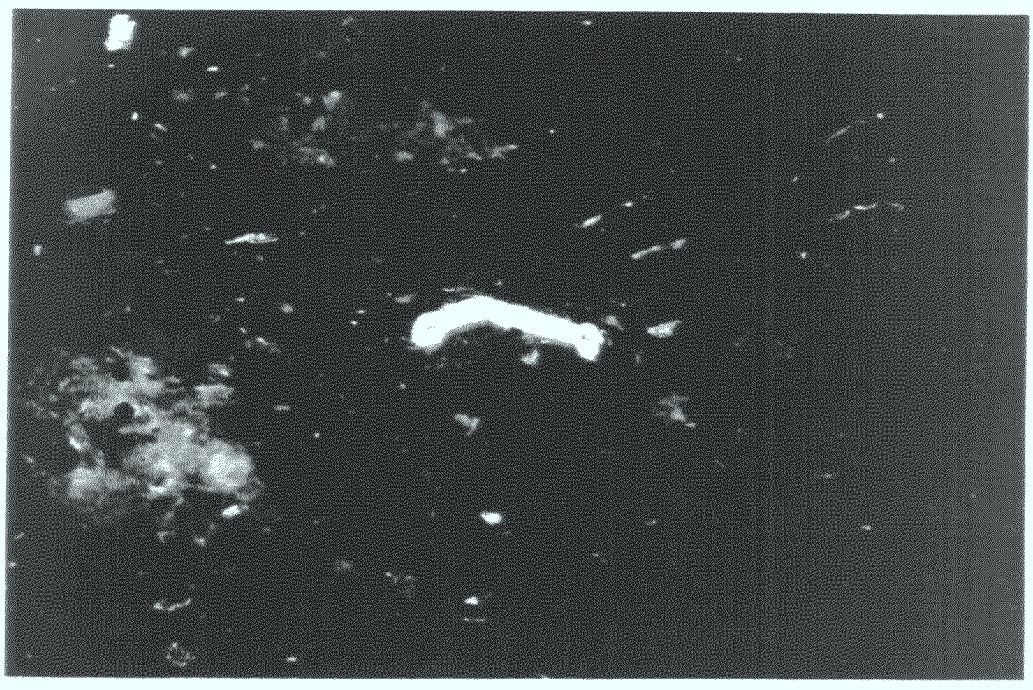


3

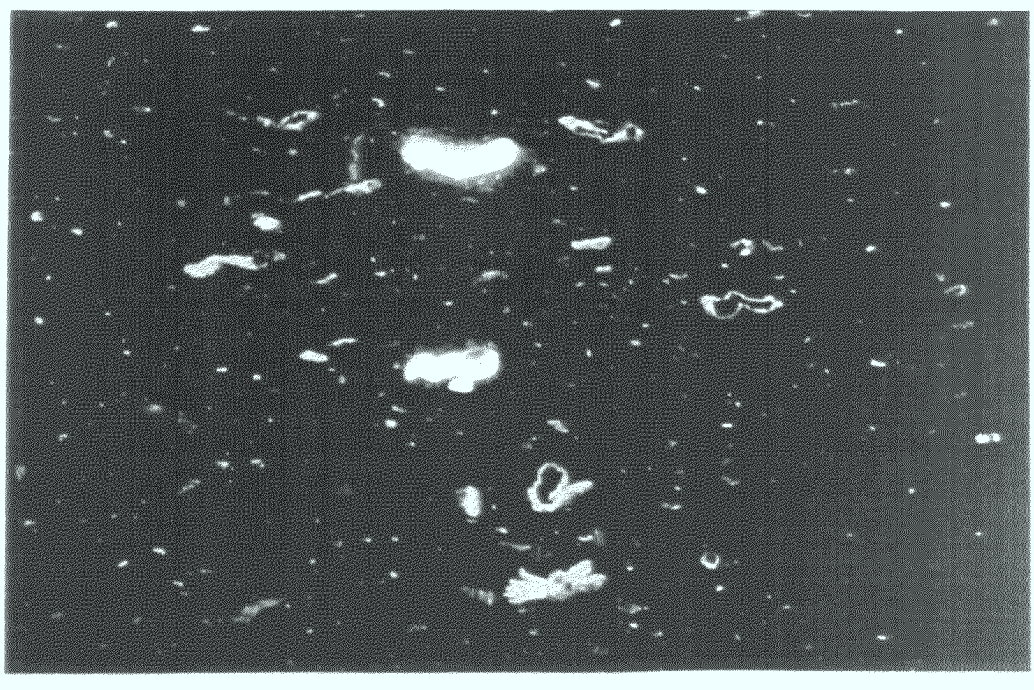
Plate 2



1

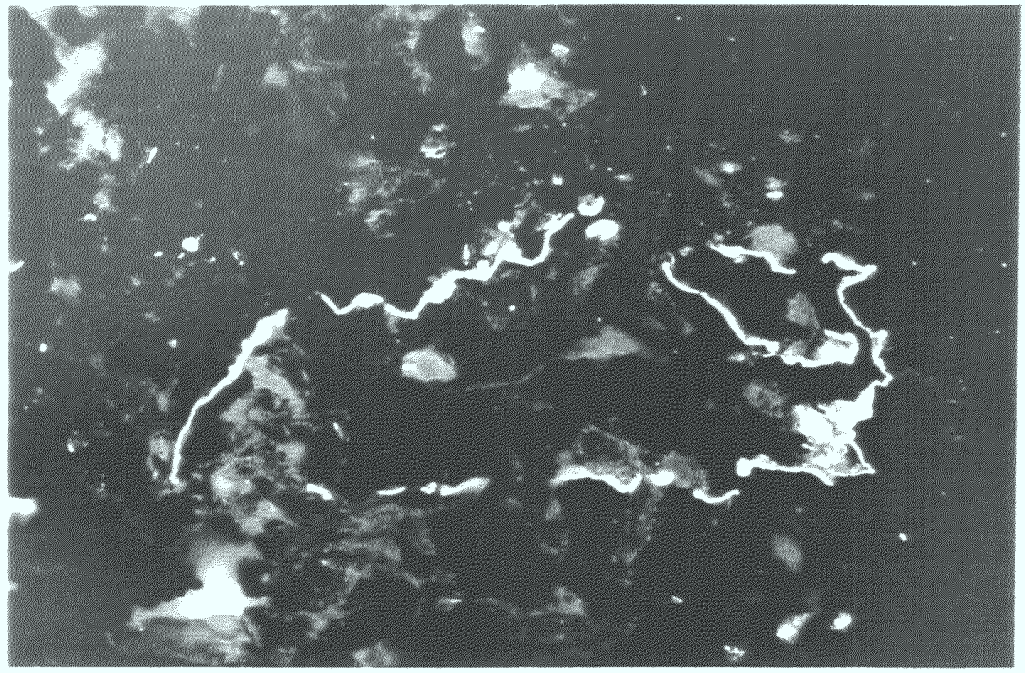


2

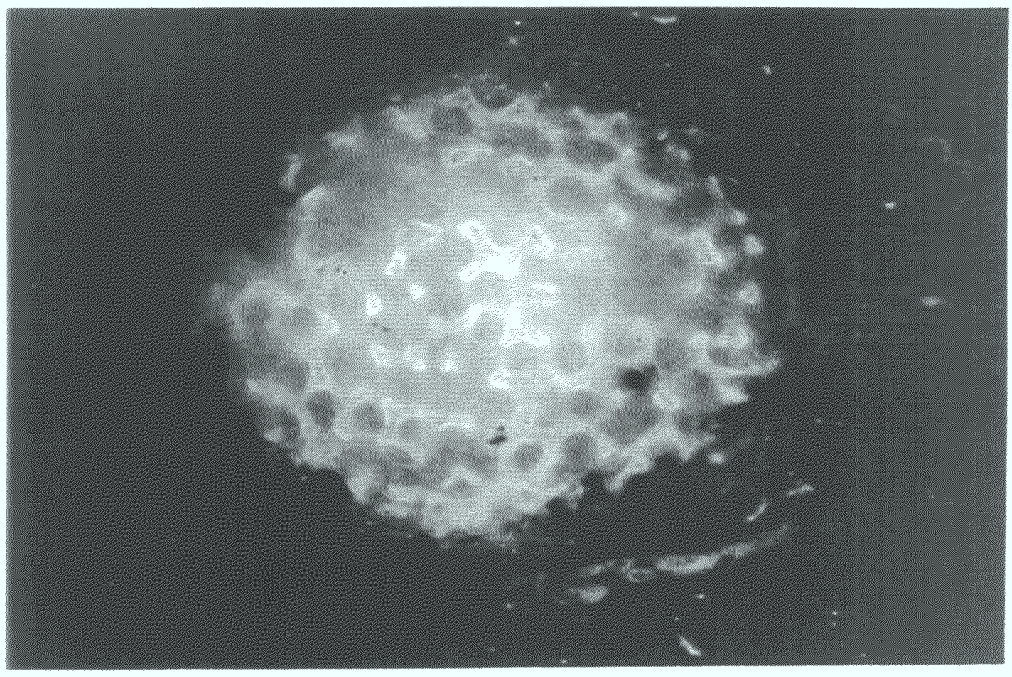


3

Plate 3



1



2

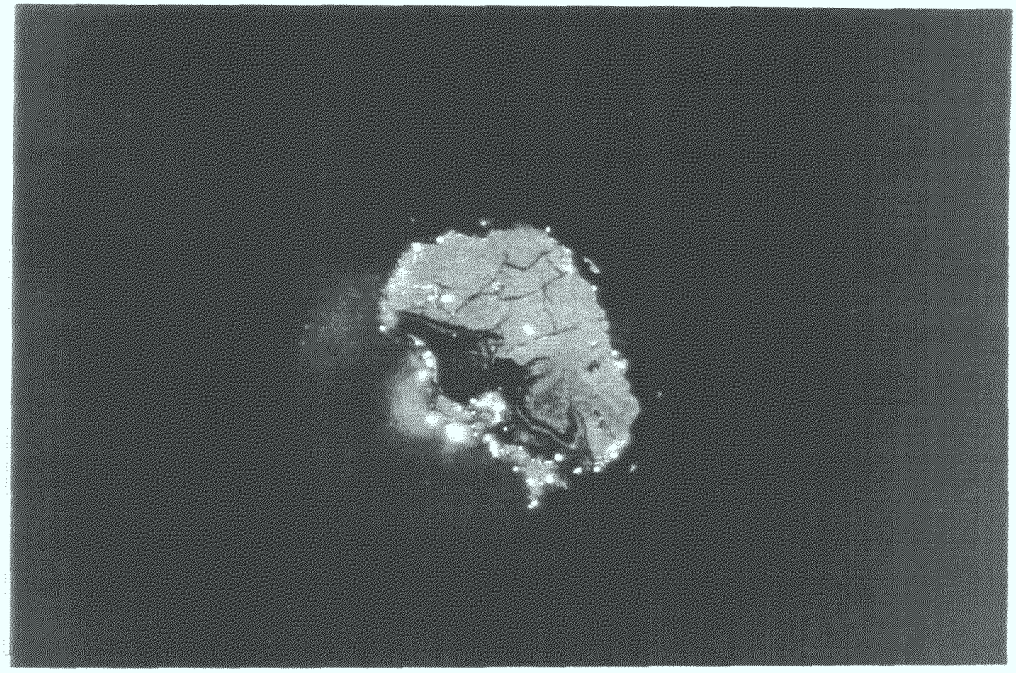


3

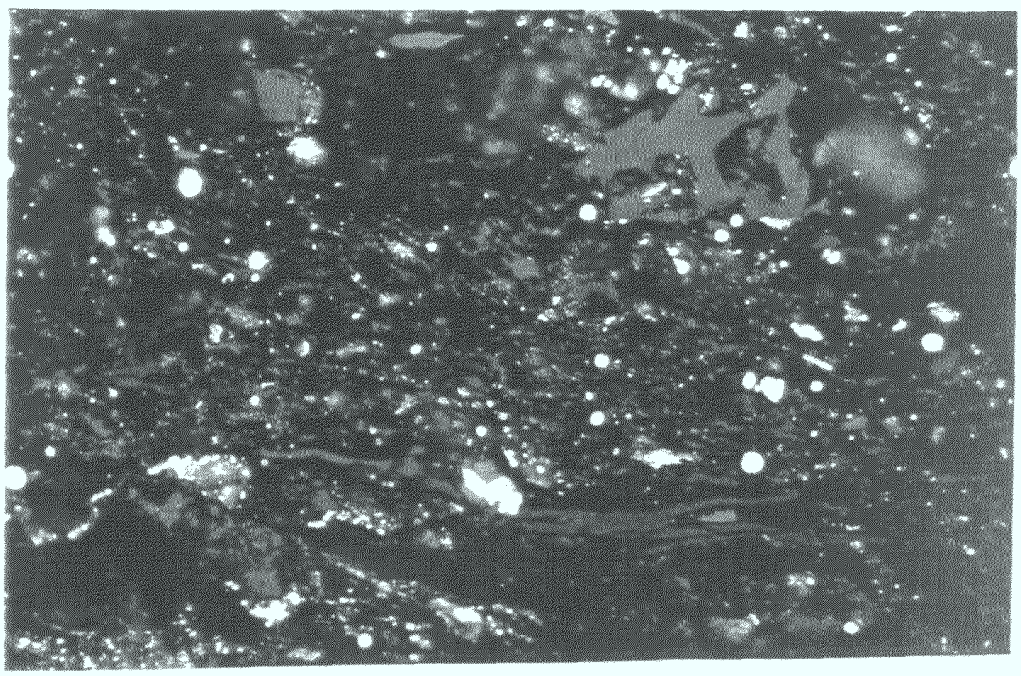
Plate 4



1



2



3

Forschungszentrum Jülich

Jül-3700
September 1999
ISSN 0944-2952